Technische Universität München

TUM School of Life Sciences

The Human Metabolism of the Bioactive Prenylated Flavonoid Xanthohumol from Hops (*Humulus Lupulus*)

Lance Buckett

Vollständiger Abdruck der von der TUM School of Life Sciences der Technischen Universität München zur Erlangung des akademischen Grades eines Doktors der Naturwissenschaften (Dr. rer. nat.) genehmigten Dissertation.

Vorsitz: Prof. Dr. Wilfried Schwab

Prüfer der Dissertation:

1. Prof. Dr. Michael Rychlik

2. apl. Prof. Dr. Thomas Skurk

Die Dissertation wurde am 13.01.2023 bei der Technischen Universität München eingereicht und durch die TUM School of Life Sciences am 12.07.2023 angenommen.

Acknowledgements

First and foremost, I would like to thank my parents, who have supported me throughout my doctoral studies and my entire life. Secondly, my brother and sisters, you are the backbone of the family and getting advice from all of you is always wonderful, everyone is so clever and you have helped guide me on this incredible journey. Thank you to the rest of my family including the newly married ones you are all the foundation to my brothers and sisters. Without a foundation, a building cannot stand tall. To my nephew's and nieces it is always a joy to visit you. To Franziska, thank you for putting up with me during the long road of getting this work completed.

My sincere thank you to Prof. Rychlik you have changed my life completely for the better and I believe without our meeting in 2016 none of this research would have materialised. You have guided me and allowed me to grow into the scientist I am today. Thank you! Many thanks to Prof. Jan Frank and Prof. Phillipe Schmitt-Kopplin you are both great advisors and without both your support some of the work would have been impossible. To the Analytical food chemistry working group where all the fun began and is still ongoing! I will never forget my time with you guys and reflecting on my time there makes me smile! Thank you to everyone.

Regarding my friends in Germany, I do not want to put names here as you know who you are and to write thank you letters would probably be longer than this thesis, but thank you so much for the fun times in this fascinating land. To my friends in New Zealand, I'll be back one day. Thank you for understanding why I left. I miss all of you. And lastly, the researchers who studied the molecule Xanthohumol. Reading about this fascinating molecule has completely changed my life and led to me moving across the world. On that note, I think the journey is not over and it is just the end of the beginning.

Life is a wondrous phenomenon

Albert Szent-Gyorgyi

This page is intentionally left blank.

Abstract

For centuries, researchers have examined the intricate details of metabolic processes, yet our understanding remains incomplete. Recent advances in metabolomics, aided by mass spectrometry and increasingly powerful computers, have provided greater insight into the functions of the metabolome within the context of untargeted metabolomics. However, this approach has certain limitations, including its reliance on indirect statistical methods and uncertainty regarding the metabolites identified. The most precise method of comprehending metabolomics is through a directed approach, entailing the creation of standards when there is no commercial availability. This study endeavoured to discover how humans metabolise xanthohumol, a prenylated flavonoid present in hops. Xanthohumol is being assessed as a natural product to address covid-19, cancer and Crohn's disease. Synthesising metabolites and stable isotopes was crucial in comprehending the human metabolic pathway of xanthohumol. Isotopes were first applied to enhance the analysis of non-metabolised compounds in beer, hops, and hop tea using stable isotope dilution analysis as the gold standard of analytical mass spectrometry methods. The study quantified six prenylated flavonoids, including two previously unquantified in beer, namely xanthohumol-C and isoxanthohumol-C. The second part involved synthesising the primary prenylated flavonoid metabolites identified in human blood plasma after consuming xanthohumol. The metabolites comprised of hydroxylated, sulfated and glucuronidated products, and a majority of them corresponded with a human blood sample taken post-ingestion of a xanthohumol capsule. The study's concluding assessment is based on a human trial involving xanthohumol; a comparison was carried out of the pharmacokinetics for both micellular and native formulations. The outcome yielded the initial method of quantifying human metabolites of xanthohumol, conclusively demonstrating that the micellular formulation boosts bioavailability by over a five-fold increase. The results indicated the importance of monitoring metabolites, given their diversity, over deconjugated compounds. Additionally, further research is required to examine the impact of metabolic changes on xanthohumol bioactivities and comprehend the effects of xanthohumol on human health.

Zusammenfassung

Seit Jahrhunderten werden die komplizierten Details der Stoffwechselprozesse erforscht, doch unser Verständnis ist immer noch unvollständig. Große Fortschritte in der Metabolomik mit Hilfe der Massenspektrometrie und immer leistungsfähigeren Computern haben mehr Details als je zuvor über die Funktionen des Metaboloms im Rahmen der ungezielten Metabolomik enthüllt. Sie hat jedoch gewisse Einschränkungen, da es sich eher um einen intirekten statistischen Ansatz handelt und die gefundenen Metaboliten nicht mit Sicherheit bestimmt werden können. Der genaueste Weg zum Verständnis der Metabolomik ist ein zielgerichteter Ansatz, der die Synthese von Standards erfordert, wenn diese nicht im Handel erhältlich sind. Ziel dieser Arbeit war es, zu verstehen, wie der Mensch Xanthohumol, ein prenyliertes Flavonoid aus Hopfen, verstoffwechselt. Xanthohumol ist ein Naturstoffkandidat für die Behandlung von Covid-19, Krebs und Morbus Crohn. Um den Humanstoffwechsel von Xanthohumol zu verstehen, ist die Synthese von Metaboliten und stabilen Isotopen erforderlich. Die Isotope wurden zunächst eingesetzt, um die Analyse der nicht metabolisierten Verbindungen in Bier, Hopfen und Hopfentee mit Hilfe des Goldstandards der Analyse, der Stabilisotopenverdünnungsanalyse, zu verbessern. Dabei wurden sechs prenylierte Flavonoide quantifiziert, von denen zwei, Xanthohumol-C und Isoxanthohumol-C, zuvor noch nie in Bier quantifiziert wurden. Im zweiten Teil wurden die wichtigsten prenylierten Flavonoid-Metaboliten synthetisiert, die nach dem Konsum von Xanthohumol im menschlichen Blutplasma gefunden wurden. Zu den Metaboliten gehörten Hydroxylierungs-, Sulfatierungs- und Glucuronidierungsprodukte, und die meisten wurden mit einer menschlichen Blutprobe nach dem Verzehr einer Xanthohumol-Kapsel abgeglichen. Die abschließende Bewertung der Arbeit war eine Humanstudie zu Xanthohumol, bei dem die Pharmakokinetik einer mizellulären und einer nativen Formulierung verglichen wurde. Das Ergebnis war die erste Methode zur Quantifizierung von Xanthohumol-Metaboliten beim Menschen, wobei nachgewiesen wurde, dass eine mizelluläre Formulierung die Bioverfügbarkeit um mehr als das fünffache erhöht. Die Ergebnisse zeigen, dass aufgrund ihrer Vielfalt und Menge auch die konjugierten Metaboliten in Studien zur Bioverfügbarkeit berücksichtigt werden müssen. Darüber hinaus sind Untersuchungen über die Rolle der metabolischen Veränderungen auf die Bioaktivität von Xanthohumol notwendig, um die Auswirkungen von Xanthohumol auf die menschliche Gesundheit zu verstehen.

I. Table of contents

II. Figures

III. Tables

IV. List of abbreviations

Prenylated flavonoids

6-PN, 6-Prenylnaringenin (5,7-dihydroxy-2-(4-hydroxyphenyl)-6-(3-methylbut-2-en-1-yl)chroman-4-one)

8-PN, 8-Prenylnaringenin (5,7-dihydroxy-2-(4-hydroxyphenyl)-8-(3-methylbut-2-en-1-yl)chroman-4-one)

DMX, Desmethylxanthohumol (3-(4-hydroxyphenyl)-1-(2,4,6-trihydroxy-3-(3-methylbut-2-en-1-yl)phenyl)propan-1-one=

DXN, Dihydroxanthohumol ((E)-3-(4-hydroxyphenyl)-1-(2,4,6-trihydroxy-3-(3-methylbut-2-en-1-yl)phenyl)prop-2-en-1-one)

IXN, Isoxanthohumol, (7-hydroxy-2-(4-hydroxyphenyl)-5-methoxy-8-(3-methylbut-2-en-1-yl)chroman-4-one)

IXN-C, Isoxanthohumol-C (2-(4-hydroxyphenyl)-5-methoxy-8,8-dimethyl-2,3-dihydro-4H,8H-pyrano[2,3-f]chromen-4-one)

Mb, Mulberin (2-(2,4-dihydroxyphenyl)-5,7-dihydroxy-3,8-bis(3-methylbut-2-enyl)chromen-4-one)

XN-C, Xanthohumol-C ((E)-1-(5-hydroxy-7-methoxy-2,2-dimethyl-2H-chromen-6-yl)-3-(4-hydroxyphenyl)prop-2-en-1-one

XN, Xanthohumol (2',4,4'-trihydroxy-6'-methoxy-3'-prenylchalcone)

Metabolites of prenylated flavonoids

6-PN-7-O-GlcA, (2S,3S,4S,5R,6S)-3,4,5-trihydroxy-6-((5-hydroxy-2-(4-hydroxyphenyl)-6-(3-methylbut-2-en-1-yl)-4- oxochroman-7-yl)oxy)tetrahydro-2H-pyran-2-carboxylate.

6-PN-7-O-sulfate, 5-hydroxy-2-(4-hydroxyphenyl)-6-(3-methylbut-2-en-1-yl)-4-oxochroman-7-yl hydrogen sulfate.

6-PN-E-OH, (E)-5,7-dihydroxy-6-(4-hydroxy-3-methylbut-2-en-1-yl)-2-(4-hydroxyphenyl) chroman-4-one.

8-PN-4'-O-sulfate, 4-(5,7-dihydroxy-8-(3-methylbut-2- en-1-yl)-4-oxochroman-2-yl)phenyl hydrogen sulfate.

8-PN-7-O-GlcA, (2S,3S,4S,5R,6S)-3,4,5-trihydroxy-6-((5-hydroxy-2-(4-hydroxyphenyl)-8-(3-methylbut-2-en-1-yl)-4-oxochroman-7-yl)oxy)tetrahydro-2H-pyran-2-carboxylate.

8-PN-E-OH, (E)-5,7-dihydroxy-8-(4-hydroxy-3-methylbut-2-en-1-yl)-2-(4-hydroxyphenyl)chroman-4-one.

IXN-4'-O-sulfate, (4-(7-hydroxy-5-methoxy-8-(3-methylbut-2-en-1-yl)-4-oxochroman-2-yl)phenyl hydrogen sulfate)

IXN-7-O-GlcA, (2S,3S,4S,5R,6S)-3,4,5-trihydroxy-6-((2-(4-hydroxyphenyl)-5-methoxy-8-(3-methylbut-2-en-1-yl)-4-oxochroman-7-yl)oxy)tetrahydro-2H-pyran-2-carboxylate.

IXN-(E)-OH, (E)-7-hydroxy-8-(4-hydroxy-3-methylbut-2-en-1-yl)-2-(4-hydroxyphenyl)-5-methoxychroman-4-one.

XN-4'-O-sulfate, (E)-4-(3-(2,4-dihydroxy-6-methoxy-3-(3-methylbut-2-en-1-yl)phenyl)-3-oxoprop-1-en-1-yl)phenyl hydrogen sulfate

XN-7-O-GlcA, (2S,3S,4S,5R,6S)-3,4,5-trihydroxy-6-(3-hydroxy-4-((E)-3-(4-hydroxyphenyl)acryloyl)-5-methoxy-2-(3-methylbut-2-en-1-yl)phenoxy)tetrahydro-2H-pyran-2-carboxylate.

XN-(E)-OH. (E)-1-(2,4-dihydroxy-3-((E)-4-hydroxy-3-methylbut-2-en-1-yl)-6-methoxyphenyl)-3-(4-hydroxyphenyl)prop-2-en-1-one

XN-(Z)-OH, (E)-1-(2,4-dihydroxy-3-((Z)-4-hydroxy-3-methylbut-2-en-1-yl)-6-methoxyphenyl)-3-(4-hydroxyphenyl)prop-2-en-1-one)

Analytical

APCI, Atmospheric chemical ionisation

AUC, Area under the curve

CE, Capillary electrophoresis

DAD, Diode array detector

ESI, Electrospray ionisation

HPLC, High-performance liquid chromatography

HCS, High content screening

HR-MS, High-resolution mass spectrometry

LC-MS/MS, Liquid chromatography-tandem mass spectrometry

LOD, Limit of detection

MS/MS, Tandem mass spectrometry

m/z, mass to charge ratio

NMR, Nuclear Magnetic Resonance Spectroscopy

QQQ Triple quadrupole

UV, Ultraviolet visible

Biochemical

ABC, ATP binding cassette

BSA, Bovine serum albumin

CYP450, Cytochrome P450

DNA, Deoxyribonucleic acid

Glut1, Glucose transporter 1

GSH, Glutathione

GST, Glutathione S-transferase

HDL, High density lipoprotein

LDL, Low density lipoprotein

MDR1, Multi-drug-resistance protein 1

MRSA, methicillin resistant staphylococcus aureus

NADPH, Nicotanamide adenine dinucleotide phosphate

UGT ,Uridine diphosphate glucuronosyltransferase

SLC, solute carrier

SULTs, Sulfotransferases

1. Theoretical Background

1.1 History of dose and toxicity, modern medicine and food as medicine

Paracelsianism is the early practice of modern-day medicine and originated in the mid-16th century. The father of the modern theory of Paracelsianism was Paracelsus (born Theophrastus Bombastus Philippus Aureolus von Hohenheim). Paracelsianism originates from alchemy using the term "Insertion of chemistry into medicine" and is when clinical practice started employing simple chemical reactions to produce medicine with increased efficacy, deemed Iatrochemistry [1]. The basis of Iatrochemistry is primitive and, therefore, not practised today. However, it has led to the development of medical practices in the modern-day era of "evidence-based applications on scientific practices". The importance of Paracelsus was not realised until hundreds of years later once his famous phrase "the dose is the poison" in German, "Alle Dinge sind Gift, und nichts ist ohne Gift; allein die dosis machts, daß ein Ding kein Gift sei" was understood and this concept is stated in many biochemistry textbooks [2]. The meaning of Parceluses's phrase still holds up value today (nearly 500 years later), affecting the design and efficacy of many pharmaceutical compounds and food products. Generally, food is non-toxic, but when contaminated with, e.g. mycotoxins, it can potentially be toxic, such as with aflatoxin-B1. The aflatoxin-B1 is toxic, but if the dose is below the harmful threshold, it will not harm the consumer. However, aflatoxin-B1 is highly carcinogenic and often present in peanut butter. However, suppose that threshold is higher than the allowed amount. In that case, the peanut butter can be blended with a lower content, permitting the peanut butter to be safer for human consumption and not contributing to waste in certain countries [3]. However, such practice is illegal in the European Union, and for genotoxic compounds, no minimum threshold is considered safe [4].

A different argument that "the dose makes the medicine" is also a valid point. It is the basis of many drugs, nutritional and food products, as the minimum threshold for therapeutic efficacy (dose) needs to be met for a phenotypic response to occur [5]. Hence, the dose of a compound, including compounds in everything consumed, needs to be known when discussing metabolomics as these methods are very sensitive and hit compounds might not have sufficient concentrations to elicit an effect. The complex matrices of compounds should elicit a phenotype of a parent organism or otherwise not contribute a health benefit. Sometimes this fact is complicated as the evaluation should include whether a substance acts in unison with other compounds, as these can have additive or synergistic impacts (i.e. the cocktail effect). Later discussed will be whether a compound in a beer named xanthohumol (XN) might be responsible for a range of health benefits due to an observation that beer consumption causes less liver damage than pure ethanol when given at the same concentration [6 7].

Not all medicine is related to chemistry, i.e. psychology uses a more holistic approach by changing the way we think with therapy, thus improving health [8]. Although many arguments state that changes in the brain are a chemical reaction causing these changes, further research into these matters is required and is psychiatric based practices [9]. Therefore, understanding the psychology and chemistry of distinct processors is essential in realising how compounds affect individuals. Lastly, adding to the complexity of modern medicine is that the individual responses to compounds and foods are different as our genomic and postgenomic, amongst other makeups, are personalised, although at the same time, 99% similar. Therefore, personalised medicine and nutrition are believed to sustain humans in the future. Nevertheless, the costs of personalised medicine are excessive and unaffordable for most people [10].

One aspect of food chemistry involves studying the biochemistry underlying the "dose that makes the medicine". An essential component of this examination involves determining how to assess the potential bioactivities of compounds. Classically, the assessment process for bioactivity evaluation is first understanding a target (e.g. receptor/enzyme), and a direct way is understanding a disease, where initially molecular targets are elucidated. Identifying the target and the elicitor is achieved by observing an increase or decrease of a said effect or development of an inhibitor by compound design. Once the characterisation of the enzyme target is achieved, the structural description of the active site needs to be addressed for the "bioactive" design. Furthermore, the design of a bioactive candidate is only applicable when it is theoretically synthesisable or extractable; otherwise, it has limited uses in pharmaceuticals. Within a food context, many strides are undertaken in producing an essential component of a food's stuff via enrichment. For example, folates are essential vitamins essential for cell growth/division that selective breeding techniques in strawberries can enrich [11]. A different approach for finding bioactive compounds is high content screening (HCS), also known as cellomics. It utilises purified compounds or complex mixtures, incubates them with various cell types, and observes phenotypic changes [12]. The methodology of HCS tests so many different compounds simultaneously and is the first approach in bioactive identification. In scanning 100's – 1000's compounds, a positive hit is bound to find something bioactive for a disease/enzyme target. Historically compounds were naturally derived, but new databases have allowed the evaluation of synthetic compounds. Newer types of HCS tools can use computer modelling to find "hits", also known as lead compounds forming the basis of drug design.

Food chemistry is a broad scientific field that intertwines many natural science disciplines such as law, physics, biochemistry, chemistry, biology, statistics and mathematics, among other fundamental studies. Food chemistry applies the chemistry, and biochemical principles approach, e.g. to minimise risk and hazards allowing the general public to consume safer food. As we enter the age of preventive medicine, food chemistry is moving towards a portion of food as medicine. Where a doctor prescribes food to treat a given disease or reduce harm, i.e. people with diabetes are usually prescribed strict diets rich in polyphenols, and the elderly have exciting textures in their food to stimulate consumption while retaining a high energy content [13] [14] [15]. Another aspect is using food to provide medicinal properties; some examples are vitamin fortified

food, such as the golden rice project with a biotechnological approach enriched rice with β-carotene (precursor to Vitamin A) and has the chance to impact half the global population's nutrition [16] [17]. Therefore, it is desired to incorporate bioactive compounds into specific products that increase their efficacy. Another example of this concept is "XanWellness", a product that was to aid in the antioxidant activity of a beverage by enrichment with XN [18]. Similar to the activities of vitamin C in fortified juices, the polyphenol XN protects the DNA from damage and, thus, was stated as an elixir [19]. Although the 'XanWellness' drink has had some problems with stability and whether it was correct to claim that it 'protects against DNA damage' is still being debated, it has since been withdrawn from the market [20] [21] [19].

A primary goal of the brewing industry is to produce a less harmful beer, but this is very difficult due to the toxicity of ethanol, as the balance of benefits needs to be tightly controlled. However, new marketing strategies of many breweries is non-alcoholic beers are "healthy", but the evidence is not based on human trials and is limited. To return to Theophrastus' statement, "the dose is the poison"; therefore, the "dose" of beer should be consumed in moderation. Although there is a lot to be said for this statement, such as the reasons why moderate beer consumption statistically increases life expectancy, even though it contains toxins such as ethanol and mycotoxins. [22] [23]. Therefore, is the consumption of beer good or bad for health? Meta-analysis has correlated that moderate consumption of alcohol leads to a longer lifespan, but the mechanisms behind this observation are unknown [23]. One of many compounds may be working in unison to provide a health effect as long as the dose of beneficial compounds is over a certain threshold, while ethanol should be below the toxicity threshold as it is known that excess beer consumption causes various diseases. Intertwining food as medicine and medicine as food is a complicated matter; due to the cost and amount of data needed for evaluation, the subject has been a matter of many debates. On average, developing a medicine requires 100's if not 1000's million Euros, and regarding food health claims, this expensive process is not required by law [24]. As such, many bogus medicines and health supplements without any scientific bases are on the market, which promotes the need for thorough investigations [25].

To enable food as a medicine is an attractive commodity as it bypasses medical costs and indicates that people can enjoy the benefits by only eating everyday meals [25]. To achieve this, one must elucidate the dose required and decipher whether one food/bioactive will harm the consumer or whether the dose promotes a claimed health effect. Additionally, food chemists discover potential harm from the everyday foods we eat. A recent example is that heating starchy foods cause a carcinogen, "acrylamide", to be formed in high concentrations [26] Now, the regulations in the EU recommend that potato fries in restaurants are fried at a specified temperature to limit harm to the general public [27]. The temperature recommendation does not protect the people cooking at home but will decrease the cancer risk for the general public in the long run. In this thesis, a compound found in beer (XN) is studied to see what might happen during metabolism in humans. Many compounds are 'pro-drugs', although this term is used to describe 'pro-bioactives' as the compounds

discussed are not drugs. The answer to the question of whether XN can be used for medicinal purposes on its own, or as a supplement to a healthy human diet in a drink formula, is not yet fully understood.

Another critical issue is the nutraceutical potential of XN, where many multidisciplinary topics need to be intertwined and used to answer these questions. The most famous related compound is resveratrol, a compound commonly found in red wine, where it correlates with increasing cardiac health, contributed by many Mediterranean type diets[28]. Accordingly, studies suggest that beer has similar effects on moderate drinkers. Many studies correlate beer consumption with increased longevity, and a likely family of compounds that may be responsible are polyphenols [23]. It is thought that polyphenols reside in the grain, and additional polyphenols from hops, such as XN and other polyphenols, contribute to the observed health effects [29]. In other, more specific studies, rats that consumed alcohol had significantly less liver damage than another group that was fed alcohol enriched with XN [30].

1.2 Human metabolism

Today, Human metabolism is a basis of biochemistry, "studying the molecule mechanisms behind all things living" [2]. Metabolism primarily explains the modification of a given compound once it enters a body where it is changed by many different processors, including modifications that begin via chewing, for example, saliva secretes enzymes that can hydrolyse and modify components moving down through the digestive system [2]. The food, along with the components that are absorbable and essential to the person consuming food, are then transported down into the digestive tract. Digestion further contributes to food degradation from the macromolecular structure towards breaking down into the molecular level. Peptidases break the proteins down into more accessible, digestible and valuable peptides. Lipases break down triglycerides into simpler free fatty acids (fats). Glycoside hydrolases start working on the saccharides, further degraded by certain amylases allowing more useful components for catabolism to suit the needs of the host. Food is a complicated matrix that supplements life as we know it, where some parts of the diet are essential for humans as they cannot produce compounds solely by Anabolism. In addition, we break up our food into simpler building blocks which we modify and build new structures that make living organisms, e.g. humans. Another aspect is the gut microbiome which is the bacteria within the gut. These modify certain compounds into more useful components for both organisms, termed biological synergism [31].

Mainly investigations into metabolism mechanisms use metabolomics which studies the metabolome (the identification of all small mass compounds with a mass usually below 1500 Daltons [32]. A part of understanding human metabolism is with metabolomics to correlate the processors within the systems biology approach; hence the primary tool used is mass spectrometry, but supplemented via other "Omic" fields, such as, genomics and proteomics. However, if plasma is the analytical medium some information might be missed as the metabolism of XN does not begin in the liver, and various changes occur before absorption of XN by the gut. In addition intervention trials might modify the host causing metabolic differences on an

individual basis. For example, it is known that people with irritable bowel syndrome are more likely to have metabolic syndrome, which increases the health risks associated with human metabolism, and thus might give skewed results [33]. Furthermore, dietary flavonoids might regulate gut microbiota homeostasis and thus change how gut metabolism functions during investigations and might not represent the general metabolism. Therefore, to break down the steps, investigations focus on the more straightforward transfers and modifications of foreign molecules (xenobiotics) that enter the body via predictive enzymatic reactions. However, the power of metabolomics is also capable of following the bacteria modifications [34].

1.2.1 Phase I

Generally, phase I metabolism is the modification of non-polar compounds by a series of enzymes resulting in increased polarity (water soluble) or more liable compounds via incorporation of specific functional groups, such as, hydroxyl groups, the liberation of hydroxyls or other C-H activations, amongst others. The most crucial process of phase I metabolism is carried out by a superfamily of enzymes, cytochrome p450's (CYP450), named after the strong absorption of light at λ 450 nm [35]. Phase I metabolism is the first line of detoxification and sets up compounds for excretion and further modification possibilities, for example, phase II conjugation will be introduced later in section 1.2.2. The mechanism of the hydroxylation of a xenobiotic (Figure 1) starts with the incorporation into the active site of the CYP450 (there are putatively 57 known genes encoded in humans' DNA) [36]. The interaction of the CYP450 (membrane-bound enzymes located in the mitochondria) and water in the active site of the CYP450, which is coordinated with iron (Fe) in the ferric state Fe3+ (1.) is then excluded from the active site allowing the xenobiotic entry (2.). The next step (3.) is the movement of an electron into the Heme, changing the state of the Fe3+ into a ferrous state, Fe3+, which directs the electron towards O2. The radicalised O2 is then able to then scavenge a further electron from the Nicotinamide adenine dinucleotide phosphate (NADPH) of cytochrome P450 reductase (4.). The short-lived radicalised O2 is capable of oxygenating substrates via an alternative pathway named oxidation shunt. Step (5.) involves the addition of 2H+, which coordinate with the radical that cleaves itself, resulting in water leaving the P450 in a state of a highly reactive iron (IV) oxo species where the substrate is introduced (7) and hydroxylation occurs. (8) The substrate then leaves the active site and returns to the ground ferric state, where the cycle repeats depending on the availability of substrates and NADPH pool. One other enzyme plays a role in the process, named Cytochrome b5, and enhances the redox potential of the p450 oxidative system (a sort of biocatalyst) [37].

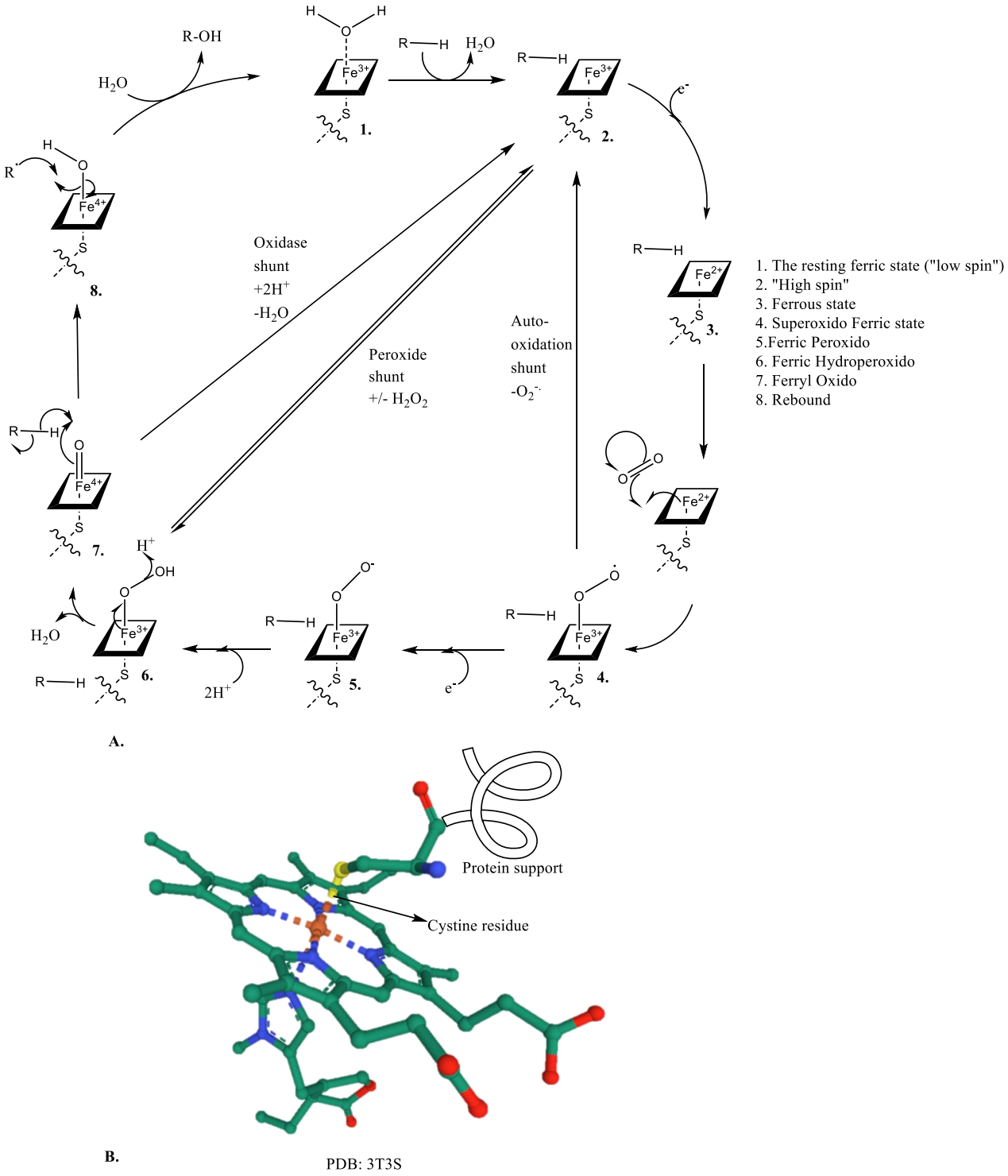

Figure 1: Possible Cyp450 catalysed hydroxylation mechanism (A) and the Heme core coordinated with Pilocarpin (B) [35 38 39 40].

Different reactions other than oxidation in phase I include cyclisation, reduction and hydrolysis [37]. These reactions are facilitated via an array of enzymes, including Flavin monooxygenases, cyclooxygenases, aldehyde dehydrogenases, alcohol dehydrogenases and epoxide dehydrogenases [31] Although a purpose of phase I metabolism is detoxifying the xenobiotics, it can activate them into a toxic compound, such as, epoxides, which are products of phase I metabolism and some are very harmful carcinogens [41]. An example is the epoxide formation of 2-naphthylamine during phase I metabolism and was one of the first compounds found to cause cancer (it is present in cigarette smoke) via epoxide formation from phase I metabolism [42]. The epoxide of the 2-naphthylamine is partially stabilised by the delocalised electrons, which provides a long enough half-life for it to reach DNA where damage can occur [42]. Interestingly, 2-naphthylamine mainly causes bladder cancer due to phase II enzymes modifying the compound until it reaches the bladder, where glucuronidases remove glucuronide and the CYP450s adds an epoxide causing harm from mutating DNA [43]. The devastating effects of epoxides not only result in changes at the DNA level but also deplete glutathione (GSH), another factor used in detoxifying compounds by conjugation and is outlined below [44]. Since the discovery that 2-naphthylamine can activate into a carcinogen, the compound is used less in industry because of the potential risk and hazards [20].

Phase I metabolism of prenylated flavonoids is well documented and usually is investigated by incubating an isolated compound with pooled liver microsomes (reformed vesicle-like parts of the endoplasmic reticulum rich in metabolic enzymes) and supplying excess NADPH for shuttling electrons as depicted in Figure 1. To illustrate the known combinations, an investigation was performed by supplying human liver microsomes with XN and isoxanthohumol (IXN) while supplementing NADPH as a co-substrate. The aim of the study carried out by Nikolic et al. 2005 investigated whether more potent phytoestrogens were produced and showed that in-vitro oxidation, demethylation and epoxide intermediates were detected upon LC-MS/MS analysis (Figure 2) [45]. XN is additionally spontaneously converted to IXN in the gut acidic environment, and demethylation into 8-prenylnaringenin (8-PN) can occur. The knowledge that the gut microbiota is responsible for the activation of XN to 8-PN was suggested by the fact that when germ-free mice were fed XN, no 8-PN metabolites were detected, whereas feeding mice with microbiota produced 8-PN. [46]. Another study on the in-vitro phase I metabolism of 8-PN and IXN showed that predominantly hydroxylation occurred on the prenyl group and that trans (*E*) isomer is favoured, most likely due to the lower internal energy of this conformer [47]. Furthermore, the in-vivo analysis of the metabolism of XN in rats after 1000 mg doses identified further metabolites explaining similar pathways as the in-vitro studies classifying more than 14 phase I metabolites [48]. For example, epoxidation, hydroxylation, methylation, acetylation, and cyclisation of the prenyl side chain occurred. See Figure 2 for an overview of the Phase I metabolism of XN.

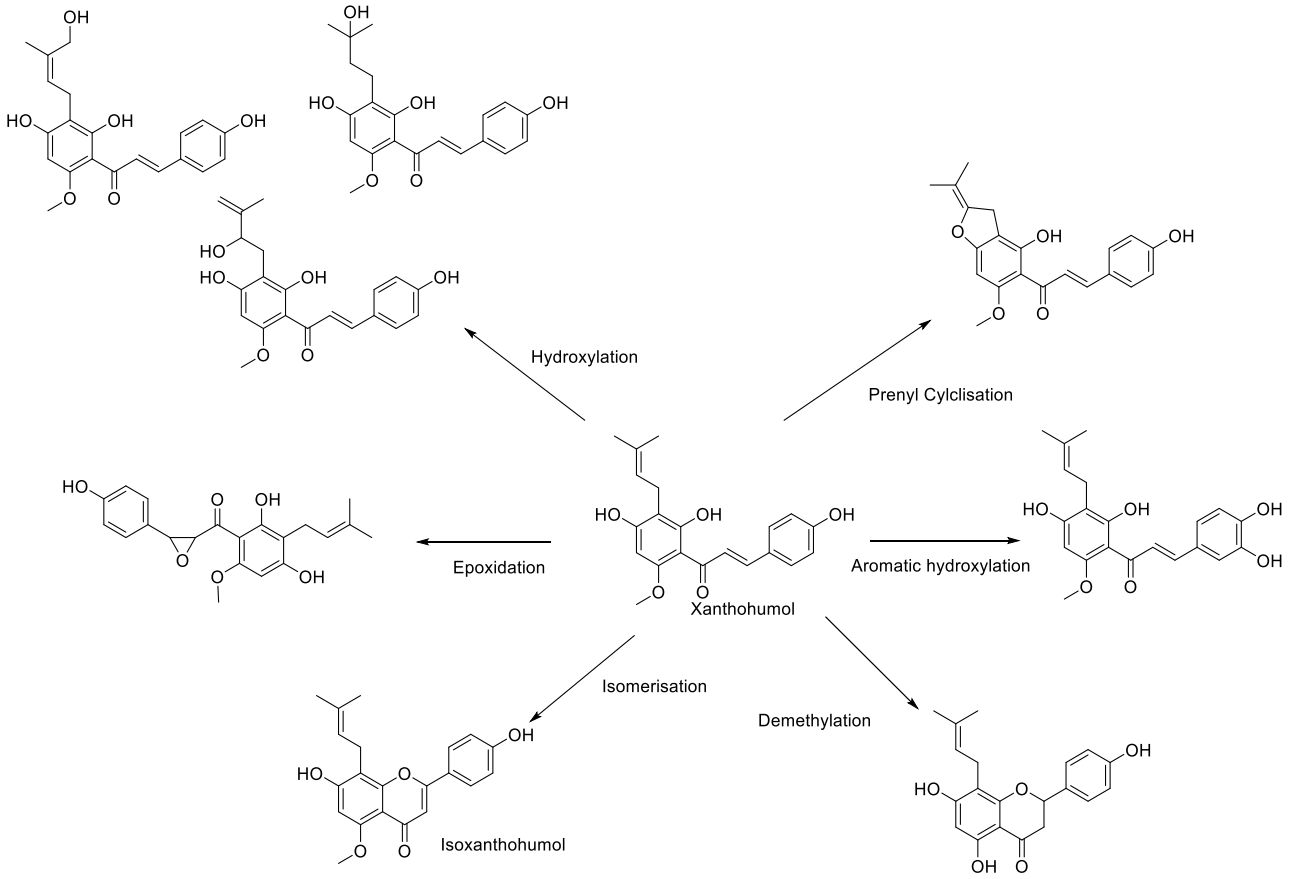

Figure 2: Some examples of phase I metabolites found in various studies. Depending on the dose of XN given mostly, hydroxylation of the prenyl group predominates regarding phase I metabolites [46] [45] [47].

Although, all phase I metabolism studies on XN are complicated by the fact it is a CYP450 inhibitor and might require a certain threshold of concentrations above a particular value for hydroxyls to be detected in the circulatory system [22] [49]. To date, no known hydroxylated metabolites have been found in humans after XN supplementation. Additionally, little is known about which bioactivities these compounds have at a cellular level, as activation of epoxides could be damaging to DNA/GSH, or the phase I metabolites might even be activated towards a more phytoestrogenic compound [45]. Before the work carried out in this thesis, no phase I synthetic products were chemically synthesised, and only a few studies investigated their microbial metabolism. Furthermore, hydroxylated products of XN were only identified tentatively based on MS/MS patterns. Therefore, reference standards with corresponding nuclear magnetic resonance (NMR) spectra would greatly complement XN metabolism and bioactivity studies.

The bioactivities of some hydroxylated XN (XN-OH) metabolites were investigated by Herath et al., 2003 revealed no antibacterial or anti-malarial activity, and they were not cytotoxic [50]. 8-Prenylnaringenin-OH (8-PN-OH) has potential bioactivities via information from a patent which suggests it might have uses in treating gout [51]Although that data is limited, it might explain why the non-metabolite XN is listed in clinical trials for treating Crohn's disease, the only active clinical trial [52]. 6-Prenylnaringenin-OH (6-

PN-OH) has not been previously described or observed in-vivo. Additionally, XN-OH showed a different reactivity than the rest of the prenylated flavonoids, which might be explained by the chalcone forms' flexibility. No bioactivity studies on 6-PN-OH are known, but some analogues might reveal some information on the bioactivities of this suspected metabolite. For example, the analogue Artocarmin D (having an additional alkene group in the C ring and an extra hydroxyl on the phenol B ring) is under investigation into anti-malarial and anti-tobacco viral activities [53]. Thus, synthetic production of the tentatively identified metabolites complements in-vitro bioactivity investigations and might unequivocally identify XN metabolism pathways.

1.2.2 Phase II

Phase II metabolism involves the addition of a functional group that modifies the host compound to become highly soluble compared to the pre-metabolite. The increased solubility of the compound allows the xenobiotic to be transported into the blood, transferred to the kidneys (where additional conjugation may occur), and excreted in the urine (renal excretion), thus eliminating any further interaction with biological processors and quenching the xenobiotic. The other route of excretion is the biliary route, in which compounds are excreted from the gallbladder into the small intestine after hepatic metabolism and are excreted in the faeces. Compounds larger than 300 daltons are usually excreted in the bile, while smaller compounds are excreted by the kidneys. Phase II metabolism primarily involves the transfer of either sulphate, glutathione, acetate, methyl and glucuronic acid functional groups to the xenobiotic. The main site within the cell where phase II metabolism takes place is in the cytosolic space. Therefore, for xenobiotic metabolism to occur, the compound must enter the cell. Crucially, the prenyl group on prenyl flavonoids is thought to aid cellular uptake [54]. Unlike humans, cats use taurine conjugation as a major pathway for the excretion of bile acids, providing an example of why animals are not always a suitable model for assessing human metabolism [55]. It is therefore necessary to carry out human trials when assessing the potential effects of a pharmaceutical or nutraceutical product or when understanding the effects of a bioactive compound in food on humans.

With regard to the phase II metabolism of the prenylated flavonoids found in hops, a number of compounds have been identified either via in-vitro, animal and human intervention studies. Originally, XN isolated from hops was incubated with human liver microsomes, which showed that the main metabolic pathway was via glucuronidation (all metabolites were only tentatively identified due to a lack of reference standards). The enzyme UDP-glucuronosyltransferases (UGT) facilitated this bioreaction by transferring glucuronic acid from uridine to 5'-diphospho-glucuronic acid, a very important xenobiotic detoxification step in human metabolism. [56]. The UGTs are only able to conjugate glucuronides on an oxygen, nitrogen, carboxy and sulfur groups, although XN only hydroxyl groups are possible as the compound does not contain other functional groups supporting glucuronidation sites. The most important UGT in humans regarding the glucuronidation of XN are UGT 1A8, 1A9, 1A10, 1A1,1A7, and 2B7 [57]. Another type of phase II metabolism

is the conjugation of glutathione to various xenobiotic substrates via glutathione-S-transferase (GST) contrary to the glucuronidation, glutathione is able conjugate to different electrophilic centres e.g. the Michael system in XN. Interestingly, the administration of XN has demonstrated that the concentration of α-GST increased and might contribute to the broader bioactivities of XN. Glutathione adducts are usually detected as n-acetyl-cysteine conjugates which are also termed mercapturic acid conjugates [58]. However to date no known conjugates of GSH (or mercapturic acids) with XN are reported.

Sulfate conjugation is a metabolic pathway conjugating a sulfo group towards an alcohol or amine group. The conjugation of sulfo towards xenobiotics is facilitated via sulfotransferases (SULTs) and most commonly from 3'-Phosphoadenosine-5'-phosphosulfate as the sulfate donor. Regarding XN and SULTs enzymes, 1A1, 1A2, and 1E1 are the most active isoforms when evaluated using recombinant enzymes and supplying XN [57]. Sulfation is also microbially facilitated by the fungi *Mucor hiemalis* and *Absidia coerule* and helped the identification of the human metabolism pathway by engendering reference compounds [59]. Further conjugation with acetate groups is another detoxification step in humans and is carried out with acetyl-transferases enzymes [60]. To complicate the matter of metabolism any combinations of phase I metabolite can occur and, therefore many combinations of the phase II metabolites of XN are possible. Consequently, to predict which metabolites are formed only assumptions are made as the complexity of metabolism is rather "non specific" (Figure 3 is a general overview of XN conjugates in humans). Previous to the report here only one known synthetic pathway for a sulfated prenylated flavonoid metabolite from hops was known. Although, characterisation was only performed via mass spectrometry and the position of the sulfate was thus unknown [23] [61].

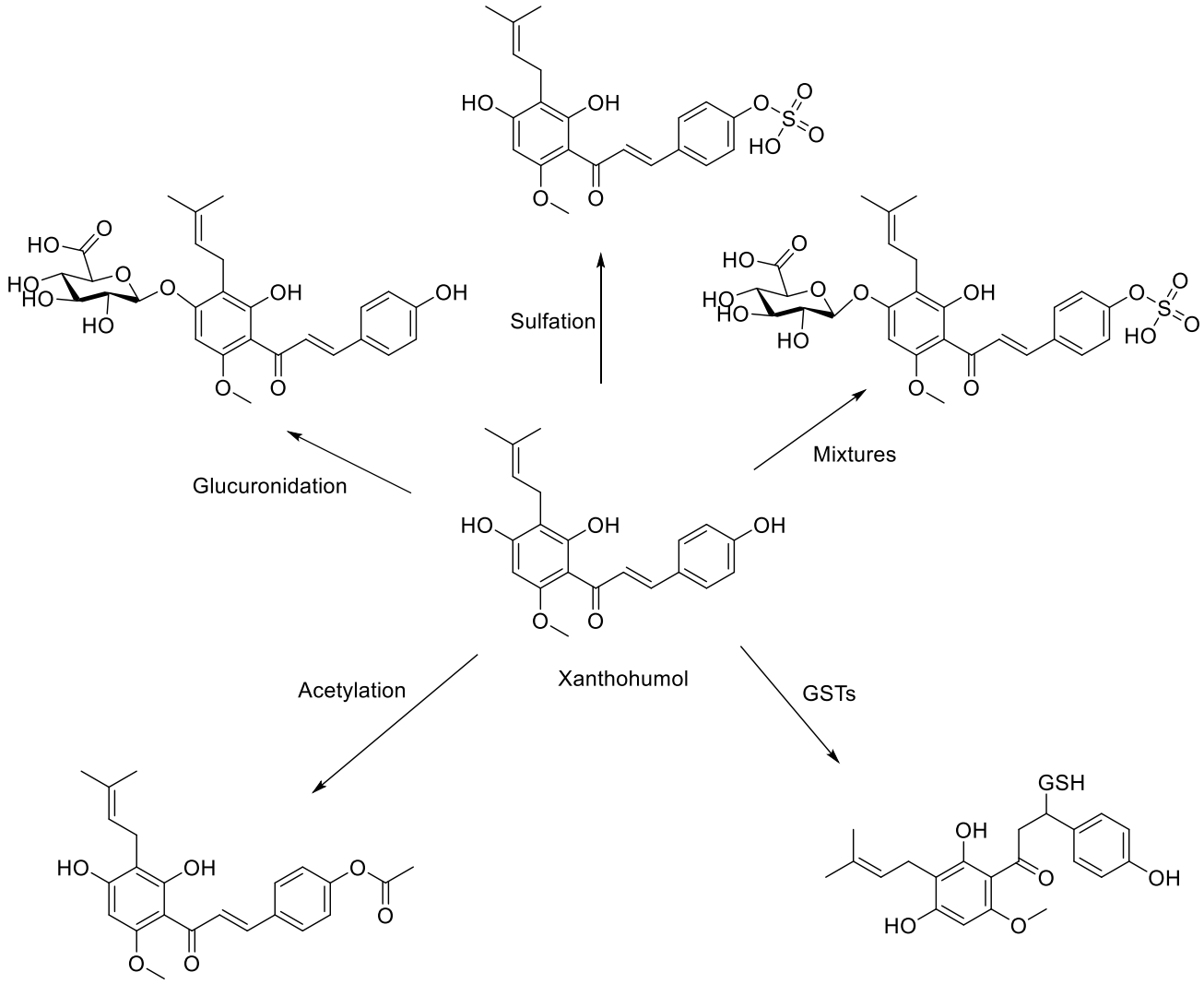

Figure 3: Possible examples of phase II metabolites of hop prenylated flavonoids [62]. Note the glutathione can also have n-acetylcysteine adducts.

In terms of bioactivities only the glycosylated analogues of XN have been investigated previously, but none of glucuronide conjugates [63]. The latter conjugates are interesting as analogous investigations carried out on naringenin chalcone glucuronide showed histamine release inhibition bioactivities, which might extrapolate to prenylated flavonoids [64]. Tronina 2013 et al. revealed that xanthohumol 4′-O-β-D-glucopyranoside is a better antioxidant and additionally, xanthohumol 7-O-β-d-(4‴-O-methyl) glucopyranoside are better at slowing cancer cell growth than the aglycone. The same was confirmed for 6- and 8-PN glucuronic acid by Fang et al. 2019. who used biosynthetic methods for production [65]. Due to the rarity of the glucuronides only analogues of XN metabolites have been investigated in bioactivity studies. For instance, the compound icaritin-7-O-glucuronide together with some glycosides, such as Icarisid J and Icarisid E shows inhibitory effects to xanthin oxidase [66] [67] [68]. Further applications for these metabolites in bioactivity and quantification experiments such as cell culture especially on cancer cell lines are required as virtually no free compounds are found in-vivo [69]. Regarding previous studies on sulfates and bioactivities only analogues can be

discussed. One of these studies suggested sulfated prenylated flavonoids have little to no anti-fungal, antibacterial, anti-fungal and protozoal effects [70].

1.2.3 Phase III "metabolism"

The last type of metabolism is not actually "metabolism" as no real reaction or change takes place to the xenobiotic, but is the active removal (or transport) of a given substance out of the cell and into the extracellular matrix known as phase III transport ("metabolism"). Carried out by two different transporter family clusters, the ATP binding cassette (ABC) and the solute carrier (SLC) facilitate transport of xenobiotics out of the cell. The ABC comprises of around 20 carries over seven families of transporters and the SLC is around 52 families of transporters. The transporters and carriers responsible for phase III transport are distributed in various tissues in the human body and not ubiquitously found, i.e. tissue specificity helps control and regulate the accumulation of xenobiotics and many of these phase III processors are very concentrated in the liver. Therefore, hepatic clearance is vital in observing the oral bioavailability of a certain compound due to the liver having concentrated metabolic enzymes and especially the transporters [71]. The phase III transport can have a basal level or an upregulated response from an elicitor, i.e. xenobiotic and is thus a critical step in the overall metabolism of prenylated flavonoids [72]. Without excretion of xenobiotics compounds would bio accumulate and cause harm to a host organism. However, the excretion step is critical to the efficacy of a drug as if a compound is excreted rapidly a bioactive response would likely not happen making the medicine or bioactive compound essentially ineffective. Hence, these processes are highly investigated within food chemistry and the pharmaceutical industry. One other transport mechanism is phase 0 metabolism; the active uptake of a given substance into a cell and will not be discussed.

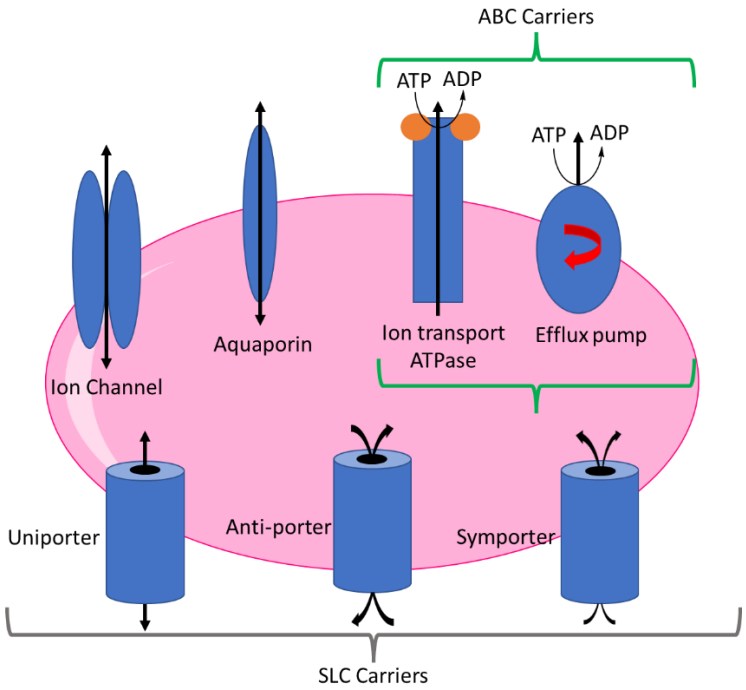

Figure 4: Classification of transporters according to Döring, B. and Petzinger, E. 2014 [72].

Regarding the transporters capable of assisting migration of molecules through the lipid bilayer either in the mitochondria or on the lipid bilayer surrounding the cell there are a multitude of different classes of proteins assisting in the process. Figure 4 has a simplified diagram representing the classifications of type of transport for each protein class and within many families each with specific functions that transport compounds around the cell. Ion channels are selective "holes" in the cell membrane and are controlled via concentration gradients and specific peptides in the pore are able to control ions travelling through either by charge interactions or size. Another specific ion channel are aquaporins, which control the water through osmosis, an important function for action potentials in neurons. Both of these do not assist in xenobiotic transport. The ABC carriers consist of two classes, the ATPases facilitate the transfer of ions utilising the energy from ATP, a classic example is the proton pump, which is involved in transporting protons into lysosomes changing the pH where proteins are recycled. Efflux pumps facilitate the removal of non-charged compounds and are a major pathway for the efflux of a range of xenobiotics. Similar to efflux proteins in humans some mutations in bacterial efflux pumps are responsible for some antibiotic resistance bacteria, for example methicillin resistant *Staphylococcus aureus* (MRSA) developed a efflux pump specific for fluoroquinolone [73]. XN among many prenylated flavonoids are modulators of phase III transport process making the pharmacokinetic investigations of this step essential when studying the bioavailability of XN. An important protein that is involved is Multi-drug resistance protein or p-glycoprotein 1 [37]. Prenylated flavonoids inhibit the efflux and, therefore, phase III metabolism is critical in understanding the pharmacokinetics of the family of these compounds [74] [75].

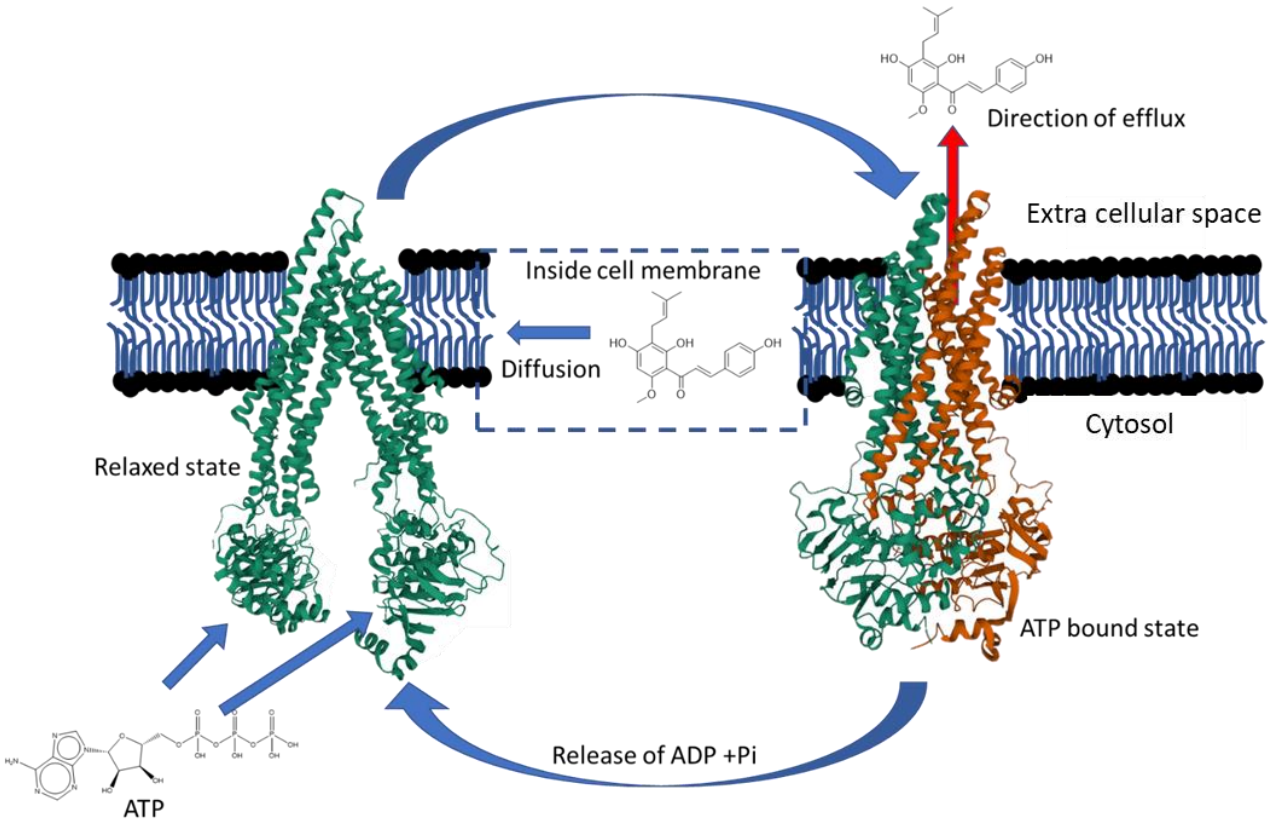

Figure 5: The hypothetical efflux of XN via MDRP1 and transport across the cell membrane with two structures open (3G5U) and closed (6RAJ) [76, 77].

Regarding the effects of XN on P-glycoprotein there are conflicting reports as Nabekura et, al. 2015 state that XN inhibits p-glycoprotein as where Gosh 2021 stated that XN does not inhibit p-glycoprotein [78, 79]. Although in comparing the two studies, Gosh 2021 used a lower concentration of XN and it was in a Poly(lactic-co-glycolic acid) nanoparticle formulation that might prevent the absorption of XN into the lipid bilayer passively. Therefore, XN might bypass the P-glycoprotein and reach the cytosolic space before being inhibition occurs (Figure 5). Another analogue of XN is named Icaritin and is rapidly excreted via P-glycoprotein and this process is inhibited by verapamil effectively increasing the prenylated flavonoids bioactivity [54]. Furthermore, the addition of a sugar moiety reduces the effectiveness of Icaritin [66]. To conclude, each step of metabolism is critical in understanding whether a compound is bioactive and hence phase I, phase II and phase III metabolism facilitate in the overall effectiveness of a drug, nutraceutical and how food changes human's overall health.

1.3 Plant metabolism

Plant metabolism is more complex than human metabolism constructing a multitude of compounds which are completely different to which is found in mammalian metabolism. Different roles attribute to how plants produce diverse compounds and one feature important in plants is the utilisation of many different organelles via compartmentalised and are plant specific. A multitude of reasons for the complexity of why plants produce so many families of compounds exist and are believed to be from an array of functions, some examples are defence, attracting insects and signalling to other plants. Even more intriguing, is plants usually lack an immune system, however, they have certain Salicylic-acid-mediated systemic acquired immunity providing the defence of plants [80]. Here only specialised (also known as secondary) metabolism will be briefly introduced as many books are written on the subject. Plant metabolism is more complex than human metabolism as more diverse small molecules are produced, thus making it a great challenge for biotechnology to recreate these processes as ten to 100s of enzymes are in use for production of natural products.

1.3.1 Specialised plant metabolites

Specialised plant metabolites are diverse and plants invest heavily in their biosynthesis even though they are not essential for a plant to survive. There are over 200,000 known specialised metabolites in the plant kingdom and they are alleged to have no specific function for the plant in terms of growth or survival and trend towards either improving the quality of life for the plant or preventing certain pathogens from infestation (known as phytoalexins) [81]. Other uses include attracting insects towards the flower so the plant can propagate via the transfer of genetic material without investing heavily in other ways of proliferation (e.g. some plants use wind requiring the construction of various structures) [82]. Many of the specialised metabolites are ubiquitous to plants, such as the flavonoids and terpenoids, but they can also be plant specific, such as prenylated flavonoids and specific alkaloids with some being extremely toxic for humans.

The biosynthesis of prenylated flavonoids is a very complex part of the metabolic and catabolic pathways represented in Figure 6 [83] [84]. Starting with L-phenylalanine, the activity of phenylalanine ammonia lyase (PAL), Cinnamate 4-hydroxylase (CA4H) and 4-Coumarate-CoA ligase (4CL) results in coumaroyl-CoA in a three step process. The coumaroyl CoA is then reacted with three malonyls via the enzyme chalcone synthase where a Claisen rearrangement along with tautomerisation results in naringenin chalone which is an important flavonoid in many other plants. Then the enzyme prenyltransferase facilitates the transfers a prenyl group to the flavonoid. The prenyltransferase identified in 2012 is not only specific to the biosynthesis of XN, but in addition can produce many other prenyl groups for bitter acids from hops and is capable of the prenylation of naringenin chalcone resulting in the very unstable compound known as desmethylxanthohumol (DMX) [85]. The DMX is finally methylated with the aid of 5-adenosyl methionine forming XN. Interestingly in hops, the enzymatic prenylated flavonoids are only XN and DMX, but it is believed the other prenylated

flavonoids found are products of degradation e.g. 6-PN and 8-prenylnaringenin (8-PN). The breakdown and reactiveness of XN results in a multitude of derivatives discussed in the prenylated flavonoids section (1.4.2).

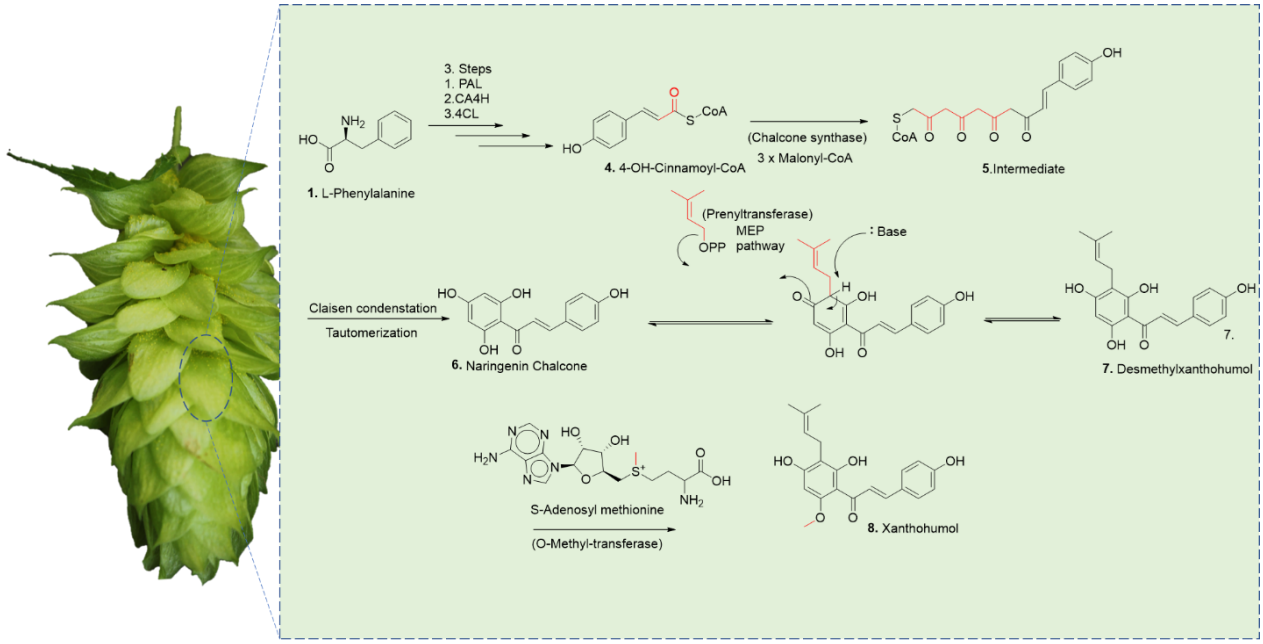

Figure 6: A simplified biosynthetic pathway of xanthohumol where critical transfers are highlighted in red. Starting with phenylalanine, 4-hydroxy cinnamoyl is produced in a 4 step reaction involving the enzymes:1, phenylalanine ammonia lyase 2. Cinnamate 4-hydroxylase and 3. 4-coumarate CoA ligase. The end product in these initial steps is 4. 4-OH cinnamoyl-CoA where an additional 3 Malonyl-CoA are transferred to 4. This undergoes a Claisen condensation and tautomerisation producing naringenin chalcone (6.). The last two steps are prenylated via a prenyltransferase and methylation via O-methyltransferase producing XN.

As the biosynthetic pathway is known sets aside an opportunity to produce genetically modified organisms (GMO) for XN production, although this is yet to be realised [86]. It is known how to produce 8-PN using GMO yeast , however with very low yields [83]. Although not applicable to hops as the prenylated flavonoid content is not so high in the roots, plant milking is another option in isolating vast quantities of rare prenylated flavonoids that might act similarly as XN regarding bioactivities [87].

1.4 Flavonoids

1.4.1 General

Plants invest approximately 20% of their energy into producing specialised metabolites, with a majority of the products being polyphenols in particular flavonoids. Flavonoids are characterised by having a pyrone gamma backbone along with three rings, and can occur in different isomers such as a chalcone having an open C ring. Flavonoids are a family of compounds found in plants consisting of a C6-C3-C6 backbone containing two phenyl rings (ring A and B) linked by three carbons (ring C). Interestingly, vitamin P was a term used between the 1930s and 1950s to explain flavonoids, although it was realised afterwards that these compounds were in fact not vitamins as they are not essential for human well being [88]. Free flavonoids are rarely found in plants and most are glycoside conjugates increasing their water solubility. Curiously, for the non-polar prenylated flavonoids in hops glycoside conjugates are unknown. Some flavonoids are able to polymerise and this forms the polyflavonoids such as condensed tannins that can contain sugar residues [82]. Many tannins are known as proanthocyanins and similarly with flavonoids the condensed tannins are sold as dietary supplements, even though it is still unknown if they contribute a health benefit [89]. The anthocyanins are responsible for the pigmentations in almost every flower and are usually blue or violet in colour [82]. The huge diversity of flavonoids has purposes for plants and the most important is pigmentation, but other functions such as attracting insects via scents, and protecting the plants from danger. The threats can range from microbial infections and making the plant taste unpleasant for mammals. The flavonoids respond and accumulate in plants once under microbial attack and as the toxicity in humans is low they might help as a byproduct [90].

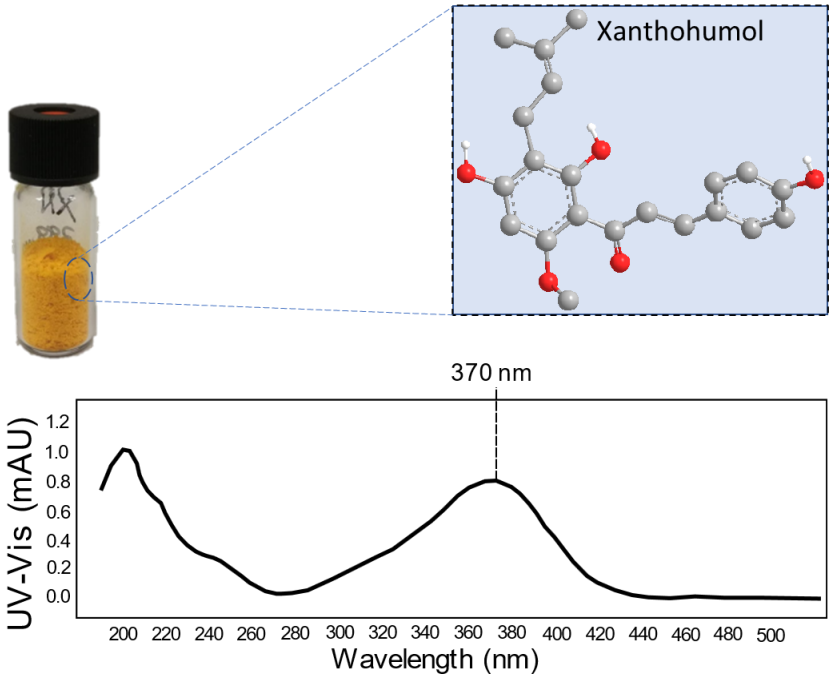

Figure 7: The colour of xanthohumol is a vibrant yellow with an example of a pure vial of XN and its structure are shown. It also absorbs UV radiation at a peak of 370 nm as depicted in the UV-Vis spectra [91].

Flavus meaning yellow in Greek is due to the vibrant colour most flavonoids possess, see Figure 7 for an example of XN colour (in the vial > 99% pure). The average daily intake of flavonoids in Europe is around 430 mg/day, where tea is the main source in a European diet, interestingly Mediterranean countries have the lowest intake. The most consumed variation of a flavonoid is a flavan-3-ol [92] . When regarding the intake of flavonoids in Europe from alcoholic beverages Denmark consumes the most with on average 15 mg followed by France, Italy, Belgium and Spain [93]. The flavonoids in general have a bioavailability that is poor and to date no flavonoid is approved by the Food and Drug Administration (FDA) nor the European Food Safety Authority (EFSA) i.e. no flavonoid prescription in the EU and the USA is permitted [21].

1.4.2 Prenylated flavonoids

Similar to flavonoids, prenylated flavonoids use the same back bones as flavonoids but contain a special functional non-polar group known as a "prenyl group", although the prenyl group can be different than a prenyl e.g. geranyl which is two prenyl groups joined together in a "chain". The diversity of the modifications is vast and the backbone is one part that is modified to varying degree depicted in Figure 8. To name a few prenylated flavonoid backbones they include dihydroflavones, flavones, chalcones, flavane isoflavanes and chalcones amongst other structures. To date the known diversity is extremely vast (over 1000) and although the "prenyl" group is not always conserved the prenylation is said to be from the original biosynthetic pathway. Further modification include the cyclisation of the prenyl group creating a pyrano group which is an example of the degradation process. In general, prenylated flavonoids are found in a low abundance in nature which limits them for dietary supplements uses whereas, the prenylated flavonoids in hops (*Humulus lupulus L,* family *Cannabacaeae*.) are rather abundant and XN is the principal prenylated chalcone found. Regarding dietary prenylated flavonoids the main source is from beer and perhaps hop tea [94]. Most of prenylated flavonoids are found in the following families, *Cannabaceae*, *Guttiferae*, *Leguminosae*, *Moraceae, Rutaceae* and *Umbelliferae*. The research here has focused on the hop (*Humulus)*. Prenylated flavonoids have similar properties (such as antioxidant activities) as their flavonoid counterparts, but with an increased bioavailability [74]. The thought is prenylated flavonoids contain a greater potential for a pharmaceutical use compared with normal flavonoids due to their increased hydrophobicity aiding the lipiophillic nature and allowing further

interactions with cell membranes. However, non-prenylated flavonoids have a higher dietary intake due to being higher concentrated in foods than prenylated flavonoids [82].

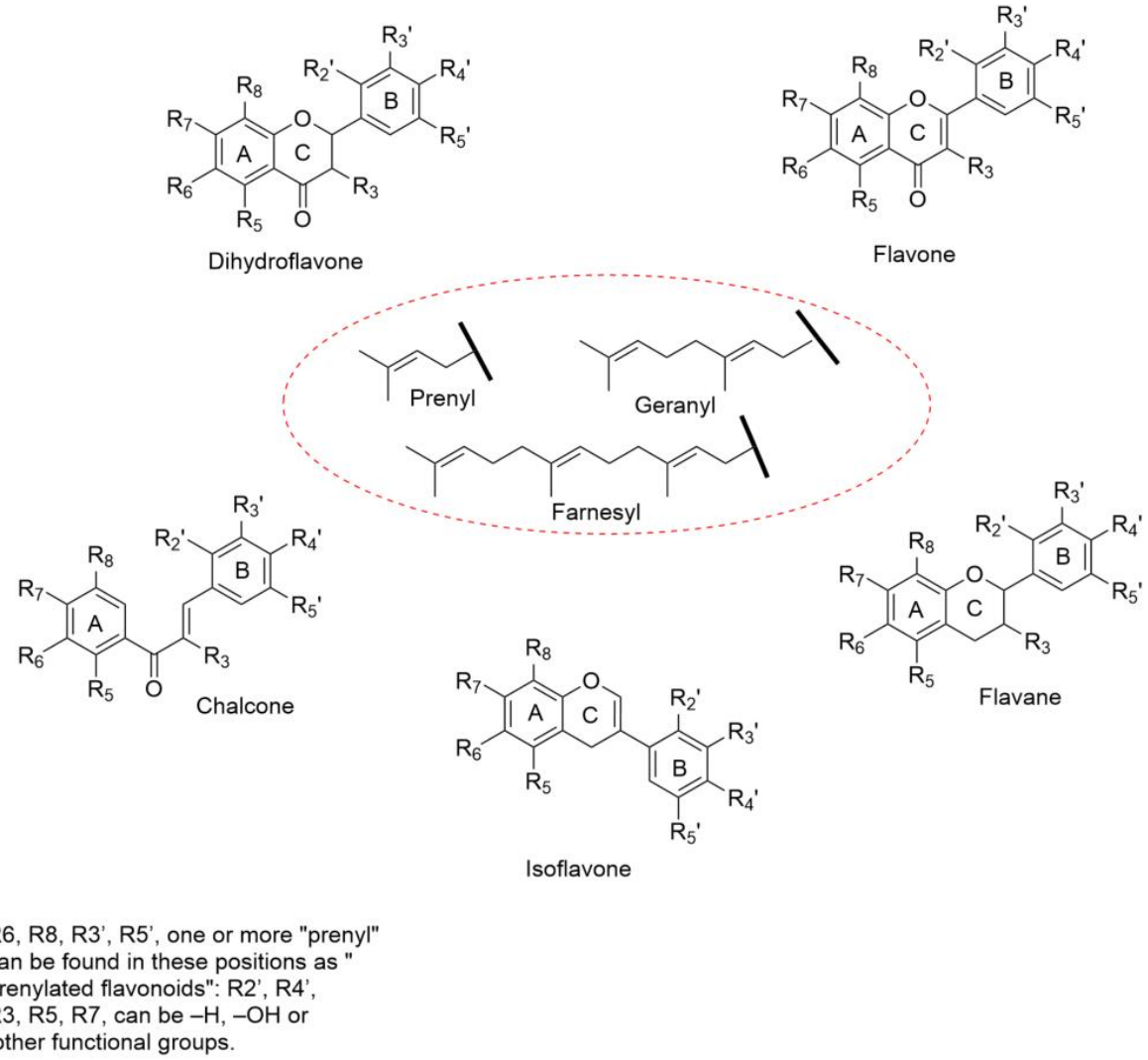

Figure 8: The backbone structures of prenylated flavonoids and their diversity.

The diversity of prenylated flavonoids is further enhanced due to the prenyl groups coming in many other alternatives which influence the bioactivities immensely. Figure 9 illustrates many variations of the prenyl group with the majority containing hydroxylated variations [95]. O-Prenylation is another type of prenylation and is much rarer than the C-prenylated flavonoids [95]. The variations of these prenyl groups modifies the bioactivity of the prenylated flavonoid dramatically. The modifications of the prenyl group are under further research as they are known to be modified either via chemical (e.g. stomach acid), bacterial (metabolism) or liver (phase I/II) metabolism. Hence, the possibilities for a lead compound are vast and simply testing the un-modified compounds in plant extracts is not enough when exploring their bioactivity [96]. An example for an altered bioactivity is an oxidised XN, named xanthohumol-C (XN-C) which changes the bioactivity from a potent tumour growth suppressor towards neuronal promoting activities. Regarding the

structural activity relationships (SAR) of prenylated flavonoids, further investigations would benefit understand XN and its influence on health. Reasons for the limited number of SAR investigations on XN are that it is challenging to obtain high yields for chemical synthesis. In addition chemical modifications of prenylated are difficult and SAR studies are time consuming and expensive [96] [97].

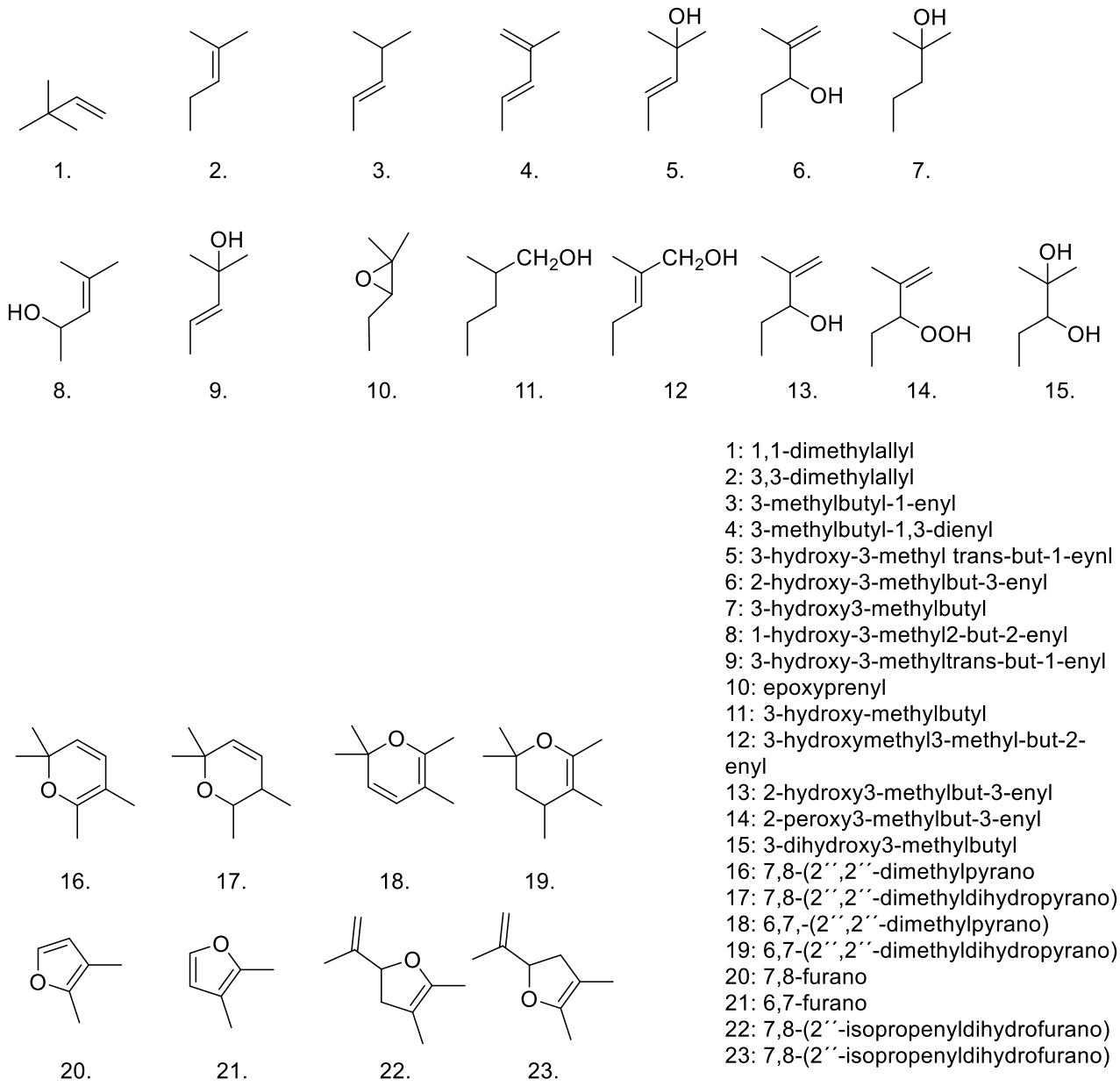

Figure 9: The diversity for the prenyl group found in many prenylated flavonoids

1.5 Bioactivities of hop prenylated flavonoids

The bioactivities of prenylated flavonoids are very broad. An early observation in the 1950s regarding prenylated flavonoids in hops (see Figure 10 for classifications [98]) was that female harvesters of hops menstrual cycle were influenced in a negative manner [99]. It was not found that the responsible compound is most likely 8-PN until many years later in 1999 [100] [98]. It is now fact that 8-PN is the most potent known phytoestrogen compound, which has led to many debates on whether beer itself is estrogenic, but regarding this matter the concentration is far too low and one would need to consume a deadly dose (from the ethanol alone) for ill effects to become apparent before estrogenic effects are in effect (the dose makes the poison) [101]. Although, many observations state that XN is demethylated into DMX in the gut and then can cyclise into 6-PN and 8-PN, thus having potential for estrogenic activities. None the less, the concentrations formed from the conversion in-vivo are still far too low for ill effects from beer consumption [47]. Regarding XN concentrates this has been under looked and might possess a risk to consumers from daily nutraceutical consumption. A more recent innovation has been the hydrogenation of the Michael system in XN and thus keeping the core structure but preventing the ability of XN cyclisation into IXN. The synthetic non-natural compound dihydroxanthohumol (DXN) maintains the bioactivities of XN and is a pure pharmaceutical approach due to DXN being non-natural [102].

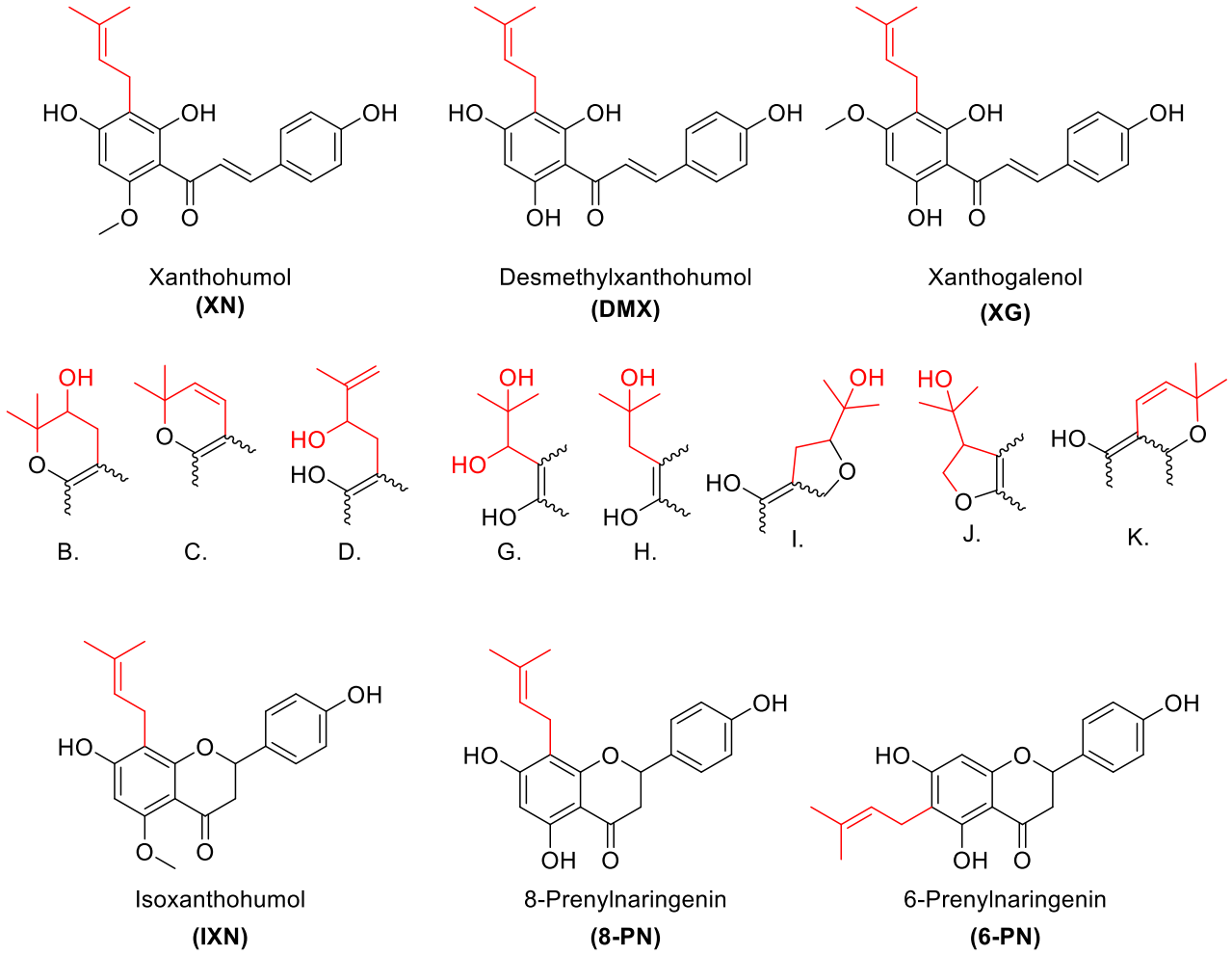

Figure 10: The naming classification of the prenylated flavonoids found in hops. The naming is consisting of the main backbone (Black) followed by the letter corresponding to the prenyl group modification (red). For example 8-Prenylnarningenin-C is the 8-prenylnaringenin backbone followed by the letter C functional group. So far combinations of 30 are known but it is likely that more combinations of the prenylated flavonoids from hops are found. Note functional groups E and F are diprenylated compounds and are not shown.

1.5.1 Antioxidant and anti-microbial potential of xanthohumol

Antioxidants are compounds which have the ability to help prevent oxidation and absorb radicals or highly reactive chemical species (ROS) that are capable of damaging cells leading to a less healthy biological system [103]. In terms of food research antioxidants retard rancid forming reactions and extend shelf-life of a range of products [104]. The antioxidant capabilities of XN and related prenylated flavonoids are very strong and therefore extensive research has been carried out to investigate whether a dietary source might prevent a range of diseases protecting humans in a similar mechanism as Vitamin-C and Vitamin-E [105]. It is thought that the strongest effects are from radical scavenging and they correlate with protection of lipid peroxidation [103]. Additionally, it is believed that scavenging of superoxide anions occurs, but other pathways are possible activities e.g. nitric oxide radical scavenging capabilities [106]. A caveat of antioxidants is in certain conditions they might cause harm as themselves can be radicalised and interact with vital cellular processors [20].

Interestingly investigations that probed the type of antioxidant activities of XN compared three different assays. The free radical neutralising potential is characterised often via ABTS·+ (Trolox equivalent antioxidant capacity), the 2,2-diphenyl-1-picrylhydrazyl (DPPH) radical assays and the ferric reducing antioxidant power assay (FRAP) [103]. All are standard assays measuring the antioxidant potential of antioxidants, but do not necessarily function on all compounds equally. The DPPH assay functions via a cation but XN did not react well [105]. Regarding the ABTS·+ and FRAP assay both performed with higher values than 0.3 versus 1 with the compound Trolox (a vitamin E analogue). Revealing that the antioxidant potential of XN is not clear as it does not function in all assays, but it seems to function for specific assays. Though a biotechnological example showed replacing nitrates (antioxidants preventing meat spoilage) with XN improved the lifespan of sausages after 30 days of storage [104]. Furthermore, research has carried out other modifications of XN adding acyl groups of various lengths resulting in the retention of XN antioxidant ability suggesting the chalcone backbone is most likely responsible for the antioxidant potential [105] . Comparing in-vivo studies on the antioxidant capabilities treating *Drosophila melanogaster* with XN improved their life quality greatly. The lifespan, resistance to oxidative stresses, activities of antioxidant enzymes, recovery from cold and heat shock and resistance to starvation stressors were all improved [107]. Other effects related to antioxidant potential from XN are protecting livers of mice when exposed to carbon tetrachloride and lipopolysaccharide induced depression most likely via a reduction in neuroinflammation [108] [109].

The antimicrobial of XN activities are extremely broad. There is evidence that low concentrations (15 μg/mL) of XN can prevent biofilm formation and at higher concentrations (60 μg/mL) even penetrate biofilms [110]. In addition, XN reduces the adhesion of *Staphylococci* bacteria to surfaces. These effects on bacteria leave the application for XN to help prevent biofilms accumulating on medical devices. The most active compound when comparing flavonoid analogues tested towards gram-positive (e.g. *Staphylococcus aureus* and *Rhodotorula rubra*) bacteria was XN [97]. Another study compared XN (IC50 between 9 - 80 μg/mL) against three anaerobic pathogenic bacteria, *Bacteroides fragilis*, *Clostridium perfringens* and *Clostridium*

difficile, which all cause common bacteria infections after antibiotic treatment [111]. Furthermore, the effects of XN on Methicillin-resistant Staphylococcus aureus (MRSA) are IC50s of 2.4 μg/mL [112]. As XN performs well on preventing biofilms and having bactericidal activities might lead to supplementing XN after antibiotic treatment to reduce the negative effects these treatments often cause. Other antibacterial effects of XN were demonstrated on *Listeria monocytogenes* and *Staphylococcus aureus* having potent bactericidal activities at 6.3 μg/mL [113]. A more recent evaluation on low doses (comparable to what is found in beer) demonstrated XN consumption in humans stimulated Peripheral blood mononuclear cells (PMCs) activity against fatty acids found in bacteria, and thus, suggesting a boost in immunity [114]. The finding that XN supplemented at concentrations found in beer alters PMCs is the first anecdotal evidence that the concentrations of XN in beer might have an effect in-vivo in humans [115].

To supplement the antibacterial activities of XN, many other similar effects are known. For example many antiviral applications are known such as inhibiting human immunodeficiency and bovine viral diarrhoea virus [116] [117]. Other organisms that are effected by reduction in growth and survival are fungi although only demonstrated in a mixture of hop compounds [118]. Finally, XN has insecticidal properties and due to all the anti pathogenic activities is perhaps this is why the hops invest energy to produce these compounds [119] [120]. The effects of XN on coronaviruses will be discussed further in section 1.5.5.

1.5.2 Xanthohumol and Metabolic syndrome

The medical condition metabolic syndrome is characterised by a variety of different factors that include obesity, low "High density lipoprotein" (HDL) levels, elevated low density lipoprotein (LDL), increased blood pressure, high fasting blood sugar levels and excess triglyceride levels. The syndrome does not need all of the listed concerns to be elevated and only requires three in any combination for a diagnosis [121]. The risks of developing serious diseases when having metabolic syndrome is very high and they include cardiovascular disease and type II diabetes [61]. The increasing amount of humans (approximately 25-34% of adults in the USA) have varying degrees of metabolic syndrome, making the disease a major problem for humanity [33]. Therefore, medicines are being developed to treat the underlying causes for example, Orlistat treats obesity by inhibiting certain lipases blocking the breakdown of fats into useable energy. More radical approaches involve interventions such as surgery. One strong candidate for the treatment of metabolic syndrome is XN as it has the ability to disrupt various enzymatic and biosynthetic pathways that contribute to this disease.

In a mice model where the animals were fed a very high fat food and a dose of XN equating upwards to 60 mg/kg blood plasma levels of LDL cholesterol IL-6, insulin and leptin levels were dramatically reduced [121] . In addition, the triglycerides and the body weight of the XN treated mice weight were lowered indicating that XN had an effect on many markers for metabolic syndrome. In a different mice

study aimed at feeding mice at a much lower dose of 2.5 mg/kg/bw of XN (a micellarised formulation), in a diseased model represented by obesity and insulin resistance, resulted in a significant reduction in weight and improved glucose tolerance compared to the wildtype [122]. Investigations on humans and preventing metabolic syndrome with XN supplementation resulted in no change in the lipid and glucose metabolism parameters following a 12 mg daily dose. Although, it was revealed that the DNA was protected [19]. Therefore, further intervention trials are required on humans perhaps with higher doses of XN or via a different formulation of administration.

The biochemical processors behind the effects seen in animal interventions biochemical assays are used to explain the mechanisms of action. One such is that XN inhibits triacylglycerol synthesis and apolipoprotein B (apoB) secretion when investigated in-vitro on HepG2 cells. The Diacylglycerol acyltransferase (DGAT) enzyme is a key component in triglyceride synthesis and hence inhibiting the formation of triglycerides is believed that it would assist in obesity reduction. Enhanced by evidence that knockout mice lacking the DGAT enzyme are resistant to obesity and live rather healthy lives makes this a candidate target for many drugs that are aimed at obesity [123]. The other protein function that XN inhibits is the apoB protein, essential in the formation of LDL, and thus, in transporting fats. If apoB is elevated it can lead to heart disease. Accordingly, reduction of this protein is believed to regulate metabolic syndrome, although the mechanisms of its function are only partially understood. To further support XN and its effects on metabolic syndrome it also inhibits cholesteryl ester transfer protein activity as an essential function that transfers cholesterol from HDL, ("good cholesterol") to LDL ("bad cholesterol") [124].

One major drug named Anacetrapib is successful in reducing heart attacks significantly, although it has since been abandoned by Merck due to the drug accumulating in the fat tissue of the trial participants. Hence no cholesterol ester transfer protein drug targets are currently on the market. GLUT-1, also erythrocyte/brain hexose facilitator (gene: SLC2A1), is a transport protein in the cell membrane of pancreatic β-cells, cells of the mammalian blood-brain barrier and many other tissue types, which facilitates the transport of glucose, as well as other hexoses and pentoses and vitamin C across the cell membrane [61]. Furthermore, XN inhibits Farnesoid X receptor (FXR), a member of the nuclear receptor family, a common receptor found in the intestine and liver cells, supports systemic metabolic homeostasis through regulating bile acid, glucose, lipid metabolism, and energy homeostasis [71]. The effects of XN on metabolic syndrome are broad and it might one day aid in the treatment of metabolic syndrome. Although improvements on the formulation for XN treatment has a caveat that it can form in the gut the highly estrogenic 8-PN. However, the removal of the Michael system (DXN) does not change the activity in treating rats with metabolic syndrome [102]. Without the Michael system the formation of 8-PN is not possible [125]. To conclude XN might reveal new drug targets and perhaps a formulation might allow treatment of metabolic syndrome in the future [52] [126].

1.5.3 Xanthohumol effects on cancer, gene and cell regulation

Cancer is another disease which contributes to many deaths in the world and hence countless compounds are envisaged to combat this terrible disease [127] [20]. The observations that cancer cell growth was reduced by supplementation of XN has been observed in various cancer cells represented in Table 1. although the list is not exhaustive and further anticancer activities are summarised in the review by Girisa. S. et al 2021 [127] . The effectiveness of XN against cancer is not as strong as usual chemotherapeutics (Pemetrexed, a chemotherapeutic agent inhibits thymidylate synthase at nM levels [128]) but due to the inhibition of XN on many xenobiotic efflux enzymes using it in conjugation with more potent chemotherapeutics might make a more meaningful drug i.e. a concoction [129]. The clinical dose of XN might be too high for its effectiveness with the current doses given and it is undesired to give very large doses or too often if a substance is rapidly excreted.

Table 1: The cell lines effected from XN exposure in-vitro for specific cancers.

Tissue	$IC_{50}/EC_{50}/LD_{50}$	Cell line
Breast cancer	1.22 - 23.0 μM	MCF-7
	23.0 μM	T47-D
	7.1 μM	Sk-Br-3
	6.7 μM	MDA-MB-231
Cervical cancer	7.9 μM	HeLa
	20.08 μM	Ca Ski
Colon cancer	3.6 μg/ml	HCT-15
	10 μM	HT-29
Liver cancer	22.8 μM	HepG2

Although no clinical trial has directly measured the anticancer effects of XN as previously stated the DNA damage markers were lowered when feeding healthy humans XN [19]. Therefore, most studies investigate the effects on cancer cell lines which revealed some biochemistry targets, but could not conclude on XN use against cancer [129]. The easiest marker to observe is reduction in tumour growth, such as using a mice model displaying a certain cancer in a tumour form e.g. Cholangiocarcinoma. Supplementing mice that display Cholangiocarcinoma tumours XN reduced tumour growth [130]. Other effects of XN are inhibiting Topoisomerase I activity which would be enhanced with combination of efflux transporter inhibitors hence XN is a primary candidate [131]. Furthermore, XN changed the cell cycle phases of an human alveolar adenocarcinoma cell line (A549) where many of the cells paused in the in sub G1 and S phase a process where DNA is produced and many chemotherapeutics target. Therefore, combination of XN would deem more

potent in cancer cells as they would pause the cell cycle where a more potent DNA killer drug would target [132] [133].

1.5.4 Dermatology and xanthohumol

Many cosmetics aim and are advertised at rejuvenating skin health and preventing acne. Due to XN having a rather broad antimicrobial and antioxidant properties many investigation on improving skin health are described [134] [135]. In addition, XN and its effects on cancer are described and some related to skin disorders e.g. effects on reducing melanoma cells via an array of cell targets and reduced tumour growth [111]. By administrating XN towards skin hypo pigmenting was lessened by reducing the melanogenic pathways in melanoma cells [136] [137]. The mechanism of action is a complex process as Melanogenesis involves over 125 genes, but evidence suggest that XN plays a role in tyrosinase type enzymes, at the transcriptional level [136]. Via interacting with the microphthalmia-associated transcription factor (MITF), a known oncogene, XN might underline melanoma cell proliferation [136]. Therefore, skin cancer may be reduced via removing the pigments in skin cancer (inhibition of Melanin) and acne by killing certain bacteria [137] [138] [139]. These are some reasons that XN is thought to lead into the development of new cosmetics focusing on skin whitening. Other prenylated flavonoids that are similar to XN isolated from *Sophra flavescens* have potential in treating eczema [67]. In combination with inhibiting melanoma along with its antioxidant and antibacterial activities XN shows promising results and might be added to certain skin creams [135]. Hence, XN is stated by some as an anti-aging skin agent from these effects. To conclude, skin health related to XN has the ability to aid in new medical technology. Furthermore, many medicinal products are derived from fish collagen which needs sterilisation usually from UV irradiation. The process of sterilisation destroys or partially destroys the important collagen fibre. It has been shown during sterilisation of the fish collagen by UV light irradiation having XN at 1,15% of collagen can prevent the degradation while retaining the sterilisation factor [134].

1.5.5 Xanthohumol and Covid -19

In early 2020 (late 2019) an outbreak of a severe acute respiratory syndrome (SARs) virus in the city of Wuhan China was revealed, which spread rapidly and ferociously throughout the globe resulting in a global pandemic. The virus is commonly named Covid-19. Fortunately, a few vaccines are now available and are helping curb the impact that this virus is currently having on the globe [140]. Although, the vaccines appear to reduce mortality in populations at risk, small molecule inhibitors that prevent covid-19 are urgently required [141]. Additionally, the virus is rapidly mutating changing the vaccines' efficacy, which specifies that alternative treatments are essential in curbing the virus's impact on humanity. Molnupiravir an anti-viral that inhibits RNA replication is on the market for treating viral infections and is approved in many countries and even more have emergency authorisation [142]. Molnupiravir provides a 30% increase in survival in critically

ill patients regarding covid-19 [143]. Concerningly, Covid-19 is mutating at an unprecedented speed and the mutations are commonly in the S-glycoprotein and RNA Directed RNA Polymerase regions of Covid-19 [141]. The S-glycoprotein in Covid-19 is especially important for recognition from antibodies that are produced from the current vaccines. Therefore, due to these mutations in the S-glycoprotein the covid-19 vaccines are impending less efficient. Another common mutation location on Covid-19 is on the RNA directed RNA Polymerase, which would imply that Molnupiravir would not have the greatest effect in treatment. Therefore, the search for other mechanisms of actions against covid-19 are essential [141]. Furthermore, resistance is already seen in remdesivir treatment an RNA Directed RNA Polymerase target [144]. Hence remdesivir clinical trials were unsuccessful [145].

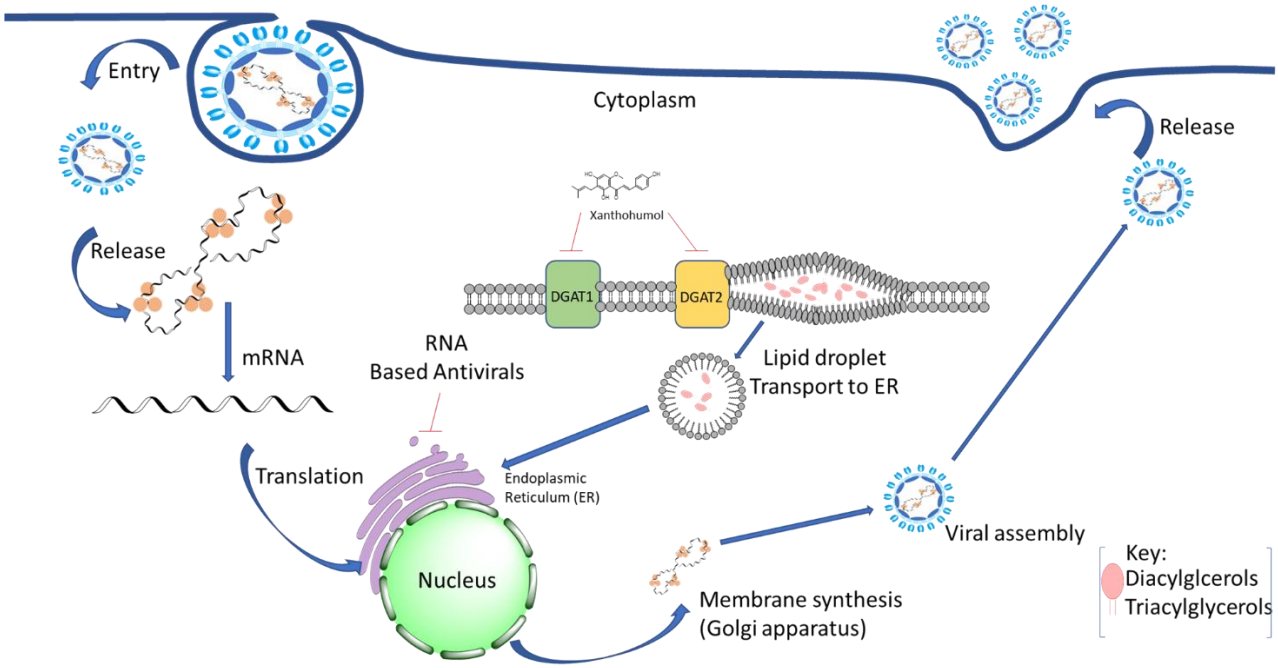

Figure 11: The cycle of Covid-19. Entering the cell using specific receptors that allow entry the genetic material is released where the mRNA is liberated and translates the code of the virus to replicate in the endoplasmic reticulum. Producing the proteins essential for viral progression, most anti-viral drugs target this part (RNA-dependent RNA polymerase) of the virus's life-cycle. The new virus protein replicates transfer to the Golgi apparatus where viral assembly takes place. The requirement of lipid drops is essential at this step as without fatty acids the virus cannot build the membrane coat which allows entry and protects the RNA from damage. XN inhibits the formation of lipid drops therefore, the virus cannot assemble and release thus stopping virus propagation **[146].**

XN is a lead compound in the treatment of covid-19 [147] [148]. The most evidenced based mechanism of action is via inhibition of the diacylglycerol transferase 1 and 2 which is the same mechanism XN has against metabolic syndrome [102]. Covid-19 requires DAG1/2 to replicate as extensive formation of lipid droplets allows viral replication (See figure 11 for a simplified replication cycle for covid-19). i.e. by inhibiting this process the virus cannot replicate or release as there is not enough material for the cell to surround itself in lipid coat. In addition, the viral nucleo capsid protein up-regulates DGAT1/2 expression to facilitate replication making lipid droplets essential for viral replication. The authors Yuan et al. 2021 additionally tested

the efficacy of XN treatment on hamsters infected with covid-19 and demonstrated that the virus was not released in the lung cell and was unlikely to propagate between hosts [146]. To further supplement the effects of XN on lipid drop formation it is a known Pan-Inhibitor of Coronaviruses including Covid-19 (IC50 of 7.51 μM) among many other viruses, targeting the Main Protease [145]. For these reasons Covid-19 treatment from XN is undergoing a human trial as it has a multitude of benefits, however, the clinical trial against covid-19 is currently suspended due to limited funds [149].

1.6 Analytical methods on hop prenylated flavonoids

The small size of all things chemical in nature leads to the scientific challenge to visualise the chemical makeup of biological matrixes. Therefore, technology has developed various methods that allow scientific observations of compounds [150]. Unfortunately, XN and its related compounds are mostly observed indirectly, i.e. by spectroscopic or spectrometric methods. There are assumptions made during the analytical work and the best way forward is reducing steps of error such as derivatisation and complicated work-up steps where losses are not accounted for making analytical work a challenge. Many analytical methods for the quantitation of prenylated flavonoids are known and will briefly be discussed along with other methods which monitor the response from XN or related compounds treatment [151].

1.6.1 Non-targeted analysis of prenylated flavonoids

1.6.1.1 Metabolomics

Metabolomics is usually the analysis of all molecules at a given mass range usually between 100 and 1500 Daltons. Most commonly the tools that are used in metabolomics study the metabolome, which is a complex array of different classes of compounds, that are not only derived from bodily processors (endogenous), but also from influence caused by the environment (exogenous). To date the metabolomic details on XN found in hops is very limited although it has helped identify the mechanisms behind XN and metabolic syndrome reducing plasma markers of ROS and dysfunctional lipid oxidation in the muscle tissue of Zucker rats [152]. A metabolic approach in understanding XN effects on humans is yet to be carried out.

1.6.1.2 Proteomics

Unlike metabolomics the proteomic path is looking at the proteome (the entire protein complement of a cell tissue or organism). Proteomics is more of a indirect observation to investigate how a compound influences a biological system at the protein level [153]. Interestingly, the Michael system on XN is highly reactive towards cysteine residues the addition of which is an irreversible process [108]. Cysteine is a very important amino acid in the structural motifs of proteins and XN supplementation might change the proteome

from the interaction with cysteine [154]. One observation in leukaemia cells is the modification of cysteine residues of IκB kinase enzyme complex (IKK) and the cell immune response nuclear factor NF-kappa-B p65 by XN leads to inhibition of the NF-κB activation pathway [154]. The proteomic approach was applied for this observation via mutation of the cystine residue which caused the effects from XN to be diminished. Furthermore, XN and XN-C bioactivities were demonstrated via a proteomic approach resulting in changes to the endoplasmic reticulum and influencing cell cycle proteins [155]. To conclude, proteomic approaches have demonstrated further modulation of the proteome by XN exposure especially in oxidative stress, proteosome systems and import neuronal network proteins [156].

1.6.1.3 Genomics

Genomics is another feature in the omics world and focuses on changes at the DNA level including post translational modifications of amino acids. To date, genomic influences from XN exposure have not been carried out. There is one study which demonstrated XN causes DNA fragmentation and cell cycle arrest in the S-phase, although the mechanism behind is not fully understood [132]. Another use for genomic research was expressed sequence tagging and allowed the elucidation for the biosynthetic pathway of XN discussed previously [84].

1.6.1.4 Foodomics

As a rather new addition to the "omics" world is the study of all things in food components focusing on functionality, sensation, nutritional value and safety amongst others [157]. In-principal foodomics, uses many "omic" fields of study, but exclusively applies it in a food context ultimately investigating the quality of food. Although beer and tea are beverages they are covered within the field of foodomics even though by definition they are not food. However in a food context the prenylated are sometimes used. This is due to prenylated flavonoids in hops contributing to flavour and the said benefits from consumption [158]. Even more relevant to the foodomics approach is the diversity of the prenylated flavonoids as it is not so simple as only the biosynthesised compounds found in hops are found as over 30 variations of prenylated flavonoids are known [98] [159]. Therefore, the identification of further compounds would contribute to understanding the effects of beer and hop products on human health.

1.6.1.5 Lipidomics

The lipidomic approach yet focuses on the lipid content or influence from a target compound. As the prenylated flavonoids are not a lipid, but XN and related prenylated flavonoids seem to influence the metabolism and synthesis of the lipids many lipidomic studies have evaluated metabolic changes at the lipidome level. The latter were mainly looking at metabolic syndrome and newly discovered effects on Covid-19 [121].

1.6.2 Targeted analysis of the prenylated flavonoids found in hops

1.6.2.1 Seperation of analytes

One important pre-analytical method is the separation of analytes to minimise effects from non desired compounds that might interfere with a given signal. The said interference of compounds is known as the matrix effect and varies depending on how the data is acquired. As it is difficult to separate compounds so they are individually eluted many different techniques are used to compensate for or reduce the matrix effect, one such is using separation science to "clean" the point at where data for the said analyte is acquired [150]. Regarding XN separation science is rather simple as the conventional and commonly used reverse phase chromatography techniques is sufficient, although many different techniques have been trialled. The said method of separation can be on-line, i.e. during analysis, or off-line which is when separation (isolation) is carried out and afterwards acquisition of the data is performed. The most commonly applied approach for XN and related prenylated flavonoids is high performance liquid chromatography (HPLC). Relying on pumps and solvents of various polarities the analyte is washed through an absorbent material at high pressures. Separation methods that have been applied to XN include high performance thin-layer chromatography, gas chromatography (after derivatisation), capillary electrophoresis (CE) and counter current chromatography [151]. NMR is a method that does not separate compounds physically, but can separate compounds via spectrum and relaxation theories and has also had applications in quantifying XN using a process called qNMR.

1.6.2.2 Non-mass spectrometry based methods

Most of the methods for the analysis of prenylated flavonoids involve liquid chromatography separation, although a fast way which requires less work up is using the assistance of immunochemistry/radio-immunoassays, i.e. using antibodies specific to certain prenylated flavonoids that are coupled to a immuno/radiolabel tag [151] [160] [161]. Once washed, the antibodies retain to the samples with a degree of specificity where the concentrations are evaluated using fluorescence or radio spectroscopic methods. Regarding prenylated flavonoids and immunoaffinity based methods only two assays have been developed. One targeting 8-PN, in biological matrices which was successful in quantifying concentrations during human trials investigating the use of 8-PN for possible menopausal treatment [161] [162]. However, concerns were raised regarding unspecific binding (cross reactivity) to glucuronic acid conjugates [151]. The other was an enzyme-linked immunosorbent assay (ELISA) targeting with specificity XN, IXN and 8-PN with quantifiable result [160]. Limitations of the method were the sensitivities as with many other analytical techniques they are higher [151]. HPLC coupled with a variety of detectors is most likely the most accessible method for analysing the quantity of prenylated flavonoids. UV utilises the Beer lambert law $A = \varepsilon lc$ taking advantage of that the attenuation of light through absorption is a more robust measurement than mass spectrometry. Other detection methods include

electrochemical detectors (ECD), Chemiluminescence detection and square-wave adsorptive-stripping voltammetry. Limitations are sensitivity, cross reactivity, or and specificity hence LC-MS/MS methods dominate prenylated flavonoid analysis [151].

1.6.2.3 Mass spectrometry based methods

Although upfront costs are more expensive, LC-MS and LC-MS/MS methodologies lead prenylated flavonoid analysis in biological samples and in food products. Heron, a few details on certain methods will be introduced. As each have positives and negatives there is no one fits all answer and each technique has uses depending on the question that is investigated [150]. The most affordable mass spectrometry method is using a single quadrupole selected ion monitoring mode method [101]. Most use either atmospheric pressure chemical ionisation (APCI) and electrospray ionisation (ESI) sources, it is also noted that neither positive or negative mode is superior but should require individual testing depending on the specific mass spectrometer. However, many methods use negative polarity when analysing biological material and positive polarity regarding beer and hop products [151]. Another type of mass spectrometer method is the use of a triple quadrupole (QQQ), which has the ability to filter out fragmentation events with a much improved filter. QQQ increases selectivity, an advantage over single quadrupole methods, but at increase in the cost and size of the mass spectrometer [150]. Remarkably many mass spectrometry methods for prenylated flavonoids did not utilise an internal standard, making it rather difficult to compensate for ionisation efficiencies contributed from the matrix effect [101 163 164].

To date most reliable LC-MS/MS methods use an internal standard where commonly the compound 4,2'-dihyroxychalone is often used as when analytes are separated using C_{18} columns due to the fact that it is eluted in a similar retention time as XN (partially compensating for a matrix effect) [151]. Other internal standards include 4-hydroxyphenylpyruvic acid, naringenin, and 8-isopentylnaringenin. Most reliable methods use an internal standard however and perform matrix matched calibration (creating calibration curves before and after analysis in a matrix free from the analytes) where possible [165 166]. Thus, somewhat compensating for a matrix effect, however, it is not always possible to find a suitable matrix without the analytes present. An example, hop free beer does not exist, due to the complicated nature of the hops it is not easy to compensate for their chemical diversity. One other issue is that the matrix is separated via the LC system and thus at different retention times the matrix is different, and using a single internal standard does not compensate for these effects on ionisation of the analytes. Another, due to fluctuation in matrix during a batch of measurements each samples matrix is different, for example, blood composition between humans varies to a degree where the matrix differs in a manner which can influence the results when using matrix matched analysis. Another method that improves on matrix matched is the standard addition method. Standard addition involves direct addition of the analytes on pre-analysed samples, at increasing increments of pure standard concentrations. Once analysed the concentrations of each are calculated and creating calibration graphs where the concentration

of the unknowns are extrapolated and the compounds are quantified. The method of standard addition eliminates the matrix effect within the measurement, but does not compensate for matrices between samples. Furthermore, a very niche method is the ECHO technique [167]. The ECHO technique is a Mass spectrometry method that compensates for the matrix effect partially without the use of internal standards, but uses a pure form of analyte itself. By injecting the sample and an pure analyte (of known concentration) of the sample after a given time (for example 10 seconds) after the run has started the analyte will be eluted and in theory the known concentration standard will elute afterwards (for simplicity 10 seconds after the unknown). Thus, taking the integrals of each peak normalises the data between different matrices. Conversely compared with standard addition , ECHO partially compensates matrices between samples although not within the measurement [150].

One technique which reduces the matrix effects dramatically is stable isotope dilution analysis (SIDA) [4]. Due to this reduction in matrix effects it is said to be the gold standard of mass spectrometry methods. The principles behind SIDA are from an ecological method for approximating the population of animals in a large wild space where it is physically not possible to count each individual animal [4]. Therefore, the example used to explain is animals with a tag are released into the wild and after a set time "equilibration" a tracker tracks down a proportion of the animals (including the non-tagged animals) and counts the ratio of the tagged and the non-tagged. The ratio of the tagged and non-tagged animals is extrapolated and usually gives an accurate estimation depending on the equilibration time in chemistry termed "homogenisation of the analytes within the matrix". An expression is $\frac{[Taggeed\ animal-(non\ tagged\ animal+tagged\ animal)]}{[(non\ tagged+tagged\ animal)-non\ tagged\ animal]} = Approximate\ population$ [168]. Within mass spectrometry calibration graphs need be created beforehand so the ratio of internal standard with the analyte is calculatable as molarity and using linear regression analysis allows estimation of the concentrations (polynomial equations are possible). Additionally, the method of SIDA takes into account losses during sample work-up and in theory one can have an actual recovery of 1% with an apparent recovery that is excellent (>90) as the ratio of internal standard and reference standard behave physically the same (there are very slight isotopes differences regarding mass of isotopes) [94]. An overview of SIDA is shown in Figure 12. Previously to the work carried out in this Thesis no stable isotope dilution analysis on the prenylflavonoids found in hops was known due to a lack of available stable isotopes.

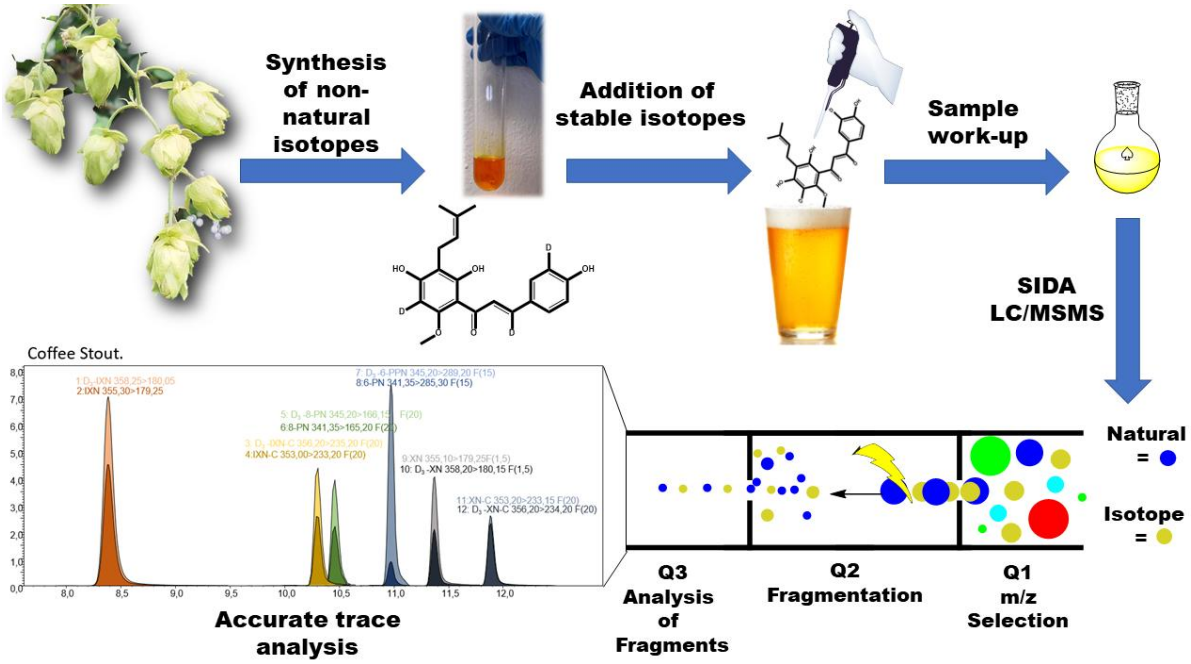

Figure 12: An overview of stable isotope dilution analysis. First, the synthesis of the non-natural stable isotopes needs to be performed. Once in a pure form they are added to the material before work-up. The sample is cleaned to remove saturation of the detector and then LC-MS/MS is used to quantify the ratio of natural compound compared to the stable isotope. Creating calibration graphs monitoring the ratio of reference compounds with internal standard allows the quantitation of the analytes of interest [94].

1.7 Pharmacokinetics of prenylated flavonoids in hops

Pharmacokinetics is the study of investigating the metabolic fate of a compound through a complex biological system using these main parameters absorption, distribution, metabolism, and elimination known as ADME. The ADME is applied most often to foreign compounds such as drugs and toxins, but this concept is also applied to foods stuff. As many different processors change a compound once it enters the system the compound(s) has(have) many different routes of modification. These parameters can be changed via the route of administration i.e. ingestion (enteral), injection (parental) and topical (local). The most favoured way of administration by patients is by oral ingestion therefore, the others will be excluded as this thesis is based on the metabolism of one compound XN and it was administered orally. However oral administration has complications via drastic changes in the stomach which is vital in XN metabolism. Drugs can be administrated as salts to overcome transfer across the epithelial layer in the stomach as sometimes charged particles are excreted rapidly. Formulations of orally administered XN in western Europe include the brand names: Xanthoflav™ (Germany), Lifenol, Naturex, and Avignon (France) [97].

1.7.1 Absorption, distribution, metabolism and elimination of xanthohumol

The initial phase of pharmacokinetics is the absorption, termed " the movement of a drug or compound across the gastrointestinal tract" [169]. Absorption studies of prenylated flavonoids are numerous and XN is not very bioavailable on it is own when investigated in rats as no XN (free) was found in the plasma after the administering 500 mg/kg [170]. Furthermore, in a separate study the oral bioavailability was deemed dose dependant between 11% low dose (1.86 mg/kg BW) and 33 % in a high dose (16.9 mg/kg BW) in rats after oral administration [171]. Due to these observations that XN absorption is low many technologies to increase the absorption have been developed. Some examples are pegylated XN (PEG-GO@XN) nanocomposites, hydroxypropyl-β-cyclodextrin complexes, Micellar formulas and bound to rice protein matrices [172] [173] [122] [174]. All of these products increased the bioavailability dramatically, although human trials with the new formulations are yet to be realised.

The term distribution is the second step in pharmacokinetics and is the delivery of the compound throughout the body/host and in very specific cases directed towards organs. A difficult biological phenomenon is crossing the blood brain barrier and depending on the compound certain salt formulations aid in this process. XN-C is seen as a promising neuroprotective agent, although it does not cross the blood brain barrier, thus making it very difficult to administer as it is not distributed where it is required. To overcome this solution researches applied the compound directly to the brain of mice which is an invasive route of distribution [173]. Thus not a desirable method for administration. One major problem with XN is that it is converted into the less desired IXN in the acidic environment of stomach [175]. To overcome this, intravenous routes of administration can distribute XN throughout the body where it is more useful. Furthermore, the micellular formulations discussed previously, protect XN from being converted to IXN. Once XN is distributed in to the blood it binds to albumin and might quench its bioactivities [176] [177]. Controlling the distribution of compounds can be as simple as combing a cytotoxic compound with a hormone or hormone analogue. Therefore, will accumulate in the area where the hormone is active e.g. coupling a cytotoxic compound with thyroxin. This approach is yet to be realised with prenylated flavonoids most likely due to the efficacy of action is not absolute and not extremely toxic [129].

The third part of ADME is metabolism either via chemical degradation (e.g. acid in stomach), and bacteria or liver metabolism. Most research regarding the pharmacokinetic approaches focused on this area as it is plausible to study simpler models such as in-vitro systems. Initially, Yilmazer M. et al. 2001 incubated XN with rat liver microsome to mimic liver metabolism. The results showed that upon NADPH supplementation three main phase I metabolites were formed [178]. The same laboratory group then further increased the knowledge by using human liver microsome and provided the co factor UDP-glucuronic-acid [62]. Concurrently, mice and rats studies followed revealing a multitude of glucuronides and sulfates and confirmed the dosing was safe [171, 179]. Human trials commenced. Most interestingly the major products are glucuronides and sulfates [180]. Elimination/Excretion is a vital point of any pharmaceutical and persistent compounds

in food due to whether something residing too long (bioaccumulation) can cause harm. The converse is that if a compound is eliminated quickly it will require constant dosing or not have a bioactive benefit. To improve bioavailability Deuteration can improve the lifetime in the system [181]. The faecal urine excretion ratio is another important factor as Van Breeman et, al. 2014 demonstrated after human supplementation of a prenylated flavonoid mixture only 2% was excreted in the urine i.e. the main route of excretion should be via faeces [180]. In a separate study in rats it is known that 89% of XN metabolites are excreted in the faeces [48].

1.8 Chemical synthesis of hop prenylated flavonoids

As many of the compounds essential for the analysis of prenylated flavonoids are not commercially available or do not have known synthetic protocols it is required to understand synthetic approaches. Here is the basis of their design, which is based from previous in-vivo and in-vitro studies that confirmed or tentatively identified XN metabolites. One thought is that in the work presented here vast amounts of XN (> 10 g) as a starting material for many reactions was required. Since XN is expensive to purchase commercially different approaches were foreseen. It is known that some synthetic methods exist in the literature. The most simplest synthesis starts with naringenin as a precursor, and using a catalyst 3,5-Octanedione, 6,6,7,7,8,8,8-heptafluoro-2,2-dimethyl-, europium complex (europium (III) FOD), which facilitates the prenylation of naringenin via Claisen-cope rearrangement [182] . The following step would require the methylation and subsequent opening of the chalcone using KOH. Furthermore an alternative method synthesised the demethylated derivate of XN named DMX [183] which was followed by the total synthesis represented in Figure 13 in all requiring seven steps and accomplishing a 10% overall yield [184]. Due to the complexity of the synthetic methods the isolation from natural sources was considered the most straight forward way to obtain XN in quantities useful for supplementation.

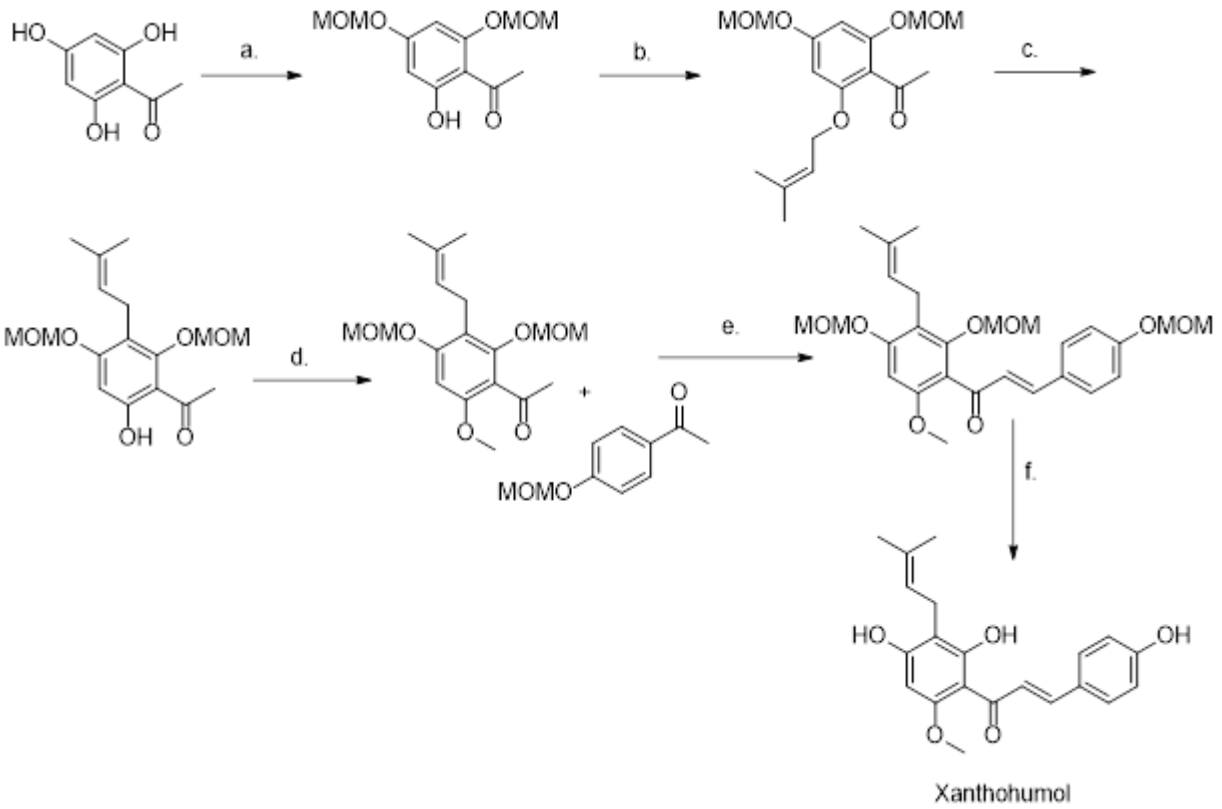

Figure 13: The total synthesis of XN aadapted from Khupse and Erhardt 2007. (a) MOMCl (3 eq), diisopropyl ethyl amine (3 eq), CH_2Cl_2, RT (60%); (b) 3-methyl-2-butene-1-ol (1.5 eq), diethylazodicarboxylate (1.6 eq), PPh3 (1.2 eq), toluene/THF, RT (80%); (c) N,N-dimethylaniline, reflux, 200 °C (64%); (d) $(CH_3O)SO_2$ (2 equiv), K_2CO_3 (2 eq), acetone, reflux (82%); (e) MOMCl (3 eq), diisopropyl ethyl amine (3 eq), CH_2Cl_2, RT (90%); (f) aqueous NaOH, MeOH, reflux (60%); (g) concentrated HCl (pH 1), MeOH/H2O, RT (72%); (h) can occur spontaneously upon heating and by acid or base catalysis . Khupse et, al. 2007 [182].

1.8.1 Isolation of prenylated flavonoids from hops

Starting in 1913 the isolation of XN was carried out by Powers et al. 1913 who described a yellow powder that was isolated from the lupulin gland [185]. The need for elucidation of various compounds at this time was paramount as brewing was in a discovery age in terms of chemistry. The isolation of XN that Powers et, al. 1913 achieved was critical for subsequent investigations on XN research. Although the work resulted in the wrong chemical formula annotation ($C_{13}H_{14}O_3$ where it should be $C_{21}H_{22}O_5$) the naming of the interesting compound "Xanthohumol" was given and the description of the bright orange substance was defined. Additionally, Powers et, al. 1913 treated the newly found compound XN with NaOH and stated it increases water solubility. Powers et al did not know at the time but they were producing IXN which they described that XN was turning a light yellow colour and increasing its water solubility. It was not just an observation, but a major discovery in how XN is metabolised and about which products are found in the

brewing process. It was not until 1957 by Verzele et, al. 1957 that the structure of XN was correctly elucidated [186].

As the brewing waste has a high content of XN it is desired that simple and green extraction methods are developed as there is high financial gain by providing a useful component of an otherwise wasted product. One of the most wide spread techniques for extraction of XN is the use of organic solvents which was initially provided by the pioneers of understanding the constituents of hops and is still wide spread in hop analysis today. Although, this is a great method new discoveries in "Green chemistry" have seen an increasing use in XN extraction. One of these is using super critical CO_2 at a very high pressure to pull the XN into solution [187] . Advantages of this method are that it is does not produce harmful waste of organic solvent and is rather selective depending on the pressures used. The green chemistry approach has developed into using pressurised hot water extractions and deep eutectic solvents [188] [189]. Precipitation methods have also been investigated using a variety of salts e.g. NaCl to remove the chlorophyll and fats from the hops making purification simpler [190]. Although the previous methods are great in producing high yields they might not give extremely pure extracts therefore, other methods were developed to produce very pure XN such as chromatographic separation and counter current chromatography [159] [191] [192]. The isolation methods of XN have come a long way and each progressive step in higher yields supports the development of XN for uses in disease prevention and the future development of novel biotechnological uses e.g. as an insecticide [119] [120].

1.8.2 Modification and isotope enrichment of prenylated flavonoids in hops

Most investigations looked at the biological transformation of prenylated flavonoids and very few have chemically modified them. As the metabolism of XN produces 8-PN, 6-PN and IXN their synthesis was required. Reportedly, isoxanthohumol-C (IXN-C) and XN-C are deemed important and were thus additionally synthesised. A variety of synthetic methods to obtain XN related prenylated flavonoids are known. The most simple is IXN, which requires only treatment with base in an aqueous environment [175]. To obtain 8-PN and 6-PN a simple demethylation reagent using a Lewis acid or magnesium iodide etherate is capable of demethylating XN [187]. Furthermore, LiCl is a great cheap candidate for the demethylation of XN [193]. These methods were applied in the manuscript I Appendix 5.1.

Hydroxylation while retaining a prenyl moiety is possible via Riley-Oxidation mimicking phase I metabolism products [194]. The C-H oxidation is possible due to the active allylic position in the prenyl group. Sulfates are further metabolites that are required and sulfation was previously carried out by Legette et, al. 2014 although the authors only applied MS analysis and did not purify or characterise the position of the sulfate group as there are three possibilities – 7-O, 5-O and 4'O positions [61].

Glycosylation is the reaction between a glycosyl acceptor and a glycosyl donor and, via the assistance of an activator or promoter. Forming a glycosidic bond. During the transition step assisted by the promoter a cation glycosyl is formed which is stabilised with an oxocarbenium ion. The nucleophile and

glycosyl acceptor form a glycosidic bond via two different orientations either attack from the top or bottom face of the flat oxocarbenium ion. Thus, two different stereoisomers are possible the α (If the attack is from above) and β (if attack is from below) isomers. Forming either 1,2 trans or 1,2 cis depending on which direction the glycosidic bond is formed. [195]. To summarise nature tends to produce β (1,2-cis) rather than the α (1,2-trans) O'linked glucuronic acid. Therefore, to synthesise metabolites of glucuronic acid the stereospecificity is required. The important α position glycoside is difficult to synthesise. To control α formation glucuronidation synthetically in general requires no neighbour group participation [195]. A common glycosylation method is Schmidt glycosylation and utilises Lewis acids, such as TMSOTf or BF3 in solvents like Et_2O. Schmidt glycosylation is likely the most popular method currently due to the simple control between α and β isomer control [196]. Another method is Koenigs–Knorr glucuronidation, which proceeded Schmidt glycosylation utilising halide activation and being the basis of Schmidt [197]. Koenigs–Knorr is facilitated by a substitution reaction between a glycosyl halide and an alcohol to give a glycoside through an SN2 mechanism. Glucuronidation was applied from Jongkees and Withers 2011 using the Koenigs–Knorr approach [198]. The hydroxylation sulfation and glycosylation (glucuronidation) using the previous methods and principles were applied to Manuscript II. Section 3.2.

Many attempts to enrich hop related prenylated flavonoids isotopically have been attempted and some were successful. The examples discussed have many uses in medical imagining, analytical methodology and in discovering biochemical pathways. One detail that has not been researched regarding the labelled hop prenylated flavonoids is kinetic isotope effects for understanding mechanisms of actions in many XN enzyme targets. The initial enrichment of XN isotopes used ^{13}C labelled phenylalanine and glucose and incubated fresh hop cuttings that were left for eight days. The purification of XN from the hop cuttings that were feed labelled glucose resulted in isotopically enriched XN. The hop cuttings have contributed to the elucidation for the biosynthetic pathway in hops [84]. Although, upon thorough analysis of the isotopes produced it was noticed that the non-enriched product remained, thus it is not suitable for stable isotope dilution analysis [4 150]. Reasons are that the signals of the non- isotopologues will interfere with calibration graphs making the data revision very complicated. Another limitation is hops need to be in season, which makes the method accessibly seasonal i.e. September through October in Europe. Therefore, the feeding of hop cones was not considered. The authors further made radio-labelled isotopes of XN which should allow medicinal studies to identify which organs XN accumulates [199]. Further research is required for the use of labelled compounds in human studies and in medicinal imaging. The basis from Khupse and Erhardt 2007 (total synthesis of XN) was the scaffold for the total synthesis of C13 labelled XN substituting a [^{13}C]-iodomethane rather than iodomethane. Ultimately enriching XN with [$^{13}C_5$] in a 7 step synthesis [184 200]. ^{13}C labelling is desired as deuterium is possible to interact with certain hydrophobic interactions, however the method is considerably more expensive and usually leads to low yields from the multiple steps required [201]. Most recently a method focused on

naringenin prenylation in a 6 step synthetic pathway and by adding deuterated methyl iodide to yielding XN where the methoxy group is OD_3 [202]. The last two examples are suitable for SIDA.

2. Objectives

The overall goal of this research was to create new methods for evaluating the metabolism of XN provided by hops in humans. At the timing of this publication the compound XN is undergoing clinical trial for the treatment of Chron's disease and covid-19. XN is only seen as a supplement as established evaluations have not identified whether XN promotes health benefits conclusively and the metabolism is not fully understood. Current formulations of XN fit for human consumption are concentrated extracts derived from hops and in a dietary context XN is found in beer. In addition, XN is under research for use as a food preservative. Ultimately the analysis of XN and how it is metabolised is critical to understand the future of XN biotechnological applications. Furthermore, no analytical methods have quantified XN metabolites in humans. Thus, leaving out critical information about the quantity of metabolites in circulation. As no reference compounds were available the production of new isotopologues for the SIDA of prenylated flavonoids derived from XN was required. The first synthetic approach aimed at creating stable isotopologues for uses in the gold standard of analytical methods characterising the content of XN and related prenylated flavonoids in a range of beverages that contain XN e.g. hops, beer and hop tea. The second aim was to develop new synthetic methods for metabolites of XN ranging from sulfate, hydroxylation and glucuronidation products which represented a broad range of XN human metabolites. The synthesised compounds had uses in the identification of metabolites unequivocally, along with the tentative annotation of isomeric compounds that had similar MS/MS fragmentation but different retention times. The third aim was the estimation of the pharmacokinetics of XN metabolites in humans after the consumption of native XN compared with a micellarised formulation. These objectives overall assisted in understanding how the potent bioactive XN compound is metabolised and revealed the quantity and pharmacokinetics of the metabolites in humans after XN consumption.

3. Results

The work carried out resulted in the publication of three peer reviewed manuscripts. The first major part of this project led to the synthesis of stable isotopologues of XN and derivatives, namely XN, XN-C, IXN, IXN-C, 6-PN and 8-PN. With these standards, the first ever reported SIDA of prenylated flavonoids in hop products was carried out. With its greater sensitivity compared to other analytical approaches, this method can serve as the gold standard for quantifying prenylated flavonoids in beer (which is the highest dietary source of prenylated flavonoids in the human diet). In general the synthesis of stable isotopologues was the first publication that carried out the SIDA on hop prenylated flavonoids and might have uses in future analysis and quantified prenylated flavonoids in beer. The SIDA on prenylated flavonoids in beer is a great method for quantification and found typical concentrations of total prenylated flavonoid content found in beer and hops with comparable results (723–2456 μg/L) to other investigations [165]. The prenylated flavonoid content is very unlikely to contribute to health or taste and in addition the dealcoholisation process for alcohol free beer might remove prenylated flavonoids and should be further investigated. [158].

In the second major part of this work, the human metabolites of XN and derivatives were synthetised, namely xanthohumol-*Z*-OH, xanthohumol-*E*-OH, isoxanthohumol-*E*-OH, 6-prenylnaringenin-*E*-OH, 8-prenylnaringenin-*E*-OH, isoxanthohumol-4'-*O*-sulfate, 8-prenylnaringenin-4'-*O*-sulfate, 6-prenylnaringenin-7-*O*-sulfate, IXN-7-*O*-GlcA, XN-7-*O*-GlcA, 8-prenylnaringenin-7-*O*-GlcA and 6-prenylnaringenin-7-*O*-GlcA. These metabolites were for the first time unequivocally identified by matching them to a human blood sample. Previous biochemical approaches did not provide enough material for unequivocal identification.

Lastly, a human trial compared the consumption of two formulations of XN and was the first time metabolites of XN were quantified in-vivo. Finally, the work demonstrated the complexity and metabolism profile of XN in humans, moreover provided evidence that a micelle formulation of XN is 7 times superior than administering native XN.

3.1 Manuscript I : Stable isotope dilution analysis of the major prenylated flavonoids found in beer, hop tea and hops [94]

3.1.1 Information about my contribution as an author.

Author contributions from myself were conceptualising that carrying out SIDA on prenylated flavonoids from hops will improve the field of XN analytics with focusing on the ultimate goal of investing the human metabolism. Furthermore, I carried out the synthesis and purification of the reference compounds and all deuterated compounds useful for SIDA . This includes the identification of all 13 compounds by NMR, MS, HPLC and LC-MS/MS and tuning each compound to the QQQ mass spectrometer. The analytical method was developed by myself and I performed the measurements of all samples. The initial writing of the manuscript and interpretation of the data was additionally carried out by me. I contributed partially (over 50%) of sample work up.

Permission to reprint the article

The research focused on the growing interest in prenylated flavonoids derived from hops (Humulus lupulus) due to their potential health benefits, including anti-cancerous activities and the treatment of metabolic syndrome. These compounds have shown promise in clinical trials, prompting the need for robust analytical methods to determine their concentrations in various products such as food, supplements, and beverages. The gold standard analytical method employed in this study is SIDA. This method is preferred for its ability to compensate for matrix effects and losses during sample preparation. Since commercial standards for prenylated flavonoids were unavailable, the synthesise of seven different isotopologues of these compounds using various strategies, including microwave assistance, acid-base catalyst with deuterated substance, and Strykers catalyst was carried out. The synthesised prenylated flavonoid isotopologues were then utilised in the development of the first SIDA method on hop prenylated flavonoids. This method successfully quantified six natural prenylated flavonoids (Isoxanthohumol, Isoxanthohumol-C, 8-Prenylnaringenin, 6-Prenylnaringenin, Xanthohumol, and Xanthohumol-C) in beer, hop tea, and hops, demonstrating its applicability across different products. The analytical method, SIDA-LC-MS/MS, underwent validation, with limits of detection (LODs) and limits of quantification (LOQs) ranging from 0.04 to 3.2 μg/L for all analytes. Notably, the simplicity of the clean-up process in the developed method opens the possibility of applying it to measure prenylated

flavonoids in clinical samples in the future. Overall, this study provides a comprehensive approach to analysing and quantifying prenylated flavonoids in various matrices, contributing to the understanding of their potential health benefits and paving the way for future applications in clinical research.

3.2 Manuscript II: Synthesis of human phase I and phase II metabolites of hop (*Humulus lupulus*) prenylated flavonoids [69]

3.2.1 Information about my contribution as an author.

My contributions to the second manuscript were designing the methodology for the synthesis of the sulfates, glucuronides and hydroxyls of all prenylated flavonoid conjugates in the manuscript and producing enough precursors for the synthesis of all prenylated flavonoids i.e. XN, XN-C, IXN, IXN-C, 8-PN and 6-PN. I investigated the production methods for the glucuronic acid donor and the initial synthesis of each, XN-7-O-GlcA, IXN-7-O-GlcA, 8-PN-7-O-GlcA, 6-PN-7-O-GlcA. In addition I discovered the conversion of IXN-O-GlcA to XN-O-GlcA when carrying out deprotection step. Furthermore, interpretation of the majority of NMR, HPLC, and LC-MS/MS data was carried out by myself. The development of the LC-MS/MS method for analysis was my work alone along with the work-up of the blood samples. I partially contributed in spiking the blood with the desired concentration of internal standards and handled all blood samples until no biological risk was apparent (once the addition of MeOH was carried out).

This study delved into the exploration of in-vivo activities of hop prenylated flavonoids, with a specific focus on the metabolism of XN - a compound known for its diverse positive health effects. Existing research utilising untargeted methods has revealed that XN undergoes a metabolic pathway involving degradation into 8-prenylnaringenin and 6-prenylnaringenin, spontaneous cyclisation into IXN, and subsequent demethylation by gut bacteria. Additional metabolic transformations, including hydroxylation, sulfation, and glucuronidation, lead to a variety of isomers. However, previous investigations often relied on surrogate or untargeted approaches for metabolite identification, introducing potential errors in absolute identification.

This study introduces a synthetic approach to generating reference standards crucial for the accurate identification of human XN metabolites. The synthesised metabolites were then analysed using qTOF LC-MS/MS. Several of these metabolites were successfully matched to a human blood sample obtained after the consumption of 43 mg of micellarized XN. Notably, the research identified isomers of the reference

standards by comparing their identical mass fragmentation patterns with different retention times. This method unequivocally pinpointed the presence of XN metabolites in the human circulatory system.

The findings underscore the importance of employing in-vitro bioactive testing with metabolites rather than the original compounds, as free compounds are seldom found in human blood. This comprehensive approach not only advances our understanding of XN metabolism but also provides a reliable framework for future research exploring the health benefits associated with hop prenylated flavonoids.

3.3 Manuscript III: The pharmacokinetics of individual conjugated xanthohumol metabolites show higher bioavailability of micellar than native xanthohumol in a randomized, double-blind, crossover trial in healthy humans [203]

3.3.1 Information about my contribution as an author.

The work carried out by myself in the third manuscript was the work-up of all blood samples (until the addition of MeOH), however I only partially contributed to spiking the blood samples with internal standards. Handling of the blood samples during the potentially infectious phase was done by me alone. The coordination of getting the blood samples from the university of Hohenheim and correspondence between the working groups was also my contribution. The LC-MS/MS method was developed by myself along with the measurements of all samples and the interpretation of all the data. I calculated the concentrations of each compound and dilutions required to produce all calibration graphs. Lastly, I wrote the initial draft of the manuscript and coordinated the submission process.

Permission to reprint the article

Access and permission to reprint the article in this Thesis between Lance Buckett and John Wiley and Sons was given according to License Number 5637021005492.

This study explores the potential health benefits of prenylated chalcones and flavonoids, focusing on XN, a compound commonly found in beer but known for its poor absorption and rapid metabolism, limiting its bioavailability. The work conducted a randomized, double-blind, crossover trial involving five healthy volunteers to compare the oral administration of a single 43 mg dose of XN in native and micellar formulations. The results reveal that in plasma, unmetabolised free XN constitutes 1% or less of total plasma XN. The study quantifies major human XN metabolites and demonstrates that the micellar formulation significantly enhances the oral bioavailability of XN. Specifically, the area under the plasma concentration–time curve of xanthohumol-7-O-glucuronide is five times higher, and its maximum plasma concentration is more than 20 times higher compared to native XN. The complexity of XN metabolism is highlighted, showcasing the efficient conversion of the parent compound into predominantly glucuronic acid and, to a lesser extent, sulfate conjugates. The findings suggest that micellar XN serves as a more effective delivery form, surpassing the bioavailability of native XN. This underscores its potential utility in future human trials, emphasizing the importance of formulation strategies in enhancing the efficacy of bioactive compounds for improved health outcomes.

4. Discussion and Conclusion

The exploration of human metabolism and the intricate interactions between the human body and foreign substances at the molecular level lies at the heart of biochemistry. The field of metabolomics investigating human metabolism seeks to unravel these complex relationships, aiming to comprehend how various compounds may engage with receptors and enzymes, ultimately triggering bioactive effects. The primary objective of this thesis was to improve analytical methods for investigating the metabolism of prenylated flavonoids, with a specific focus on examining the metabolic fate of XN in humans after oral consumption.

To achieve a comprehensive understanding, the analytical framework employed in this research was founded on the direct synthesis of internal standards, specifically stable isotopologues. This approach provided a robust foundation for the subsequent analytical endeavours. Additionally, the synthesis of new reference compounds played a pivotal role in facilitating the unambiguous identification of human metabolites following XN consumption. The synthesis of these compounds not only enriched the analytical toolkit but also enabled precise annotations of metabolites arising from the human metabolism of XN.

The analytical strategy further involved the amalgamation of stable isotopologues as internal standards with the newly synthesised reference compounds representing human metabolites. This integrative approach was instrumental in quantifying XN during a human trial, offering insights into the intricate web of metabolic transformations. The successful unravelling of how XN is metabolised demanded a nuanced comprehension of both plant and human metabolism, coupled with insights into pharmacokinetics. Moreover, a grasp of synthetic chemical methods proved essential, facilitating the identity of XN metabolic pathways and metabolites that might have otherwise eluded detection.

The multifaceted nature of this investigation extended beyond the laboratory, necessitating a profound appreciation of the statement "the dose is the medicine." Understanding the interplay between XN supplementation, as well as the concentrations found in beer, and their potential contributions to health benefits became a goal of the work. Moreover, acknowledging the inherent limitations of this framework was paramount to ensuring the validity of extrapolations drawn from the experimental findings. This study represents a comprehensive exploration of XN metabolism in humans, integrating advanced analytical methodologies, synthetic chemistry, and a profound understanding of plant and human biochemistry. The findings not only contribute to the growing body of knowledge in metabolomics but also hold implications for the broader understanding of the potential health benefits associated with XN supplementation and its presence in beer and or in capsule supplementations.

4.1 Manuscript I: Stable isotope dilution analysis of the major prenylated flavonoids found in beer, hop tea and hops

The successful production of stable isotopologues and their application in the analysis of beer, hops, and hop tea has significantly advanced our understanding in three key areas. Firstly, the synthesis of new isotopologues was achieved through various methods. Notably, the acid-base catalysed hydrogen/deuterium exchange emerged as a viable approach, accessible to a wide range of laboratories [94]. Additionally, the microwave-assisted method enabled the enrichment of deuterium in the flavonoid backbone, and successfully applied to a SIDA method. Secondly, the utilisation of SIDA proved to be an excellent strategy for quantifying the prenylated flavonoid content in beer and hop products, such as tea. The novel method introduced is characterised by enhanced robustness, featuring a straightforward liquid-liquid extraction process. Remarkably, the limits of detection achieved with this new method are outstanding, comparable to the most sensitive techniques available [151]. Specifically, the limits of detection (LOD) ranged from 0.04 to 3.2 μg/L, surpassing the minimum literature value of 3 μg/L. These advancements represent a significant contribution to the field, not only by expanding the synthetic approaches for isotopologues but also by introducing a more robust and sensitive method for analysing prenylated flavonoids in beer and hop products.

The findings have the potential to impact various laboratories and researchers engaged in the study of isotopologues of XN and their applications in the field of food and beverage analysis.[151]. Moreover, the developed method stands out as the exclusive approach that successfully analysed XN-C and IXN-C in beer. This revelation brought to light that the concentrations of these compounds are insufficient for eliciting bioactive modulations following beer consumption. Given that XN-C and IXN-C are currently under investigation for their potential health effects, there arises an opportunity for the development of a brewing method that specifically enriches these compounds. This could prove to be beneficial in enhancing the bioavailability of XN-C and IXN-C in beer. The ongoing exploration of the health effects of XN-C and IXN-C suggests a potential role in providing neuronal protection. However, it is essential to underscore that further investigations into the mechanisms of action are imperative. This underscores the need for continued research to elucidate the precise ways in which XN-C and IXN-C may exert their neuroprotective effects. Such insights could pave the way for the development of targeted strategies for enhancing the health-promoting properties of beer through the modulation of these specific compounds [173].

A further finding presented in Manuscript I demonstrated that alcohol-free beer samples exhibited lower concentrations of prenylated flavonoids compared to their counterparts with alcohol [94]. Considering that flavonoids contribute to the taste profile of beer, it raises the question of whether a slight enrichment of prenylated flavonoid content in beer could potentially enhance its flavour. This observation opens the door to a discussion within the brewing community about the sensory implications of manipulating prenylated flavonoid levels and how it might positively impact the overall taste experience of alcohol-free beer

[6]. In a related context, the initial publication investigating prenylated flavonoid content in hop tea unveiled their presence, albeit at extremely low concentrations. Interestingly, the study suggested that these low concentrations may not significantly contribute to the flavour profile of hop tea or offer notable health benefits. This underscores the importance of understanding not only the presence but also the sensory impact and potential health implications of bioactive compounds in beverages like hop tea.

In the meantime, other research groups have provided different synthetic methods for XN isotopologues production to the literature, with the most recent being the methylation of the methyl group of naringenin at step three in a six-step synthesis [202]. A disadvantage to this step is that it requires synthetic methods in six steps which is costly and time-consuming. Furthermore, the introduction of the stable isotope is located only in the methyl group. However, since Andrusiak et al. 2021 used $^{13}CH_3I$ in their synthesis, it has the advantage of ^{13}C (instead of ^{2}H) enrichment due to less apparent effects of isotope exchange that deuterium possess [202]. The authors succeeded in producing a stable isotopologue of XN however to the publication date of this work no further SIDA had quantified XN in any matrix e.g. food, beer or blood plasma.

The method described in Manuscript I, while informative, has some limitations as it only assessed 15 beers that represent a typical range consumed in Europe. To further enhance the study's comprehensiveness and applicability, it would be advantageous to expand the analysis to encompass a more extensive array of beer styles. This broader sampling would enable the identification of patterns in prenylated flavonoid content across various beer types, providing a more nuanced understanding of how these compounds are distributed within the spectrum of beers available in the market. Additionally, a more extensive analysis could contribute to an enhanced understanding of the fate of prenylated flavonoid content throughout different brewing processes and how it evolves across diverse beer styles. This exploration is crucial for gaining insights into the factors influencing the concentration of these compounds in the final product.

Moreover, a larger sample size would facilitate a more robust investigation into whether the concentrations of prenylated flavonoids are consistently at levels that could potentially confer health benefits. This expanded dataset would not only provide a more comprehensive picture of the variability in prenylated flavonoid content but also aid in establishing connections between these concentrations and potential health impacts, thereby advancing our understanding of the nutritional aspects of beer. Hence, broadening the scope of the study to include a diverse array of beer styles would offer a more representative and nuanced perspective, shedding light on the patterns, dynamics, and potential health implications of prenylated flavonoid content in beer. [204]. Some factors which were ignored regarding the analysis were impacts of dry hopping and the content in very dark beers. Boronat et al. 2020 stated that a very dark beer contained 9.5 mg/L prenylated flavonoids, nearly five times the total content found using the SIDA method [29]. In a food context, a more analytical focus could be applied to analysing the prenylated flavonoid content during the dealcoholising process of beer, as prenylated flavonoids might contribute to the taste or quality of the beer which is implied by the results in manuscript I (see appendix 5.1)[158].

A vital issue that brewers are focusing on regarding beverage technology is the taste and quality of alcohol-free beer, and it has been noted that the taste threshold of XN is approximately 700 μg/L and IXN 450 μg/L [158]. As most of the beer styles measured in the SIDA study are within this range IXN (< 700 μg/L), perhaps prenylated flavonoids contribute to a bitter taste. In addition, as the work here showed that alcohol-free beer contained much less prenylated flavonoids, further research by increasing the sample number would benefit the brewing industry. Boronat et al. 2020 observed the same phenomenon regarding alcohol-free beer containing less prenylflavonoids [29]. Once the effect is understood, alcohol-free beers with increased amounts can be engineered towards similar levels in alcohol-containing beer.

In addition, the isotopically labelled prenylated flavonoids might have further uses in other biotechnology. The synthetic method of enriching prenylated flavonoids with deuterium could produce radiolabelled compounds by substituting the D_2O with T_2O or TDO. If XN becomes a pharmaceutical, this would be vital in medicinal radiochemistry applications. Labelling XN and related prenylated flavonoids with radioactive isotopes would enable the identification of which organs might bioaccumulate XN, which is essential in distribution studies [205]. Furthermore, deuteration can increase the bioavailability of a compound in a biological system, e.g. Deutetrabenazine showed a 44% increase in AUC against its non-deuterated counterpart Tetrabenazine [206]. Hence, deuterated XN and related prenylated flavonoids may persist in the body for longer and increase their effects [181].

The concentration of XN across many beers is relatively low and might not elicit bioactivity. However, recently a human trial supplementing 0.125 mg in total noticed changes to the immune system (see section 1.5.1). The low concentration is in the range of dark beer and fresh hop beers published in manuscript I. Therefore, the low dose in some beers is within the critical concentration for an observed bioactive effect and might contribute to an increased immunity [114]. Further studies (using beer rather than pure XN) similar to Jung et al. 2022 would reveal whether this is the case or not. No studies have looked at the synergism of bioactivities between the prenylated flavonoids from beer, which brings back the topic of "food as medicine" and the "dose makes the medicine". It has previously been shown that beer might be safer to consume than pure alcohol in mice, but further research is required on whether this is relatable in humans and which role natural products such as XN play in that regard [30].

4.2 Manuscript II: Synthesis of human phase I and phase II metabolites of hop (Humulus lupulus) prenylated flavonoids

The innovative aspect of this research lies in the development of synthetic methods for glucuronides, sulfates, and hydroxylated prenylated flavonoids from hops, which, prior to this work, were not available. These synthetic approaches are poised to become foundational in future studies focusing on the metabolism of XN. The newly established standards generated through these methods should find widespread applications, particularly in bioactivity testing. This advancement allows for a more precise representation of the actual processes occurring in blood plasma after XN consumption, providing a valuable tool for understanding the metabolic fate of XN. The utility of these synthetic standards extends beyond bioactivity testing. They might be instrumental in conducting inhibition assays on specific enzymes such as p-glycoprotein and cytochrome P450 [207]. These assays are crucial for investigating whether the metabolites derived from XN are responsible for the bioactivities observed in in-vitro studies. This approach helps bridge the gap between in-vitro and in-vivo studies, offering a more comprehensive understanding of the potential mechanisms underlying the bioactive effects of XN. Furthermore, the research contributes to the documented knowledge on the impact of glycosylation on flavonoid activity. It is well-established that glycosylation, such as O-glycosylation, can modify the activity of flavonoids [208]. For instance, O-glycosylation may reduce antioxidant activity, but interestingly, it can enhance antimicrobial activities. This nuanced understanding of the relationship between glycosylation/glucuronidation and activity is crucial for interpreting the biological effects of prenylated flavonoids and provides a valuable foundation for future studies in this field.

The evaluation of certain factors in prenylated flavonoids, particularly those derived from hops, has not been thoroughly conducted. Specifically, in the context of sulfation, it has been observed that XN-sulfate exhibits reduced cytotoxic activity against human cancer cell lines in comparison to its non-sulfated counterpart. Suggesting that the process of sulfation can impact the biological activity of these compounds, and further investigations are needed to comprehensively understand the implications of such modifications in prenylated flavonoids, particularly those derived from hops [59]. Therefore, as the standards have been produced bioactivity testing is paramount in understanding the bioactive effects of XN consumption, however this was not carried out due to limited time and resources.

Efforts were made to combine the isotopologues generated from the synthesis described in manuscript I (Appendix, section 5.1.) with glucuronic acid, but no successful outcomes were achieved. An alternative approach for generating stable isotopes of the metabolites involves employing labelled glucuronic acid. This method is commonly practiced in the synthesis of various commercial stable isotopologue conjugates [205]. This alternative strategy may offer a viable pathway to obtain the desired labelled metabolites and warrants further exploration in the context of your research or experimentation. The incorporation of stable isotopes for enrichment in hydroxylation and sulfation functional groups has not been attempted. The

use of sulfur isotope ^{33}S, theoretically resulting in only a 1 m/z increase compared to ^{32}S, is not deemed suitable for SIDA due to potential signal overlap with the natural ^{13}C in XN, accounting for approximately 23% of m/z +1.

To control the location of a metabolite conjugate in the synthesis methods, employing protection groups like MOM-Cl to safeguard hydroxyl groups was considered. Depending on the molar ratio of the protecting group, this approach could facilitate the synthesis of glucuronides in other OH position of prenylated flavonoids. This strategy holds promise for expanding the repertoire of reference compounds, contributing to a more diverse set of metabolites for further investigations [183]. The levels of 4'-O-GlcA were found to be considerably lower in abundance in human blood plasma than the 7-O-GlcA. These diminished quantities suggest that they may not exert a significant influence on the observed phenotypic changes following XN consumption in-vivo [115]. The Koenigs–Knorr glycosylation of IXN-C and XN-C produced low yields, and the reaction may not be practically feasible within the established conditions described in manuscript II. Consequently, an alternative approach involving biosynthesis was employed for the generation of these compounds. This adaptation in the synthetic strategy was necessary to overcome the limitations encountered with the conventional chemical synthesis method.

The compound DXN is of significant interest in ongoing research due to its unique property of not cyclising into the potent phytoestrogen 8-PN. Despite its potential as a pharmaceutical candidate, the metabolism of DXN in humans has yet to be thoroughly investigated. The Koenigs–Knorr reaction, which is known to work with IXN (flavanone) as a starting material but not with XN (chalcone), presents an interesting avenue for exploration with DXN. However, the conventional Koenigs–Knorr couplings involve deprotection steps that could result in a mixture of both the flavanone and the chalcone forms, making the process more complex. Considering the challenges associated with the Koenigs–Knorr reaction, further research into alternative methods of glucuronidating DXN is warranted. The synthesis of glucuronidated standards would be particularly beneficial for understanding the metabolism of DXN. This is crucial given that DXN, despite sharing similar bioactivities with XN, is not estrogenic and has a significantly reduced ability to convert into an estrogenic compound.

The hydroxylation of prenyl groups with SeO2 represented an area that requires further investigation, particularly regarding the mechanism that is yet to be fully understood [194] [106]. Theoretically, the hydroxylation process should yield only the *E* isomer. However, experimental results, confirmed by COSY NMR spectra, revealed the production of a mixture of both *E* and *Z* conformers. This discrepancy, highlights the need for a more comprehensive understanding of the underlying mechanisms at play. To gain better control over isomer formation, exploring different solvent systems is suggested. Typically, 1,4-dioxane is a commonly used solvent in such reactions, but its omission in our experimentation is noted, due to safety concerns. The choice of solvent can indeed influence reaction outcomes, and investigating alternative solvent systems may provide valuable insights into achieving greater selectivity in isomer formation during the

hydroxylation process when using SeO2. This optimisation could contribute to a more precise and controlled synthesis of prenylated compounds with specific geometric isomers.

The synthetic methods outlined in the manuscript appear to have overlooked a significant class of metabolites and mixed metabolites present in blood samples as found in Appendix 5.3. Combining each synthetic method of glucuronidation and sulfation could potentially lead to the production of these further metabolites. However, it is anticipated that such an approach would necessitate extensive use of protecting groups and considerably more complex synthetic procedures. The cost and purification challenges associated with XN, coupled with its complexity, deterred the implementation of this strategy in the current work. As newer, cleaner, and higher-yielding processes for obtaining XN precursors emerge, future methodologies may indeed explore the synthesis of these mixed metabolites. The ability to access larger quantities of XN precursor materials may alleviate the cost and purification challenges, making such endeavours more feasible (Section 1.8.1). Furthermore, the investigation of "non"-natural derived XN analogues, such as tetrahydroxanthohumol (TXN), which involves removing the Michael system in XN and alkene in the prenyl group, is noteworthy. This modification in TXN prevents the formation of 8-PN in the gut (similar to DXN), thereby avoiding the production of the estrogenic compound while still retaining the desired bioactivities [115]. Although human trials on the metabolism of TXN have not been conducted, this area remains open for future investigations, offering potential insights into the biological effects and safety profile of this modified compound.

From a biotechnological perspective, the synthesised metabolites demonstrate increased solubility in water. For instance, the logP of XN-7-O-GlcA is 2.0 compared to XN, which has a logP of 3.9, making it more soluble in water. Given that beer primarily consists of water, there is considerable research interest in engineering the brewing process to enhance the content of prenylated flavonoids, which are generally not very water-soluble [204 7 188]. One potential application of these findings is the addition of the synthesised products to a beverage or the development of a highly active yeast capable of glucuronidation/glycosylation of prenylated flavonoids during the dry hopping phase. This approach, in theory, could increase the prenylated flavonoid content in the final beer product. By leveraging the glucuronidation pathway and incorporating a specialized yeast strain for prenylated flavonoid metabolism, it becomes possible to enrich beer with these bioactive compounds. This biotechnological strategy offers a promising avenue for creating functional beverages with enhanced prenylated flavonoid content, potentially imparting additional health benefits to the consumers beyond the typical properties of traditional beer [83].

4.3 Manuscript III: The pharmacokinetics of individual conjugated xanthohumol metabolites show higher bioavailability of micellar than native xanthohumol in a randomized, double-blind, crossover trial in healthy humans

The findings in Manuscript III have validated the metabolism of XN using two different formulas and have indicated that micelles offer superior bioavailability compared to the administration of native XN. This challenges the traditional notion of "The dose makes the medicine," as discussed in the thesis introduction. In this context, even when the doses were equivalent (43 mg), the overall bioavailability varied significantly (5 times higher in micelles) [5]. As a result, a more accurate statement might be "the dose and drug administration make the medicine," emphasizing not only the quantity but also the method of administering the drug as crucial factors in determining its efficacy. This revised perspective underscores the importance of considering not just the dosage but also the formulation and delivery method when assessing the therapeutic impact of a drug or compound.

Elucidating aspects of the metabolic pathways associated with XN, specific attention was directed towards phase I metabolism, with a particular emphasis on the demethylation process, which could occur either in the gut or through cytochrome P450 (CYP) modifications. The resulting metabolites, 8-PN and 6-PN, were examined, and their representation in human plasma was investigated, particularly in the forms of 6-PN-7-O-GlcA and 8-PN-7-O-GlcA. Notably, the observation that all samples exhibited a higher concentration of 6-PN compared to 8-PN (as a glucuronic acid conjugate) suggested that the demethylation step predominantly originates from XN and not IXN. This inference aligns with existing knowledge indicating that the cyclisation of demethylated-XN (DMX) favours the formation of 6-PN. Conversely, a higher concentration of 8-PN would have suggested that the demethylation step occurs from IXN, as it is less likely for 6-PN to form after this particular step in the metabolic pathway. Moreover, previous work delved into experimental setups involving pure DMX and acid-based reactions, revealing a consistent trend where more 6-PN was formed [209]. Interestingly, this outcome mirrored the in-vivo (human) results, as the calculated average concentration of 6-PN-7-O-GlcA, determined using the area under the curve (AUC) method, across all participants was 35 nmol/L/h [209]. In contrast, the corresponding concentration for 8-PN was 20 nmol/L/h. In conclusion, the investigation shed light on the intricate metabolic (and perhaps microbial) transformations of XN, emphasising the role of demethylation in generating key metabolites, with a nuanced consideration of the preferential formation of 6-PN over 8-PN [49]. The alignment of in-vitro and in-vivo findings contributes valuable insights into the understanding of XN metabolism and its implications in human physiology.

The absence of hydroxylated prenylated flavonoids in the study findings might be attributed to the inhibitory effect of XN on specific cytochrome P450 enzymes in humans, namely CYP1B1 and CYP1A1. These enzymes play a crucial role in the hydroxylation processes involved in the formation of

certain metabolites. The inhibition of CYP450 enzymes by XN has implications for the in-vivo metabolic pathways of the compound. In essence, the hindrance of CYP1B1 and CYP1A1 activity limits the ability of these enzymes to catalyse hydroxylation reactions, leading to the observed absence of hydroxylated prenylated flavonoids in the scope of the study [49]. Furthermore, it is suggested that the inhibition may either completely prevent the formation of hydroxylated metabolites or reduce their concentrations to levels below the limit of detection (LOD) of the analytical methods employed in the study. The inability to detect these metabolites could be attributed to their absence or, alternatively, their presence at concentrations below the sensitivity threshold of the analytical techniques used. This information underscores the significance of considering enzyme inhibition effects when studying the metabolism of compounds like XN, as it directly influences the profile of metabolites formed in-vivo. The findings contribute to a comprehensive understanding of the interactions between XN and cytochrome P450 enzymes, providing valuable insights into the potential impact of XN on the overall metabolic landscape in humans.

Phase II metabolism, particularly glucuronidation and sulfation, plays a pivotal role in the active metabolism of XN (assuming XN refers to a specific compound or substance). This intricate biochemical process involves the addition of specific molecules, such as glucuronic acid or sulfate, to the parent compound (XN) or its metabolites. In the case of XN, glucuronidation is notably favoured at the 7-O position across all glucuronides, while sulfation predominantly occurs at the 4'O-position. The preference for glucuronidation at the 7-O position suggests a specific molecular interaction between XN and the active site of glucuronosyltransferase, an enzyme responsible for catalysing the glucuronidation process. This selectivity may be attributed to the three-dimensional confirmation of the 7-O position, which seems to be particularly compatible with the active site geometry of glucuronosyltransferase. The specificity of this interaction is crucial for understanding the biochemistry of XN metabolism, as it influences the efficiency and effectiveness of the glucuronidation process. It's worth noting that the phenomenon observed in the metabolism of XN parallels findings in the metabolism of naringenin, a related non-prenylated flavonoid. This suggests a conserved or similar enzymatic preference for the 7-O position in the glucuronidation process among structurally related compounds. The comparative analysis between XN and naringenin sheds light on shared metabolic pathways and enzymatic preferences, providing valuable insights into the broader context of flavonoid metabolism. On the other hand, the prevalence of sulfation at the 4'O-position in XN metabolism indicates a distinct preference for this specific location during the sulfation process. This preference might be influenced by the active site characteristics of the sulfotransferase enzyme involved in this phase of metabolism. Elucidating the structural and chemical factors that contribute to the selective sulfation at the 4'O position could enhance our understanding of the nuanced interactions between XN and sulfotransferase.

In summary, the in-depth analysis of XN metabolism reveals that the 7-O position is favoured in glucuronidation, likely due to the specific conformation that interacts favourably with

glucuronosyltransferase. Additionally, sulfation predominantly occurs at the 4'O position, suggesting specificity in the sulfation process. The parallels with naringenin metabolism underscore the importance of considering related compounds in understanding the intricacies of flavonoid metabolism [210]. Furthermore, the AUC for sulfates was more significant than the glucuronides and thus had an increased value of bioavailability, which was demonstrated with XN the sulfate conjugates and glucuronides over 24 h having a similar AUC (around 250 nmol/L/h), although, much different Cmax values (Xn-7-O-GlcA, 190 nmol/L and XN-7-O-sulfate, 40 nmol/L) [211].

Phase III metabolism, characterised by an apparent enterohepatic circulation of XN metabolites, adds another layer of complexity to the understanding of XN's fate within the body. This observation suggests that there is a cycle of excretion from the liver into the gut, followed by reabsorption, possibly contributing to the prolonged presence of XN metabolites in the systemic circulation. The second peak visible in the pharmacokinetic data, occurring within five hours, indicates a potential reabsorption of metabolites, highlighting the importance of considering the gastrointestinal tract as a dynamic player in the overall metabolism of XN. Analysing the pharmacokinetics of all XN metabolites collectively reveals a rapid conjugation process occurring with the micelle formulation, taking approximately one hour. This initial phase of conjugation is a crucial step in preparing the metabolites for elimination. The observed Cmax (maximum concentration) at around three hours, in the native formulation, suggests a peak concentration of XN or its metabolites in the systemic circulation. Understanding the timing of these events is essential for optimising dosing regimens and predicting the duration of therapeutic effects.

The potential role of p-glycoprotein (P-gp) inhibition in modulating XN bioavailability adds an intriguing layer to the pharmacokinetic profile. P-gp, a membrane transport protein, is known to influence the absorption and distribution of various compounds, including drugs and natural products. Inhibition of P-gp may enhance the absorption of XN and possibly impact its metabolism. The suggestion that inhibiting P-gp could also inhibit the glucuronidation process implies a complex interplay between transport mechanisms and metabolic pathways. This insight into the interconnection of absorption and metabolism can guide strategies to improve the efficacy of XN-based formulations. The reference to mulberin, a prenylated flavonoid found in mulberry, as a potent glucuronosyltransferase inhibitor provides a potential strategy for modulating XN metabolism. The inhibitory effect of mulberin on glucuronidation suggests a broader spectrum of compounds with the capacity to influence this phase of metabolism. Moreover, the mention of cannabinoids from Cannabis Sativa inhibiting UDP-glucuronosyltransferases highlights the diversity of natural compounds that could be explored to fine-tune XN metabolism.

The proposal to couple XN with a glucuronosyltransferase inhibitor opens avenues for enhancing the bioactivity potential of XN. By inhibiting the glucuronidation process, which is a key mechanism in the detoxification and elimination of compounds, the concentration of active XN in the body could

be prolonged. This potential strategy suggests a more nuanced approach to pharmaceutical research, emphasising the importance of combination therapies and exploring synergies between XN and other natural compounds. The in-depth exploration of XN's Phase III metabolism sheds light on its enterohepatic circulation, conjugation kinetics, and the potential modulation of its bioavailability through P-gp inhibition and glucuronosyltransferase inhibition. These findings provide a foundation for designing strategies to optimize the pharmacokinetic profile of XN, offering insights that can be valuable in the development of pharmaceutical formulations with enhanced bioactivity and therapeutic efficacy.

The data presented in manuscript III provides valuable insights into the potential pharmaceutical applications of XN, particularly in terms of dosing and its metabolic profile. The study administered 43 mg of XN in a micellar formula, resulting in sustained plasma levels of its metabolites above 100 nmol/L for the first hour, with minimal free XN detected in the circulatory system [102]. The rapid excretion of XN metabolites occurred after 90 minutes, maintaining concentrations at around 30 nmol/L for approximately 24 hours. One crucial implication of these findings is the scheduling of XN dosing for potential pharmaceutical use, especially in the context of treating COVID infections. The observation that plasma levels of XN metabolites above 100 nmol/L are required for efficacy suggests a dosing regimen of every 90 minutes to maintain therapeutic levels. Conversely, if XN remains effective at 30 nmol/L, a daily dose may be sufficient. However, the challenge arises from the fact that almost no free XN is found in circulation, raising questions about how to accurately assess its pharmaceutical value.

The study emphasises the need to explore the bioactivities of XN metabolites before committing to further development or investment in the pharmaceutical potential of XN. While it's known from other flavonoids, such as naringenin glucuronide, that metabolites can exhibit enhanced bioactivity compared to the aglycone form, the specific bioactivities of XN metabolites remain unknown. This uncertainty complicates the assessment of XN's pharmaceutical value, and further research is essential to clarify the therapeutic potential of its metabolites. Moreover, the discussion points out a critical consideration regarding the study's sample size. Although statistically significant, the low number of participants, coupled with an insufficient representation of both male and female subjects, raises concerns about the generalizability of the findings. While existing knowledge indicates that certain flavonoids, like 8-PN and 6-PN, exhibit consistent pharmacokinetic parameters across genders, a more comprehensive investigation is warranted to discern potential absorption pattern differences between males and females for XN.

In summary, the data from manuscript III underscores the complexity of harnessing XN for pharmaceutical purposes. It highlights the need for further research to elucidate the bioactivities of XN

metabolites, address the limitations in sample size and gender representation, and ultimately determine the feasibility of developing XN as a pharmaceutical agent.

In conclusion, a crucial future aspect that demands investigation in the realm of prenylated flavonoids metabolism, particularly focusing on XN, is the potential interaction with red blood cells during the centrifugation step in blood separation. The majority of analytical methods employed to study prenylated flavonoids metabolism traditionally utilize plasma as the primary analytical medium. However, it remains uncertain whether prenylated flavonoids and their metabolites may be binding to the red blood cell component during the centrifugation process.

Given that many metabolites identified in plasma are glucuronides and sulfates, there exists the possibility that these metabolites could be adhering to the glycogen-rich surface of erythrocytes. This introduces the intriguing prospect that analysing whole blood might unveil entirely different pharmacokinetic profiles than those previously reported based on plasma analysis alone (as this is yet to be realised). To gain insights into this potential phenomenon, a recommended approach involves employing blood partitioning assays. These assays involve analysing the content of each metabolite in both the red blood cell fraction and the plasma fraction subsequent to centrifugation. By comparing the results of these fractions, it becomes possible to determine whether the compound, in this case, XN and its metabolites, exhibits affinity for red blood cells. This information is crucial as compounds adhering to red blood cells may have their bioactivities affected or even quenched. In essence, a comprehensive understanding of the interaction between prenylated flavonoids and red blood cells during blood separation is essential for refining the interpretation of pharmacokinetic profiles. This consideration underscores the need for future research endeavours to delve into blood partitioning assays and assess the content of metabolites in both plasma and erythrocyte fractions, providing a more accurate depiction of the compound's behaviour in the circulatory system.

4.4 Discussion of hop prenylated flavonoids and metabolism

The comprehensive body of work presented in this study introduces a novel method for the analysis of prenylated flavonoids, with a particular focus on those found in hops, beer, and tea. Additionally, the research delves into the exploration of the human metabolism of these prenylated flavonoids. The significance of this analysis lies in the accurate quantification of prenylated flavonoids, especially considering their prevalence in the Western diet, notably in beer. XN is among the most consumed prenylated flavonoid by humans, particularly through the consumption of beer. This dietary source is of particular interest due to the potential health benefits associated with high-hopped beer. There is growing evidence suggesting that the concentrations of prenylated flavonoids in such beverages might offer protection against liver damage, and anecdotal reports even hint at potential immune-supportive effects [108]. However, existing tests often correlate the bioactivities of XN without fully considering the effects of metabolism, which might reveal different mechanisms to be exploited.

The present studies addresses this gap by aiming to identify the metabolic processes that occur during the human metabolism of prenylated flavonoids. Establishing this baseline knowledge was deemed necessary before delving into investigations aimed at uncovering specific metabolism pathways. The work encountered several limitations, primarily stemming from the scarcity of commercial standards for prenylated flavonoids from hops and the complexity of methods required to obtain analytical standards. The lack of readily available commercial standards necessitated the development of synthetic approaches to generate these standards. This step was crucial for the subsequent investigation into the metabolism of prenylated flavonoids. The complexity of these synthetic methods underlines the challenges inherent in studying prenylated flavonoids, emphasising the need for robust analytical techniques to accurately quantify and characterise these compounds in biological samples. This body of work lays the foundation for a deeper understanding of prenylated flavonoids' role in human metabolism. By introducing a new analytical method and addressing the limitations posed by the scarcity of standards, the study paves the way for future investigations into the metabolic pathways of prenylated flavonoids, contributing valuable insights into their potential health effects.

The initial phase of this work laid the groundwork for subsequent investigations on three interconnected levels. Firstly, the production of significant quantities of XN was pivotal, serving as the foundation for various synthetic methods in subsequent research. A cost-effective and efficient method involving a simple NaCl precipitation process to remove chlorophyll was employed. Despite successful chlorophyll removal, residual unknown components persisted, necessitating normal phase column chromatography to attain synthesis grade XN. Once an ample quantity of XN was available, it became the basis for generating all metabolites detected in human plasma and was utilised in all publications produced [94 69 203].

Secondly, reference compounds such as IXN, 6-PN, 8-PN, XN-C, and IXN-C played a crucial role in understanding metabolism. These compounds served as a backbone for modification in synthetic methods, facilitating a comprehensive exploration of metabolic pathways. Thirdly, internal standards,

represented by deuterated counterparts of XN, IXN, 6-PN, 8-PN, XN-C, and IXN-C, were fundamental for accurate quantification using the SIDA methodology. This approach not only enabled precise quantification of XN and related prenylated flavonoids in the main dietary intake source, beer, but also laid the foundation for a range of internal standards in subsequent analyses.

The quantification of prenylated flavonoids in beer was a crucial step, leading to further considerations. As the concentration of prenylated flavonoids in beer is relatively low, it became necessary to optimise analytical methods for enhanced sensitivity. Additionally, the use of 2D NMR data such as HSQC and HMBC permitted structural elucidation, along with prompting the exploration of alternative biochemical approaches, including enzymatic deconjugation. The final phase aimed at refining existing methods, deviating from conventional approaches of deconjugating metabolites. Matrix-matched calibration, utilizing the internal standards from the initial work, formed the basis for this improvement. However, it's notable that bioactivities of XN on the human trial, particularly in areas like lipid metabolism, were not investigated. The expensive nature and low bioavailability of XN, along with the protective effect of micelles against gut degradation, were acknowledged as challenges. The discussion touched upon drug delivery and emphasised the importance of understanding these factors in the context of XN's potential pharmaceutical applications. The multi-level investigation demonstrates a comprehensive approach, from synthesis and modification to quantification and optimisation, in understanding the metabolism and potential bioactivities of prenylated flavonoids, particularly XN. The work sets the stage for future research addressing challenges and refining methodologies for a more thorough exploration of prenylated flavonoids in human health and nutrition.

The future of XN supplementation might be sampling of clinical studies in real time sampling throughout the digestive system, as the research here only implied that 8-PN and 6-PN are being formed in the gut [212]. One key area of research focuses on designing smart pills with the ability to monitor and modulate the metabolism of xenobiotics within the gastrointestinal tract. This involves understanding how the body processes and metabolises drugs, nutrients, and other foreign substances. By incorporating sensors and analytical tools into smart pills, the aim is to gather real-time data on the metabolic processes occurring in the gastrointestinal system. This information can be invaluable for tailoring treatments to individual patients, optimising drug dosages, and minimising side effects. Furthermore, the integration of drug delivery mechanisms within smart pills opens up new possibilities for targeted and controlled release of therapeutic agents. Smart pills can be designed to deliver drugs to specific locations in the gastrointestinal tract, ensuring optimal absorption and efficacy. Optimising targeted drug delivery approach has the potential to improve treatment outcomes while minimizing systemic side effects. However, despite the promising potential of incorporating XN metabolism and drug delivery into ingestible smart pills, there are several technical challenges that need to be addressed.

Biocompatibility: Ensuring that the materials used in smart pills are biocompatible and safe for ingestion is crucial. The smart pills should not cause harm to the gastrointestinal tract or interact

adversely with the body's physiological processes. Power Supply: Smart pills require a reliable and safe power source to operate sensors and drug delivery mechanisms. Designing efficient power supply systems that can function within the confined space of a pill is a technical challenge. Communication and Data Transmission: Establishing robust communication systems for transmitting real-time data from smart pills to external devices is essential. This involves addressing issues related to signal strength, interference, and data security. Miniaturisation: Shrinking the size of sensors, actuators, and other components to fit within the constraints of a pill while maintaining functionality is a considerable challenge. Regulatory Approval: Meeting regulatory standards for safety and efficacy is a crucial hurdle in translating smart pill technology from research to clinical practice. Ensuring compliance with regulatory requirements is essential for widespread adoption. Despite these challenges, ongoing research and technological advancements continue to push the boundaries of ingestible smart pill technology. Overcoming these hurdles holds the potential to revolutionise the field of gastroenterology, offering more personalised and effective diagnostics and treatments for gastrointestinal diseases. In the realm of ingestible smart pills, the incorporation of xenobiotic (XN) metabolism and drug delivery is a critical aspect that holds great promise for advancing clinical treatment of various diseases discussed in the introduction (section 1.5). Integrating XN metabolism and drug delivery functionalities into smart pills might significantly enhance its therapeutic potential and diagnostic capabilities.

The administration of XN can vary, and the method of delivery can influence its bioavailability and subsequent health effects. Here are different types of administration and their potential implications: Oral Administration: XN can be obtained through the consumption of hop-containing products, such as beer. However, the concentration of XN in beer is relatively low, and excessive alcohol consumption may counteract potential health benefits. XN supplements are available in various forms, including capsules and tablets. This method allows for controlled dosages, and supplements may provide a more concentrated and standardized amount of XN compared to dietary sources. Oral administration can potentially contribute to antioxidant and anti-inflammatory effects. Some studies suggest that XN may have protective effects against certain chronic diseases, including cardiovascular disease and cancer [207]. Topical Administration: Creams and Lotions: XN can be formulated into topical creams and lotions for application to the skin . This mode of administration allows for direct absorption through the skin [134 135]. Topical application may be explored for its potential in skincare, as XN exhibits antioxidant properties that could contribute to protecting the skin from oxidative stress and aging. Research in this area is ongoing. In some research settings, XN has been administered intravenously for experimental purposes. Intravenous administration is typically employed in research studies to investigate specific pharmacological effects and is thus so far only carried out in animal studies. It may allow for a more rapid and controlled delivery of XN, but it is not a common route for practical use in the general population. Nanoparticle Formulations of XN improve its solubility and bioavailability [203]. Therefore, nanoparticle formulations may enhance the therapeutic potential of XN by overcoming limitations related to its poor solubility. This could lead to improved bioavailability and increased effectiveness and might protect XN

from the undesired conversion into IXN. Finally, food products containing XN such as energy bars or functional beverages, might provide a convenient and palatable way to consume the bioactive compound. This approach would allow for the integration of XN into daily dietary habits. The health effects would be similar to those associated with oral administration, with potential benefits for overall health and wellness [213]. It's important to note that while XN shows promise in preclinical studies, more research, including clinical trials, is needed to fully understand its safety and efficacy in various administration forms. Additionally, individual responses to XN may vary, and potential interactions with medications should be considered.

4.5 Overall conclusion

To answer the question of how the bioactive compound XN in hops is metabolised in humans, various compounds were synthesised. For example in manuscript I., six reference compounds and their equivalent stable isotopologues (deuterated enriched) of XN, IXN, 6PN, 8-PN, XN-C and IXN-C were produced. The standards were then used to quantify the most abundant prenylated flavonoids in beer using the gold standard method for quantification, SIDA. The analysis of prenylated flavonoids in various beers revealed further knowledge about amounts of prenylated flavonoids typically found in beer as beer is the highest dietary intake of prenylated flavonoids known. It was additionally first time that XN-C and IXN-C have been detected and quantified in beer. Furthermore, it is the first time hop tea was investigated for the presence of any prenylated flavonoids although their concentration was extremely low and most likely does not contribute health effects or taste.

In the second part 13 metabolites were synthesised that have uses in understanding the biochemistry of XN and its observed bioactivities at a cellular level. The metabolites included the most prominent XN-7-O-GlcA, IXN-7-O-GlcA, 8-PN-7-O-GlcA, 6-PN-7-O-GlcA, XN-4'-O-sulfate, IXN-4'-O-sulfate, 8-PN-4'-O-sulfate and 6-PN-7-O-sulfate metabolites amongst others. Using the synthesised metabolites unequivocally identified several human metabolites after XN consumption and calculating their presence in human blood plasma. Future uses for the new metabolites include observing cell absorption and blood partitioning assays. It is critical that bioactivity testing on these compounds is carried out in the future, however, this was not carried out in this work due to the lack of laboratory facilities with that capability.

The final part of the investigation was a human trial quantifying XN metabolites in humans after the consumption of a micellular and native formulation, the first of its kind. The study revealed that micellarised XN is five-fold more effective when considering oral administration than the native form. There were also hints that XN undergoes enterohepatic recirculation. Overall 28 metabolites were found and the pharmacokinetic profiles identified. The work presented demonstrates that following the metabolism of one compound is more complex than previously thought and simple beverages such as beer and tea contain more prenylated flavonoid variations than previously known. Bringing everything back to Paracelsianism "the dose makes the poison (medicine)" the typical concentrations of XN found in beer is low and demonstrates that during metabolism most XN is conjugated. Although the dose of XN reaching cell targets is minimal, bioactive effects of the metabolites on humans cannot be ruled out. A future requirement is assessing the bioactivity of the metabolites and then perhaps XN might lead to an array of new nutraceuticals and pharmaceuticals. As the in-vitro and animal studies show, XN prevents a selection of health disorders, and is promising for treating acute covid-19 and liver damage. However, the results from the rapid metabolism of XN demonstrate the need to lessen the amount of phase II metabolism unless bioactivity evaluation reveals the glucuronide and sulphated products are potently bioactive, which cannot be ruled out.

5. Appendix

5.1 Stable isotope dilution analysis of the major prenylated flavonoids found in beer, hop tea and hops [94].

frontiers in Nutrition

ORIGINAL RESEARCH
published: 15 December 2020
doi: 10.3389/fnut.2020.619921

Stable Isotope Dilution Analysis of the Major Prenylated Flavonoids Found in Beer, Hop Tea, and Hops

*Lance Buckett[1], Simone Schinko[1], Corinna Urmann[2,3], Herbert Riepl[2,3] and Michael Rychlik[1]**

[1] Chair of Analytical Food Chemistry, Technical University of Munich, Freising, Germany, [2] Organic-Analytical Chemistry, Weihenstephan-Triesdorf University of Applied Sciences, Straubing, Germany, [3] Campus Straubing for Biotechnology and Sustainability, Technical University of Munich, Straubing, Germany

Prenylated flavonoids from hops (*Humulus lupulus*) have become of interest in recent years due to a range of bioactivities. The potential health benefits of prenylated flavonoids include anti-cancerous activities and treatment of the metabolic syndrome among others. Since prenylated flavonoids from hops have shown pharmaceutical potential in clinical trials, robust analytical methods to determine their concentrations in food, supplements, and beverages are required. One such, the gold standard of analytical methods, is stable isotope dilution analysis due to its ability to compensate matrix effects and losses during sample work-up. As no commercial standards were available, the synthesis of seven different prenylated flavonoid isotopes utilizing various strategies (microwave assistance, acid base catalyst in the presence of deuterated substance and lastly, the use of Strykers catalyst) is described. The produced prenylated flavonoid isotopes were then applied in the first stable isotope dilution analysis method that quantified six natural prenylated flavonoids (Isoxanthohumol, Isoxanthohumol-C, 8-Prenylnaringenin, 6- Prenylnaringenin, Xanthohumol, and Xanthohumol-C) in beer, hop tea and hops to prove its applicability. The SIDA-LC-MS/MS method was validated resulting in LODs and LOQs for all analytes between 0.04 and 3.2 μg/L. Moreover, due to the simple clean-up the developed method allows the prospect for measuring clinical samples in the future.

Keywords: beer (analysis method for), stable isotope dilution analysis (SIDA), xanthohumol, xanthohumol C, isoxanthohumol, isoxanthohumol C, 8-prenylanaringeninx, 6-prenylnaringenin

OPEN ACCESS

Edited by:
Sascha Rohn, Technische Universität Berlin, Germany

Reviewed by:
Michal Halagarda, Kraków University of Economics, Poland
Giuseppe Annunziata, University of Naples Federico II, Italy

***Correspondence:**
Michael Rychlik
michael.rychlik@tum.de

Specialty section:
This article was submitted to Food Chemistry, a section of the journal Frontiers in Nutrition

Received: *21 October 2020*
Accepted: *26 November 2020*
Published: *15 December 2020*

Citation:
Buckett L, Schinko S, Urmann C, Riepl H and Rychlik M (2020) Stable Isotope Dilution Analysis of the Major Prenylated Flavonoids Found in Beer, Hop Tea, and Hops. Front. Nutr. 7:619921. doi: 10.3389/fnut.2020.619921

INTRODUCTION

Prenylated flavonoids (PF) derived from hops have undergone an increased interest in recent years regarding their potential for improving health and uses in treating various disorders. Xanthohumol (XN), the most prevalent PF in hops shows an effect on metabolic syndrome (perhaps via modulation of glucagon -like-peptide-1), prevention of DNA damage, and has anti-cancer properties (1–4) Interestingly, many of XN plant metabolites and degradation products (**Figure 1**) possess bioactivities (4, 5). 8-Prenylnaringenin (8-PN) is the most potent phytoestrogen known so far (6). In addition 6-Prenylnaringenin (6-PN), the isomer of 8-PN, is slightly estrogenic, but also shows an anti-proliferative effect on different cancer cell lines (7). Another PF, Xanthohumol-C (XN-C), initiates differentiation in neuronal precursor cells and is neuroprotective (8). Accordingly, it seems to be a candidate for treating neurodegenerative diseases (9). The isomerized XN-C,

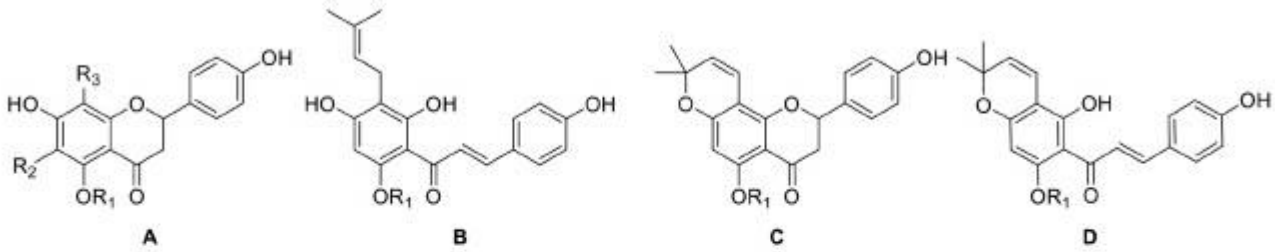

FIGURE 1 | Structures of the prenylated flavonoids **(A)** Isoxanthohumol (R1=CH3, R2=H, R3=Prenyl), 8-Prenylnaringenin (R1=H, R2=H, R3=prenyl): 6-prenylnaringenin (R1=H, R2=Prenyl, R3=H). **(B)** Xanthohumol (R1=CH3). **(C)** Isoxanthohumol-C (R1=CH3). **(D)** Xanthohumol-C (R1=CH3).

isoxanthohumol-C (IXN-C) shows only a slight differentiation inducing effect and accordingly, that makes the chalcone structure all the more interesting (10). Clinical trials show that PFs have a pharmaceutical use as non-modified forms (flavones) or by slight modifications e.g., removal of the Michael system (i.e., cyclization of chalcones into flavanones, or hydrogenation of the Michael system) (11–13). Further studies investigating the *in-vivo* effects are required to fully understand the beneficial properties of PF concerning different diseases and, therefore, robust and sensitive analytical methods that target the bioactive hop compounds are needed, for example, stable isotope dilution analysis (SIDA) (1). To date, SIDA has not been applied for analysis of hop PFs.

Common analytical methods applied on PF found in hops are HPLC, immunoassays, square-wave adsorptive-stripping voltammetry, high performance thin layer chromatography, MALDI, and LC-MS/MS using two different ionization sources (APCI and ESI) (1, 14–16). Some of the caveats of the current methods are: (i) they require expensive development of antibodies, (ii) are not specific enough, (iii) rely on expensive SPE clean-up, (iv) have no internal standard, or (v) use a single internal standard which might have unseen errors due to matrix effects in MS measurements (1, 17). All the disadvantages of the methods above are overcome by SIDA, the current analytical gold standard in mass spectrometry (18). The advantages of SIDA compared to LC-MS/MS using an internal standard are that it can compensate the matrix effect and work up errors as only the ratio of the isotopolog is measured. The isotope labeling of the IS, guarantees accuracy also in sample workup due to having nearly the same physical and chemical properties as the analyte i.e., losses during workup are retained as the ratio of A/IS, which is commonly accepted to be constant (18). Combined with a simple clean up, SIDA is a rapid analysis method, which is suitable for large scale intervention trials. Therefore, we aim to develop the first SIDA method on hop PFs and test the appropriateness by quantifying PF content in beer, hops, and hop tea.

As the name suggests, SIDA requires the use of isotope-labeled substances. So far, XN was isotope-labeled via multi-step synthesis or plant feeding experiments. Initially, Berwanger et al. produced a ^{13}C-XN by feeding hop flower cuttings with different labeled precursors and concluded that universally labeled ^{13}C glucose was the best supplement with 9.41% of the product labeled (19). Additionally, the same research group produced ^{14}C XN at 318 microCi/mmol (20). More recently, (21) carried out the successful total synthesis of XN enriched with ^{13}C (21, 22). The total synthesis of XN used seven steps producing a yield of 5.7%. Both of the above options are time consuming and expensive with low yields and no methods for other PFs other than XN are described. Furthermore, plant feeding experiments are generally poorly suited for SIDA, due to the presence of unlabeled isotopologues. In this study an approach to produce isotopically labeled PFs enriched with deuterium by utilizing various methods e.g., Strykers Cat, acid base catalyzation and microwave enrichment is described (23–27). The produced stable isotopes were then applied and validated using an LC-MS/MS-SIDA method to quantify the natural occurring PFs in a few selected samples of beer, hops, and hop tea.

MATERIALS AND METHODS

General Experimental Information

All reactions were carried under inert atmosphere of argon or nitrogen unless stated. All chemicals were of technical grade unless stated. TLC monitoring was carried out during all reactions. The TLC plates used for development were silica on alumina 60 F254 (Merck). For TLC development a solvent system of 60:40 EtOAc:Hexane was utilized (Merck, Deutschland) and the stain was prepared using CAM-reagent: Ammonium molybdate tetrahydrate (Sigma aldrich) (3 g), cerium ammonium sulfate dihydrate (Sigma aldrich) (1 g), sulfuric acid 10% 100 mL (Sigma aldrich), stirred vigorously and filtered twice through filter paper (H 1/2 filter paper Schleicher & Schuell). TLC plates were dipped in the stain and heated using a heat gun until the TLC plates turned blue and dark spots formed. The analytical standards that underwent qNMR were dissolved in 600 µL MeOD-d4 (≥99.8% D, Sigma Aldrich, USA) with NMR tubes (177.8 × 4.97 mm, Bruker, USA). Staff members at the Chair of Molecular Sensory Science at the Technical University Munich carried out the NMR and qNMR experiments with a Bruker Advance II 400 MHz and 500 MHz NMR spectrometer. Data evaluation was conducted on MestReNova (Mestrelab Research, Spain) software. All samples that underwent LC-MS/MS analysis were filtered using a 0.22 µm filter (Chromafil® Xtra PVDF-20/13, 0.20 µm, Ø 13 mm; Macherey-Nagel).

LC-MS/MS Analysis

Preparation of Standard Solutions

Each analytical and internal standard underwent quantitative NMR (qNMR) in methanol-d6 to determine the concentration before being made up to a final concentration of 1 mg/mL and placed in −80°C freezer. An exception is D3-8-PN and D3-XN-C the concentrations of which were calculated using HPLC-UV from calibration graphs produced by the standard compounds 8-PN and XN-C as the amounts produced in the reactions were too low for qNMR.

LC-MS/MS Parameters

The chromatographic separation of the analytes was performed on a Shimadzu Nexera X2 UHPLC system (Shimadzu, Kyoto, Japan). The LC-parameters used solvent (A) H2O (0.1% FA) with ACN (0.1%) FA, solvent (B) with the initial solvent settings started at 25% B and increased to 35% B at 4 min where it remained until being linearly increased from 35 to 95% at 12.5 min. At 12.5 min the solvent remained at 95% B for 3.5 min until returning over 1 min back to 25%. Overall, each run took 22.5 min. The MS instrument operated in the positive electrospray ionization (ESI) mode for all analytes. The column (Restek Raptor FluoroPhenyl 2.7 μm 100 x 2.1 mm) protected with a precolumn with penta fluoro propyl phenol (PFPP) Shimadzu, Velox EXP Guard 2.1 x 5 mm) was equilibrated for 5 min between each injection. Samples were injected at 1 μL, the flow was set at 0.3 μL/min and the column oven was set to 30°C. Using an additional valve after the column, the solvent flow was introduced into the mass spectrometer at 4 min after injection to prevent the instrument from matrix contamination. The LC was coupled to a triple quadrupole mass spectrometer (LCMS-8050, Shimadzu Corporation, Kyoto, Japan). Parameters for MS were as follows: heating gas at a flow 10 L/min, nebulizing gas flow 3 L/min, drying gas flow 10 L/min, heat block temperature 400°C, desolvation line temperature 250°C, interface temperature 300°C, interface voltage 4 kV, and collision-induced dissociation gas pressure 270 kPa. The mass spectrometer worked in the scheduled multiple reaction monitoring (MRM) mode for MS/MS measurements. Optimized voltages and collision energies, the retention time of each analyte are listed in **Table 1**. The LabSolutions software (Shimadzu, Kyoto, Japan) was utilized for data acquisition and data analysis.

Analytical HPLC

The analytical HPLC analysis utilized a Shimadzu HPLC-DAD (SPA-M20A) coupled with a liquid chromatograph system (LC-20 AD, Shimadzu, Kyoto, Japan). Samples were automatically injected with an autosampler (SIL-20A HAT, Shimadzu, Kyoto, Japan) and a degassing unit (DGU-20A3R) was used when solvent system was active. Analyte separation used a C18 (YMC-Pro pack, 3 μm, 12 n, 150 x 3 mm Machery-Nagel) with a precolumn (C18, 8 x 3 mm). The mobile phase consisted of 0.1% FA in HPLC grade water as solvent A and 0.1% FA in ACN as solvent B. The flow rate was set 0.3 ml/min with gradient starting at 50% B for 2.0 min, and then gradually increasing solvent B to 90% at 11.0 min. The mobile phase remained at 90% for a further 2.5 min before being returned to 50% B. The column was equilibrated for 5 min between injections of 10 μL. Chalcones were monitored at 370 nm and flavanones at 290 nm. 8-PN was used for the calibration of D3-8-PN and XN-C was used for D3-XN-C at 0.56, 1.1, 1.7, 2.2, 2.8, 3.3, 3.9, 4.4, and 5.0 mg/L in ACN (see **Supplementary Material**).

Sample Preparation

Beer

Fifteen beers that represented a cross section of brewery products of Bavaria were purchased from local supermarkets. They were opened and degassed using sonication. A 1 mL aliquot of each beer was placed into a 4 mL vial and IS were spiked at various concentrations, deuterated isoxanthohumol (D3-IXN) at 6.99 μM, deuterated isoxanthohumol-C (D3-IXN-C), and deuterated xanthohumol (D3-XN-C) at 0.14 μM, deuterated 8-prenylnaringenin (D3-8PN) at 0.29 μM, deuterated 6-prenylnaringenin (D3-6-PN) at 0.15 μM and deuterated xanthohumol (D3-XN) at 0.14 μM. 1 mL of EtOAc was added and the vials mixed using a vortex (Vortex Genie 2, Scientific Industries). Taking the supernatant, which was repeated 3 times, the combined organic phase of the samples was dried under N2 (set at 30°C) and resolved in 1 mL ACN.

Hops

Using a method derived from Stevens et al., a packet of pelletized hops (Columbus, 15.6% α-acid, USA HOPS) of a high alpha acid (15.6% AA) was purchased from the local brewing shop and ground frozen using a mortar and pestle (28). 0.1 g of the powder was taken and extracted using sonication and 100 mL of EtOAc for 15 min. Samples (0.1 mL) were spiked with IS, dried and re-dissolved in 1.0 mL of ACN.

Hop Tea (5%)

A brand of hop tea was purchased from the local supermarket and two different preparations were investigated. One tea bag was prepared following the instruction on the packet. 100 mL of boiling (distilled) water was added to one tea bag and brewed for 5 min. Once the tea was at room temperature the IS were spiked and the solution was dried using a N2 drier and a heating plate set at 30°C. Another sample of tea was crushed using a mortar and pestle and prepared the same as the hop pellets.

Method Validation and Statistical Analysis

The developed method and workup procedures were validated according to the procedure of Vogelgesang and Hädrich (29). All LC-MS/MS data was collected and integrated using lab solutions software (Shimadzu Europa GmbH) and data transferred into Microsoft excel where all calculations were performed using excel functions (Microsoft Corporation, USA).

Preparation of Calibration Graphs

Calibrators of all 6 analytes (Reference standards) were spiked against their internal standards (IS) in ACN at the following molar ratios [n(Ref)/n(IS)]: IXN, 14 points: 100:1, 80:1, 60:1, 40:1, 20:1, 10:1, 7.50:1, 1:1, 1:20, 1:40, 1:60, 1:80, 1:100 (R^2 = 0.9982). IXN-C 12 points: 100:1, 60:1, 25:1, 10:1, 7.5:1, 5:1,1:1, 1:20, 1:40, 1:60, 1:80, 1:100. (R^2 = 1). 8-PN, 14 points: 25:1, 15.:1, 12.5:1, 9.7:1, 7.5:1, 5.0:1, 4.4:1, 3.9:1, 3.3:1, 2.8:1 1.7:1,

TABLE 1 | The MRM profiles of the isotopologues compared with the MRM profiles of the reference compounds being analyzed.

Analyte-D_3	D_3-XN	D_3-IXN	D_3-6-PN	D_3-8-PN	D_3-IXN-C	D_3-XN-C
MRM-1	358.20–180.15 (CE:−21.0)	358.25–180.05 (CE:−26.0)	345.20–289.20 (CE:−16.0)	345.20–166.15 (CE:−25.0)	356.20–235.20 (CE:−22.0)	356.20–234.20 (CE:−20.0)
MRM-2	358.20–302.20 (CE:−12.0)	358.25–302.15 (CE:−17.0)	345.20–167.10 (CE:−27.0)	345.20–167.15 (CE:−24.0)	356.20–234.70 (CE:−23)	356.20–81.10 (CE:−16.0)
MRM-3	358.20–181.15 (CE:−23.0)	358.–301.20 (CE:−15.0)	345.20–166.15 (CE:−28.0)	345.20–288.20 (CE:−16.0)	356.20–82.10 (CE:−44.0)	356.20–111.15 (CE:−33)
Analyte-Ref	**XN**	**IXN**	**6PN**	**8-PN**	**IXN-C**	**XN-C**
MRM-1	355.10–179.25 (CE:−21.0)	355.30–179.25 (CE:−24.0)	341.35–165.20 (CE:−29.0)	341.35–165.20 (CE:−18.0)	353.00–233.20 (CE:−22.0)	353.20–233.15 (CE:−21.0)
MRM-2	355.10–299.30 (CE:−12.0)	355.30–299.30 (CE:−15.0)	341.35–285.30 (CE:−15.0)	341.35–285.25 (CE:−15.0)	353.00–191.20 (CE:−32.0)	353.20–191.10 (CE:−31.0)
MRM-3	355.10–113.25 (CE:−23.0)	355.30–172.15 (CE:−9.0)	341.35–123.10 (CE:−37.0)	341.35–123.0 (CE:−33.0)	353.00–109.20 (CE:−35.0)	353.20–109.15 (CE−33.0)
Deuterium Enrichment	m/z +3	m/z + 3	m/z +4	m/z +4	m/z +3	m/z +3

0.1:1, 0.05:1, 0.04:1 ($R^2 = 0.9995$). 6-PN 11 points: 20:1, 15:1, 12.5:1, 5.9:1, 1.98:1, 1.5:1, 1.3:1 0.65:1, 0.43:1, 0.2:1, 0.002:1. ($R = 0.9999$). XN, 11 points: 100:1, 80:1, 60:1, 40:1, 20:1, 1:1, 1:20, 1:40, 1:60, 1:80, 1:100 ($R^2 = 0.9996$). XN-C, 10 points: 80:1, 60:1, 40:1, 20:1, 1:1, 1:20, 1:40, 1:60, 1:80, 1:100 (R^2 0.9997). The calibration graphs were formed from the LC-MS/MS data collected and from integration of the area of each peak using lab solutions software (Shimadzu Europa GmbH). The area of each peak A(ref)/A(IS) was then plotted into Microsoft excel (Microsoft Corporation, USA) against the known n(ref)/n(IS). Mandel testing confirmed linearity of the graphs and the equation resulted in determining the concentration of the prenylated flavonoids found in the samples (30). See **Supplementary Material** for each plotted calibration graph. Each calibrant level was injected 3 times and are the average value reported.

Precession, Limits of Detection and Limits of Quantification

The LOD concentrations were initially estimated by DIN 32645 (31). A hop free beer, a kindly gift of the TUM Research Center Weihenstephan for Brewing and Food Quality., served as blank matrix. Activated charcoal 1 g was added to the hop free beer (50 mL) and the solution was left to stirring for 1 h before being filtered through filter paper. The hop free beer was extracted three times with EtOAc (50 mL) and then concentrated to dryness and dissolved in ACN. The blank matrix was then spiked with the corresponding amounts of analytes near the estimated LOD to apply the method by Vogelgesang and Hädrich (29): IXN (0.18, 0.70, 1.3, 1.8 μg/L, and IS at 1 μg/L), IXN-C (0.05, 0.35, 0.2, 0.5 μg/L, and IS at 0.5 μg/L), 8-PN and XN (0.25, 1.0, 1.8, 2.5 μg/L, and IS at 2.0 μg/L), 6-PN (0.16, 0.64, 1.1, 1.6 μg/L, and IS at 1.0 μg/L), XN-C (0.2 μg/L, 0.8 μg/L, 1.4 μg/L, 2.0 μg/L and IS at 0.5 μg/L). For recoveries the matrix was spiked at 4 different levels (2 low and 2 high). IXN low level, 0.004, 0.009 mg/L (D_3-IXN 0.0025 mg/L), and high 2.5, 4.0 mg/L (D_3-IXN at 2.5 mg/L). IXN-C low level, 0.004, 0.009 mg/L (D_3-IXN-C 0.0025 mg/L), high level 0.5, 0.05 mg/L (D_3-IXN-C 0.1 mg/L). 8-PN, low level 0.004, 0.009 mg/L (D_3-8-PN, 0.0025 mg/L). High level 0.5, 0.25 (D_3-8PN, 0.1 mg/L). 6-PN low level 0.004, 0.009 mg/L (D_3-6-PN 0.00125 mg/L). High level 0.5, 1.0 mg/L (D_3-6PN 0.25 mg/L). XN, low level 0.004, 0.009 mg/L (D_3-XN 0.0025), and high level 0.5, 1.0 mg/L (D_3-XN 0.5 mg/L) XN-C low level, 0.004 mg/L and 0.009 mg/L (D_3-XN-C: 0.0025 mg/L), and high level 0.025, 0.05 (D_3-XN-C 0.05 mg/L). Each sample underwent the same extraction in section Beer, and molarity of each compound was calculated using linear regression using the calibrations graphs prepared above. The ratios of the theoretical spiked vs. the calculated values determined the recoveries, LOD and LOQ. Precision was checked by triplicate determination of a mixed sample being injected 9 times and the RSD of ratios of the A(ref)/A(IS) calculated. Intra-daily precision was determined by measuring 3 samples twice during one day and the inter-daily precision was determined by measuring a sample 3 times weekly using double injections.

Calculation of the Prenylated Flavonoid Content

The concentration of each analyte in each sample was calculated by taking the integrated area ratio of the analyzed reference compound (unknown) compared to the peak area of the spiked internal standard. The ratio of A(ref)/A(IS) was then used with linear regression equation reported in each excel graph to calculate the concentration [i.e., n(unknown)/n(IS)] in the samples in triplicate +− SD. The total PF content was calculated from the sum of each analyte using the excel function. The concentration of the PF in samples are expressed as the mean +− SD.

Analytical HPLC

To characterize and quantify labeled XN-C and 8-PN analytical HPLC was necessary. HPLC using a LC-20 AD Shimadzu Prominence HPLC System (Shidmadzu Kyoto, Japan) coupled with a SPA-M20A prominence diode array detector. And a YMC-

Pack Pro C18, S-3 µm, 12 n, 150 x 3 mml. D, precolumn: 8 x 3 mm (Machery-Nagel, Düren, Germany) column. The retention times and UV profiles were compared with the non-deuterated compound (see **Supplementary Material**). The non-deuterated forms of XN-C and 8-PN were constructed into calibration solutions of 5.0, 4.4, 3.9, 3.3, 2.8, 2.2, 1.7, 1.1, and 0.6 mg/L. Upon evaluation of the graphs equations of XN-C $y = 0.00001x + 0.0724$, $R^2 = 0.998$ and 8-PN $y = 42810x + 1007$, $R^2 = 0.999$ were used to quantify the concentration of the D3-XN-C and D3 8-PN.

RESULTS AND DISCUSSION

Synthetic Results

As no commercial isotopically labeled standard of any prenylated hop flavonoid were available all isotopologues were synthesized (**Figure 2**) before SIDA was carried out (for detailed synthesis instruction see **Supplementary Material**). First, the isotope labeled standard of IXN was synthesized using wet chemistry, cyclisation following (32), with all protic solvents replaced by deuterated equivalences (32). To produce isotopically labeled xanthohumol (D_3-XN), 6-prenylnaringenin (D_3-6PN), 8-prenylnaringenin (D_3-8PN) and isoxanthohumol (D_3-IXN) two synthetic methods were combined. One, the removal of aryl methyl ethers by LiCl in DMF and the other, enrichment of deuterium by D_2O and catalyst mixtures of Pt (30%)/C, Pd (30%)/C, Rh (10%)/Al. (26, 33). Using this approach, four isotopically labeled standards (D_3-IXN, D_3-6-PN, D_3, 8-PN, and D_3-XN) were created in 1 pot (**Supplementary Material**) reaction. A recent method using the demethylation and microwave approach has greatly improved the yields for production of non-deuterated 6- and 8-PN (27). The synthesized D_3-XN and deuterated IXN (by wet chemistry approach) were then further reacted into D_3-XN-C and D_3-IXN-C using a known selective cyclisation of the prenyl-group (10).

To overwhelm the electronically activation of the Michael system of XN, Stryker catalyst, which selectively lead to hydrogenation of the double bond, was used to synthesize the isotope labeled standard dihydroxanthohumol (DXN) by using a deuterated form rather than conventional donation of protons (**Supplementary Material**) (23, 34).

Mass Spectrometry of Synthesized Isotopes

The enrichment of deuterium in the isotopologues were confirmed using MS (see **Table 1**) and NMR analysis (**Supplementary Material**). In MS analysis, PFs fragmentate mainly via retro-diels alder which leads in case of the natural chalcone XN to the A-ring fragment (m/z 179) and the B-ring fragment (m/z 120). The fragmentation pattern of the isotopolog shows an A-ring (m/z 180), which leads to the assumption, that one deuterium is exchanged on the A-Ring. Furthermore, it can be concluded from fragmentation pattern, that one deuterium is exchanged on the B-Ring and one on the Michael system (**Figure 3**). Importantly no labeling is in the prenyl side chain as this would not be visible in MRM fragmentation and the fragment ion would have the same m/z as the precursor ion. A similar pattern can be seen in the analysis of D_3-IXN, D_3-6PN, and D_3-8PN (**Table 1**). In case of the DXN derivative the high resolution mass spectrometry showed the incorporation of only one deuterium on the former α, β-unsaturated double bond (**Supplementary Material**), leading to the assumption that keto-enol equilibration does not save the deuterium in α-position from being exchanged. The NMR analyses confirmed the results of the mass spectrometry and are shown in the **Supplementary Material**.

The SIDA method should allow a simple, rapid and robust analysis concerning prenylflavonoids (PFs) for quantification in beer, hop products and future *in vivo* experiments. For the latter the DXN derivative is suitable, since the Michael system suggests a reduced bioavailability. All substances have a natural distribution of isotopes (in particular carbon-12 and carbon-13) and for an accurate SIDA there needs to be a certain increase in the mass making the difference measurable by mass spectrometer. The fact that DXN only has one D label made it not viable to be used in the SIDA method. However, the isotope analogs of the main natural prenylflavonoids D_3-IXN, D_3-IXN-C, D_3-8-PN, D_3-6PN, D_3-XN, and D_3-XN-C were deemed viable as they all had an increase between m/z of +3 to +4 Daltons. **Table 1** shows a summary of the results for collisions energies and the mass transitions that were selected during the MRM optimizations and were incorporated into the LC-MS/MS method (35).

Method Validation

Calibration for SIDA was performed by measuring mixtures of the reference standards and the internal standards at known concentrations. The response factor was obtained by linear regression plots after testing linearity according to (30). The calibration curves for each compound plotted are Area(ref)/Area(IS) over the n(ref)/n(nIS) and resulted from a triple injection (**Supplementary Figures**). The LOQ and LOD was calculated in Microsoft Excel (Microsoft Corporation, USA) according to the requirements of Vogelgesang and Hadrich, i.e., blank matrices were spiked with reference compounds and internal standards at known concentrations near an estimated LOD (29). The samples were worked up according to section Beer and analyzed in triplicate and concentrations of each analyte were compared to the theoretical values. The LOD was set at the 95% confidence level, where the maximum peak of a blank would be detected (29). The LOQ was set at four times the LOD. In a sense the LOQ and LOQ was a recovery test, but performed at an extreme. Therefore, additional recoveries, were tested at different concentrations of analytes and not above the LOQ. The recoveries were determined on a low (0.004–0.009 mg/L) and a high level (0.025–4.0 mg/L) resulting in 81.0–113.3% (see **Table 2**) for each specific analyte.

The LOD and LOQ (**Table 2**) are similar to previously reported values, although the levels for XN and IXN presented here are lower. Stevens et al., using a triple quadrupole LC-MS/MS system with selective reaction monitoring, reached a LOQ of 10 ng/mL, which is at least double of the values measured here (LOQ 0.3–3.74 ng/mL) (28). The improvement is probably due to the use of SIDA with the carrier effect using

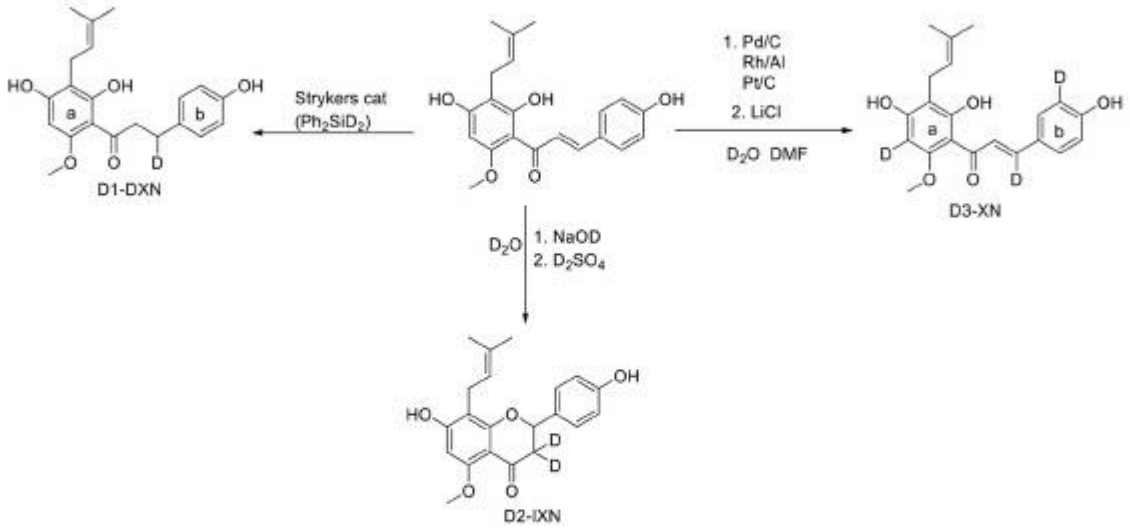

FIGURE 2 | The synthetic approaches applied to synthesize isotope labeled prenylated flavonoids.

internal standards eluting simultaneously with the analytes (28). However, using the more conventional method, i.e., comparing the signal to noise ratio, might provide a lower LOD than the method of Vogelgesang, and Hadrich, as it has less stringent criteria by not spiking blank matrixes and reporting the response (29). Using a single quadrupole MS PFs were analyzed in urine with LODs between 0.2 and 0.6 ng/mL (36). Additionally, in the method described here only 1 μL of sample was injected into the MS and therefore, room for improvement might be possible as increasing the injection volume might increase the sensitivity. Perhaps for the analysis of clinical samples this would be necessary.

Quantification of Hop Prenylated Flavonoids in Samples Using SIDA

For SIDA a simple LLE method was developed. It enabled a faster work up than solid phase extraction (SPE). Furthermore, it has been reported that LLE is superior in regards to retaining the PF as SPE results in poor recoveries for some analytes as each PF is eluted at different retention factors (1). This was also observed by us using SPE in the development of the analytical method. Spiking LLE samples with labeled standards allowed minimal clean-up steps and less losses of analytes due to the ratio of each analyte against the internal standard remaining constant throughout the work-up process as the physical properties of the internal standard and the analyte are virtually identical. Therefore, regardless of the total losses of analyte the concentration can be calculated as long as the analyte and the internal standard ratio is detectable. The matrix effect during beer analysis was anticipated by utilizing SIDA due to the respective labeled internal standards being eluted at the same time. A structurally different internal standard has a different elution time than the analyte, which can lead to large errors as there is no compensation for the matrix suppression or enhancement that may occur. Additionally, here for the first time we report the quantitation of IXN-C and XN-C in beer, which are relatively unstudied prenylated flavonoids. Lastly, it is the first SIDA method that has been utilized on prenylated flavonoids found in hops.

LC-Parameters

The LC method was designed so that sugars and carbohydrates that may have been extracted during the LLE were mostly omitted by diverting the initial 6 min of LC to waste. Additionally, the elution of the compounds of interest was devised to the isocratic phase of the method enabling a more uniform peak shape. The PFPP LC column used has been reported by Sus et al. (37) to be very suitable to separate prenylated flavonoids due to the phenolic-phenolic interactions (37). Additionally, compared to the C_{18} phase, no apparent retention time shifts were observed with the PFPP stationary phase (38). Thus, most of the analytes are eluted separately and IXN-C and 8-PN are almost base line separated (**Figure 4**) which is not a problem in MS quantification.

Quantification of Prenylated Flavonoids in Beer, Hop Tea, and Hops

In order to prove the applicability of the new SIDA we quantified the PFs in different beers as summarized in **Table 3**. As the selection of beer samples are neither representative nor comprehensive, our results may only indicate the principle distribution of PFs in the different beer types. The total concentrations of PFs reported by (28) were between 43 and 4000 μg/L, and in European beers between 43 and 2680 μg/L (28, 39). Here we report comparable results between 723 and 2456 μg/L (see **Table 3**). A more recent analysis of beer polyphenols revealed a range of prenylated flavonoids of 0 and 9500 μg/L and highest containing beers were stouts and IPAs with an average range between 1.900 and of 2190 μg/L (40). The values of the stouts in general are comparable to

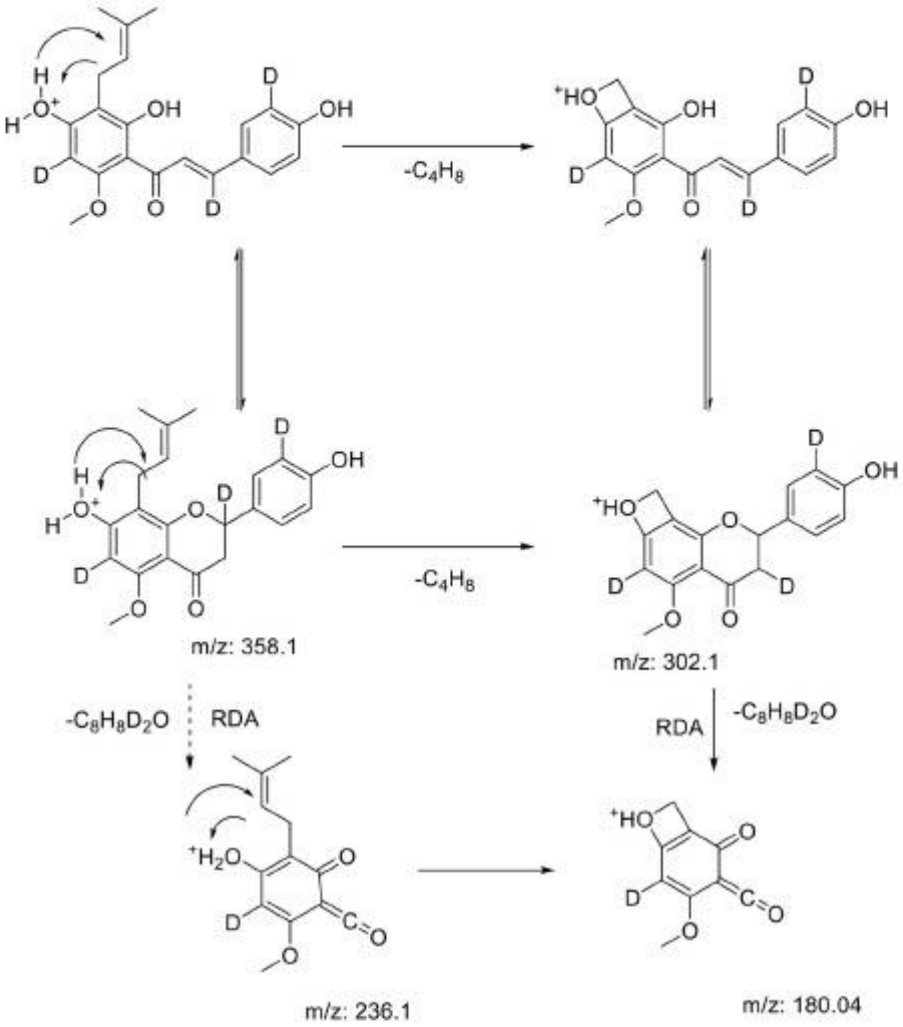

FIGURE 3 | Fragmentation patterns of the prenylated flavonoids in hops adapted from Stevens et al. (35). The example given here is our proposed scheme using MRM information for the fragmentation of D_3-XN. RDA is retro Diels Alder rearrangement. All fragments were observed during MRM of deuterated products.

our values (2445 μg/L), and only one sample (a black IPA with 9500 μg/L PF) which was not analyzed in our study, contained vastly more PF. It is worth mentioning that the alcohol free beer has a significantly reduced prenylated flavonoids content (1350 μg/L) compared to the IPA with alcohol (2400 μg/L). Obviously, the process of removing alcohol from beer seems to remove total PF content and reduce the amounts of compounds in the chalcone form, which are considered as desirable.

The amount of XN-C and IXN-C is very low in all beer samples, but it is shown that IXN-C is higher than XN-C in all beers measured, except for the double IPA. This is not surprising, since most of the XN is also converted to IXN during the brewing process (41). Interestingly, the amount of XN-C in the coffee stout is similar to the amount of IXN-C, which could suggest a stabilization process. This could be due to Maillard reaction products, which are supposed to stabilize XN from cyclizing in dark beer (42, 43). The double IPA is a heavily dry hopped beer and that might explain the higher XN-C amounts compared to IXN-C as the hops are not boiled to the extent of other beers. The chroman-like flavonoids XN-C and IXN-C are relatively unstudied and might confirm that they may add to the hepatoprotective properties that are said to outweigh the ethanol effects from beer consumption (44). However, this would need further research as little is known regarding the bioactivities of XN-C and IXN-C right now.

Furthermore, the concentrations of PFs in hop tea was investigated. However, the concentrations are so minimal that it would be very surprising if a health effect or taste modulation occurs (**Table 4**) (45). Drinking a tea that is brewed would only have 6.5 μg PF (based on 300 mL). Comparing this to the consumption of an alcoholic free beer which would contain 440 μg is vastly different. One optimistic observation

TABLE 2 | The LOD, LOQ recovery and precision determined in the hop free beer matrix of each analyte quantified using the developed SIDA method.

Analyte	LOD µg/L	LOQ µg/L	Recovery% High 2-points ($n = 3$)	Recovery % Low 2-points ($n = 3$)	Intra-day Precision RSD% ($n = 3$)	Inter-day Precision RSD% ($n = 3$)	Injection Precision RSD% ($n = 9$)
IXN	0.07	0.30	89.4–105	95.0–104	3.3	6.0	0.51
IXN-C	0.21	0.84	89.9–102	93.6–113	4.1	4.5	4.2
8-PN	0.32	1.3	106–109	108–113	2.09	8.2	4.87
6-PN	0.94	3.74	89.7–104	91.0–101	1.52	3.12	3.42
XN	0.06	0.24	90.0–109	90.9–93.0	3.15	0.51	1.24
XN-C	0.19	0.78	82.6–93.8	81.0–91.6	2.43	0.45	2.77

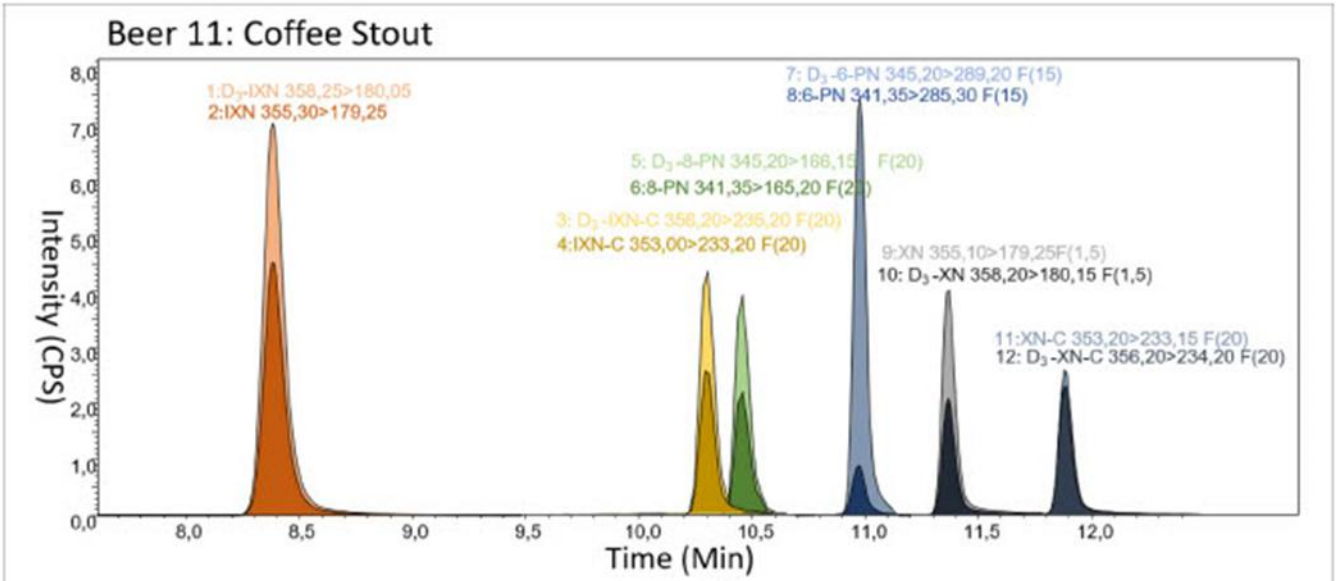

FIGURE 4 | LC-MS/MS analysis of a beer spiked with the isotopically labeled standards. The spectra show the separation of all analytes along with selected fragmentation for qualifier and quantifier. F is the factor increased for each peak size relative to D_3-IXN e.g., D_3-IXN-C peak is increased 20 fold as it reveals significantly lower amounts in beer.

is that IXN concentrations in brewed tea is not increased, which might imply that using hot distilled water does not cause cyclisation to the less desired IXN, contrary to boiling hops, a process essential in the manufacture of beer, where most XN is thermally cyclized into IXN (41). Perhaps a formulation of hop tea comprised from hop pellets or XN extract might be an alternative supplement as they contain very high concentrations of prenylated flavonoids of 11.200 mg/kg reported here with the main compound being XN (6640). Although the solubility of XN in hot water is not high (46, 47). However, the solubilization of other (e.g., IXN, 6PN, 8PN) PF at room temperature in water is higher, which might make tea formulations of hops a viable, but extremely bitter tasting dietary source (47).

CONCLUDING REMARKS

The synthesis of the deuterated labeled internal standards applicable for prenylated flavonoids analysis has been developed using three different methods. Firstly using a microwave assisted demethylation while simultaneously enriching compounds with deuterium was envisaged and applied. Second, utilizing functional groups such as a Michael system and Strykers Cat incorporating deuterium and lastly, we have also shown that a method does not need a microwave reaction, which some laboratories could be limited by a lack of resources. By contrast, acid and base reactions are also suitable to introduce deuterium. Using the synthesized products we conducted a robust SIDA method for the analysis of six different PF found in beer and hops with comparable results (723–2456 µg/L) to other investigations. For a statistical differentiation of the beer types a broader and more comprehensive sampling would be necessary. Regarding the investigation of the PF content in hop tea it contains extremely low concentrations of PF, i.e., it is very unlikely the content is contributing to health or taste (45). The method here uses a fast clean-up of LLE of samples containing PF and compensates for losses during workup by the addition of isotopically labeled internal standards. The LOD and LOQ are excellent and precision is within the DIN 32645

TABLE 3 | Concentration of prenylated flavonoids found in 15 beer styles using the developed SIDA method: ± (SD μg/L, $n = 3$).

	IXN μg/L	IXN-C μg/L	8-PN μg/L	6-PN μg/L	XN μg/L	XN-C μg/L	Total μg/L
1. Helles (pale lager)	1160 (36)	12.0 (0.73)	19.7 (2.29)	46.7 (0.4)	19.8 (1.7)	1.9 (0.11)	1260
2. Festbier (festival beer)	1110 (26)	25.6 (6.30)	25.3 (1.14)	51.8 (0.90)	19.2 (2.5)	2.3 (0.09)	1234
3. Lager	627 (2.5)	13.7 (0.22)	14.4 (0.58)	14.2 (0.1)	22.1 (1.4)	1.9 (0.10)	693
4. Pilsner beer	989 (4.8)	20.5 (0.74)	7.0 (0.28)	22.8 (0.2)	10.1 (0.7)	1.8 (0.07)	1051
5. Hopped wheat beer A	1260 (53)	28.7 (0.74)	42.0 (1.07)	278 (5.6)	425 (35.1)	8.3 (0.45)	2042
6. Hopped wheat beer B	1400 (93)	15.4 (1.07)	36.5 (1.20)	120 (6.7)	411 (18.2)	10.2 (0.69)	1993
7. Double IPA	1320 (14)	12.8 (1.08)	50.6 (2.24)	421 (9.7)	500 (22.5)	16.1 (1.19)	2331
8. IPA	1540 (280)	14.1 (0.24)	54.6 (2.59)	368 (15.9)	464 (49.4)	5.1 (0.39)	2446
9. IPA alcohol free	1150 (147)	21.7 (4.96)	31.5 (1.98)	104 (3.2)	21.7 (3.9)	2.9 (0.37)	1332
10. Dunkel (dark beer)	1170 (128)	14.9 (1.35)	101.0 (7.55)	355 (3.1)	728 (30.0)	5.6 (0.20)	2375
11. Coffee stout	1480 (51)	23.4 (0.47)	88.7 (4.12)	351 (11.2)	483 (4.8)	18.8 (0.79)	2445
12. Bock beer	1550 (39)	19.0 (0.69)	50.3 (2.49)	156 (3.0)	99.3 (4.3)	4.4 (0.50)	1879
13. Doppelbock beer A	915 (15)	17.3 (1.75)	47.7 (2.64)	203 (2.40)	155 (29.9)	7.6 (0.09)	1346
14. Doppelbock beer B	1460 (80.6)	25.4 (1.67)	35.5 (1.45)	63.6 (0.6)	27.5 (1.8)	2.1 (0.25)	1614
15. Wheat bock beer	579 (13.9)	15.5 (1.00)	22.5 (1.12)	91.2 (3.2)	59.5 (3.9)	3.2 (0.20)	771

TABLE 4 | The concentration of the prenylated flavonoids in hops and hop tea ± (SD μg/L).

	IXN	IXN-C	8-PN	6-PN	XN	XN-C	Total
Hop pellets Columbus, μg/kg	4250	151	4.46	75.5	6640	76.9	11,200
15.6% α-acid (n=2)	(274)	(1.86)	(0.16)	(11.4)	(78.2)	(1.54)	
Hop tea (μg/bag) (n=2)	14.4 (2.44)	28.1 (0.52)	5.93 (0.52)	<LOD	17.9 (0.49)	3.12 (0.13)	69.0
Hop tea brewed (μg/L) (n=3)	3.4 (0.110)	12.4 (0.81)	1.58 (0.06)	<LOD	3.46 (0.49)	<LOD	20.8

guidelines for analytical methods of trace analysis (31). In future applications this method is applicable to measuring food samples, for freshness, food fraud and due to SIDA could be applied to biological samples as well. The validation results support that deuteration of PF is an easy pathway to producing labeled PFs and apply them to SIDA in quantifying PF in beer, hop tea and hops. The ongoing research regarding the bioactivities of these compounds provides a need for further analytical methods to be developed. The next step would be applying these methods to future clinical trial samples, such as blood, feces, and urine after consumption of beer or supplements. Reports of hop PF are already confirmed by urine analysis for biomarkers or in animal studies although SIDA is yet to be utilized (12, 48).

DATA AVAILABILITY STATEMENT

The raw data supporting the conclusions of this article will be made available by the authors, without undue reservation.

AUTHOR CONTRIBUTIONS

LB and CU wrote the manuscript and did the MS and NMR analysis of compounds synthesized. LB and MR

designed the experiments for the microwave synthesis of the labeled XN, 6-PN, 8-PN, IXNC and XNC. LB carried out the synthetic work for all analytes excluding the stryker cat reaction of XN. LB and SS carried out the SIDA analysis including interpretation of the data. LB, SS, and CU carried out the preparative HPLC. SS performed the HPLC calibration graphs of XN-C and 8-PN. HR and CU designed the stryker cat synthesis of the xanthohumol and carried out the synthetic work for the DXN. All authors contributed to reading the article and proofing it before publication.

FUNDING

The European Foundation for Alcohol Research (ERAB) reference EA 18 69. Wissenschaftliche Station für Brauerei in München e.V.

ACKNOWLEDGMENTS

Many thanks to Friedrich Ampenberger (Dipl.-Brmst.) for producing the hop free beer at TUM Research Center Weihenstephan for Brewing and Food Quality. Many thanks to Dr. Richard Hammerl and Dr. Oliver Frank for carrying out the NMR measurements at the chair of Food Chemistry and Molecular Sensory Science at the Technical University of Munich (TUM). Moreover, we thank the Barth Haas group for donating the CO_2 spent hop extract for xanthohumol purification. We would also like to thank Dr. Biendl from the Hallertauer Hopfenveredelungsgesellschaft m.B.H. to provide the hop product for the isolation of XN used in the synthesis of DXN.

SUPPLEMENTARY MATERIAL

The Supplementary Material for this article can be found online at: https://www.frontiersin.org/articles/10.3389/fnut.2020.619921/full#supplementary-material

REFERENCES

1. Nikolic D, Van Breemen RB. Analytical methods for quantitation of prenylated flavonoids from hops. *Curr. Anal. Chem.* (2013) 9:71–85. doi: 10.2174/157341113804486554
2. Venturelli S, Burkard M, Biendl M, Lauer UM, Frank J, Busch C. Prenylated chalcones and flavonoids for the prevention and treatment of cancer. *Nutrition.* (2016) 32:1171–8. doi: 10.1016/j.nut.2016.03.020
3. Barrea L, Annunziata G, Muscogiuri G, Arnone A, Tenore GC, Colao A, et al. Could hop-derived bitter compounds improve glucose homeostasis by stimulating the secretion of GLP-1? *Crit Rev Food Sci Nutr.* (2019) 59:528–35. doi: 10.1080/10408398.2017.1378168
4. Bolton JL, Dunlap TL, Hajirahimkhan A, Mbachu O, Chen SN, Chadwick L, et al. The multiple biological targets of hops and bioactive compounds. *Chem. Res. Toxicol.* (2019) 32:222–33. doi: 10.1021/acs.chemrestox.8b00345
5. Osorio-Paz I, Brunauer R, Alavez S. Beer and its non-alcoholic compounds in health and disease. *Crit Rev Food Sci Nutr.* (2020) 60:3492–505. doi: 10.1080/10408398.2019.1696278
6. Milligan S, Kalita J, Pocock V, Heyerick A, Cooman L, Rong H, et al. Oestrogenic activity of the hop phyto-estrogen, 8-Prenylnaringenin. *Reproduction.* (2002) 123:235–42. doi: 10.1530/rep.0.1230235
7. Venturelli S, Niessner H, Sinnberg T, Berger A, Burkard M, Urmann C, et al. 6- and 8-prenylnaringenin, novel natural histone deacetylase inhibitors found in hops, exert antitumor activity on melanoma cells. *Cell Physiol Biochem.* (2018) 51:543–56. doi: 10.1159/000495275
8. Chia-Leeson O, Riepl H, Urmann C. Biotransformation of the promising neuro-regenerative hop chalcone xanthohumol c. *Planta Med.* (2019) 85:277. doi: 10.1055/s-0039-3399972
9. Kirchinger M, Bieler L, Tevini J, Vogl M, Haschke-Becher E, Felder TK, et al. Development and characterization of the neuroregenerative xanthohumol c/Hydroxypropyl-β-cyclodextrin complex suitable for parenteral administration. *Planta Med.* (2019) 85:1233–41. doi: 10.1055/a-1013-1276
10. Oberbauer E, Urmann C, Steffenhagen C, Bieler L, Brunner D, Furtner T, et al. Chroman-like cyclic prenylflavonoids promote neuronal differentiation and neurite outgrowth and are neuroprotective. *J Nutr Biochem.* (2013) 24:1953–62. doi: 10.1016/j.jnutbio.2013.06.005
11. Pichler C, Ferk F, Al-Serori H, Huber W, Jager W, Waldherr M, et al. Xanthohumol prevents DNA damage by dietary carcinogens: results of a human intervention trial. *Cancer Prev Res.* (2017) 10:153–60. doi: 10.1158/1940-6207.Capr-15-0378
12. Paraiso IL, Revel JS, Choi J, Miranda CL, Lak P, Kioussi C, et al. Front cover: targeting the liver-Brain axis with hop-Derived flavonoids improves lipid metabolism and cognitive performance in mice. *Mol Nutr Food Res.* (2020) 64:2070034. doi: 10.1002/mnfr.202070034
13. Zhang Y, Bobe G, Revel JS, Rodrigues RR, Sharpton TJ, Fantacone ML, et al. Improvements in metabolic syndrome by xanthohumol derivatives are linked to altered gut microbiota and bile acid metabolism. *Mol Nutr Food Res.* (2020) 64:1900789. doi: 10.1002/mnfr.201900789
14. De Keukeleire J, Ooms G, Heyerick A, Roldan-Ruiz I, Van Bockstaele E, De Keukeleire. D. Formation and accumulation of α-Acids, β-Acids, desmethylxanthohumol, and xanthohumol during flowering of hops (Humulus lupulus l.). *J Agric Food Chem.* (2003) 51:4436–41. doi: 10.1021/jf034263z
15. Kac J, Mlinarič A, Umek A. HPTLC determination of xanthohumol in hops (humulus lupulus l.) and hop products. *J Planar Chromat.* (2006) 19:58–61. doi: 10.1556/JPC.19.2006.1.10
16. Moreira MM, Carvalho AM, Valente IM, Gonçalves LM, Rodrigues JA, Barros AA, et al. Novel application of square-Wave adsorptive-stripping voltammetry for the determination of xanthohumol in spent hops. *J Agric Food Chem.* (2011) 59:7654–8. doi: 10.1021/jf2011485
17. Wyns C, Derycke L, Soenen B, Bolca S, Deforce D, Bracke M, et al. Production of monoclonal antibodies against hop-derived (Humulus lupulus l.) prenylflavonoids and the development of immunoassays. *Talanta.* (2011) 85:197–205. doi: 10.1016/j.talanta.2011.03.047
18. Rychlik M, Asam S. Stabilisotopenverdünnungsanalysen zur quantifizierung organischer spurenkomponenten in der lebensmittelanalytik. *Umweltwissenschaften und Schadstoff-Forschung.* (2009) 21:470–82. doi: 10.1007/s12302-009-0082-0
19. Berwanger S, Zapp J, Becker H. 13 C-labelling of xanthohumol in hop cones (*Humulus lupulus*). *Planta Med.* (2005) 71:530–4. doi: 10.1055/s-2005-864154
20. Berwanger S, Frank N, Knauft J, Becker H. Biosynthetic 14C-labelling of xanthohumol in hop cones. *Mol Nutr Food Res.* (2005) 49:857–60. doi: 10.1002/mnfr.200500040
21. Ellinwood DC, El-Mansy MF, Plagmann LS, Stevens JF, Maier CS, Gombart AF, et al. Total synthesis of $[^{13}C]_{2-}$, $[^{13}C]_{3-}$, and $[^{13}C]_{5}$-isotopomers of xanthohumol, the principal prenylflavonoid from hops. *J Label Compd Rad.* (2017) 60:639–48. doi: 10.1002/jlcr.3571
22. Ellinwood D, Blakemore P. Total synthesis of a series of 13C-labeled isotopomers of xanthohumol: the primary prenylated chalcone in the inflorescence of hops plants. *Abstr Pap Am Chem Soc.* (2017) 253:1. doi: 10.1021/np070158y
23. Brestensky DM, Huseland DE, McGettigan C, Stryker JM. Simplified, "one-pot" procedure for the synthesis of [(Ph3P)CUH]6, a stable copper

hydride for conjugate reductions. *Tetrahedron Lett.* (1988) 29:3749–52. doi: 10.1016/S0040-4039(00)82105-X
24. Lee DW, Yun J. Direct synthesis of stryker's reagent from a cu(II) salt. *Tetrahedron Lett.* (2005) 46:2037–9. doi: 10.1016/j.tetlet.2005.01.127
25. Vaidyanathan S, Surber BW. Microwave mediated hydrogen deuterium exchange: a rapid synthesis of 2H-substituted benzimidazole. *Tetrahedron Lett.* (2005) 46:5195–7. doi: 10.1016/j.tetlet.2005.05.110
26. Fang Z, Zhou GC, Zheng SL, He GL, Li JL, He L, et al. Lithium chloride-catalyzed selective demethylation of aryl methyl ethers under microwave irradiation. *J Mol Catal A-Chem.* (2007) 274:16–23. doi: 10.1016/j.molcata.2007.04.013
27. Urmann C, Riepl H. Semi-Synthetic approach leading to 8-Prenylnaringenin and 6-Prenylnaringenin: optimization of the microwave-assisted demethylation of xanthohumol using design of experiments. *Molecules.* (2020) 25:4007. doi: 10.3390/molecules25174007
28. Stevens JF, Taylor AW, Deinzer ML. Quantitative analysis of xanthohumol and related prenylflavonoids in hops and beer by liquid chromatography–tandem mass spectrometry. *J Chromatogr A.* (1999) 832:97–107. doi: 10.1016/S0021-9673(98)01001-2
29. Vogelgesang J, Hadrich J. Limits of detection, identification and determination: a statistical approach for practitioners. *Accredit Qual Assur.* (1998) 3:242–55. doi: 10.1007/s007690050234
30. Mandel J. *The Statistical Analysis of Experimental Data.* New York, NY: Dover Publications (1964).
31. Verlag M. *Chemische Analytik; Nachweis-, Erfassungs- Und Bestimmungsgrenze; Ermittlung Unter Wiederholbedingungen Begriffe, Verfahren, Auswertung.* Berlin: Auswertung, Beuth Verlag (2008).
32. Miles CO, Main L. The kinetics and mechanism, and the equilibrium position as a function of pH, of the isomerisation of naringin and the 4′-rhamnoglucoside of 2′,4,4′,6′-tetrahydroxychalcone. *J Chem Soc Perkin Trans.* (1988) 2:195–8. doi: 10.1039/P29880000195
33. Atzrodt J, Derdau V, Fey T, Zimmermann J. The renaissance of H/D exchange. *Angew.* (2007) 46:7744–65. doi: 10.1002/anie.200700039
34. Mahoney WS, Brestensky DM, Stryker JM. Selective hydride-mediated conjugate reduction of.alpha..beta.-unsaturated carbonyl compounds using [(Ph3P)CuH]6. *J Am Chem Soc.* (1988) 110:291–3. doi: 10.1021/ja00209a048
35. Stevens JF, Ivancic M, Hsu VL, Deinzer ML. Prenylflavonoids from humulus lupulus. *Phytochemistry.* (1997) 44:1575–85. doi: 10.1016/s0031-9422(96)00744-3
36. Wyns C, Bolca S, De Keukeleire D, Heyerick A. Development of a high-throughput lC/APCI-MS method for the determination of thirteen phytoestrogens including gut microbial metabolites in human urine and serum. *J Chromatogr B Analyt Technol Biomed Life Sci.* (2010) 878:949–56. doi: 10.1016/j.jchromb.2010.02.022
37. Sus N, Schlienz J, Calvo-Castro LA, Burkard M, Venturelli S, Busch C, et al. Validation of a rapid and sensitive reversed-phase liquid chromatographic method for the quantification of prenylated chalcones and flavanones in plasma and urine. *NFSJ.* (2018) 10:1–9. doi: 10.1016/j.nfs.2017.11.001
38. Turowski M, Yamakawa N, Meller J, Kimata K, Ikegami T, Hosoya K, et al. Deuterium isotope effects on hydrophobic interactions: the importance of dispersion interactions in the hydrophobic phase. *J Am Chem Soc.* (2003) 125:13836–49. doi: 10.1021/ja036006g
39. Stevens JF, Page JE. Xanthohumol and related prenylflavonoids from hops and beer: to your good health! *Phytochemistry.* (2004) 65:1317–30. doi: 10.1016/j.phytochem.2004.04.025
40. Boronat A, Soldevila-Domenech N, Rodríguez-Morat,ó J, Martínez-Huélamo M, Lamuela-Raventós RM, de la Torre R. Beer phenolic composition of simple phenols, prenylated flavonoids and alkylresorcinols. *Molecules.* (2020) 25:2582. doi: 10.3390/molecules25112582
41. Kamiński DM, Gaweda K, Arczewska M, Senczyna B, Gago,ś M. A kinetic study of xanthohumol cyclization to isoxanthohumol – a role of water. *J Mol Struct.* (2017) 1139:10–16. doi: 10.1016/j.molstruc.2017.03.027
42. Magalhães PJ, Dostalek P, Cruz JM, Guido LF, Barros AA. The impact of a xanthohumol-Enriched hop product on the behavior of xanthohumol and isoxanthohumol in pale and dark beers: a Pilot scale approach. *J Inst Brew.* (2008) 114:246–56. doi: 10.1002/j.2050-0416.2008.tb00335.x
43. Stevens JF. Xanthohumol and Structurally Related Prenylflavonoids for Cancer Chemoprevention and Control. In: Pezzuto JM, Vang O, editors. *Natural Products for Cancer Chemoprevention: Single Compounds and Combinations,* Cham: Springer International Publishing (2020). p. 319–350.
44. Pinto C, Cestero JJ, Rodríguez-Galdón B, Macías P. Xanthohumol, a prenylated flavonoid from hops (Humulus lupulus l.), protects rat tissues against oxidative damage after acute ethanol administration. *Toxicol.* (2014) 1:726–33. doi: 10.1016/j.toxrep.2014.09.004
45. Intelmann D, Batram C, Kuhn C, Haseleu G, Meyerhof W, Hofmann T. Three tAS2R bitter taste receptors mediate the psychophysical responses to bitter compounds of hops (Humulus lupulus l.) and beer. *Chemosens Percept.* (2009) 2:118–32. doi: 10.1007/s12078-009-9049-1
46. Schönberger C. *The Processing of Hops.* Sawston; Cambridge: Woodhead Publishing (2006). p.123–148. doi: 10.1533/9781845691738.123
47. Magalhães PJ, Guido LF, Cruz JM, Barros AA. Analysis of xanthohumol and isoxanthohumol in different hop products by liquid chromatography-diode array detection-electrospray ionization tandem mass spectrometry. *J Chrom A.* (2007) 1150:295–301. doi: 10.1016/j.chroma.2006.08.019
48. Quifer-Rada P, Martínez-Huélamo M, Chiva-Blanch G, Jáuregui O, Estruch R, Lamuela-Raventós RM. Urinary isoxanthohumol is a specific and accurate biomarker of beer consumption. *J Nutr.* (2014) 144:484–8. doi: 10.3945/jn.113.185199

Conflict of Interest: The authors declare that the research was conducted in the absence of any commercial or financial relationships that could be construed as a potential conflict of interest.

5.2 Supplementary information. Manuscript I: Stable isotope dilution analysis of the major prenylated flavonoids found in beer, hop tea and hops [94].

frontiers

Supplementary Material

1 Synthesis of reference standards

1.1 Xanthohumol

XN was produced from a CO_2 hop extract waste of the cultivar Hallertau Taurus cultivar. To 100 g of the dry hop extract, 1,2 L of acetone (technical grade VWR) was added and stirred for approx. 1 h using a magnetic stir plate. The solvent extract was filtered with grade H 1/2 filter paper (Schleicher & Schuell) and evaporated leaving a dark green viscous extract (approx. 65 g). To the extract 50 mL of MeOH (VWR) was added along with 50 mL NaCl (0,2 M) solution causing a green precipitate (PPt) to form which was again filtered leaving an orange solution. The methanol was removed by rotation evaporation causing a further PPt to form, which was collected and subjected to flash chromatography by silica gel (mesh 70-230 mesh Sigma Aldrich, Deutschland) using 99:1 DCM:MeOH as an eluent. Fractions were checked for XN by TLC (Rf = 0.5) and pooled together resulting in an orange powder approx. 640 mg of XN. 1H NMR (400 MHz, MeOD) δ 7.80 (d, J = 15.5 Hz, 0H), 7.67 (d, J = 15.6 Hz, 0H), 7.50 (d, J = 8.6 Hz, 1H), 6.83 (d, J = 8.6 Hz, 1H), 6.02 (s, 0H), 5.27 – 5.09 (m, 1H), 3.90 (s, 1H), 3.23 (d, J = 7.1 Hz, 1H), 1.76 (s, 1H), 1.65 (s, 1H). 13C NMR (101 MHz, MeOD) δ 192.66, 164.74, 162.28, 161.00, 159.61, 141.88, 129.82, 127.06, 124.47, 122.84, 115.44, 107.99, 105.10, 90.22, 54.75, 47.60, 24.56, 20.88, 16.47.

1.2 Isoxanthohumol

Argon was not utilised for this reaction. Using a method from Wihelm et al. 2006. XN (1 mM) was dissolved in 50 mL of a 1% NaOH (aq. w.v) (Wilhelm and Wessjohann, 2006). The reaction was on an ice bath and allowed to reach room temperature while stirring overnight. The solution was finally treated with 50% H_2SO_4 (aq. v.v) until the pH was neutralised causing a yellow PPt to form. Workup consisted of three times extraction using added EtOAc and a final wash of brine. The organic phase was dried using anhydrous Na_2SO_4 (VWR) and the product was subjected to Flash chromatography EtOAc:Pentane. 40:60% using silica gel (mesh 70-230 mesh Sigma Aldrich, Deutschland). Fractions containing IXN were check by TLC (Rf = 0.2) pooled and concentrated. Preparative HPLC (System 1) was used to purify. The reaction produced a 98% conversion according to HPLC, but only 34.8 mg was collected by preparative HPLC. ^{1}H NMR (400 MHz, MeOD) δ 7.80 (d, J = 15.5 Hz, 1H), 7.67 (d, J = 15.6 Hz, 1H), 7.50 (d, J = 8.6 Hz, 2H), 6.83 (d, J = 8.6 Hz, 2H), 6.02 (s, 1H), 5.27 – 5.09 (m, 2H), 3.90 (s, 3H), 3.23 (d, J = 7.1 Hz, 3H), 1.76 (s, 4H), 1.65 (s, 3H).^{13}C NMR (101 MHz, MeOD) δ 192.92, 164.27, 164.27, 163.83, 158.80, 131.67, 131.67, 128.86, 123.89, 116.24, 109.95, 109.95, 93.42, 79.99, 55.96, 46.21, 25.96, 22.70, 17.90.

1.3 Isoxanthohumol-C

To 50 mg of XN 1% NaOH solution (20 mL) was added on ice. The reaction was left overnight and subsequently neutralised with drops of 50 % vv H_2SO_4 until a yellow PPt forms. The PPt was collected and dissolved in 50 mL of EtOAc and extracted 3-fold before the organic fraction was washed twice with water and a final brine solution. Na_2SO_4 was then used to dry the organic phase before the reaction was concentrated and directly dissolved in 5 mL of dry THF under argon atmosphere. To the reaction DDQ (64 mg) was added and the reaction was refluxed for 2 h.

Subsequently, the addition of a 1% $Na_2S_2O_3$ (2.5 mL) was used to quench the reaction. EtOAc (25 mL) was added to the reaction along with a further 2.5 mL of $Na_2S_2O_3$. This was repeated 3 times until the organic phase turned yellow. The yellow organic phase was further washed with H_2O (25 mL) 3 times and then finally with (25 mL) brine. The organic phase was further dried with Na_2SO_4, filtered, and concentrated before being dissolved in MeOH. The final preparation was purification using HPLC system 1. Yielding 7.62 mg. ^{1}H NMR (400 MHz, MeOD) δ 7.38 – 7.27 (m, 2H), 6.86 – 6.76 (m, 2H), 6.52 (d, J = 10.2 Hz, 1H), 6.11 (s, 1H), 5.53 (d, J = 10.1 Hz, 1H), 5.36 (dd, J = 12.8, 2.9 Hz, 1H), 3.83 (s, 3H), 3.05 (dd, J = 16.6, 12.8 Hz, 1H), 2.71 (dd, J = 16.6, 3.0 Hz, 1H), 1.42 (d, J = 8.3 Hz, 6H). ^{13}C NMR (101 MHz, MeOD) δ 192.34, 163.54, 161.96, 160.55, 159.00, 131.03, 128.89, 127.70, 116.74, 116.37, 106.34, 104.10, 94.71, 80.34, 56.37, 46.13, 28.38.

1.4 Xanthohumol-C

An adaption to the method of Stevens et al. 1997 and Roeher et al 2018 (Stevens et al., 1997; Roehrer et al., 2018). XN (0,28 mM) was dissolved in 5 mL dry THF in a heated out double necked flask. The flask was left in an ice bath for 5 minutes before DDQ (0,28 mM) was added and the reaction turned black/green. The reaction was taken to reflux for 1 h before addition of a 1% $Na_2S_2O_3$ (aq.) was added to quench the reaction. Aqueous work up included 3 times wash with $Na_2S_2O_3$ in water (25 mL) and 25 mL of EtOAC: Followed by a further 3 times washing of the organic phase with H2O. The organic phase was collected and dried with Na2SO4 and evaporated before flash chromatography. The crude reaction was dry loaded and eluted using 20:80 EtOAc: hexane. The first compound that eluted was XN-C. Yield: 47%. Final clean-up was performed with HPLC System 1.1H NMR (400 MHz, CD3CN) δ 7.81 – 7.67 (m, 2H), 7.57 – 7.44 (m, 2H), 6.89 – 6.77 (m, 2H), 6.62 (d, J = 10.0 Hz, 1H), 6.03 (s, 1H), 5.53 (d, J = 10.0 Hz, 1H), 3.94 (s, 3H), 1.43 (s, 6H). 13C NMR (101 MHz, CD3CN) δ 194.28, 164.16, 163.02, 161.57, 161.27, 144.13, 131.42, 128.29, 126.69, 125.36, 116.91, 107.01, 103.93, 92.78, 79.17, 56.54, 28.59.

1.5 8-Prenlnaringenin and 6-Prenylnaringenin

An adaption from Urmann and Riepl 2020 and Wilhelm et al 2006. XN (1 mM) was added into a double necked flask along with LiCl (20 mM) and KI (2 mM) (Wilhelm and Wessjohann, 2006; Urmann and Riepl, 2020). Argon was added to protect the reaction along with 4 mL DMF. The reaction underwent reflux for 4 h and then was left at room temperature overnight. To quench the reaction 1,5 mL of HCl (25%) was added causing a yellow precipitate to form. EtOAc (25 mL) was added and the reaction was washed with $Na_2S_2O_3$ (aq) and further washed with H_2O 4 times 25 mL. Brine was used in the final stage and further dried using Na_2SO_4. The reaction was filtered and columned using silica gel 99:1 DCM:MeOH. The fractions that contained 8- and 6-PN were then separated using sephadex LH20 with methanol as an eluent. Yielding 0,2mM (20%) of a mixture of 6 and 8-PN this was separated using preparative HPLC. Using system 1. 6-PN. 8-PN. ^{1}H NMR (400 MHz, MeOD) δ 7.32 (d, J = 8.6 Hz, 2H), 6.82 (d, J = 8.6 Hz, 2H), 5.93 (s, 1H), 5.32 (dd, J = 12.8, 3.0 Hz, 1H), 5.14 (t, J = 8.7, 5.9, 2.9, 1.5 Hz, 1H), 3.17 (d, J = 7.4 Hz, 2H), 3.08 (dd, J = 17.1, 12.8 Hz, 1H), 2.71 (dd, J = 17.1, 3.1 Hz, 1H), 1.62 (d, J = 1.4 Hz, 4H), 1.57 (d, J = 1.4 Hz, 3H). ^{13}C NMR (101 MHz, MeOD) δ 198.17, 166.07, 163.14, 161.57, 158.89, 131.58, 131.39, 128.93, 123.93, 116.26, 109.03, 103.36, 96.37, 80.26, 49.00, 43.97, 25.96, 22.48, 17.88. 6-PN ^{1}H NMR (400 MHz, MeOD) δ 7.35 – 7.28 (m, 2H), 6.81 (d, J = 8.6 Hz, 2H), 5.93 (s, 1H), 5.31 (dd, J = 13.0, 2.9 Hz, 1H), 5.19 (t, J = 7.2 Hz, 1H), 4.58 (s, 1H), 3.20 (d, J = 7.2 Hz, 2H), 3.10 (dd, J = 17.1, 13.0 Hz, 1H), 2.68 (dd, J = 17.1, 3.0 Hz, 1H), 1.75 (s, 3H), 1.65 (s, 3H). ^{13}C NMR (101 MHz, MeOD) δ 197.85, 165.93,

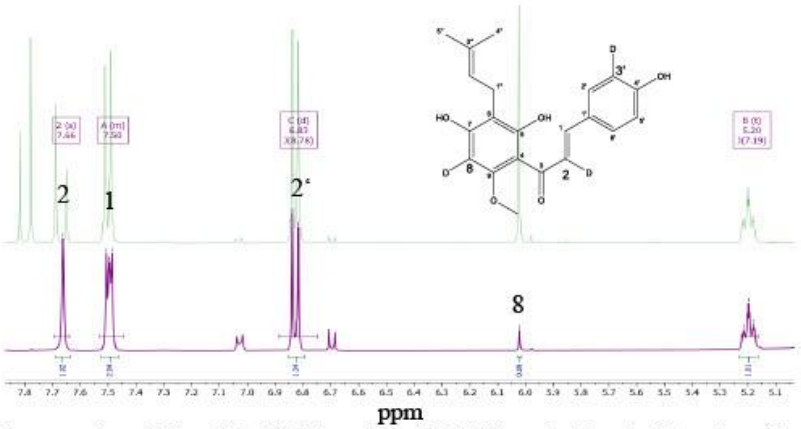

Figure 1. The superimposition of D_3-XN (purple) with XN (green). The doublet of position 2 is gone and 3' is reduced to 1 proton and position 8 is only visible for some residual signal from remaining proton.

The ESI + data of D_3-IXN showed that there is a mass increase of +3. The NMR data showed which protons were exchanged. Figure 5, shows the spectrum of D_3-IXN and due to the lack of the proton at 6.0 ppm we can confirm that the aromatic proton equivalent to position 8 in Figure 3 is exchanged. Similar to XN the doublet in position 1 after the deuteration is now a singlet. And at 3.75 ppm the proton see Figure 4. Therefore, it is similarly deuterated as the XN.

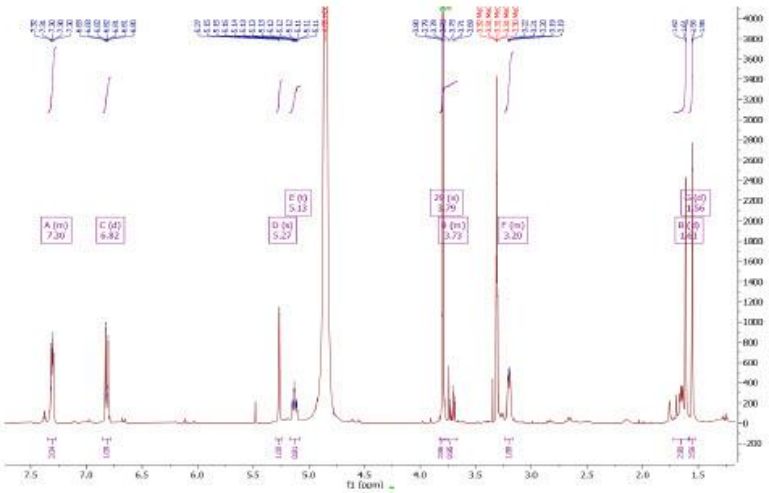

Figure 2: D_3-IXN NMR spectra. The protons equivalent to the D3-XN are exchanged.

The ESI+ of D_3-6-PN represents an m/z of +4: Therefore, the assumption is that 4 protons have been exchanged. The NMR shows that there are a different degree of labelling compared with XN. The NMR spectrum in Figure 5 demonstrates that no aliphatic proton was exchanged, although there is

162.56, 158.98, 131.59, 131.25, 128.99, 123.88, 116.30, 109.66, 103.19, 95.40, 80.45, 44.20, 25.94, 21.87, 17.84.

2 Synthesis of Isotopically labelled standards

2.1 D_3-Xanthohumol, D_3-Isoxanthohumol D_3-6-Prenylnaringenin and D_3-8-prenylnaringenin

To the extracted XN (50.3 mg) 5 mL of DMF and 5 mL D_2O, approx. 1 mg Pd (30%)/C, approx. 1 mg Pt/C and approx. 1 mg Rh (10%)/Aluminium was added into an 80 mL quartz microwave reaction flask with a magnetic stir bar (CEM). Microwave (Discover SP, CEM) was set to react for 150°C, 2 min, 10 bar, 150 w with vigorous stirring set. After the reaction had cooled 138 mg of LiCl was added and the reaction allowed to stir for 5 min before being raised to 250°C, 10 min, 20 bar, 250 w. The reaction was cooled, and TLC (50:50 EtoAc: Pentane) showed that there were three spots (Rf 0.8, 0.5 0.2) had formed. Subsequently 80, µL of D_2SO_4 was added causing a precipitate to form. For workup 25 mL of EtOAc and 25 mL $Na_2S_2O_3$ (aq) was used for the initial extraction followed by 2 times EtOAc: water extraction. The organic phase was dried using Na_2SO_4, filtered and evaporate. The sample was then dissolved in 3 mL of MeOH and prepared using preparative HPLC system 1. Yields: D_3-XN 5.07 mg, D_3-IXN 4.38 mg , D_3-6-PN, 1.13 mg, D_3-8-PN 0.4 mg (confirmed by HPLC).

ESI + 358.20. D_3-XN ^{1}H NMR (400 MHz, Methanol-d_4) δ 7.66 (s, 1H), 7.50 (t, J = 8.0 Hz, 2H), 6.83 (d, J = 8.8 Hz, 1H), 5.20 (tt, J = 7.2, 1.4 Hz, 1H), 3.90 (s, 3H), 3.23 (d, J = 7.2 Hz, 2H), 1.76 (s, 3H), 1.65 (s, 3H). 13C NMR (101 MHz, MeOD) δ 194.01, 166.16, 163.74, 162.39, 161.04, 161.00, 131.35, 131.25 , 131.14, 130.28, 128.45, 116.88, 116.16, 109.40, 106.46, 91.66, 56.18, 49.64, 25.96, 22.27, 17.87.

ESI + 358.25., D_3-IXN ^{1}H NMR (400 MHz, Methanol-d_4) δ 7.34 – 7.27 (d, J = 8.2 Hz, 2H), 6.84 – 6.77 (d, J = 8.2 Hz, 2H), 5.29 – 5.24 (s, 1H), 5.17 – 5.11 (t, 1H), 3.81 – 3.77 (s, 3H), 3.26 – 3.17 (d, J = 7.6 Hz, 2H), 1.63 – 1.60 (d, J = 1.4 Hz, 3H), 1.57 – 1.54 (d, J = 1.3 Hz, 3H). ESI+ 6-PN 345.20. 1H NMR (400 MHz, MeOD) δ 7.35 – 7.30 (m, 2H), 6.83 (d, J = 8.8 Hz, 1H), 5.32 (s, 1H), 5.18 (t, J = 7.2 Hz, 3H), 3.21 (d, J = 7.2 Hz, 21H), 3.17 – 3.08 (m, 2H), 2.73 – 2.62 (m, 2H), 1.76 (s, 3H), 1.65 (s, 3H). ESI + 8-PN 345.20 – due to the low amounts of 8-PN produced and a contaminant that was not able to be separated during preparative HPLC in the reaction no NMR was possible, although some information from the NMR could be deduced.

The ^{1}H NMR spectra of D_3-XN (Figure 1) has a total of three protons missing compared to that of XN when using the sum of integrals. The protons that are exchanged with deuterium are of 7.84-7.75 ppm (100%) of 6.86-6.79- (75%) exchanged of 6.05 ppm (91%) exchanged which is estimated by the lack of a signal (See Figure 3). The exchanged protons coincide with the MS data reported in the results section as the m/z is plus 3 protons. Additionally, further evidence is in the multiplicity of the NMR spectra allowing us to confirm that one of the Michael system is exchanged due to the multiplicity of the signal at 7.67 ppm (Proton in position 2) being a singlet compared a doublet in normal XN (Figure 1).

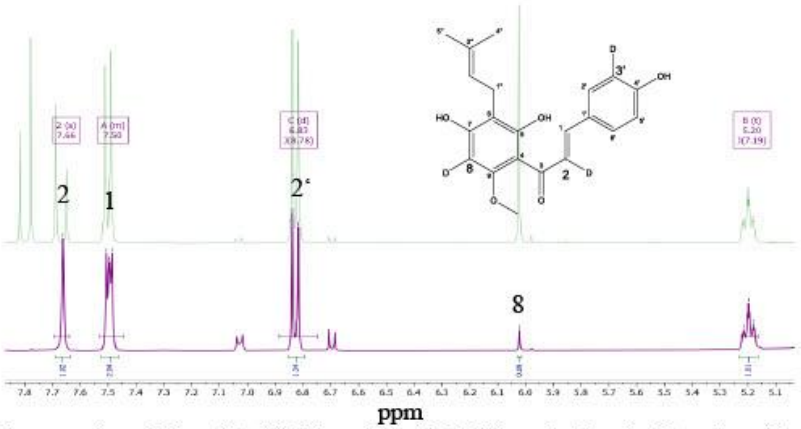

Figure 1. The superimposition of D_3-XN (purple) with XN (green). The doublet of position 2 is gone and 3' is reduced to 1 proton and position 8 is only visible for some residual signal from remaining proton.

The ESI + data of D_3-IXN showed that there is a mass increase of +3. The NMR data showed which protons were exchanged. Figure 5, shows the spectrum of D_3-IXN and due to the lack of the proton at 6.0 ppm we can confirm that the aromatic proton equivalent to position 8 in Figure 3 is exchanged. Similar to XN the doublet in position 1 after the deuteration is now a singlet. And at 3.75 ppm the proton see Figure 4. Therefore, it is similarly deuterated as the XN.

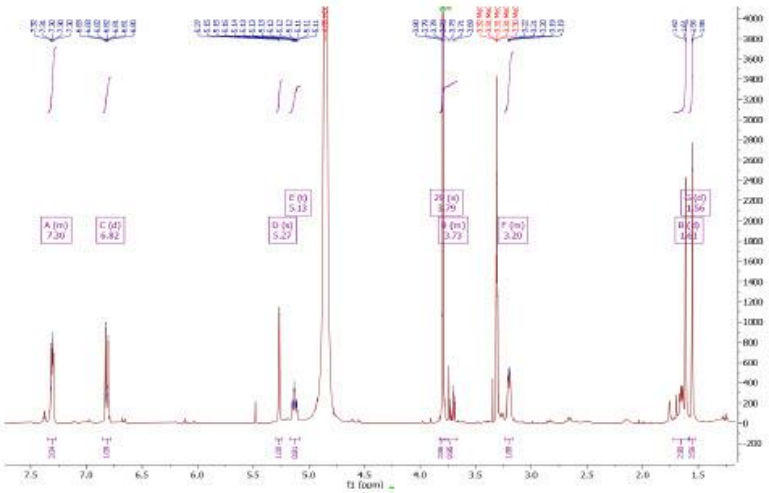

Figure 2: D_3-IXN NMR spectra. The protons equivalent to the D3-XN are exchanged.

The ESI+ of D_3-6-PN represents an m/z of +4: Therefore, the assumption is that 4 protons have been exchanged. The NMR shows that there are a different degree of labelling compared with XN. The NMR spectrum in Figure 5 demonstrates that no aliphatic proton was exchanged, although there is

the similar degree of deuteration as D3-XN there is additional deuteration in the aromatic ring which is calculated by the integrals of each peak compared to non-deuterated 6-PN. Although, it is difficult to calculate the degree accurately due to the low concentration of the sample in the NMR. Hence, the degree of deuteration is closer to 4.

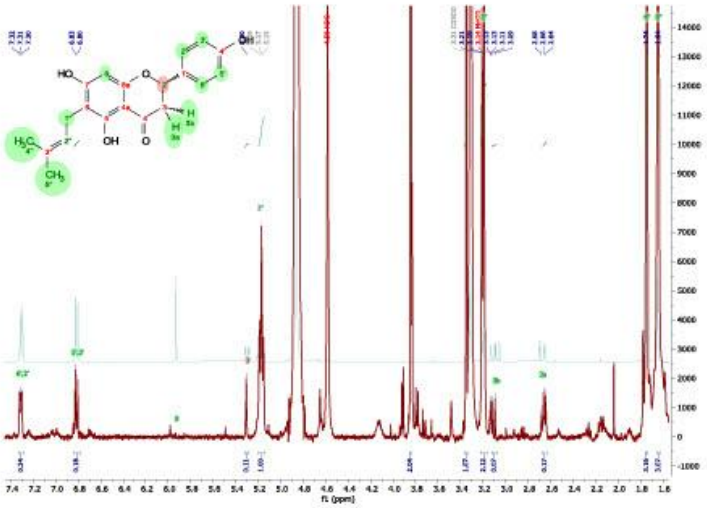

Figure 3: D_3-6-PN (Red) superimposed with 6-PN (cyan). Position 8 is completely exchanged. Based on the integrals all aromatic have some degree of deuteration which collectively is near 4 from the MS results.

Similar to the D_3-6-PN, D_3-8-PN showed an m/z of +4: The D_3-8-PN was produced in amounts that were not sufficient for 1H NMR and there was a contaminant at 8.09 min (see Figure 4) that could not be removed after several attempts of preparative HPLC. Therefore, to characterise the sample it underwent HPLC and MS analysis.

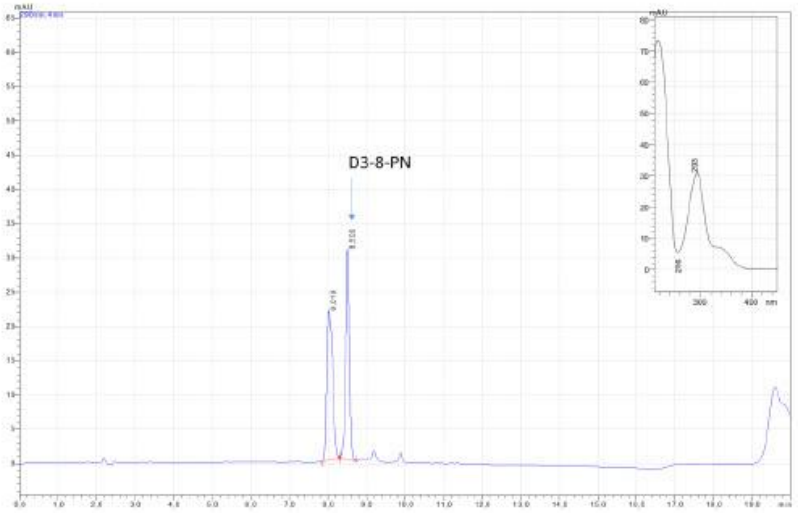

Figure 4: HPLC chromatogram of D_3-8-PN and the contaminant. The retention time and the UV profile (top right) of D_3-8-PN is the same as non-deuterated 8-PN.

2.2 D_3-Isoxanthohumol (non-microwave)

XN, 0.14 mM was dissolved in D_2O with the addition of NaOD (250 µL). The reaction was left on an ice bath overnight and afterwards 84 µL of D_2SO_4 was added causing a yellow precipitate to form. The D_2O was removed by evaporation, and further enrichment was achieved by the addition of fresh D_2O and refluxed, along with a few mg of Pd/C 10%, for 6 h. The process was repeated. Work up was by the addition of EtOAc and water (DI) and the organic phase was collected the EtOAc was repeated three times until a final wash of the organic phase with brine. The organic phase was collected dried using Na_2SO_4 (anhydrous), filtered and evaporated. Columned using 99:1 DCM:MeOH. Fractions that contained d_3 -IXN were collected. The final preparation utilised preparative HPLC system 2. Yield 98%. ESI+ 358.14. IXN ^{1}H NMR (400 MHz, Methanol-d_4) δ 7.31 (d, J = 8.5 Hz, 7H), 6.81 (d, J = 8.6 Hz, 18H), 6.12 (s, 1H), 5.28 (dd, J = 12.8, 3.0 Hz, 2H), 5.14 (t, 1H), 3.80 (s, 4H), 3.21 (d, J = 6.0 Hz, 2H), 2.98 (dd, J = 16.7, 12.8 Hz, 1) 2.71 – 2.60 (m, 2H), 1.62 (s, 4H), 1.56 (s, 5H). ^{13}C NMR (101 MHz, Methanol-d_4) δ, 192.92, 164.27, 163.83, 158.80, 131.67, 131.67, 128.86, 123.89, 116.24, 109.95, 109.95, 93.42, 79.99, 55.96, 46.21, 25.96, 22.70, 17.90.

2.3 D_3-Isoxanthohumol-C and D_3-Xanthohumol-C

To prepare D_3-IXN-C, XN was treated the same as section 2.3.2 and then further treated by dissolving D_3-IXN 20 mg in 5 mL THF followed by the addition of 36 mg of DDQ. The reaction was taken to reflux and left to react for 4h before being quenched by the addition of 2.5 mL a 1% Na_2SO_4 solution. Workup included 3 times wash with H_2O: EtoAC 50:50 and the H_2O fraction washed 3 times with equal amounts of EtOAc. The organic phase was collected and dried with Na_2SO_4 and evaporated before flash chromatography. The crude reaction was dry loaded and eluted using 20:80 EtOAc: pentane. XN-C was prepared the same way as d_3-IXN-C although d_3-XN (4 mg) was the starting material. Preparative HPLC system 1 was used in the final clean-up of both compounds.

Yielding, d_3-IXN-C 4.76 and d3-XN-C 1.13 mg. D_3-IXNC NMR ESI$^+$ (356.15) ^{1}H NMR (400 MHz, Methanol-d_4) δ 7.32 (d, J = 8.5 Hz, 1H), 6.83 (d, J = 8.6 Hz, 1H), 6.53 (d, J = 10.1 Hz, 1H), 6.11 (s, 0H), 5.54 (d, J = 10.1 Hz, 0H), 5.36 (s, 0H), 3.83 (s, 1H), 1.43 (s, 1H), 1.41 (s, 1H). ^{13}C NMR (101 MHz, Methanol-d_4) δ 28.37 (4", 5"), 28.66, 45.44 (3), 56.38 (OCH3), 79.19 (3"), 80.26 (2), 94.70 (6), 104.12 (8), 106.35 (4a), 116.38 (5', 3'), 116.74 (1"), 127.72 (2"), 128.91 (6', 2'), 131.04 (1'), 159.01 (4'), 160.56 (7, 8a), 161.95, 163.51 (5), 192.45 (4). D_3-XN-C ESI + 356.20 ^{1}H NMR (500 MHz, MeOD) δ 7.71 (d, J = 7.9 Hz, 1H), 7.52 (q, J = 4.1 Hz, 2H), 6.83 (d, J = 8.8 Hz, 1H), 4.88 (s, 1H), 3.93 (d, J = 20.8 Hz, 3H), 3.35 (s, 5H), 1.34 (s, 6H).

D_3-IXN-C was produced from D_3-IXN (non-microwaved) by the selective prenyl cyclisation using DDQ, a known reaction that was initially carried out by Mahoney et al. (Mahoney et al., 1988)Upon preparative HPLC there were 2 major product, which one was D_3-IXN-C. The same method was applied to XN using the same molar equivalent and resulted in D_3-XN-C. Figure 8, shows the protons that were exchanged which is the equivalent to non-microwave D_3-IXN, therefore the compounds are stable enough to perform harsh reactions and retaining the deuteration.

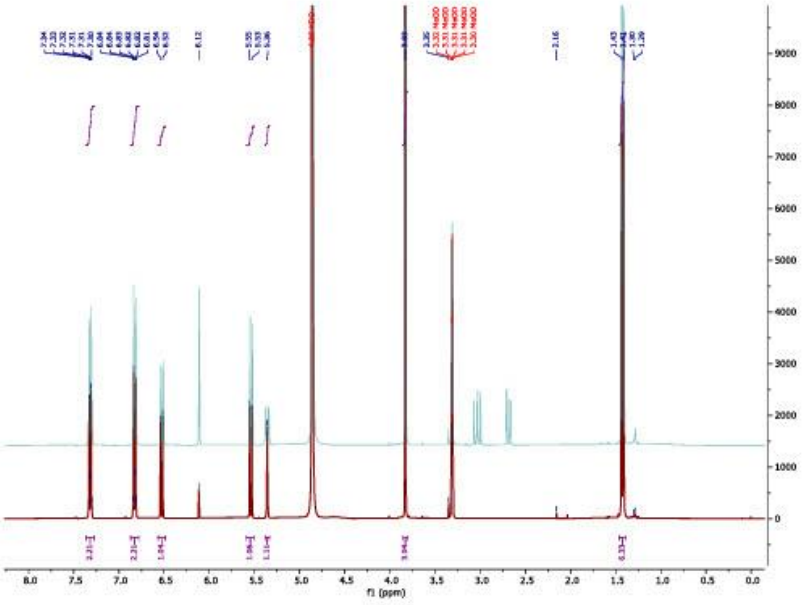

Figure 5: D-3-IXN-C (red) that was synthesised from non-microwave D3-IXN superimposed with IXN-C (Cyan).

The exact same procedure using the same molar equivalent of DDQ was applied to a proportion of the D_3-XN (See section 2.3.3), the results show that the equivalent positions were deuterated. Position 2, 8 and 15 (See Figure 9).

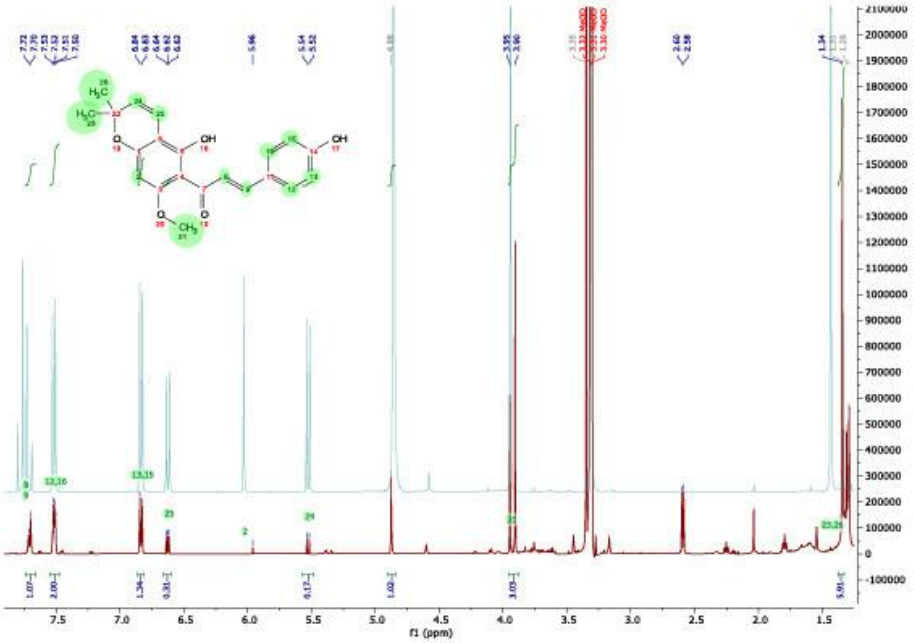

Figure 6: XN-C (cyan) superimposed with D3-XN-C (red). The assignments are for XN-C and therefore, it is possible to see which protons are exchanged. Due the lack of a peak (position 8 and 2).

The NMR (Figure 10) shows that the deuterium exchange using a non-microwave approach has a different deuteration pattern than with microwave assistance. First, using the NaOD and D_2SO4 causes both protons at position 2 to be exchanged. The structure of the non-microwaved acid/base catalysed reaction that formed D_3-IXN. There was partial deuterium exchange for proton 8 which can explain the m/z of 358.14 value observed during MS analysis. Although upon attempts to demethylate the D_3-IXN to produce D3-8PN were unsuccessful the cyclisation of the prenyl group was achieved as mentioned before.

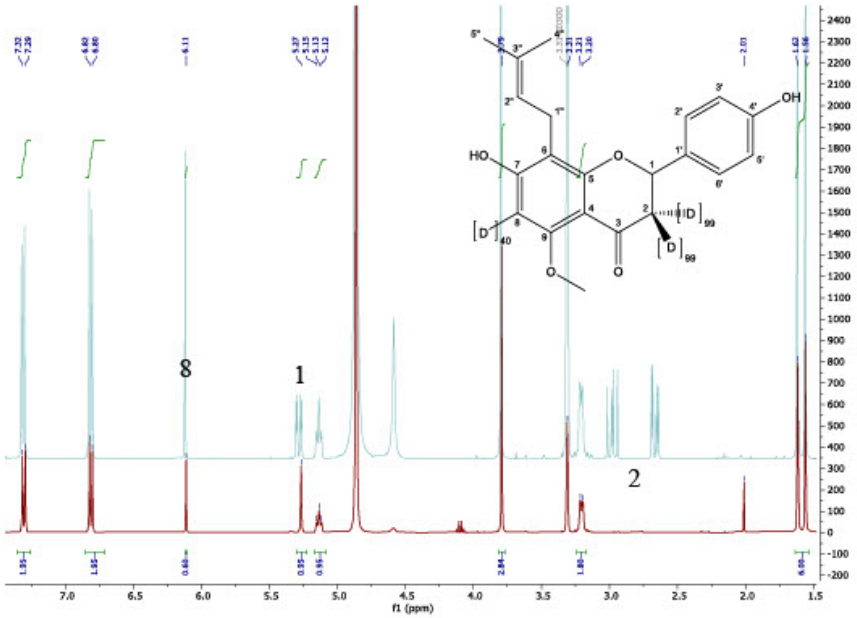

Figure 7: D3-IXN (Red) superimposed with IXN (Cyan). The protons that are exchanged are in position 2. Take not the position 1 is now a singlet indicating the complete conversion of the protons as in IXN this is a double indicating the proximity to two protons.

2.4 Isotope labelled DXN (xanthohumol-derivative without Michael system)

Preparation of DXN

a) Ph_2SiD_2

5 g dichlordiphenylsilane was dissolved in 30 ml THF (rotisolv) in a three necked reaction vessel equipped with a nitrogen inlet, condenser and relief vent. 640 mg LiD was added and the suspension is refluxed under nitrogen for 48 h. After cooling, the suspension is filtered through a glass frit, filled with a dense bed of celite (2 cm). The clear filtrate is stripped from THF by soft application of vacuum and carefully distilled under nitrogen, using a short-path vacuum distillation apparatus ("balltube")(Büchi Mod.).

b) Stryker catalyst

To prepare the Stryker catalyst, the method according to Lee is followed, with the exception of using Ph_2SiD_2.(Lee and Yun, 2005)

c) DXN

Afterwards, 44 mg deuterated Stryker catalyst was suspended in 6 ml dry benzene in a Schlenk tube under nitrogen atmosphere. 390 mg Ph_2SiD_2 was added and after 10 min stirring, 100 mg xanthohumol was added. After stirring over night at room temperature, 5 ml D_2O was added followed by 15 ml EtOAc. The aqueous phase was separated and the organic phase was mixed with 2 g silica gel G60. The solvent was removed and the resulting dry load mixture was subjected to the top of a small column of silica gel G60 (length 2 cm, diameter 1 cm) and eluted with EtOAc, 75 ml. This crude fraction containing also phosphane and some silane decomposition products was chromatographically purified. After removing the solvent, the residue was dissolved in 5 mL methanol and filtrated over glass wool. Methanol was removed under nitrogen stream, the residue was dissolved in acetonitrile/water (2/3) and the cleaning procedure started using solid phase extraction with a Hypersep C_{18} column (1000 mg 6 mL; Thermo). The product was eluted using acetonitrile/water 35/65 and these fractions were lyophilized to remove the solvent. The residue was then purified using preparative HPLC (System 4). After lyophilization of the product fractions, the product was obtained as a white powder (7.2 mg). HRMS-ain positive ionization mode(IT TOF; Shimadzu): $[M+H]^+$ 358.1761 (predicted 358.1759; $\Delta = 0.2$mDa; $\Delta = 0.56$ ppm) for the sum formula of $C_{21}H_{23}DO_5$. D_2-XN ^{1}H NMR (400 MHz, Methanol-d_4) 7.02 (d, $J = 8.3$ Hz, 2H), 6.685 (d, $J = 8.7$ Hz, 2H), 5.966 (s, 1H), 5.159 (t, J=7.3Hz), 3.811(s, 3H), 3.183 (m, $J = 7.8$ Hz, J=7.33Hz, 3H), 2.814 (t, J=7.8 Hz, 1H), 1.737 (s, 3H), 1.634 (s, 3H) . ^{13}C NMR (400 MHz, MeOD) δ 206.5, 165.76, 163.81, 162.64, 156.52, 133.88, 131.31, 130.29, 124.26, 116.15, 109.25, 105.76, 91.24, 55.88, 47.46, 25.95, 22.21, 17.86, 14.42.

3 Preparative and analytical HPLC

3.1.1 Preparative HPLC System 1

The preparative HPLC was carried out using a YMC-ACTUS Tri art column (Triart C18, 150 x 20.0 mm, 1.D. S-5 µm, 12 nm) connected with YMC-Guardpack Pro (C18, 30 x 10.0 mml.D. S-5 µm, 12 nm) guard column. The HPLC system comprised of a BESTA pump system (Besta Type HD 2-400 pump, Wilhelmsfeld, Germany) coupled to a Sapphire variable wavelength detector (Ecom, Prague, Czech Republic). The wavelength was set to 290 nm for the initial at 0-15.5 min and at 370 nm afterwards. Samples was manually injected using a glass syringe (1 mL) and a valve (brand) initiated the set time program. The flow was set at 7.5 mL/min with HPLC grade H_2O (VWR) and MeOH (VWR) starting with a multi-step gradient of 0 min 65 % MeOH, 0.5 min 80 % MeOH, 12.3 min 80 % MeOH, 12.6 min 85 % MeOH,16.5 min 85 % MeOH, 16.8 min 90 % MeOH, 24.5 min 90 % MeOH, 25.0 min 65 % MeOH, 30.0 min 65 % MeOH. All samples were manually collected.

3.1.2 Preparative HPLC System 2

The preparative HPLC used the same as system 1 although starting with 80% MeOH and monitored only at 290 nm.

3.1.3 Preparative HPLC System 3

D_3-8-Prenylnaringenin underwent further purification due to overlapping peak with d_3-IXN. The method was a modified version of system 1. Starting at 65% MeOH and remained for 7.5 min before being raised to 80% MeOH and left for isocratic until 20 mins. Lastly, solvent B was increased to 95% for 5 minutes which the column was re-equilibrated at 65% MeOH.

3.1.4 Preparative HPLC system 4

To purify the isotope-labelled Xanthohumol derivative without Michael system the preperative HPLC-System Puriflash 250 (Interchim) and a C18-column (Phenomenex, Luna C18(2) 250x15 mm 5u) was used. The gradient used started with 40% A (acetonitrile) and 60% B (water) and raised to 95 % B within 45 minutes.

3.1.5 Chromatograms of Prep HPLC

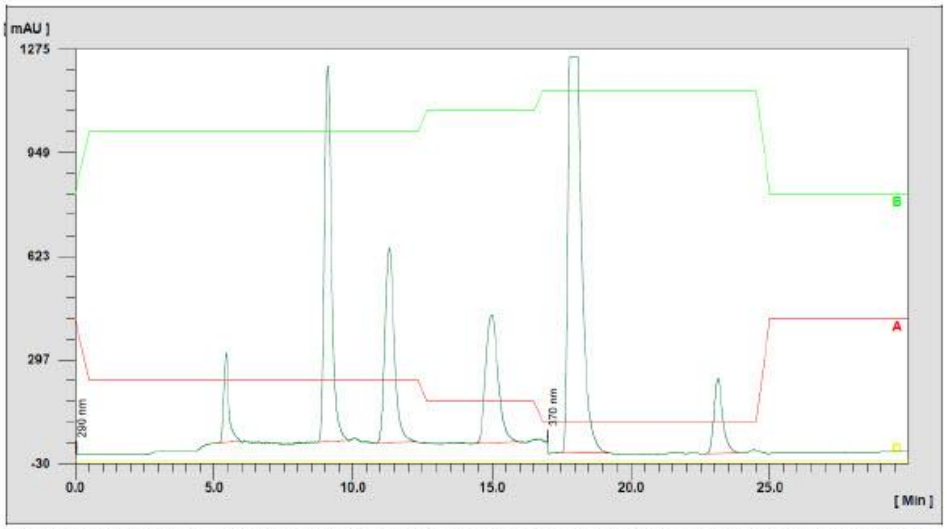

Figure 8: Preparative HPLC of Reference compounds IXN (rt=9.4), 8PN (rt=11), 6PN (rt=15) and XN (rt= 19)

11

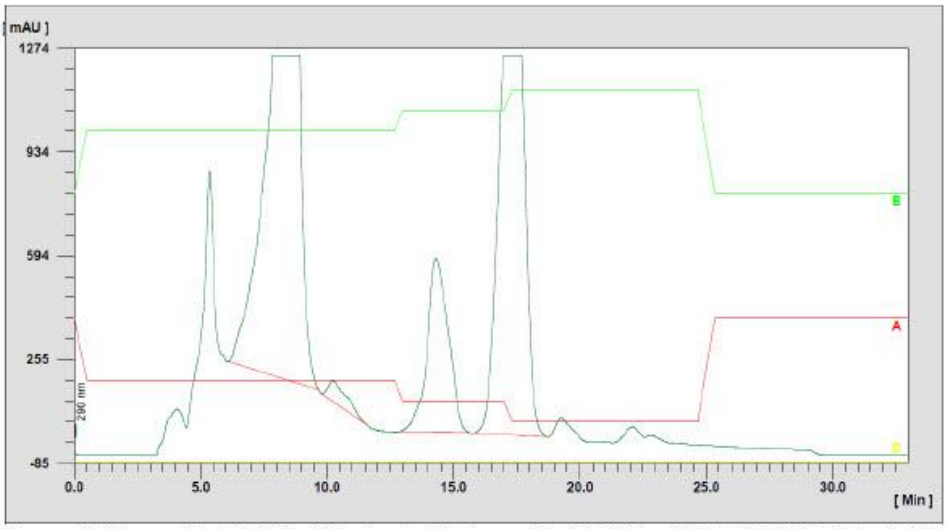

Figure 9: Preparative HPLC of Deuterated isotopes, D_3-IXN (rt = 9), D_3-6-PN(rt=10), D_3-8PN (rt =14.8) and D_3-XN (rt=19).

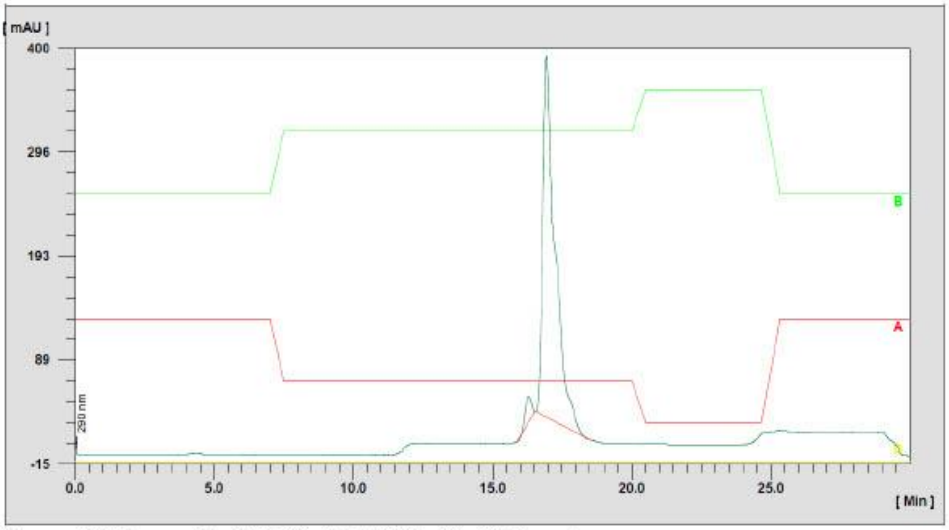

Figure 10. Preparative HPLC of D_3-8-PN after further clean up.

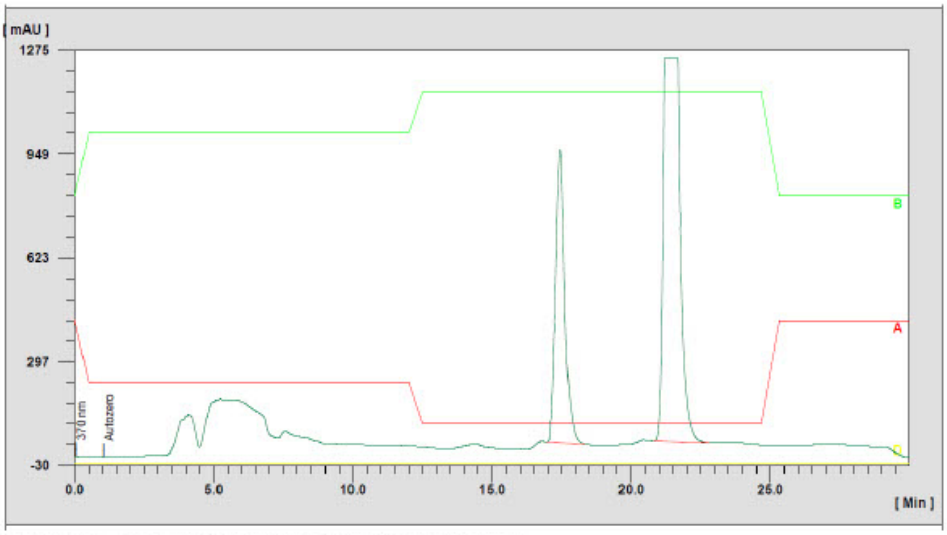

Figure 11. Preparative HPLC of D_3-XN -C (rt= 22).

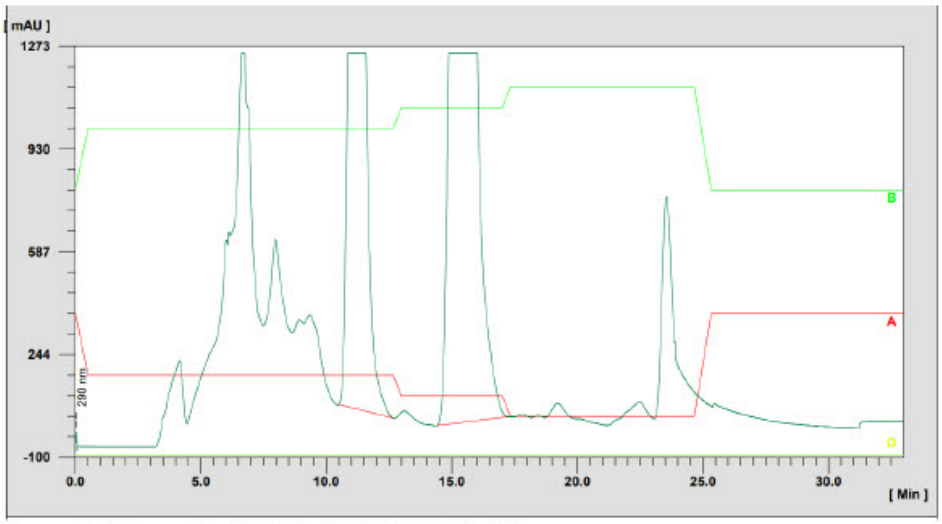

Figure 12: Preparative HPLC of D_3-IXN-C (rt = 15).

3.1.6 Analytical HPLC

13

Due to the low amounts of D_3-8-PN and D_3-XN-C synthesized, HPLC was necessary to quantify. Calibration graphs (See supplementary information) were produced using standards of 8-PN and XN-C quantified using qNMR dissolved in ACN. The calibration graphs were used to produce linear

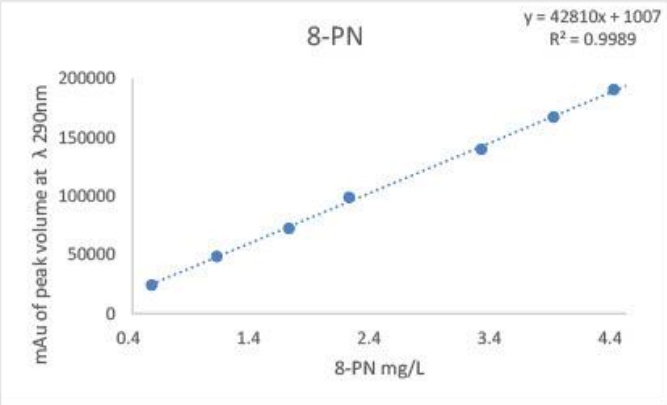

regression equations and subsequently the concentrations of D_3-8-PN and D_3-XN-C quantified.

Figure 14: The calibration graph of 8-PN. D3-8-PN concentration was calculated using the above equation.

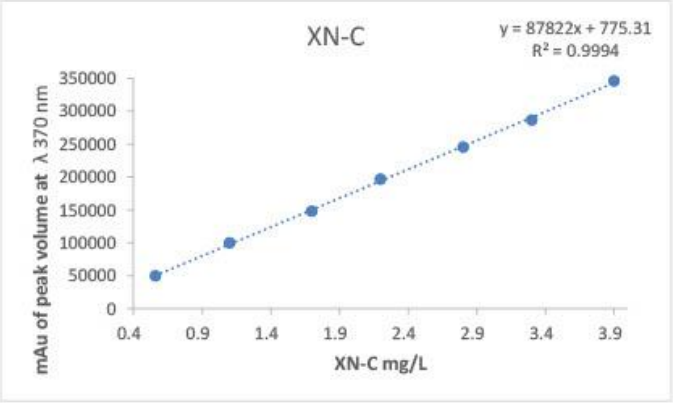

Figure 15: The calibration graph of XN-C. D3-XN-C concentration was calculated using the above equation.

4 Calibration graphs for SIDA

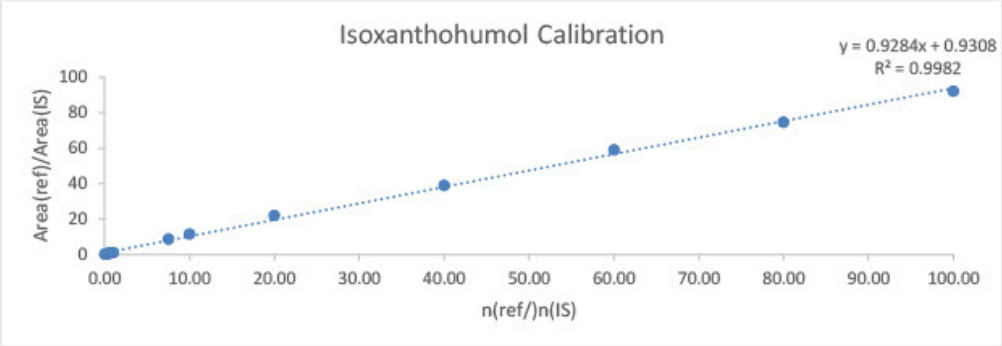

Figure 16: Calibration of isoxanthohumol

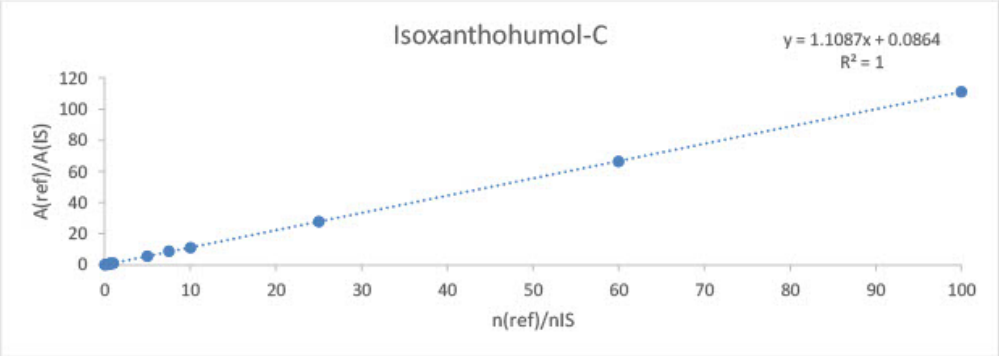

Figure 17: Calibration of Isoxanthohumol-C

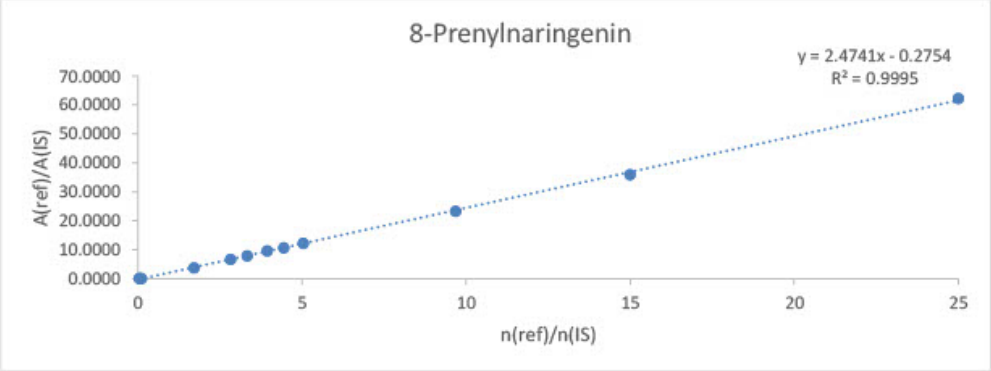

Figure 18: Calibration of 8-Prenylnaringenin

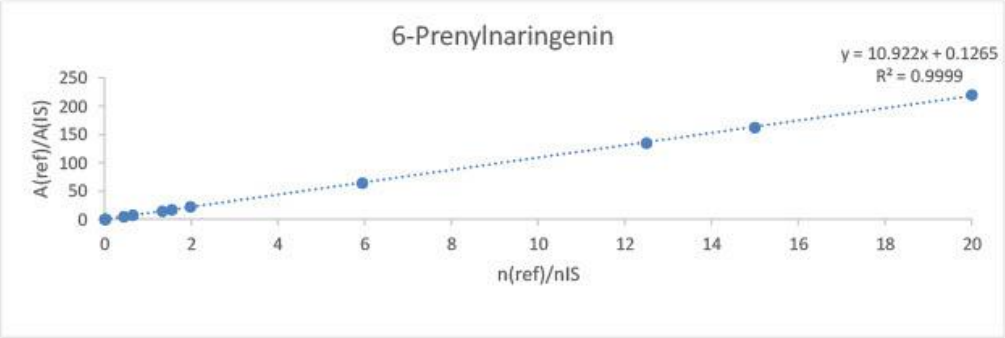

Figure 19: Calibration of 6-Prenylnaringenin

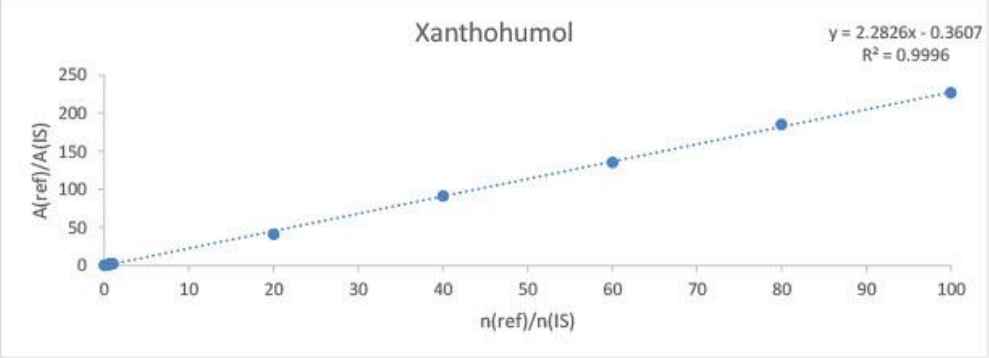

Figure 20: Calibration graph of xanthohumol

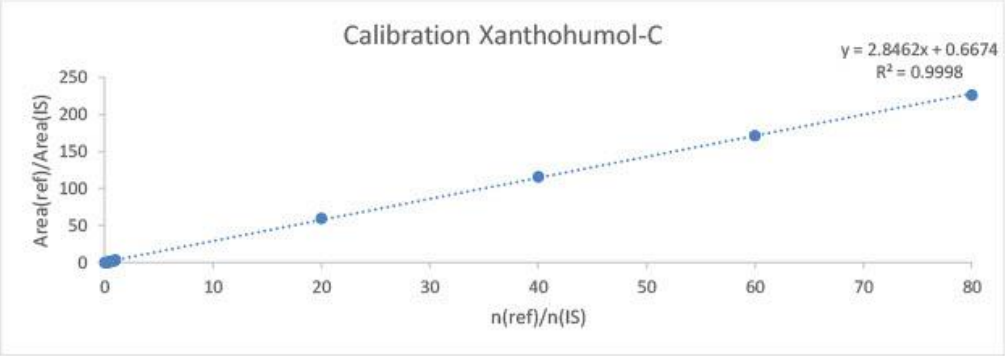

Figure 21:Calibration graph of Xanthohumol-C

5 References

Lee, D.-w., and Yun, J. (2005). Direct synthesis of Stryker's reagent from a Cu(II) salt. *Tetrahedron Lett.* 46(12), 2037-2039. doi: 10.1016/j.tetlet.2005.01.127.

Mahoney, W.S., Brestensky, D.M., and Stryker, J.M. (1988). Selective hydride-mediated conjugate reduction of .alpha.,.beta.-unsaturated carbonyl compounds using [(Ph3P)CuH]6. *J. Am. Chem. Soc.* 110(1), 291-293. doi: 10.1021/ja00209a048.

Roehrer, S., Behr, J., Stork, V., Ramires, M., Medard, G., Frank, O., et al. (2018). Xanthohumol C, a minor bioactive hop compound: Production, purification strategies and antimicrobial test. *J. Chromatogr. B* 1095, 39-49. doi: 10.1016/j.jchromb.2018.07.018.

Stevens, J.F., Ivancic, M., Hsu, V.L., and Deinzer, M.L. (1997). Prenylflavonoids from Humulus lupulus. *Phytochemistry* 44(8), 1575-1585. doi: 10.1016/s0031-9422(96)00744-3.

Urmann, C., and Riepl, H. (2020). Semi-Synthetic Approach Leading to 8-Prenylnaringenin and 6-Prenylnaringenin: Optimization of the Microwave-Assisted Demethylation of Xanthohumol Using Design of Experiments. *Molecules* 25(17), 4007. doi: 10.3390/molecules25174007.

Wilhelm, H., and Wessjohann, L.A. (2006). An efficient synthesis of the phytoestrogen 8-prenylnaringenin from xanthohumol by a novel demethylation process. *Tetrahedron* 62(29), 6961-6966. doi: 10.1016/j.tet.2006.04.060.

5.3 Synthesis of human phase I and phase II metabolites of hop (Humulus lupulus) prenylated flavonoids [69].

metabolites

MDPI

Article

Synthesis of Human Phase I and Phase II Metabolites of Hop (*Humulus lupulus*) Prenylated Flavonoids

Lance Buckett [1,*], Sabrina Schönberger [1], Veronika Spindler [1], Nadine Sus [2], Christian Schoergenhofer [3], Jan Frank [2], Oliver Frank [4] and Michael Rychlik [1]

[1] Analytical Food Chemistry, Technical University of Munich, Maximus-von-Imhof Forum 2, 85354 Freising, Germany; sabrina.schoenberger@tum.de (S.S.); veronika.spindler@tum.de (V.S.); michael.rychlik@tum.de (M.R.)
[2] Department of Food Biofunctionality (140b), Institute of Nutritional Sciences, University of Hohenheim, Garbenstraße 28, 70599 Stuttgart, Germany; nadine.sus@nutres.de (N.S.); jan.frank@nutres.de (J.F.)
[3] Department of Clinical Pharmacology, Medical University of Vienna, Währinger Gürtel 18-20, 1090 Vienna, Austria; christian.schoergenhofer@meduniwien.ac.at
[4] Food Chemistry and Molecular Sensory Science, Technical University of Munich, Lise-Meitner-Str. 34, 85354 Freising, Germany; oliver.frank@tum.de
* Correspondence: lance.buckett@tum.de

Abstract: Hop prenylated flavonoids have been investigated for their in vivo activities due to their broad spectrum of positive health effects. Previous studies on the metabolism of xanthohumol using untargeted methods have found that it is first degraded into 8-prenylnaringenin and 6-prenylnaringenin, by spontaneous cyclisation into isoxanthohumol, and subsequently demethylated by gut bacteria. Further combinations of metabolism by hydroxylation, sulfation, and glucuronidation result in an unknown number of isomers. Most investigations involving the analysis of prenylated flavonoids used surrogate or untargeted approaches in metabolite identification, which is prone to errors in absolute identification. Here, we present a synthetic approach to obtaining reference standards for the identification of human xanthohumol metabolites. The synthesised metabolites were subsequently analysed by qTOF LC-MS/MS, and some were matched to a human blood sample obtained after the consumption of 43 mg of micellarised xanthohumol. Additionally, isomers of the reference standards were identified due to their having the same mass fragmentation pattern and different retention times. Overall, the methods unequivocally identified the metabolites of xanthohumol that are present in the blood circulatory system. Lastly, in vitro bioactive testing should be applied using metabolites and not original compounds, as free compounds are scarcely found in human blood.

Keywords: metabolites; synthesis; prenylated flavonoids; hops; beer; xanthohumol; blood analysis

Citation: Buckett, L.; Schönberger, S.; Spindler, V.; Sus, N.; Schoergenhofer, C.; Frank, J.; Frank, O.; Rychlik, M. Synthesis of Human Phase I and Phase II Metabolites of Hop (*Humulus lupulus*) Prenylated Flavonoids. *Metabolites* **2022**, *12*, 345. https://doi.org/10.3390/metabo12040345

Academic Editor: Cholsoon Jang

Received: 29 March 2022
Accepted: 10 April 2022
Published: 12 April 2022

1. Introduction

Prenylated flavonoids (PF) are secondary plant metabolites found in a range of plants, notably amongst the families Cannabaceae (hops, *Humulus lupulus*), Moraceae (mulberry, *Morus Albas*), and Fabaceae (liquorice, *Glycyrrhiza. glabra*), some of which are part of the human diet [1,2]. Many prenylated flavonoids are also found in the non-food components of plants, such as mulberry trees; the highest concentrations of prenylated flavonoids are in roots and leaves [3]. Prenylated flavonoids play a role in plant defence, as they perform a range of anti-mycotic, anti-bacterial, and anti-viral activities, which is perhaps why plants invest heavily in their biosynthesis [4]. Arguably the most frequently researched prenylated-flavonoid derivative is xanthohumol (XN), a chalcone from hops, which is a main ingredient in beer production. As beer is the most heavily consumed alcoholic beverage, XN and related compounds are believed to originate solely from beer in a dietary context [5–7]. The lipophilic prenyl group of XN seems to increase the bioavailability of

We therefore investigated the synthesis of XN metabolites and compared them to the metabolome of a human blood sample in order to provide the relevant human metabolites of XN for future experiments aimed at investigating their biological activities.

2. Results and Discussion

The synthetic approaches to obtaining the analytical standards of certain metabolites of XN via the Königs–Knorr method are presented in Figure 2, including the most abundant metabolites, XN-7-O-glc and IXN-7-O-glc [18]. Additionally, we carried out in vitro glucuronidation by incubating the XN with pig-liver microsomes to further confirm the synthesised products. To achieve the hydroxylation of the prenyl group of PF while retaining the prenyl character, a Riley oxidation process was selected [19]. The sulfation used a reaction based on the work of Legette et al. (2014) that involves base acid sulfation, although the authors did not isolate the products [20]. Currently, no reference standards obtained via synthetic methods are generally available and, therefore, new methods of isolation of vast quantities of PF for synthesis make these approaches viable, as XN isolated from spent hops is more obtainable [16,21]. Understanding the metabolism will give further evidence of how these compounds interact at a biological and cellular level in vivo. A range of XN products is already available on the market and certain pharmaceutical formulations are being developed and researched, even though the exact mechanism through which they influence health has not been elucidated. Lastly, XN is already being developed in the form of bioavailable gold nano composites used in crop protection and as a food preservative [22–25].

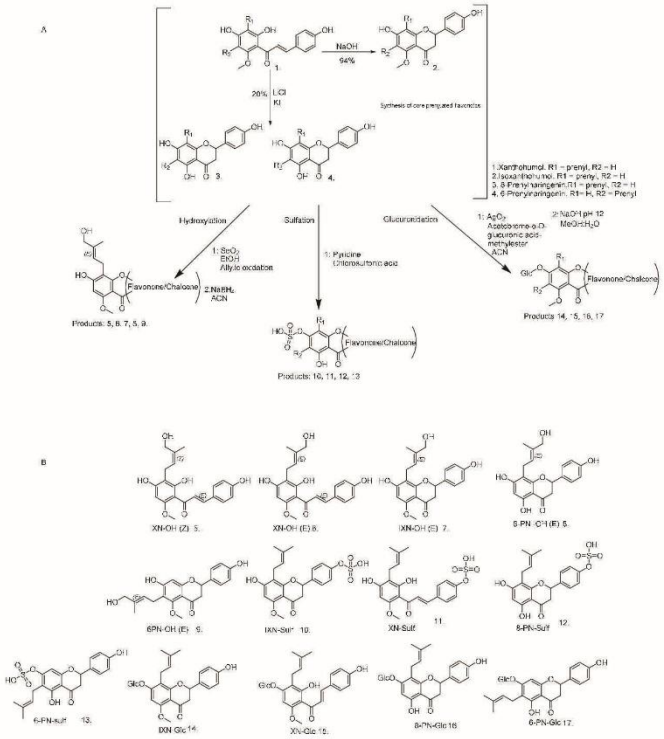

Figure 2. The generalised reaction scheme (**A**) for the synthesis of prenylated flavonoid metabolites. Products 1–4 served as the scaffold to further react into certain metabolites in either chalcone or flavanone form [18,20]. (**B**) The structures of each prenylated flavonoid synthesised (see Supplementary Information for detailed structure elucidation data).

The synthetic metabolites were characterised by HPLC, MS, LC-MS/MS, and NMR. The glucuronides were subjected to an additional enzymatic deconjugation using β-glucuronidase from *Helix pomatia* to supplement the NMR data and confirm that they were in the β-anomer configuration. The method used to chemically and biochemically (without the need for ultracentrifugation) produce some metabolites of hop prenylated flavonoid XN was successful, which might be useful for bioactivity testing and analytical methods in future work. The MRM mass spectrometry showed that the products fragmented in the same way as was observed in other in vivo studies investigating XN or related PF metabolism (see Supplementary Information) [20,26–28].

2.1. Hydroxylation of the Prenyl Group

The hydroxylation of the prenylated flavonoids showed that the Riley oxidation was successful and resulted in yields of between 10–25% in compounds **5–9**. Upon the initial analysis by mass spectrometry, the hydroxylated products all revealed an additional mass increment of 14 Da, which supported the assumption that the respective aldehydes formed (no further analysis was carried out). To reduce the aldehyde into hydroxyl, $NaBH_4$ was used, which resulted in a mass increment correlating to hydroxylation (+16). The UV spectra of compounds **5** and **6** each showed an absorption maximum of λ = 370 nm and 7–9 of λ = 290 nm, indicating that the products were in chalcone and flavanone form, respectively. Compounds **5–7** revealed an *m/z* signal at 369, while 8 and 9 showed an *m/z* signal at ~355, which suggests that the mass of a hydroxyl group (+16) was added to all the compounds. Thus, the alkene moiety of the prenyl group was retained. The MS analysis of the hydroxylation of the XN revealed two major products, as two peaks were separable in the chromatogram (see Figure 3). Once the NMR (NOESY) data were collected, they revealed that the two products were the *E* and the *Z* isomer, respectively. It is believed that trace amounts of the *Z* isomer were produced in 7–9, but none of the separation methods were able to resolve. Substances 8 and 9 produced a small shoulder, which can be visualised in the LC-MS/MS chromatogram.

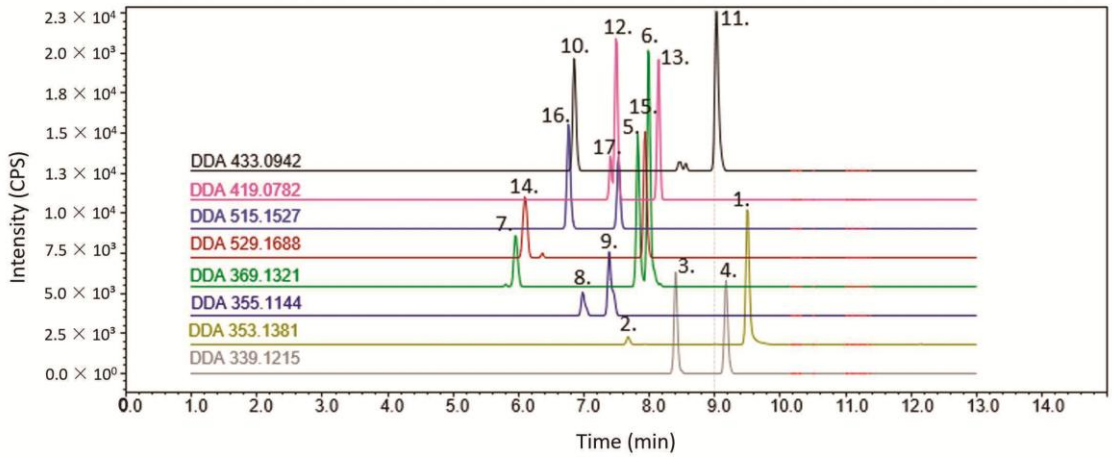

Figure 3. The DDA chromatogram (base shifted) of the analytical standards produced. Substances 1–17.

The NMR analysis further confirmed the hydroxylation of a terminal methyl group (4″ or 5″) of the prenyl moiety as the respective former signal was shifted to higher frequencies (between 3 ppm and 4 ppm, depending on the PF hydroxylated), at which point the integral was two instead of three protons in all of the analysed PFs. To confirm the stereochemistry of the products, 2D NMR experiments were carried out. The absolute confirmation was determined using a NOESY experiment via a correlation between the H2″ and the two remaining protons on the hydroxylated methyl in *E* form and the H2″ and the methyl

group in *Z* form [29]. Small secondary products that were visible in the same MRM mass chromatograms were also seen in the NMR spectra for the flavanone form, and it was assumed that they were produced, although they could not be isolated in large enough quantities in the work presented here.

Hydroxylated PFs 5–7 have only been found by in vitro incubation either with human liver microsomes or through metabolism using yeast *P. membranifaciens* [26,30]. This is the first report on the chemical synthesis of these compounds.

2.2. Synthesis of Sulfates

The sulfation of the prenylated flavonoids was successful, but was not regiospecific (yields between 50–60%). Protection chemistry, e.g., hydroxyl protection using MOM-Cl, would potentially enable a more specific conjugation, but regardless of whether one isomer is created, the other can be elucidated via the assumption that MS fragmentation patterns are similar in their identification of isomers. It was assumed that no desmethylxanthohumol derivatives formed as they were unlikely to be present due to their high instability in acidic environments, such as the stomach. However, for the quantification of the other metabolites, isolated isomers of each compound would be necessary.

2.3. Biosynthetic Glucuronidation

In our initial attempts to produce glucuronides, we used biochemical methods. This was sufficient for the production of analytical standards, but it was costly when considering the amounts (in mg) required for cell culture incubation experiments. This was mainly due to the high cost of the cofactor uridine diphosphate glucuronic acid and the antibiotic alamethicin; therefore, this approach was abandoned after the successful production of the XN-7-O-Glc and XN-4′-O-Glc. The advantage of biosynthesis is that if tentative evidence is required, it can be performed quickly, and using this approach enabled the confirmation of the XN-C-glc and IXN-C-glc. Moreover, it provided evidence about the selectivity of which isomer was produced as the synthetic glucuronidation only resulted in one major product. Only mixed Uridine 5′-diphospho-glucuronosyltransferases (UGT) were used and, perhaps, further engineering might lead to increased yields. Inadvertently, our results suggested that the enzymes from the pigs glucuronidated XN in a similar way to humans, favouring XN-7-O-glc production versus XN-4′O-glc [31].

XN-C-Glucuronide and IXN-C-Glucuronide

All the synthetic methods on the pyranone PF failed to produce enough material for an NMR, although trace amounts of xanthohumol-C glucuronide were found after the Königs–Knorr approach. Therefore, it was assumed that this is a major metabolite and only tentative evidence was obtained for the formation of XN-C and IXN-C-glucuronide. Therefore, glucuronic acid was assumed to be attached to the phenol group. This regiospecificity was evidenced by the crystal structures of the XN and IXN, revealing a strong hydrogen bond between the keto and 5-hydroxy moieties, which directs the conjugating enzyme UGT to the phenol group. Instead, any enzymatic conjugation at the 5-hydroxyl would need to overcome the energy used for displacing the hydrogen bond before the occurrence of metabolism [32].

2.4. Synthesis of Glucuronides

Initially, the Königs–Knorr reactions on the XN, as the most abundant PF in the hops, were investigated, and the conjugation was confirmed by MS (data not shown). However, deprotection, using a variety of established methods, resulted in either the destruction of the starting material or no removal of the protective acetate groups on the glucuronic acid methyl ester. Additionally, the use of KCN only resulted in the removal of the acetate groups, but failed to remove the methyl ester, making it a non-viable method for the deprotection of PF-glucuronides within the Königs–Knorr approach. Therefore, to obtain the XN-7-O-glc and IXN-7-O-glc, acetate methyl ester was first synthesised and

then deprotected by the addition of toluene sulfonic acid, resulting in the conversion of the IXN-7-O-glc into XN-7-O-glc. It seemed that the conversion between flavanone and chalcone could be partially controlled by the addition of KOH, most likely resulting in ring opening, and neutralisation allowed the formation of XN-7-O-glc along with IXN-7-O-glc, depending on the amount of KOH used. However, the reaction required the careful addition of KOH which, if added in excessive amounts, could have resulted in the destruction of the glucuronide conjugate. The same approach was applied to the 8-PN and 6-PN, but based on the observation that both 8-PN-7-O-glc and 6-PN-7-O-glc were produced, it was not deemed necessary to isolate the pure 6-PN and 8-PN. Instead, a mixture was sufficient for our analytical purposes, thus avoiding a time-consuming purification step (yield 12%). The application of Königs–Knorr on XN as a starting material resulted in only trace amounts of the glucuronide product. Therefore, IXN, which produced a yield of 21.3%, is a better starting material.

2.5. LC-MS/MS of Synthesised Analytes

In non-targeted tandem mass spectrometry, data-dependent acquisition (DDA) is a common method used to fragment a (user-defined) number of the highest ion count "masses" from the MS1 scan within certain time frames. The MS2 scans correspond to the MS1 scan, which simplifies data interpretation and was applied to analyse the synthetic products in Figure 3. The DDA of the standard mixture revealed the fragmentation of each compound corresponding to the literature and the expected fragmentation proposed therein (see Supplementary Information for details) [28].

2.6. LC-MS/MS of Analytes in Human Blood after Xanthohumol Consumption

The selection of the blood sample 1 h after dosing was based on the work of Legette et al. (2014), who demonstrated peak XN concentrations after 1 h of consumption [20]. Therefore, blood plasma samples were taken randomly from a human trial at the 1-h time point. Upon the initial analysis, the mass spectrum was saturated with components from the human plasma (as components from the blood were selected over the XN metabolites), making DDA unsuitable for human plasma; therefore, data-independent acquisition (DIA) was carried out. Contrary to the DDA, the DIA fragments of all the ions in the MS1 spectra retaining all information on all the detected compound fragments in the spectra, although it was difficult to determine the precursor for each molecule. In addition, the standard mixture was also determined using the DIA for co-chromatography and the mass-spectrometry identification of the fragmentation of the compounds in the human blood plasma ($n = 2$). Regarding the glucuronides, all the synthesised metabolites were found in the human plasma sample; therefore, the positions of the glucuronic acids were identified unequivocally. Additionally, the compounds IXN-4′-O-Glc, 8-PN-4′O-Glc, and 6-PN-4′O-Glc were tentatively identified as they possessed the same nominal mass and fragmentation pattern as the synthesised compounds (Figure 4). This coincides with the assumption of Yilmazer et al. (2001) regarding the analysis of glucuronides after enzyme incubation and confirms that they were correct, due to their identification of the same elution order on a C18 column [33].

Unlike the glucuronides, for the XN sulfates in the human plasma (Figure 5), only XN-4′-O-sulfate was identified unequivocally as no other co-chromatographing peak was found. As being tentatively identified at level 3 (Table 1) according to Schymanski et al. (2014), two other products were found, namely IXN-7-O-sulfate and XN-7-O-sulfate [34]. No IXN-4′-sulfate was found, and the most prevalent product by intensity was, tentatively, XN-7-O-sulfate.

In Figure 6, the sulphated prenylnaringenins revealed that, out of the synthesised compounds, only compound **14** (6-PN-7-O-sulfate) was found, along with the tentative compounds 8-PN-7-O-sulfate (compound **12**) and 6-PN-4′O-sulfate (compound **15**).

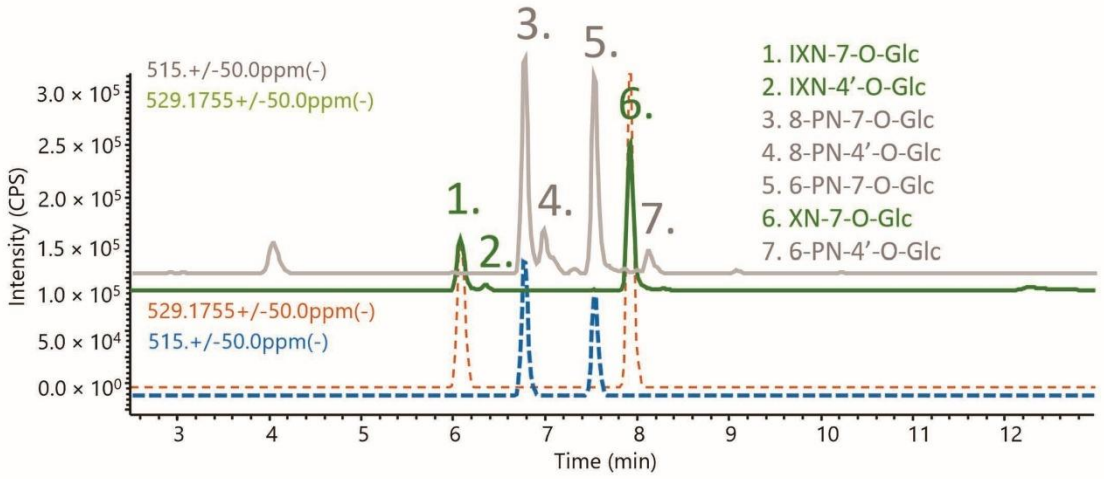

Figure 4. The identification of glucuronides after 60 min of XN consumption: co-chromatograms of the synthesised prenylated flavonoids (dashed blue, brown) and the compounds found in blood (green and gray).

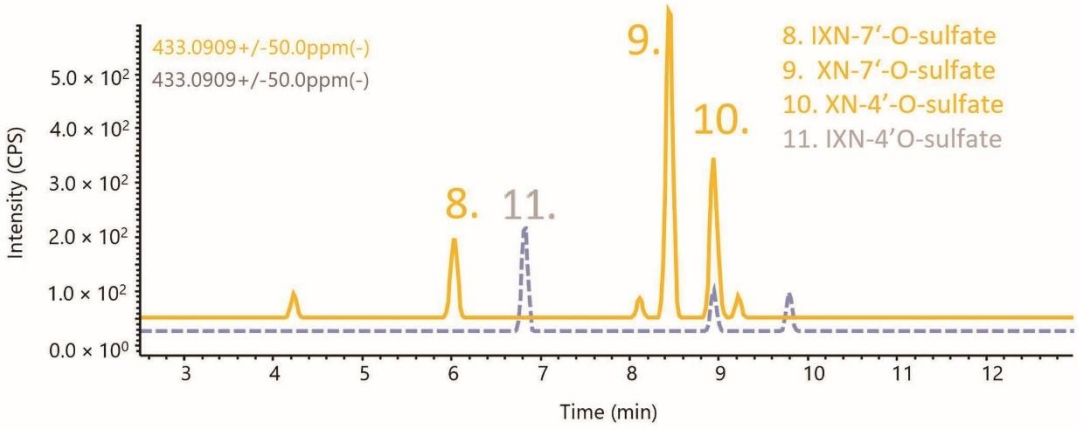

Figure 5. Co-chromatogram of the synthesised XN/IXN sulfates (gray) and analysis of human plasma (orange); compounds **8** and **9** were tentatively assigned.

Table 1. The compounds found in human blood at different levels of identification according to Schymanski, E.L. (2014) [34].

Level 1: Confirmed Structure (Reference Standard)	Level 2: Probable Structure (Ms^2)	Level 3: Tentative Structure (MS^2)	Level 4: Molecular Formula	Level 5: Exact Mass of Interest (MS)
XN-7-O-GLc	-	IXN-4′O-Glc	-	-
IXN-7-O-Glc	-	8-PN-4′-O-Glc	-	-
6PN-7-O-Glc	-	6-PN-4′-O-Glc	-	-
8-PN-7-O-Glc	-	8-PN-7-O-sulfate	-	-
XN-4′O-Sulfate	-	6-PN-7-O-sulfate	-	-
6-PN-7-O-sulfate	-	6-PN-4′-O-sulfate	-	-

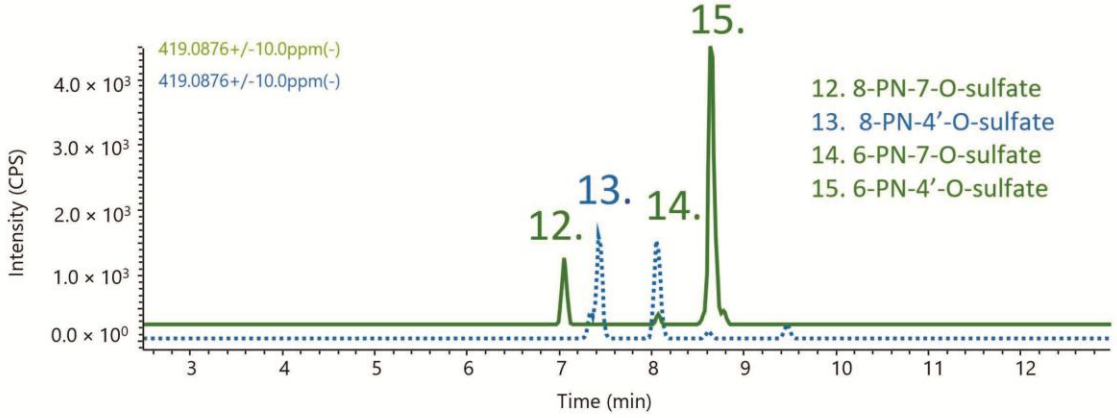

Figure 6. Co-chromatogram of the synthesised 8/6PN-sulfate, and then a human blood sample (green); compounds **12** and **15** were tentatively assigned.

The description of XN metabolism is much more complicated than XN reaching cells and inducing certain bioactivities. Once consumed, XN is modified by a series of processors, including passive and non-passive routes, resulting in the formation of many metabolites (Figure 1). Furthermore, the gut microbiota plays an important role [35]. Another factor that makes investigating the bioactivities of XN challenging is that most in vivo studies of bioactivity use mouse models. The in vivo mouse model for XN is prone to error as most mice do not have the human microbiota that are essential to study the bioactivity effects of XN supplementation [36–38]. However, some of the metabolites are probably bioactive as in vivo effects are reported from XN consumption [39,40]. Some metabolites might be rapidly excreted, which would suggest that their absorption into cells is limited, although to answer this unequivocally, a preliminary investigation using synthesised metabolites with a Caco-2 absorption assay is necessary [9,41]. As very little free XN and PF are found in human samples after XN consumption, testing the bioactivities of synthesised metabolites in vitro would provide further evidence of what might occur in vivo. A summary of the compounds found in the blood sample is shown in Table 1. No hydroxyls were found in the blood plasma sample (see Supplementary Information for the chromatograms). Hence, large-scale intervention trials should be carried out to determine whether hydroxylated prenylflavonoids are produced in rare cases. Therefore, the production of these metabolites is essential for future work on XN metabolism. Additionally, it might be that the dose of XN was not sufficient to produce sufficient quantities of t hydroxylated metabolites, or that they are quickly conjugated by phase II enzymes and thus not sufficiently long-lived. Another, less common use of the synthesised metabolites is the investigation of the concentration of metabolites in the environment, as free XN is known as a pollutant and its metabolite haves not been investigated [42].

3. Materials and Methods

3.1. General

All reactions were carried out using analytical-grade solvents unless otherwise stated. Biochemical reactions were conducted at 39 °C in an orbital shaking bath (GFL 1092, Burgwedel, Germany).

3.2. Reference Compounds

Xanthohumol, xanthohumol-C, isoxanthohumol, isoxanthohumol-C, 6-prenylnaringenin, and 8-prenylnaringenin from hops were synthesised previously [43].

3.2.1. General Reaction of Hydroxylated Prenylated Flavonoids

To hydroxylate the prenylated flavonoids, a Riley oxidation method was employed [19,44]. A reference prenylated flavonoid (1 molar e.q) was dissolved in 3 mL ethanol. Along with SeO_3 (1.2 molar equivalence), the reaction was taken to reflux for 48 h and quenched by the addition of ethyl acetate and water; subsequently, liquid–liquid extraction was carried out by washing the organic phase with water (25 mL) three times. This was employed to 6-PN, 8-PN, IXN, and XN individually. The organic phases of each reaction without further clean-up were further reacted with $NaBH_4$ at 1.2 molar equivalence (of the aldeyde) by dissolving the reactant and product of the oxidation in ACN and leaving it to stir for 30 min. The products were then subjected to liquid– liquid extraction again and washed over celite 454, concentrated and purified using preparative HPLC, and submitted to NMR, HPLC, LC-MS/MS and HR-MS analysis.

3.2.2. Synthesis of Sulphate Conjugates

In an adaption from Legette et al. (2014) [20], the general scheme was as follows. Individually selected prenylated flavonoids (50 mg) were dissolved in pyridine 1 (mL) and, subsequently, 80 µL of Chlorosulfonic acid was added, while the flask was on an ice bath. The reaction was left to stir vigorously for 30 min, followed by stirring overnight at room temperature. The following day, the reaction was quenched with the slow addition of approximately 20 mL of $NaCO_2$ until the solution stopped fizzing. All samples were submitted to liquid–liquid extraction by washing the water with 5 × ethyl acetate (EtOAc), the EtOAc fractions were washed with brine, and the rotation evaporator was set at 60 °C to remove most of the pyridine. The samples were columned through Sephadex LH-20 using MeOH for elution, concentrated, and then purified by preparative HPLC [43].

3.2.3. Synthesis of Synthetic Glucuronic Acid Conjugates

Synthesis of the glucuronic acid donor was carried out according to Jongkees and Withers (2011) in a dark environment [18]. To IXN, in a dry flask in argon atmosphere, 20 mg of IXN was dissolved in dry acetonitrile (dried with molecular sieves, Sigma Aldrich, Saint Louis, MO, USA) followed by the addition of 27 mg (1.2 eq) of acetobromo-α-D-glucuronic acid methyl ester. The reaction was left to stir for 5 min before AgO_2 (2.5 eq, 32.4 mg) was added. The reaction was left at room temperature for 20 h before being filtered through a celite plug, followed by silica gel (mesh 80–200), filtered through filter paper, and concentrated. The reaction product was resuspended in EtOAc and washed with H_2CO_3 twice, with water twice, and with brine once before being concentrated. Deprotection was conducted by the addition of $MeOH/H_2O$, changing the pH to 12, and leaving the product to stir for a further 3 h, before performing liquid–liquid extraction. Lastly, the obtained suspension was filtered through celite, and the filtrate was columned with Sephadex LH-20 and prepared with preparative HPLC according to previous work [43]. To obtain 6-PN-7-O-Glc and 8-PN-7-O-Glc, a mixture of 6-PN and 8-PN was used as starting material.

3.3. Biosynthesis of Glucuronic Acid Conjugates

3.3.1. Purification of Pig-Liver Microsomes

Enzymatic synthesis of glucuronide conjugates was performed by using pig liver. Liver microsomes were prepared according to a modified version of the method of , (1971) [45]. The liver (from a pig slaughtered less than 1 h prior) was a gift from a local butcher. The liver was transported on ice and immediately homogenised at a ratio of 4 mL to 1 g tissue with a 10% sucrose buffer containing 0.05 M tris HCl, 150 mM KCl, 0.005 M $MgCl_2$, 2 mM EDTA, and 1 mM dithiothreitol at pH 7.5. The liver homogenate was then centrifuged at 10,000× *g* for 15 min at 4 °C. Afterwards, the supernatant was removed and collected in a centrifuge tube. The supernatant was diluted with 25 mL of cold 0.0125 M sucrose solution containing 0.008 M $CaCl_2$ and 0.005 M $MgCl_2$, and was stirred a few times on ice. The solution was again centrifuged but at 1500× *g*, and at 4 °C, for 10 min. The pellet that formed was collected and rinsed with a 15-mL, 10% sucrose solution. The process was repeated twice,

but each time the pellet was dispersed (vortexed) in fresh sucrose (10%). Finally, the pellet was solved in a 0.05 M Tris-HCl buffer containing 150 mM KCl, 0.005 M $MgCl_2$, 2 mM EDTA, and 1 mM dithiothreitol pH 7.5. Aliquots (1.5 mL) were flash-frozen in liquid N_2 and stored at −80 °C until usage.

3.3.2. Glucuronidation of Flavonoids Using Pig-Liver Microsomes

A method similar to that described by Ladd et al. (2016) [46] was applied. A substrate of 2 mM was dissolved in ethanol (VWR) along with 1 mM alamethicin (Cayman Chemical Compound); the solution mixture was incubated in a vial at 39 °C for 17 h and quenched by the addition of 1 mL of cold MeOH, and the sample was centrifuged at 10,000× *g* 4 °C for 5 min. The sample was washed again and recentrifuged. The supernatants were combined and dried under N_2, reconstituted in 90:10 ACN:MeOH, and analysed or prepared by HPLC. After collecting the peaks from HPLC, the purified compounds underwent LC-MS/MS analysis and, of these compounds, XN-Glc1 and XN-Glc2 underwent NMR analysis.

3.3.3. Protein Content of Liver Microsomes

The protein content of the liver microsomes was estimated using Bradford assay and bovine serum albumin (BSA) for calibration. The reference protein BSA (lyophilized powder, crystallized, ≥98.0% GE) was made up to 1 mg/mL and diluted in a potassium phosphate buffer (pH 7) to corresponding concentrations. Calibration graphs were produced according to [47].

3.3.4. Enzymatic Digestion of Glucuronides

To confirm the β-anomer of the synthesised glucuronides, they were treated with β-glucuronidase from *Helix pomatia* (G7017, Sigma Aldrich, Saint Louis, MO, USA). A method derived from Grebenstein et al. (2017) [48] was slightly modified. The synthesised glucuronides (dissolved in ethanol) were treated with 3.4 µL of the β-glucuronidase (≥100.000 units/mL), suspended in a buffer (NaOAc 2 mM at pH 5.1) and incubated at 37 °C for 2.5 h [48]. A control was used by adding the glucuronide conjugate, but without adding any enzymes. The samples then underwent HPLC, LC-MS/MS, and NMR analysis.

3.4. Analysis of Samples

3.4.1. HPLC

Analytical HPLC was carried out using a Shimadzu LC-DAD system (Shimadzu, Kyoto, Japan; Degaser: DGU-20A3R prominence degassing Unit, Liquid Chromatograph: LC-20 AD prominence liquid chromatograph, SIL-20A HAT prominence autosampler, and SPA-M20A prominence diode-array detector) with a YMC-Pack Pro C18 column (S-5 µm, 12 nm, 150 × 10.0 mm). The preparative HPLC was performed according to Buckett et al. (2020) [43]. Regarding the biosynthesised compounds, each peak was collected using the analytical method and, after approximately 20 runs, this resulted in enough material for NMR.

3.4.2. Mass Spectrometry

MRM fragmentation of all analytes was determined by injecting 1×10^{-4} mg/L of the synthesised reference compounds directly using an autosampler (Shimadzu, nexera 2 system). The time-of-flight mass spectrometer (Shimadzu 9030) was tuned beforehand using NAI (Shimadzu) with a resolution above 40,000 at 1625.8 *m/z* in 2 kHz mode, and data-dependent acquisition (DDA) mode was selected from a range of 100–1000 Da with a threshold set at 1000 cps. The nebulizing gas flow was set at 3.0 L/min, the heating gas flow at 10 L/min, the interface temperature at 300 °C, and the desolvation temperature at 526 °C. The interface had a voltage of −40 kv, drying gas of 10 L/min, DL temperature of 250 °C, and heat block of 400 °C.

3.4.3. Nuclear Magnetic Resonance Spectroscopy

The 1D-/2D-NMR experiments for structure elucidation were performed on a 500 MHz or 600 MHz Bruker AVANCE NEO system, equipped with a triple-resonance cryo-probe (TCI, Bruker, Rheinstetten, Germany) at 300 K. Samples were either dissolved in 600 µL Methanol-d_4 or Acetone-d_6, and chemical shifts are reported in parts per million (ppm) relative to solvent signals in the ^{1}H NMR and 13C NMR spectra. All pulse sequences were taken from the standard Bruker pulse sequence library. Data processing was performed with Topspin software (version 4.1.1) or MestReNova 14.0 (Mestrelab Research, Santiago de Compostela, Spain).

3.4.4. LC-MS/MS

The synthesised compounds at approx. 2.5 µg/L and blood samples were injected (5 µL) using the following parameters and subjected to analysis with a Shimadzu Nexera UHPLC system coupled with a Shimadzu 9030 Q-ToF mass spectrometer (Kyoto, Japan). A Waters BEH c18 100 × 2.1 mm, 1.7 µm separated the analytes with acidified solvents using 0.1% formic acid, H_2O (solvent A), and ACN (solvent B). The gradient started at 20% B and ran isocratically for 4 min at a flow rate of 0.4 mL/min; it then slowly increased using a gradient at 85% B at 10.5 min and was held for 1.5 min until it was ramped up to 99% B for 2.5 min before returning to 20% B over 1 min and an equilibration time of 3 min, giving a total measurement time of 20 min. The column oven temperature was set at 40 °C. Due to the saturated mass spectra, blood sample underwent a data-independent acquisition mode to collect data. The data-independent analysis (DIA) window was set at 100–800 m/z and each MS/MS event over 20 Daltons, while CE was set at 35 V with spread of 20 V. One event was reserved for MS1 spectra and at the end of each run, a reference material (Agilent low-mass mix) was introduced using the CDS. Each run was calibrated to these masses. A blood sample from a random study participant was taken after 60 min of consumption of micellar XN (43 mg), which was determined to contain the highest amount of glucuronide conjugates (data not shown). The blood sample was directly subjected to analysis. The study included healthy volunteers and was conducted at the Department of Clinical Pharmacology, Medical University of Vienna, between October 2018 and August 2019. The independent ethics committee approved the study before its initiation (ethics number 1580/2018) and all participants gave their oral and written informed consent. In short, healthy volunteers received three capsules of native or micellar XN (43 mg) in a randomized, double-blind crossover manner for seven days. The main objectives were to determine the pharmacokinetics and compare the pharmacodynamics of two XN formulations with specific focus on anti-inflammatory effects (data not published).

3.5. Preparation of the Blood Sample

The blood samples were prepared according to van Breemen et al. (2020), although an additional 10 µL of 1 M ascorbic acid was added before centrifugation and the samples were resolved in 50 µL of 90:10 ACN:MeOH [27,48].

4. Conclusions

With the methods presented here, many phase I and phase II metabolites of XN were generated. The synthesised compounds represent common metabolites, such as phase I hydroxyls and phase II conjugates, namely, glucuronides and sulfates. This includes the most predominant glucuronide conjugates of XN. The identity of the compounds allowed the confirmation of the functional groups' positions. Due to the production of chemical standards in high enough amounts to perform an NMR analysis, an unequivocal characterisation was accomplished and a tentative identification of the analytes found in human blood, without the use of isolated standards, was obtained. The Riley oxidation was not stereospecific towards XN and produced two isomers. In the analysis of the blood, no hydroxylated compounds, nor their conjugates, were found; this does not rule out their presence, but it does reveal that they might be concentrated at extremely low levels or

not produced at the dose of XN that was given (43 mg). Furthermore, producing one or two different conjugates allows through the process of elimination to identify functional group positions without producing the analytical standard. The bioavailability of these compounds needs to be addressed in future investigations to understand the mechanism behind XN supplementation, as it is currently undergoing clinical trials and is a leading candidate natural product in the treatment of COVID-19 infection.

Supplementary Materials: The following supporting information can be downloaded at: https://www.mdpi.com/article/10.3390/metabo12040345/s1. Figure S1: Structures of the newly synthesised compounds. Classification of Compounds **1**–**4**. Figure S2: The structure of compound **5**. Figure S3: The MS/MS fragmentation of compound **5** and proposed structures and the annotation of the NMR spectra. Figure S4 the H-NOESY of XN-Z-OH showing the correlations between the free methyl group (5″) and the 2″ protons. Figure S5: An MM2 job minimisation after 1000 iterations of XN-Z-OH, showing the distances between the 2″ and 5″ protons of compound **5**. Figure S6: The structure of compound **6**. Figure S7: The MS/MS fragmentation of compound **6** and proposed structures and annotation of the NMR spectra. Figure S8: ^{1}H NOEASY of compound **6**. Figure S9: The MM2 job minimisation after 1000 irritations of XN-Z-OH, showing the distances between the 2″ and 5″ protons of compound **6**. Figure S10: The structure of compound **7**. Figure S11: The MS/MS fragmentation of compound **7** and proposed structures along with the NMR annotation. Figure S12: The ^{1}H-NOESY of compound **7**. Figure S13: The structure of compound **8**. Figure S14: The MS/MS fragmentation of compound **8** and proposed structures along with the NMR annotation. Figure S15: The structure of compound **9**. Figure S16: The MS/MS fragmentation of compound **9** and proposed structures along with NMR annotation. Figure S17: The structure of compound **10**. Figure S18: The MS/MS fragmentation of compound **10** and proposed structures along with the NMR annotation. Figure S19: H1 spectrum of (blue) IXN stacked against (red) IXN-4′-O-sulfate. Figure S20: A zoomed-in area of the carbon spectra of IXN (cyan) and IXN-4′O-sulfate (red). Figure S21: The structure of compound **11**. Figure S22: The MS/MS fragmentation of compound **11** and proposed structures and NMR annotation. Figure S23: H1 spectrum of (blue) XN stacked against (red) XN-4′O-sulfate. Figure S24: A zoomed-in area of the carbon spectra of XN (cyan) and XN-4′O-sulfate (red). Figure S25: The structure of compound **12**. Figure S26: The MS/MS fragmentation of compound **12** and proposed structures and NMR annotation. Figure S27: A zoomed-in area of the carbon spectra of 8PN (cyan) and 8PN-4′O-sulfate (red). Figure S28: The structure of compound **13**. Figure S29: The MS/MS fragmentation of compound **13** and proposed structures along with NMR annotation. Figure S30: A zoomed-in area of the carbon spectra of 6PN (cyan) and 6PN-7-O-sulfate (red). Figure S31: The structure of compound **14**. Figure S32: The MS/MS fragmentation of compound **14** and proposed structures. Figure S33: HMBC of IXN-7-O-glc. Figure S34: The structure of compound **15**. Figure S35: The MS/MS fragmentation of compound **15** and proposed structures along with NMR annotation. Figure S36: HMBC of XN-7-O-glc. Figure S37: The structure of compound **16**. Figure 38: The MS/MS fragmentation of compound **16** and proposed structures. Figure S39: HMBC of 8-PN-7-O-glc. Figure S40: The structure of compound **17**. Figure S41: The MS/MS fragmentation of compound **17** and proposed structures along with NMR annotation. Figure S42: HMBC of 6-PN-7-O-glc. Figure S43: Comparison of the ^{1}H NMR of synthesised XN-7-O-glc, biosynthesised XN-7-O-Glc, and biosynthesised 4′OH-glc. Figure S44: The fragmentation of IXN-C-glc in DDA mode. Figure S45: The fragmentation of IXN-C-glc in DDA mode. Figures S46–S51: Enzymatic digestion of glucuronide metabolites. Figure S52: The DIA of hydroxylated XN, IXN compounds. Figure S53: The DIA of hydroxylated 6 and 8-PN. Table S1. LogP values of the synthesised compounds.

Author Contributions: L.B., S.S., and V.S. designed the methodology. L.B., N.S., C.S., J.F., and M.R. conceptualised the experiments. L.B. wrote the first draft. O.F. performed the NMR measurements and data analysis/interpretation. C.S. supervised the human trial. J.F. and M.R. acquired the funding. All authors have read and agreed to the published version of the manuscript.

Funding: This research was funded by The European Foundation for Alcohol Research (ERAB) reference EA 18 69.

Institutional Review Board Statement: The independent ethics committee of the Medical University of Vienna approved the human trial (EC number 1580/2018) on 30 July 2018. The study was conducted in accordance with the Declaration of Helsinki and the Good Clinical Practice guideline.

Informed Consent Statement: All participants gave their oral and written informed consent before performed any study-related actions.

Data Availability Statement: The data presented in this study are available on request from the corresponding authors, as it has not been uploaded to an online database.

Acknowledgments: Sadia Ahmad for assisting in the preparation of the pig-liver microsomes and Herbert Forche for the fresh liver.

Conflicts of Interest: The authors declare no conflict of interest.

References

1. Yang, X.; Jiang, Y.; Yang, J.; He, J.; Sun, J.; Chen, F.; Zhang, M.; Yang, B. Prenylated flavonoids, promising nutraceuticals with impressive biological activities. *Trends Food Sci. Technol.* **2015**, *44*, 93–104. [CrossRef]
2. Awouafack, M.D.; Wong, C.P.; Tane, P.; Morita, H. Prenylated Flavonoids in Food. In *Handbook of Dietary Phytochemicals*; Xiao, J., Sarker, S.D., Asakawa, Y., Eds.; Springer: Singapore, 2020; pp. 1–23.
3. Butt, M.S.; Nazir, A.; Sultan, M.T.; Schroën, K. *Morus alba* L. nature's functional tonic. *Trends Food Sci. Technol.* **2008**, *19*, 505–512. [CrossRef]
4. Chen, X.; Mukwaya, E.; Wong, M.-S.; Zhang, Y. A systematic review on biological activities of prenylated flavonoids. *Pharm. Biol.* **2014**, *52*, 655–660. [CrossRef] [PubMed]
5. Chang, S.K.; Jiang, Y.; Yang, B. An update of prenylated phenolics: Food sources, chemistry and health benefits. *Trends Food Sci. Technol.* **2021**, *108*, 197–213. [CrossRef]
6. Wen, L.; Zhou, T.; Jiang, Y.; Chang, S.K.; Yang, B. Prenylated flavonoids in foods and their applications on cancer prevention. *Crit. Rev. Food Sci. Nutr.* **2021**, 1–14. [CrossRef]
7. Stevens, J.F.; Page, J.E. Xanthohumol and related prenylflavonoids from hops and beer: To your good health! *Phytochemistry* **2004**, *65*, 1317–1330. [CrossRef]
8. Mukai, R. Prenylation enhances the biological activity of dietary flavonoids by altering their bioavailability. *Biosci. Biotechnol. Biochem.* **2018**, *82*, 207–215. [CrossRef]
9. Neumann, H.F.; Frank, J.; Venturelli, S.; Egert, S. Bioavailability and Cardiometabolic Effects of Xanthohumol: Evidence from Animal and Human Studies. *Mol. Nutr. Food Res.* **2021**, *66*, e2100831. [CrossRef]
10. Pinto, C.; Cestero, J.J.; Rodríguez-Galdón, B.; Macías, P. Xanthohumol, a prenylated flavonoid from hops (*Humulus lupulus* L.), protects rat tissues against oxidative damage after acute ethanol administration. *Toxicol. Rep.* **2014**, *1*, 726–733. [CrossRef]
11. Miranda, C.L.; Stevens, J.F.; Helmrich, A.; Henderson, M.C.; Rodriguez, R.J.; Yang, Y.H.; Deinzer, M.L.; Barnes, D.W.; Buhler, D.R. Antiproliferative and cytotoxic effects of prenylated flavonoids from hops (*Humulus lupulus*) in human cancer cell lines. *Food Chem. Toxicol.* **1999**, *37*, 271–285. [CrossRef]
12. Urmann, C.; Bieler, L.; Priglinger, E.; Aigner, L.; Couillard-Despres, S.; Riepl, H.M. Neuroregenerative Potential of Prenyl- and Pyranochalcones: A Structure–Activity Study. *J. Nat. Prod.* **2021**, *84*, 2675–2682. [CrossRef] [PubMed]
13. Duan, X.; Tang, X.; Nair, M.S.; Zhang, T.; Qiu, Y.; Zhang, W.; Wang, P.; Huang, Y.; Xiang, J.; Wang, H.; et al. An Airway Organoid-Based Screen Identifies a Role for the HIF1α-Glycolysis Axis in SARS-CoV-2 Infection. *Cell Rep.* **2021**, *37*, 109920. [CrossRef] [PubMed]
14. Lucas, K.; Frohlich-Nowoisky, J.; Oppitz, N.; Ackermann, M. Cinnamon and Hop Extracts as Potential Immunomodulators for Severe COVID-19 Cases. *Front. Plant Sci.* **2021**, *12*, 7. [CrossRef] [PubMed]
15. Yuan, S.; Yan, B.; Cao, J.; Ye, Z.-W.; Liang, R.; Tang, K.; Luo, C.; Cai, J.; Chu, H.; Chung, T.W.-H.; et al. SARS-CoV-2 exploits host DGAT and ADRP for efficient replication. *Cell Discov.* **2021**, *7*, 100. [CrossRef] [PubMed]
16. Langley, B.O.; Ryan, J.J.; Hanes, D.; Phipps, J.; Stack, E.; Metz, T.O.; Stevens, J.F.; Bradley, R. Xanthohumol Microbiome and Signature in Healthy Adults (the XMaS Trial): Safety and Tolerability Results of a Phase I Triple-Masked, Placebo-Controlled Clinical Trial. *Mol. Nutr. Food Res.* **2021**, *65*, 2001170. [CrossRef]
17. Aghamiri, V.; Mirghafourvand, M.; Mohammad-Alizadeh-Charandabi, S.; Nazemiyeh, H. The effect of Hop (*Humulus lupulus* L.) on early menopausal symptoms and hot flashes: A randomized placebo-controlled trial. *Complement. Ther. Clin. Pract.* **2016**, *23*, 130–135. [CrossRef]
18. Jongkees, S.A.K.; Withers, S.G. Glycoside Cleavage by a New Mechanism in Unsaturated Glucuronyl Hydrolases. *J. Am. Chem. Soc.* **2011**, *133*, 19334–19337. [CrossRef] [PubMed]
19. Nakamura, A.; Nakada, M. Allylic Oxidations in Natural Product Synthesis. *Synthesis* **2013**, *45*, 1421–1451. [CrossRef]
20. Legette, L.; Karnpracha, C.; Reed, R.L.; Choi, J.; Bobe, G.; Christensen, J.M.; Rodriguez-Proteau, R.; Purnell, J.Q.; Stevens, J.F. Human pharmacokinetics of xanthohumol, an antihyperglycemic flavonoid from hops. *Mol. Nutr. Food Res.* **2014**, *58*, 248–255. [CrossRef]
21. Grudniewska, A.; Popłoński, J. Simple and green method for the extraction of xanthohumol from spent hops using deep eutectic solvents. *Sep. Purif.* **2020**, *250*, 117196. [CrossRef]
22. Zhang, J.L.; Yan, L.; Wei, P.; Zhou, R.Y.; Hua, C.J.; Xiao, M.; Tu, Y.P.; Gu, Z.J.; Wei, T.T. PEG-GO@XN nanocomposite suppresses breast cancer metastasis via inhibition of mitochondrial oxidative phosphorylation and blockade of epithelial-to-mesenchymal transition. *Eur. J. Pharmacol.* **2021**, *895*, 9. [CrossRef] [PubMed]

23. Stompor, M.; Dancewicz, K.; Gabryś, B.; Anioł, M. Insect Antifeedant Potential of Xanthohumol, Isoxanthohumol, and Their Derivatives. *J. Agric. Food Chem.* **2015**, *63*, 6749–6756. [CrossRef] [PubMed]
24. Ogunnupebi, T.A.; Oluyori, A.P.; Dada, A.O.; Oladeji, O.S.; Inyinbor, A.A.; Egharevba, G.O. Promising Natural Products in Crop Protection and Food Preservation: Basis, Advances, and Future Prospects. *Int. J. Agron.* **2020**, *2020*, 8840046. [CrossRef]
25. Khatib, N.; Varidi, M.J.; Mohebbi, M.; Varidi, M.; Hosseini, S.M.H. Replacement of nitrite with lupulon–xanthohumol loaded nanoliposome in cooked beef-sausage: Experimental and model based study. *J. Food Sci. Technol.* **2020**, *57*, 2629–2639. [CrossRef]
26. Nikolic, D.; Li, Y.; Chadwick, L.R.; Pauli, G.F.; van Breemen, R.B. Metabolism of xanthohumol and isoxanthohumol, prenylated flavonoids from hops (*Humulus lupulus* L.), by human liver microsomes. *J. Mass Spectrom.* **2005**, *40*, 289–299. [CrossRef]
27. van Breemen, R.B.; Chen, L.; Tonsing-Carter, A.; Banuvar, S.; Barengolts, E.; Viana, M.; Chen, S.-N.; Pauli, G.F.; Bolton, J.L. Pharmacokinetic Interactions of a Hop Dietary Supplement with Drug Metabolism in Perimenopausal and Postmenopausal Women. *J. Agric. Food Chem.* **2020**, *68*, 5212–5220. [CrossRef]
28. Nookandeh, A.; Frank, N.; Steiner, F.; Ellinger, R.; Schneider, B.; Gerhäuser, C.; Becker, H. Xanthohumol metabolites in faeces of rats. *Phytochemistry* **2004**, *65*, 561–570. [CrossRef]
29. Chadwick, L.R.; Nikolic, D.; Burdette, J.E.; Overk, C.R.; Bolton, J.L.; van Breemen, R.B.; Fröhlich, R.; Fong, H.H.S.; Farnsworth, N.R.; Pauli, G.F. Estrogens and Congeners from Spent Hops (*Humulus lupulus*). *J. Nat. Prod.* **2004**, *67*, 2024–2032. [CrossRef]
30. Herath, W.; Ferreira, D.; Khan, S.; Khan, I. Identification and Biological Activity of Microbial Metabolites of Xanthohumol. *Chem. Pharm. Bull.* **2004**, *51*, 1237–1240. [CrossRef]
31. Ruefer, C.E.; Gerhäuser, C.; Frank, N.; Becker, H.; Kulling, S.E. In vitro phase II metabolism of xanthohumol by human UDP-glucuronosyltransferases and sulfotransferases. *Mol. Nutr. Food Res.* **2005**, *49*, 851–856. [CrossRef]
32. Budziak, I.; Arczewska, M.; Kamiński, D.M. Formation of Prenylated Chalcone Xanthohumol Cocrystals: Single Crystal X-ray Diffraction, Vibrational Spectroscopic Study Coupled with Multivariate Analysis. *Molecules* **2019**, *24*, 4245. [CrossRef] [PubMed]
33. Yilmazer, M.; Stevens, J.F.; Buhler, D.R. In vitro glucuronidation of xanthohumol, a flavonoid in hop and beer, by rat and human liver microsomes. *FEBS Lett.* **2001**, *491*, 252–256. [CrossRef]
34. Schymanski, E.L.; Jeon, J.; Gulde, R.; Fenner, K.; Ruff, M.; Singer, H.P.; Hollender, J. Identifying small molecules via high resolution mass spectrometry: Communicating confidence. *Environ. Sci. Technol.* **2014**, *48*, 2097–2098. [CrossRef] [PubMed]
35. Zhang, Y.; Bobe, G.; Miranda, C.L.; Lowry, M.B.; Hsu, V.L.; Lohr, C.V.; Wong, C.P.; Jump, D.B.; Robinson, M.M.; Sharpton, T.J.; et al. Tetrahydroxanthohumol, a xanthohumol derivative, attenuates high-fat diet-induced hepatic steatosis by antagonizing PPARγ. *eLife* **2021**, *10*, e66398. [CrossRef] [PubMed]
36. Li, J.; Zeng, L.; Xie, J.; Yue, Z.; Deng, H.; Ma, X.; Zheng, C.; Wu, X.; Luo, J.; Liu, M. Inhibition of Osteoclastogenesis and Bone Resorption in vitro and in vivo by a prenylflavonoid xanthohumol from hops. *Sci. Rep.* **2015**, *5*, 17605. [CrossRef] [PubMed]
37. Logan, I.E.; Shulzhenko, N.; Sharpton, T.J.; Bobe, G.; Liu, K.; Nuss, S.; Jones, M.L.; Miranda, C.L.; Vasquez-Perez, S.; Pennington, J.M.; et al. Xanthohumol Requires the Intestinal Microbiota to Improve Glucose Metabolism in Diet-Induced Obese Mice. *Mol. Nutr. Food Res.* **2021**, *65*, 2100389. [CrossRef]
38. Pohjanvirta, R.; Nasri, A. The Potent Phytoestrogen 8-Prenylnaringenin: A Friend or a Foe? *Int. J. Mol. Sci.* **2022**, *23*, 3168. [CrossRef]
39. Ferk, F.; Mišík, M.; Nersesyan, A.; Pichler, C.; Jäger, W.; Szekeres, T.; Marculescu, R.; Poulsen, H.E.; Henriksen, T.; Bono, R.; et al. Impact of xanthohumol (a prenylated flavonoid from hops) on DNA stability and other health-related biochemical parameters: Results of human intervention trials. *Mol. Nutr. Food Res.* **2016**, *60*, 773–786. [CrossRef]
40. Pichler, C.; Ferk, F.; Al-Serori, H.; Huber, W.; Jäger, W.; Waldherr, M.; Mišík, M.; Kundi, M.; Nersesyan, A.; Herbacek, I.; et al. Xanthohumol Prevents DNA Damage by Dietary Carcinogens: Results of a Human Intervention Trial. *Cancer Prev. Res.* **2017**, *10*, 153–160. [CrossRef]
41. van Breemen, R.B.; Li, Y. Caco-2 cell permeability assays to measure drug absorption. *Expert Opin. Drug Metab. Toxicol.* **2005**, *1*, 175–185. [CrossRef]
42. Qi, J.; Mulabagal, V.; Liu, L.; Wilson, C.; Hayworth, J.S. A rapid UHPLC-MS/MS method for quantitation of phytoestrogens and the distribution of enterolactone in an Alabama estuary. *Chemosphere* **2019**, *237*, 124472. [CrossRef] [PubMed]
43. Buckett, L.; Schinko, S.; Urmann, C.; Riepl, H.; Rychlik, M. Stable Isotope Dilution Analysis of the Major Prenylated Flavonoids Found in Beer, Hop Tea, and Hops. *Front. Nutr.* **2020**, *7*, 11. [CrossRef] [PubMed]
44. Woodward, R.B.; Cava, M.P.; Ollis, W.D.; Hunger, A.; Daeniker, H.U.; Schenker, K. The Total Synthesis of Strychnine. *J. Am. Chem. Soc.* **1954**, *76*, 4749–4751. [CrossRef]
45. Kamath, S.A.; Kummerow, F.A.; Narayan, K.A. A simple procedure for the isolation of rat liver microsomes. *FEBS Lett.* **1971**, *17*, 90–92. [CrossRef]
46. Ladd, M.A.; Fitzsimmons, P.N.; Nichols, J.W. Optimization of a UDP-glucuronosyltransferase assay for trout liver S9 fractions: Activity enhancement by alamethicin, a pore-forming peptide. *Xenobiotica* **2016**, *46*, 1066–1075. [CrossRef]
47. Zor, T.; Selinger, Z. Linearization of the Bradford Protein Assay Increases Its Sensitivity: Theoretical and Experimental Studies. *Anal. Biochem.* **1996**, *236*, 302–308. [CrossRef]
48. Grebenstein, N.; Schlienz, J.; Calvo-Castro, L.A.; Burkard, M.; Venturelli, S.; Busch, C.; Frank, J. Validation of a rapid and sensitive reversed-phase liquid chromatographic method for the quantification of prenylated chalcones and flavanones in plasma and urine. *NFS J.* **2017**, *10*, 1–9. [CrossRef]

5.4 Supplementary information. Manuscript II: Synthesis of human phase I and phase II metabolites of hop (Humulus lupulus) prenylated flavonoids [69].

Supplementary information

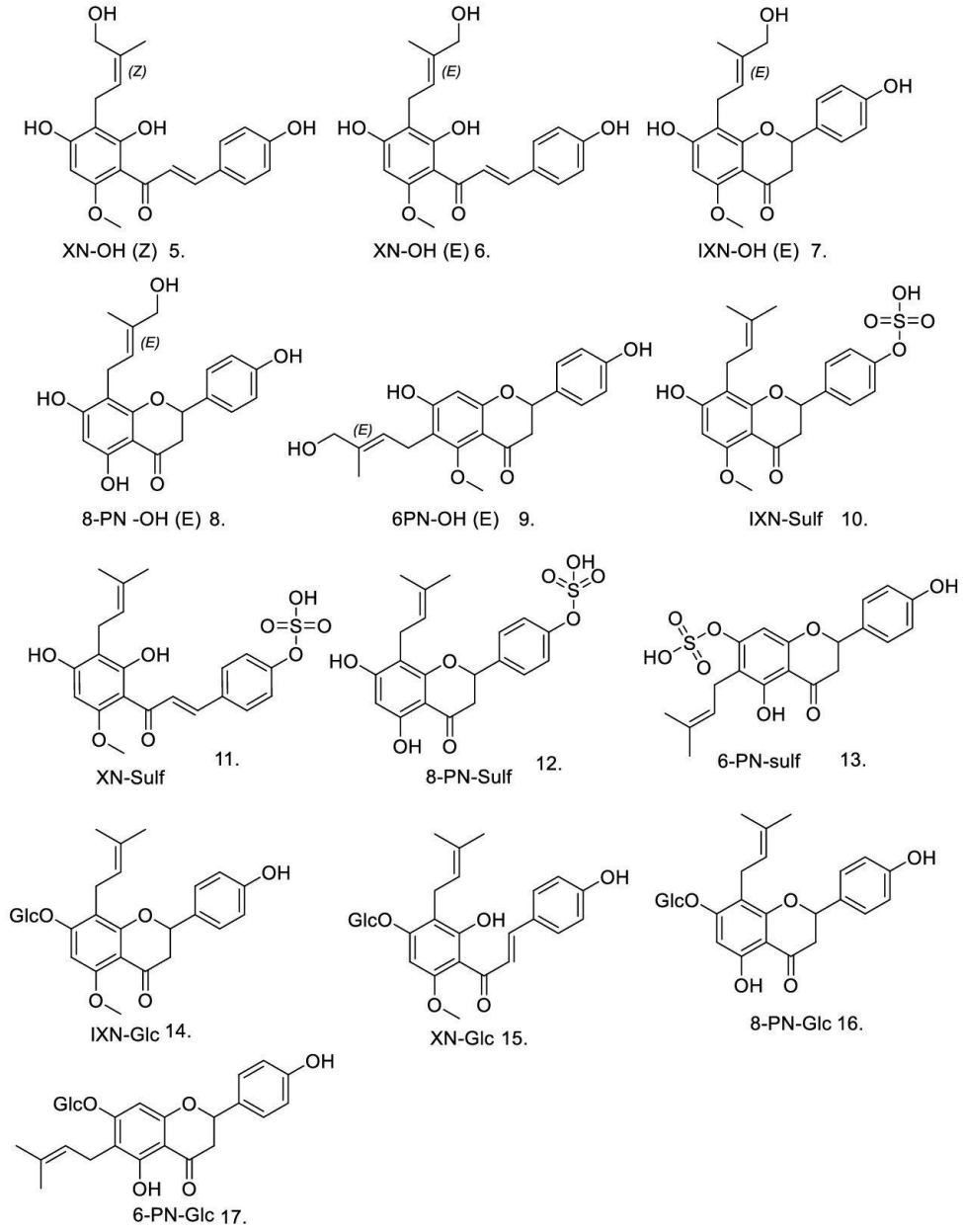

Figure S1: Structures of the newly synthesised compounds:

1. NMR and MS

Acetobromo-α-D-glucuronic acid methyl ester

ESI-: 338.90 (M+Br)

^{1}H NMR (500 MHz, $CDCl_3$) δ 6.64 (d, *J* = 4.0 Hz, 1H), 5.61 (t, *J* = 9.7 Hz, 1H, 6), 5.24 (dd, *J* = 10.3, 9.5 Hz, 1H), 4.85 (dd, *J* = 10.0, 4.1 Hz, 1H), 4.58 (d, *J* = 10.3 Hz, 1H), 3.76 (s, 3H, 22), 2.10 (s, 3H, 24), 2.05 (d, *J* = 3.1 Hz, 7H, 16, 20, 27), 1.29 – 1.22 (m, 1H), 0.07 (s, 1H). ^{13}C NMR (126 MHz, $CDCl_3$) δ 169.83, 169.63, 166.83, 85.47, 72.17, 70.46, 69.41, 68.62, 53.30, 29.85, 20.76, 20.61, 1.17. in accordance to jonkees et al. 2008 [1]

Compound 1, 2, 3, and 4

Xanthohumol, Isoxanthohumol, 6-Prenylnaringenin and 8-Prenylnaringenin were prepared previously [2].

Compound (**5.**) Xanthouhmol-Z-OH: (E)-1-(2,4-dihydroxy-3-((Z)-4-hydroxy-3-methylbut-2-en-1-yl)-6-methoxyphenyl)-3-(4-hydroxyphenyl)prop-2-en-1-one

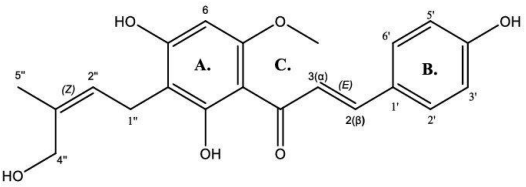

Figure S2: The structure of compound 5

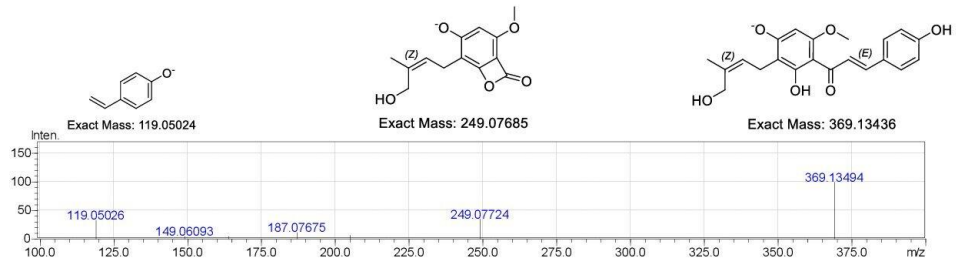

Figure S3: The MS/MS fragmentation of compound 5 and proposed structures.

^{1}H NMR (600 MHz, Acetone) δ 7.89 (d, *J* = 15.5 Hz, 1H, 3α), 7.74 (d, *J* = 15.6 Hz, 1H, 2β), 7.63 – 7.58 (m, 2H, 2', 6'), 6.94 – 6.89 (m, 2H, 3', 5'), 6.10 (s, 1H, 6), 5.34 (d, *J* = 8.6 Hz, 1H, 2''), 4.32 – 4.20 (m, 2H, 4''), 3.93 (s, 3H, OMe), 3.39 (d, *J* = 7.9 Hz, 2H, 1''), 1.72 (s, 3H, 5'').

^{13}C NMR (151 MHz, Acetone) δ 192.99 (4), 166.37 (8a), 164.10 (5), 162.16 (4'), 160.54 (7), 143.05 (2β), 135.06 (3''), 131.22 (2', 6'), 128.14 (3α), 126.14 (2''), 116.76 (3', 5'), 107.74 (4a), 105.95 (8), 92.35 (6), 61.96 (4''), 56.14 (OMe), 22.31 (1''), 21.90 (5'').

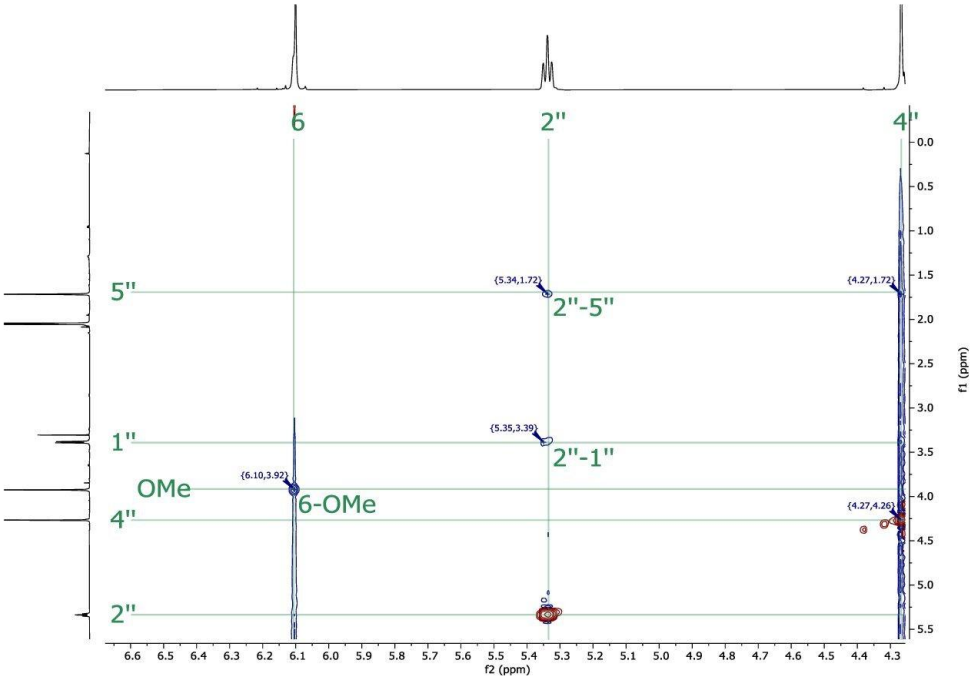

Figure S4: H-NOESY of XN-Z-OH shows the correlations between the free methyl group (5'') and the 2'' protons.

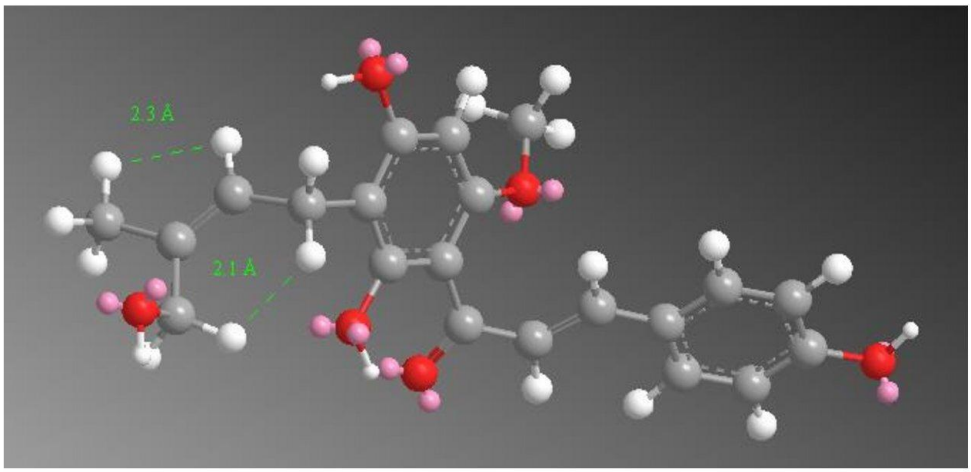

Figure S5: MM2 job minimisation after 1000 itreterations of XN-Z-OH. Showing the distances between the 2'' and 5'' protons of compound 5.

Compound (**6.**) Xanthouhmol-E-OH: (E)-1-(2,4-dihydroxy-3-((E)-4-hydroxy-3-methylbut-2-en-1-yl)-6-methoxyphenyl)-3-(4-hydroxyphenyl)prop-2-en-1-one

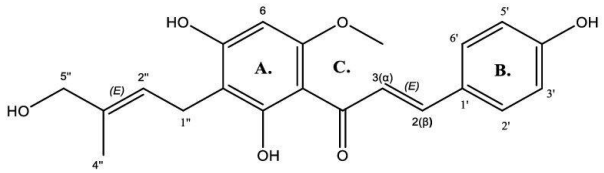

Figure S6: The strucuture of compound 6

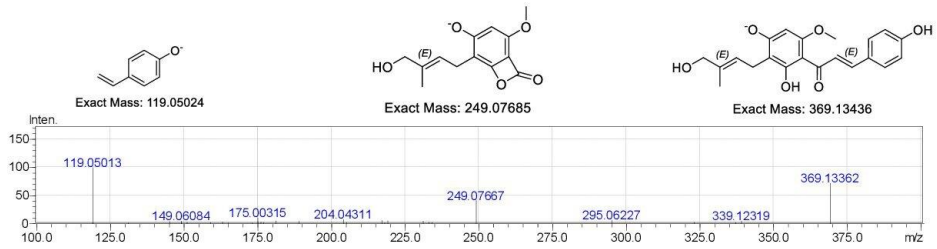

Figure S7: The MS/MS fragmentation of compound 6 and proposed structures

^{1}H NMR (600 MHz, Acetone) δ 7.88 (d, *J* = 15.5 Hz, 1H, 3α), 7.74 (d, *J* = 15.5 Hz, 1H, 2β), 7.63 – 7.58 (m, 2H, 2', 6'), 6.94 – 6.87 (m, 2H, 3', 5'), 6.16 (s, 1H, 6), 5.50 (t, *J* = 7.3 Hz, 1H, 2''), 3.92 (s, 3H, OCH3), 3.88 (s, 2H, 4''), 3.33 (d, *J* = 7.1 Hz, 2H, 1''), 1.78 (s, 3H, 5'').

^{13}C NMR (151 MHz, Acetone) δ 193.18 (4), 193.15, 166.46 (7), 165.86 (5), 162.00 (8a), 160.58 (4'), 142.99 (2β), 135.60 (3''), 131.24 (2', 6'), 128.10 (3α), 125.44 (1'), 116.75 (3', 5'), 108.56 (s, 8), 106.15 (4a)d, 91.78 (6), 68.43 (4''), 56.14 (OCH3), 21.61 (1''), 13.82 (5'').

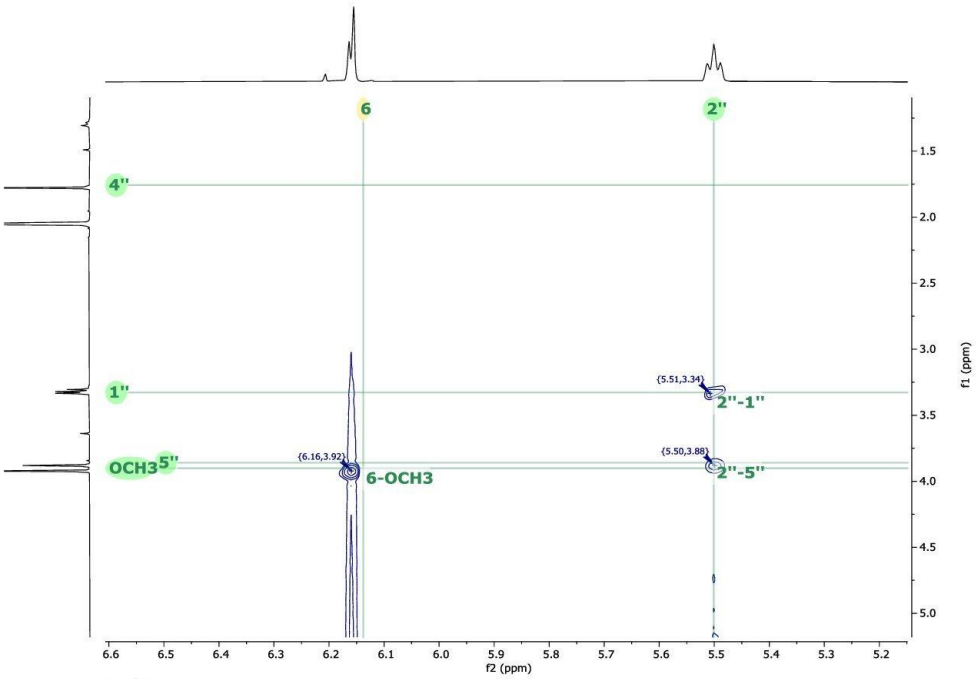

Figure S8: The ^{1}H-NOESY of compound 6

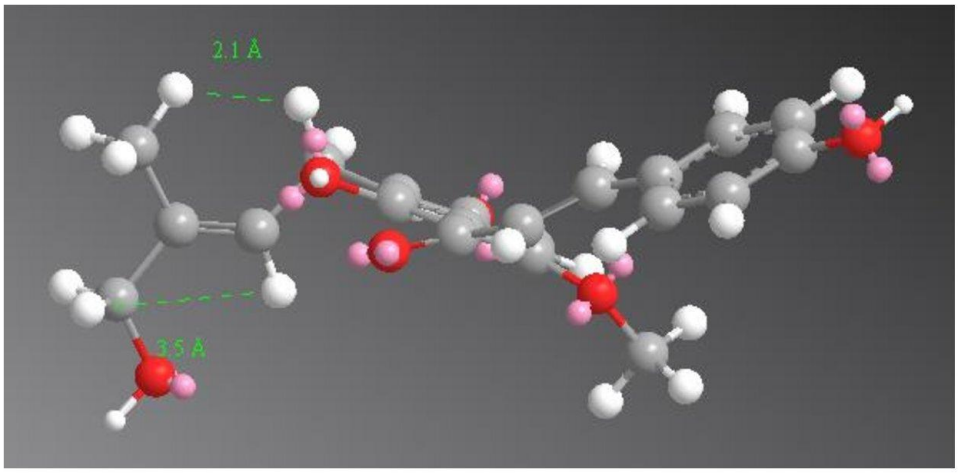

Figure S9: MM2 job minimisation after 1000 itreterations of XN-*Z*-OH. Showing the distances between the 2'' and 5'' protons of compound 6.

Compound (**7.**) Isoxanthohumol-E-OH: (E)-7-hydroxy-8-(4-hydroxy-3-methylbut-2-en-1-yl)-2-(4-hydroxyphenyl)-5-methoxychroman-4-one

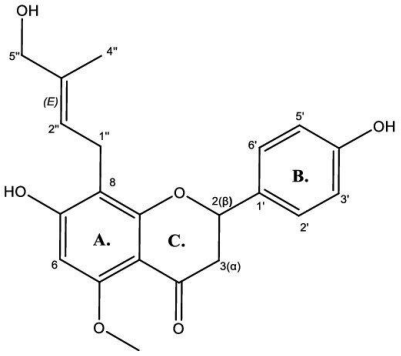

Figure S10: The strucuture of compound 7

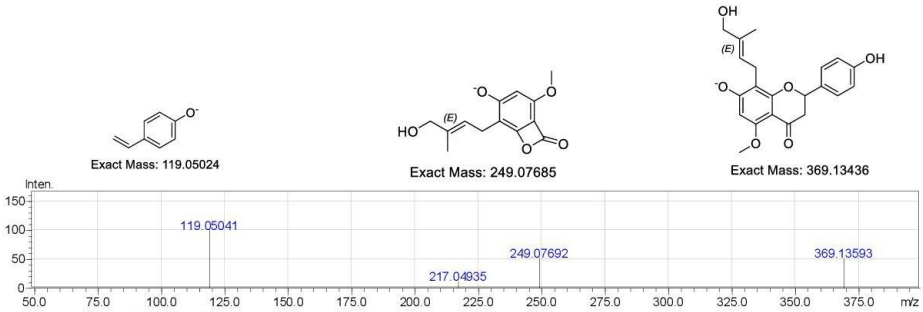

Figure S11: The MS/MS fragmentation of compound 7 and proposed structures

^{1}H NMR (600 MHz, Acetone) δ 7.39 (d, *J* = 8.5 Hz, 2H, 2', 6'), 6.89 (d, *J* = 8.5 Hz, 2H, 3', 5'), 6.23 (s, 1H, 6), 5.50 – 5.42 (m, 1H, 2''), 5.35 (d, *J* = 12.8 Hz, 1H, 2β), 3.87 – 3.83 (m, 2H, 5''), 3.74 (s, 3H, OCH3), 3.33 – 3.26 (m, 2H, 1''), 2.97 – 2.87 (m, 1H, 3α''), 2.65 – 2.57 (m, 1H, 3α'), 1.62 (s, 3H, 4'').

^{13}C NMR (126 MHz, Acetone) δ 187.81 (4), 162.02 (8a), 161.31 (7), 160.34 (5), 157.48 (4'), 134.80 (3''), 130.64 (1'), 127.84 (2', 6'), 122.57 (2''), 115.16 (3', 5'), 107.78 (8), 105.32 (4a), 92.77 (6), 78.65 (2β), 67.47 (5''), 54.98 (OCH3), 45.34 (3α), 21.17 (1''), 12.95 (4'').

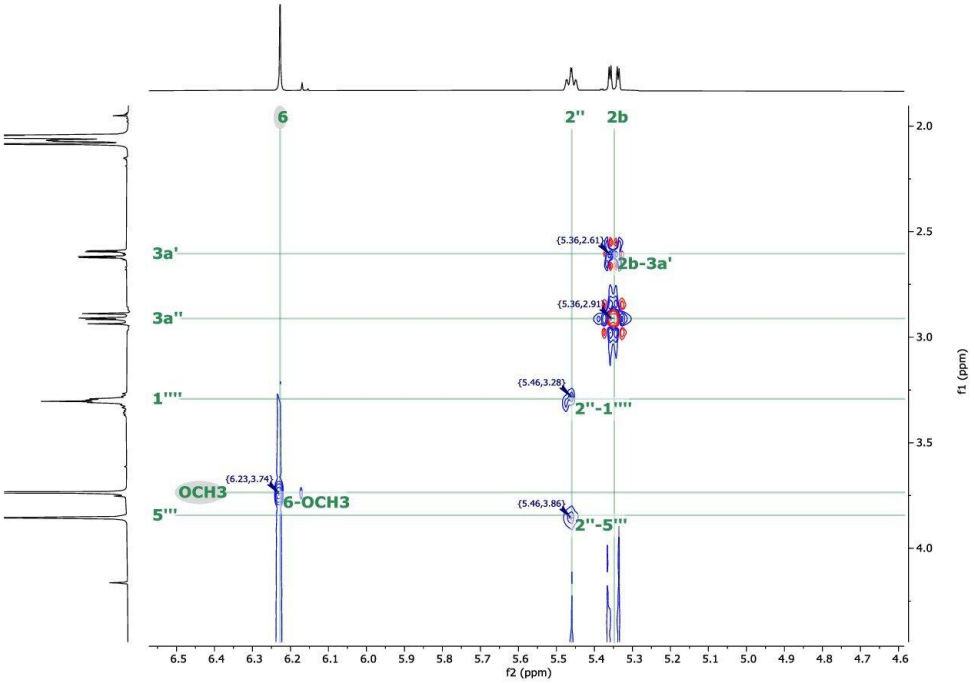

Figure S12: The ^{1}H-NOESY of compound 7

Compound (8.) 8-Prenylnaringenin-E-OH : (E)-5,7-dihydroxy-8-(4-hydroxy-3-methylbut-2-en-1-yl)-2-(4-hydroxyphenyl)chroman-4-one

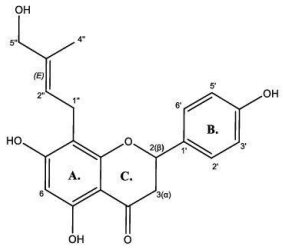

Figure S13: The structure of compound 8

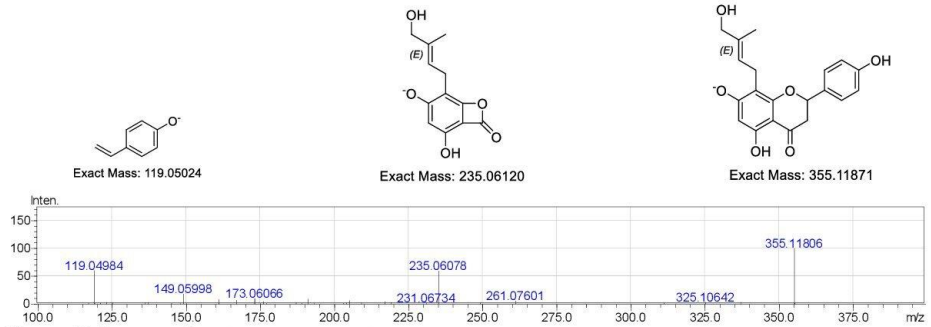

Figure S14: The MS/MS fragmentation of compound 8 and proposed structures

^{1}H NMR (400 MHz, Acetone) δ 7.41 (d, *J* = 8.5 Hz, 2H, 1', 2'), 6.90 (d, *J* = 8.5 Hz, 2H, 3', 6'), 6.04 (s, 1H, 6), 5.45 (m, 1H, 2β), 5.42 (m, 1H, 2''), 3.86 (s 2H, 5''), 3.26 (d, *J* = 7.2 Hz, 2H, 1''), 3.12 (m, 1H, 3α''), 2.75 (m,1H 3α'), 1.62 (s, 3H, 4'').

^{13}C NMR (101 MHz, Acetone) δ 197.37 (4), 165.51 (8a), 163.09 (7), 161.12 (5), 158.56 (4'), 135.75 (3''), 131.11 (1), 128.88 (1', 2'), 123.36 (2''), 116.13 (3', 6'), 108.06 (8), 103.12 (4a), 96.46 (6), 79.73 (2β), 68.38 (5''), 43.47 (3α), 21.81 (1''), 13.82 (4'').

Compound (9.) 6-Prenylnaringenin-E-OH: (E)-5,7-dihydroxy-6-(4-hydroxy-3-methylbut-2-en-1-yl)-2-(4-hydroxyphenyl)chroman-4-one

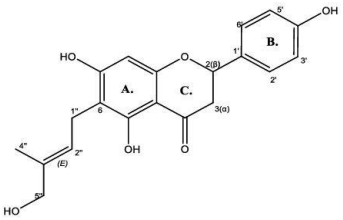

Figure S15: The structure of compound 9

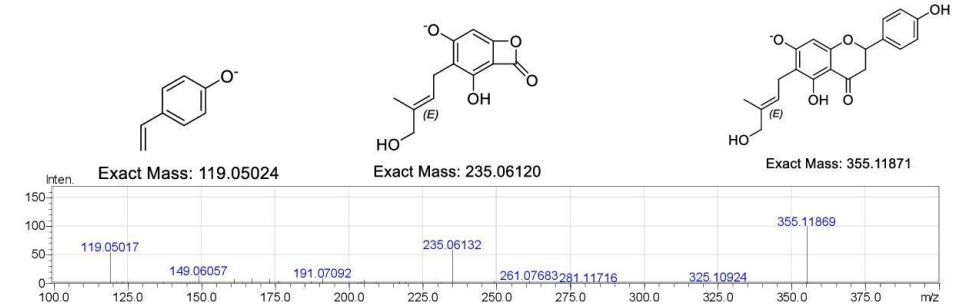

Figure S16: The MS/MS fragmentation of compound 9 and proposed structures

^{1}H NMR (500 MHz, Acetone) δ 7.51 – 7.29 (m, 2H, 2', 6'), 6.92 – 6.85 (m, 2H, 3', 5'), 6.04 (s, 1H, 8), 5.49 (t, *J* = 8.7, 7.3, 1.5 Hz, 1H, 2β), 5.45 – 5.36 (m, 1H, 2''), 3.88 (s, 2H, 5''), 3.29 (d, *J* = 7.3 Hz, 2H, 1''), 3.20 – 3.08 (m, 1H, 3α''), 2.71 (ddd, *J* = 17.1, 7.7, 3.1 Hz, 1H, 3α'), 1.77 (s, 3H, 4'').

^{3}C NMR (126 MHz, Acetone) δ 197.21 (4), 165.28 , (8a), 162.18 (5, 7), 158.65 (4'), 135.81 (3''), 130.94 (1'), 129.00 ,(2', 6'), 123.25 (2''), 116.13 ,(3', 5') 108.73 ,(6) 102.98 (8), 95.41 (4a), 79.84 (2β), 68.38 (5''), 43.59 , (3α), 21.17 (1''), 13.78 (4'').

Compound (10.) Isoxanthohumol-4'-O-sulfate: 4-(7-hydroxy-5-methoxy-8-(3-methylbut-2-en-1-yl)-4-oxochroman-2-yl)phenyl hydrogen sulfate

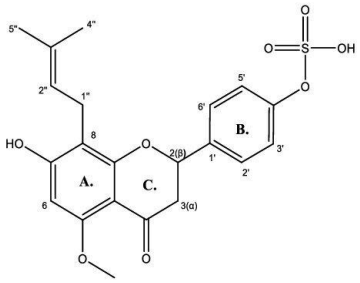

Figure S17: The structure of compound 10

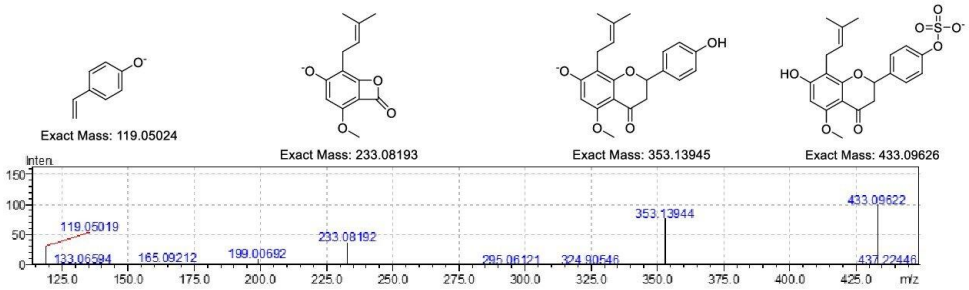

Figure S18: The MS/MS fragmentation of compound 10 and proposed structures

^{1}H NMR (400 MHz, MeOD) δ 7.51 – 7.45 (m, 2H, 2', 6'), 7.39 – 7.31 (m, 2H, 3', 5'), 6.13 (s, 1H, 6), 5.40 (dd, *J* = 12.6, 3.2 Hz, 1H, 2β), 5.15 (ddt, *J* = 8.6, 7.2, 1.4 Hz, 1H, 2''), 3.80 (s, 3H, OMe), 3.27 – 3.19 (m, 2H, 1''), 2.96 (dd, *J* = 16.7, 12.6 Hz, 1H, 3α''), 2.73 (dd, *J* = 16.7, 3.2 Hz, 1H, 3α'), 1.61 (d, *J* = 12.0 Hz, 6H, 4'', 5''),

^{13}C NMR (126 MHz, MeOD) δ 196.31 (4), 164.72 (8a), 161.79 (7), 159.86 (5) 154.05 (1') 137.17 (4'), 131.76 (3''), 128.17 (2', 6'), 123.94 (2''), 122.54 (3', 5'), 110.08 (8), 105.78 (4a), 93.65 (6), 79.62 (2β), 55.96 (OMe), 46.32 (3α), 25.95 (4''), 22.70 (1''), 17.96 (5'').

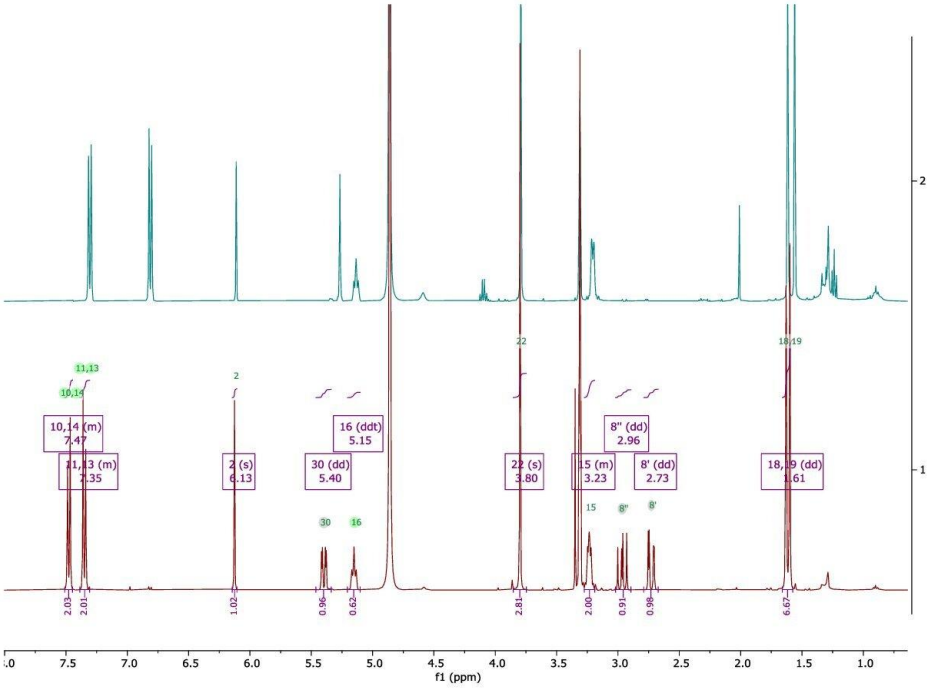

Figure S19: H1 spectrum of (Blue) IXN stacked against (red) IXN-4'-O-sulfate

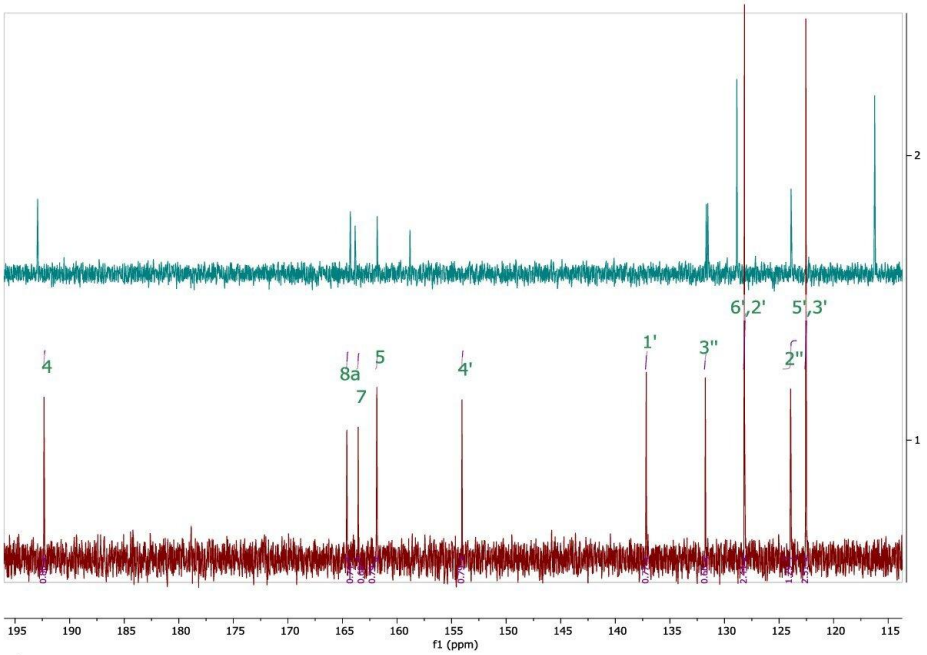

Figure S20: A zoomed in area of the carbon spectra of IXN (cyan) and IXN-4'O-sulfate (red)

To figure out the position of the sulfate group the chemical shift of that carbon should be significantly shifted upfield therefore, we looked at position 4' and carbon 7 as significant changes should occur at either of these positions. As C7 is relatively unchanged and position 4' and the 5',3' have moved to significantly (158 towards 153 and 116 towards 122 ppm repectively) ppms indicating that the sulfate is conjugated on ring B – see Figure 20.

Compound (11.): Xanthohumol-4’-O-Sulfate: (E)-4-(3-(2,4-dihydroxy-6-methoxy-3-(3-methylbut-2-en-1-yl)phenyl)-3-oxoprop-1-en-1-yl)phenyl hydrogen sulfate

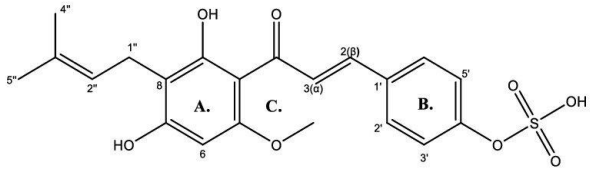

Figure S21: The structure of compound 11

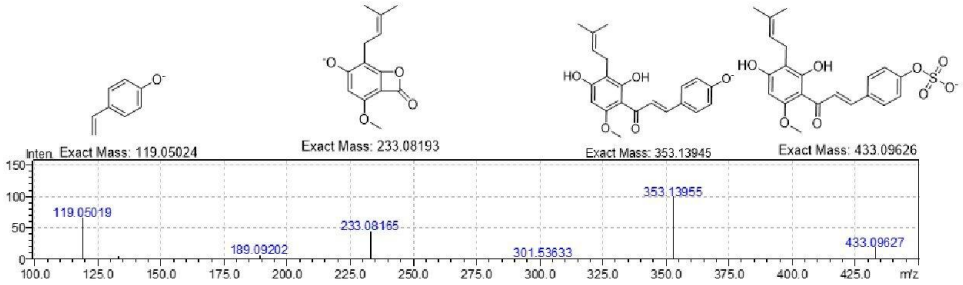

Figure S22: The MS/MS fragmentation of compound 11 and proposed structures

^{1}H NMR (500 MHz, MeOD) δ 7.89 (d, *J* = 15.6 Hz, 1H, 3α), 7.68 (d, *J* = 15.6 Hz, 1H, 2β), 7.65 – 7.61 (m, 2H, 2', 6'), 7.39 – 7.33 (m, 2H, 3', 5'), 6.03 (s, 1H, 6), 5.21 (tt, J = 7.3, 4.3, 1.5 Hz, 1H, 2''), 3.91 (s, 3H, OMe), 3.23 (d, *J* = 7.1 Hz, 2H, 1'',), 1.76 (s, 3H, 4'',), 1.65 (s, 3H, 5'')

^{13}C NMR (126 MHz, MeOD) δ 193.90 , 4, 166.22 , 8a, 164.05 , 7, 162.53 , 5, 155.58 , 4', 141.91 , 2a, 133.41 , 1', 131.35 , 3'', 130.27 , 2', 6', 128.63 , 3b, 124.21 , 2'', 122.68 , 3', 5', 109.37 , 8, 106.47 , 4a, 91.62 , 6, 56.21 , OMe, 25.98 , 4'', 5'', 22.26 , 1'', 17.88.

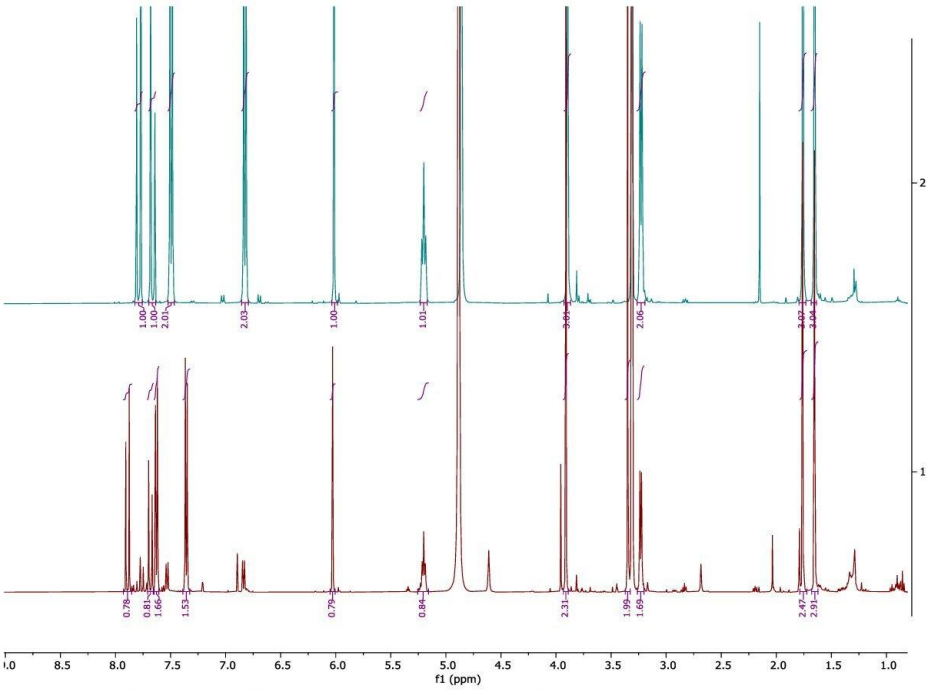

Figure S23: H1 spectrum of (Blue) XN stacked against (red) XN-4'O-sulfate

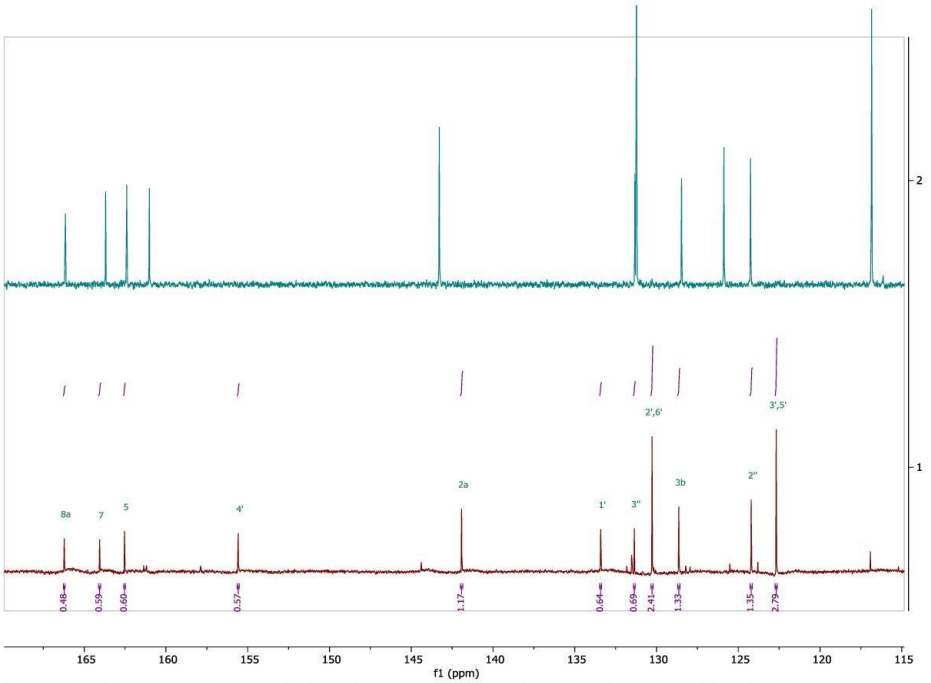

Figure S24: A zoomed in area of the carbon spectra of XN (cyan) and XN-4'O-sulfate (red)

To figure out the position of the sulfate group the chemical shift of that carbon should be significantly shifted upfield therefore, we looked at position 4' and carbon 7 as significant changes should occur at either of these positions. As C7 is relatively unchanged and position 4' and the 5',3' have moved to significantly (161 towards 155 and 116 towards 122 ppm repectively) ppms indicating that the sulfate is conjugated on ring B – See Figure 24.

Compound (12.): 8-Prenylnaringenin-4'O sulfate: 4-(5,7-dihydroxy-8-(3-methylbut-2-en-1-yl)-4-oxochroman-2-yl)phenyl hydrogen sulfate

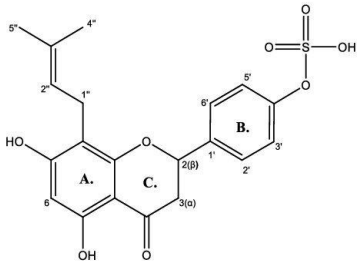

Figure S25: The structure of compound 12

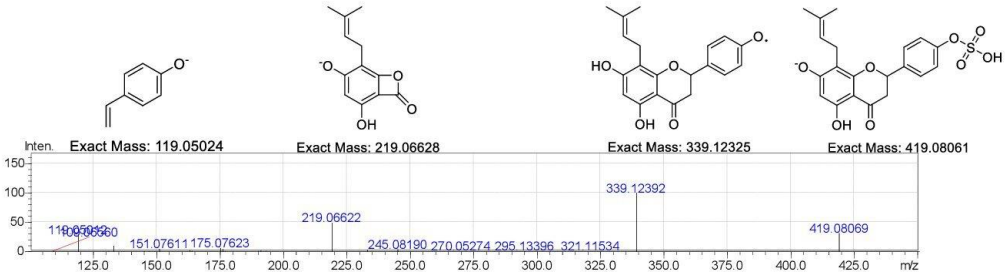

Figure S26: The MS/MS fragmentation of compound 12 and proposed structures

^{1}H NMR (500 MHz, MeOD) δ 7.53 – 7.46 (m, 2H, 2', 6'), 7.39 – 7.29 (m, 2H, 3', 5'), 5.94 (s, 1H, 6), 5.44 (dd, *J* = 12.5, 3.1 Hz, 1H), 5.15 (t, *J* = 7.2, 1.4 Hz, 1H), 3.26 – 3.13 (m, 2H), 3.17 (p, *J* = 1.7 Hz, 0H, 1''), 3.07 (dd, *J* = 17.1, 12.5 Hz, 1H, 3a), 2.79 (dd, *J* = 17.1, 3.2 Hz, 1H), 1.63 (s, 3H), 1.60 (s, 3H, 4'', 5'').

^{13}C NMR (126 MHz, MeOD) δ 196.31 (4), 164.72 (8a) 161.79 (7) 159.86 (5), 152.68 (4'), 135.67 (3''), 130.29 (1'), 126.87 (2', 6'), 122.53 (2''), 121.18 (3', 5'), 107.69 (8), 101.96 ,(4a), 95.08 (6), 78.45 (2a), 42.67 (3a), 24.56 (5''), 21.07 (1''), 16.54 (4'').

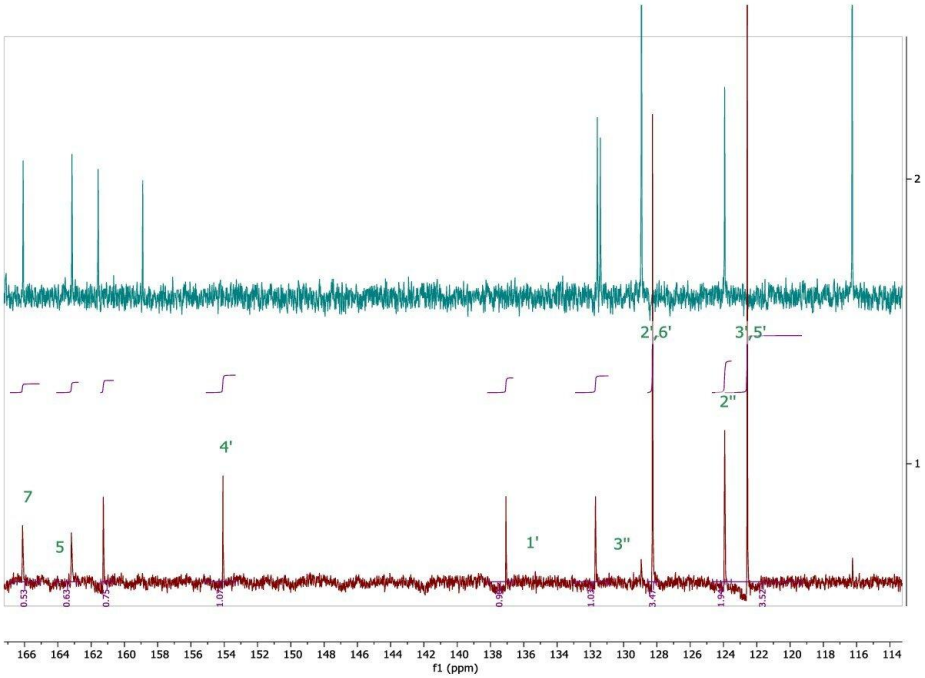

Figure S27: A zoomed in area of the carbon spectra of 8PN (cyan) and 8PN-4'O-sulfate (red)

To figure out the position of the sulfate group the chemical shift of that carbon should be significantly shifted upfield therefore, we looked at position 4' and carbon 7 as significant changes should occur at either of these positions. As C7 is relatively unchanged and position 4' and the 5',3' have moved to significantly (159 towards 154 and 116 towards 122 ppm repectively) ppms indicating that the sulfate is conjugated on ring B See Figure 27.

Compound (13.): 6-Prenylnaringenin-7-O-sulfate: 5-hydroxy-2-(4-hydroxyphenyl)-6-(3-methylbut-2-en-1-yl)-4-oxochroman-7-yl hydrogen sulfate

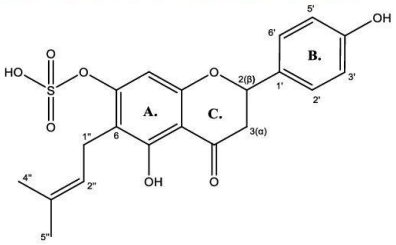

Figure S28: The structure of compound 13

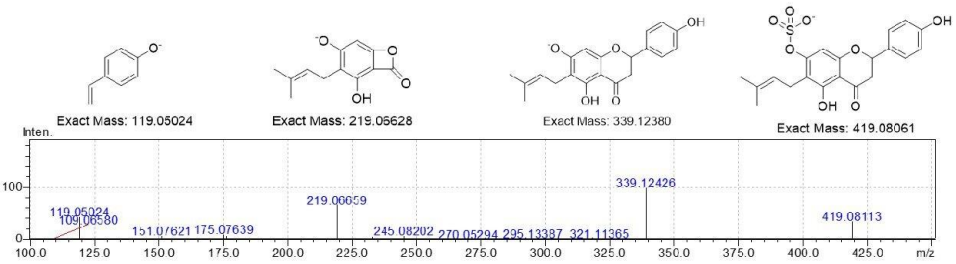

Figure S29: The MS/MS fragmentation of compound 13 and proposed structures

^{1}H NMR (500 MHz, MeOD) δ 7.30 (d, *J* = 8.7 Hz, 2H, 2', 6'), 6.81 (d, *J* = 8.7 Hz, 2H, 3', 5'), 5.90 (s, 1H, 8), 5.28 (dd, *J* = 13.0, 2.9 Hz, 1H, 2''), 5.19 (t, *J* = 7.2 Hz, 1H, 2a), 3.20 (d, *J* = 7.2 Hz, 2H, 1''), 3.07 (dd, *J* = 17.1, 13.0 Hz, 1H, 3b'), 2.65 (dd, *J* = 17.1, 3.1 Hz, 1H, 3b''), 1.75 (s, 3H, 4'',), 1.65 (s, 3H. 5'').

^{13}C NMR (126 MHz, MeOD) δ 197.21 (4), 168.01 (8a), 162.58 (7), 162.43(5) , 158.96 (4'), 131.36 (3''), 131.35 (1'), 128.98 (3', 5'), 124.18 (2''), 116.29 (2', 6'), 109.95 (6), 102.72 (4a), 96.06 (8), 80.33 (2a), 44.16 , 3b, 25.96 (5''), 21.92 (1''), 17.87 (4'').

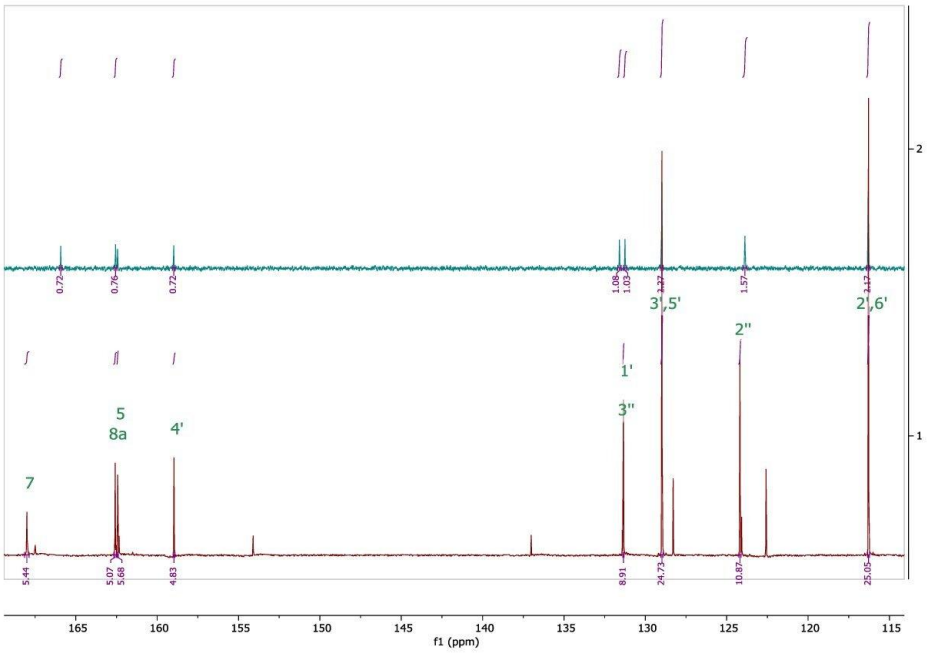

Figure S30: A zoomed in area of the carbon spectra of 6PN (cyan) and 6PN-7-O-sulfate (red)

To find out the position of the sulfate group the chemical shift of that carbon should be significantly shifted to higher PPM near where the sulfate is conjugated therefore, we looked at position 4' and carbon 7. Differing from the other sulfates the 2',6' and 3',5' signals have not moved, but position 7

has changed from 165 towards 168 indicating that the sulfate is conjugated to this position. See figure 30.

Compound (14.): IXN 7-O-Glucuronide: (2S,3S,4S,5R,6S)-3,4,5-trihydroxy-6-((2-(4-hydroxyphenyl)-5-methoxy-8-(3-methylbut-2-en-1-yl)-4-oxochroman-7-yl)oxy)tetrahydro-2H-pyran-2-carboxylate

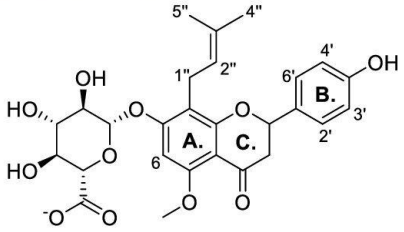

Figure S31 The structure of compound 14

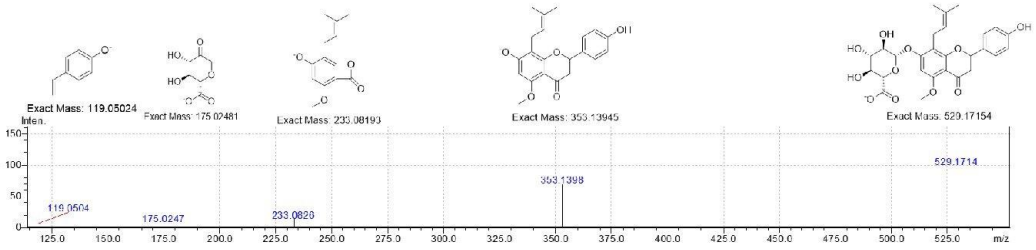

Figure S32: The MS/MS fragmentation of compound 14 and proposed structures

^{1}H NMR (500 MHz, MeOD) δ 7.34 – 7.26 (m, 2H, 2', 6'), 6.86 – 6.78 (m, 2H, 3', 5'), 6.55 (s, 1H, 6), 5.32 (t, *J* = 12.8, 9.8, 2.9 Hz, 1H, 2a), 5.19 – 5.15 (m, 1H, 2''), 5.07 (dd, *J* = 14.2, 7.0 Hz, 1H, 9), 3.86 (s, 2H, OMe), 3.71 – 3.43 (m, 2H, 10, 11, 12), 3.27 – 3.14 (m, 1H, 13), 3.03 (ddd, *J* = 16.7, 12.7, 9.5 Hz, 1H, 3b''), 2.76 – 2.66 (m, 1H, 3b'), 1.58 (d, 6H).

^{13}C NMR (126 MHz, MeOD) δ 193.19 (4), 163.22 (8a), 163.14 (7), 163.01 (5), 161.68 (4'), 158.90 (14), 131.77 (3''), 131.30 (1'), 128.96 (2', 6'), 123.89 (2''), 116.23 (3', 5'), 112.73 (8), 107.67 (4a), 102.03 (9), 93.82 (6), 80.17 (2a), 78.09 (13), 74.74 (10, 11, 12), 56.28 (OMe), 46.30 (3b), 25.95 (5''), 22.93 (1''), 18.05 (4'').

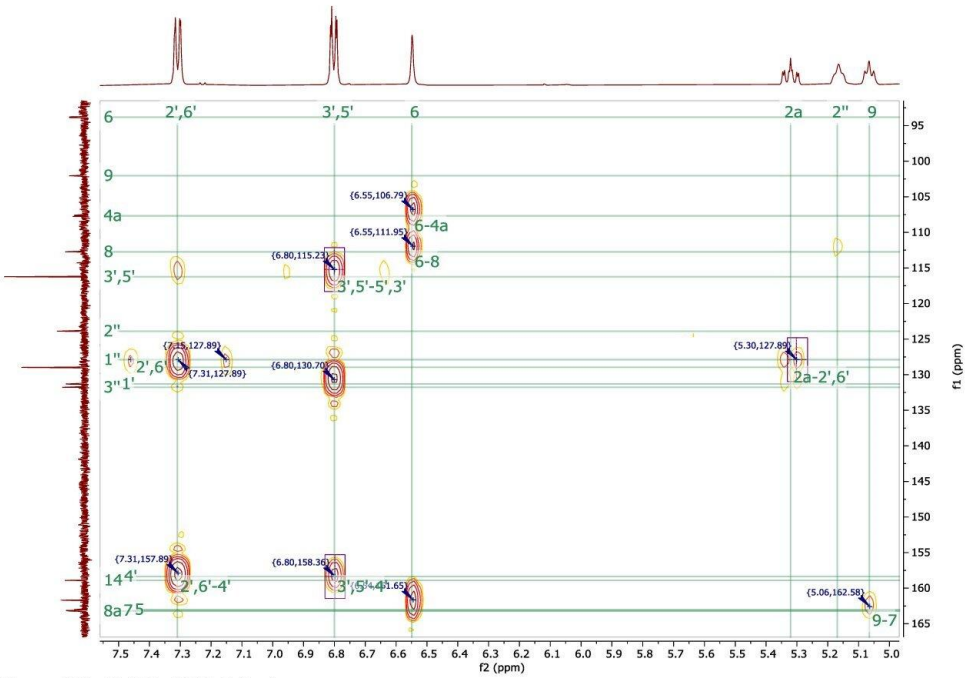

Figure S33: HMBC of IXN-7-O-glc

Indications that the glucuronide is attached to the 7 position is that there is a correlation between the anomeric proton of the glucuronide and the C7 as indicated in figure 33.

Compound (15.): XN 7-O-Glucuronide: (2S,3S,4S,5R,6S)-3,4,5-trihydroxy-6-(3-hydroxy-4-((E)-3-(4-hydroxyphenyl)acryloyl)-5-methoxy-2-(3-methylbut-2-en-1-yl)phenoxy)tetrahydro-2H-pyran-2-carboxylate

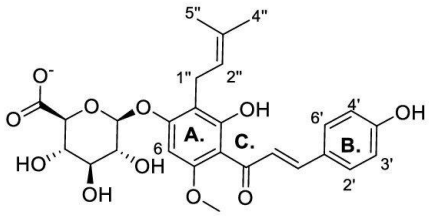

Figure S34: The structure of compound 15

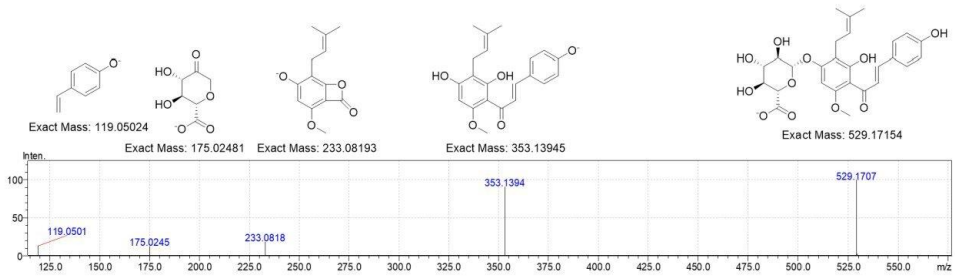

Figure S35: The MS/MS fragmentation of compound 15 and proposed structures

^{1}H NMR (600 MHz, MeOD) δ 7.78 (d, *J* = 15.5 Hz, 1H, 3b), 7.71 (d, *J* = 15.5 Hz, 1H), 7.58 – 7.47 (m, 2H, 2', 6'), 6.90 – 6.80 (m, 2H, 3', 5'), 6.40 (s, 1H, 6), 5.23 (tt, *J* = 7.2, 1.5 Hz, 1H, 2''), 5.13 (d, *J* = 7.5 Hz, 1H, 10), 4.03 (d, *J* = 9.7 Hz, 1H, 14), 3.95 (s, 3H, OMe), 3.76 – 3.64 (m, 1H, 13), 3.62 – 3.50 (m, 2H, 11, 12), 3.40 (dd, *J* = 14.1, 7.5 Hz, 1H, 1''), 3.30 – 3.26 (m, 1H), 1.72 (dd, *J* = 80.7, 1.6 Hz, 6H, 4'', 5'').

^{13}C NMR (151 MHz, MeOD) δ 194.83 (4) , 164.94 (8a), 162.30 (7), 162.17 (5), 161.28 (4'), 144.17 (2a), 131.62 (3''), 131.45 (2', 6'), 128.28 (1'), 125.56 (3b), 124.12 (2''), 116.91 (3', 5'), 112.54 (8), 108.49 (4a), 102.04 (10), 91.70 (6), 77.74 (12), 76.55 (14), 74.67 (11), 72.72 (13), 56.42 (OMe), 25.95 (5''), 22.54 (1''), 18.06 (4'').

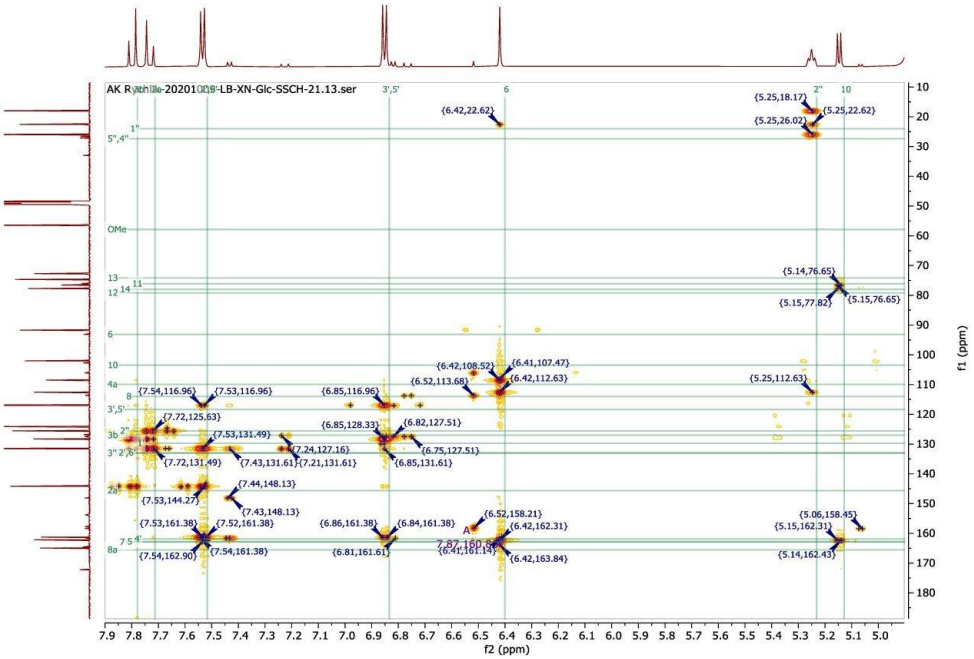

Figure S36: HMBC of XN-7-O-glc

Indications that the glucuronide is attached to the 7 position is that there is a correlation between the anomeric proton of the glucuronide and the C7 as indicated in figure 36

Compound (16.): 8-Prenylnaringenin-7-O-Glucuronide: (2S,3S,4S,5R,6S)-3,4,5-trihydroxy-6-((5-hydroxy-2-(4-hydroxyphenyl)-8-(3-methylbut-2-en-1-yl)-4-oxochroman-7-yl)oxy)tetrahydro-2H-pyran-2-carboxylate

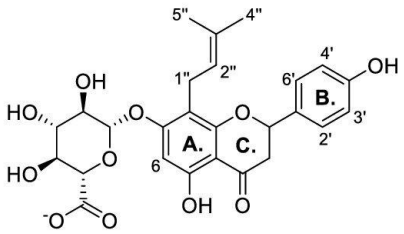

Figure S37: The structure of compound 16

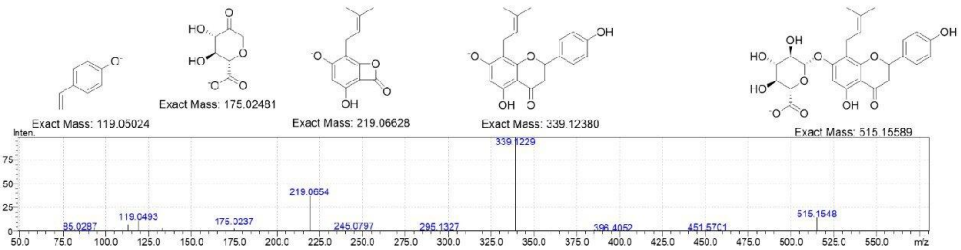

Figure S38: The MS/MS fragmentation of compound 16 and proposed structures

^{1}H NMR (600 MHz, MeOD) δ 7.37 – 7.29 (m, 2H, 2', 6'), 6.86 – 6.78 (m, 2H, 3', 5'), 6.27 (s, 1H, 6), 5.37 (t, *J* = 13.1, 3.0 Hz, 1H, 2), 5.19 (t, 1H, 2''), 5.07 (d, *J* = 10.9, 7.4 Hz, 1H, 9), 4.01 – 3.94 (m, 1H), 3.64 – 3.47 (m, 2H, 10, 11, 12, 13), 3.35 (s, 1H), 3.39 – 3.28 (m, 0H), 3.28 – 3.10 (m, 2H, 3''), 2.77 (ddd, *J* = 17.1, 14.2, 3.1 Hz, 1H, 3'), 1.61 (s, 3H), 1.57 (s, 3H).

^{13}C NMR (151 MHz, MeOD) δ 198.84 , 4, 176.82 , 14, 164.51 , 8a, 164.39 , 7, 162.75 , 5, 161.57, 159.04 , 4', 149.74, 140.64, 131.78 , 3'', 131.04 , 1', 129.09, 129.07, 123.84 (d, *J* = 3.3 Hz, 2''), 116.29 , 3', 5', 111.86 , 8, 104.73 , 4a, 101.32 , 9, 95.29 , 6, 80.66 , 2, 80.62 , 13, 77.91 , 11, 74.63 , 10, 73.18 , 12, 44.32 , 3, 25.94, 24.60 , 4'', 22.09 , 1'', 18.01.

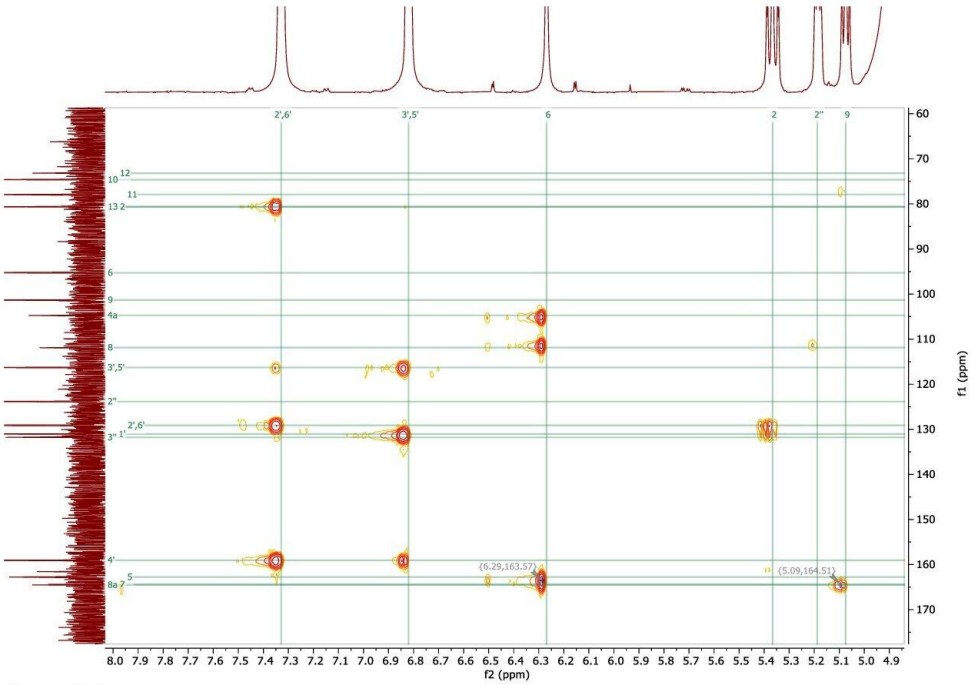

Figure S39: HMBC of 8-PN-7-O-glc

Indications that the glucuronide is attached to the 7 position is that there is a correlation between the anomeric proton of the glucuronide and the C7 as indicated in figure 39

Compound (17.): 6-Prenylnaringenin-7-O-glucuronide: (2S,3S,4S,5R,6S)-3,4,5-trihydroxy-6-((5-hydroxy-2-(4-hydroxyphenyl)-6-(3-methylbut-2-en-1-yl)-4-oxochroman-7-yl)oxy)tetrahydro-2H-pyran-2-carboxylate

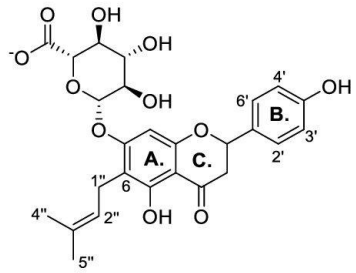

Figure S40: The structure of compound 17

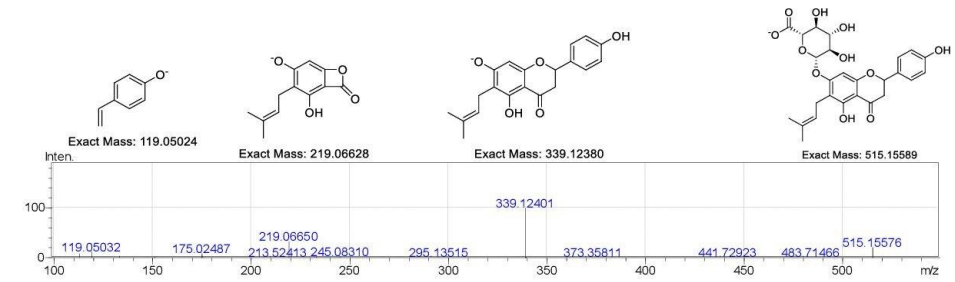

Figure S41: The MS/MS fragmentation of compound 17 and proposed structures

^{1}H NMR (500 MHz, MeOD) δ 7.33 (dd, *J* = 8.6, 2.8 Hz, 2H, 2, 6), 6.82 (dd, *J* = 8.6, 2.7 Hz, 2H), 6.27 (s, 1H, 13), 5.37 (td, *J* = 12.1, 3.0 Hz, 1H, 19), 5.18 (t, *J* = 7.4 Hz, 1H, 34), 5.11 – 5.04 (m, 1H, 23), 3.98 (dd, *J* = 9.8, 4.3 Hz, 1H, 20), 3.58 – 3.47 (m, 1H, 21, 22, 25), 3.35 (d, 0H, 33''), 3.27 – 3.10 (m, 1H, 9), 2.82 – 2.72 (m, 1H), 1.59 (d, *J* = 21.8 Hz, 7H).

^{13}C NMR (126 MHz, MeOD) δ 199.03 , 4, 164.42 , 8a, 163.08 , 7, 163.01, 161.05 , 5, 158.99 , 4', 131.78 , 3'', 131.12 , 1', 129.02 , 2', 6', 123.85 , 2'', 116.28 , 3', 5', 111.26 , 6, 105.00 , 4a, 101.42 , 9, 96.33 , 8, 80.46 , 2, 77.71, 76.63 , 13, 74.57 , 11, 72.99 , 10, 44.22, 43.98, 25.94 , 4'', 5'', 22.69 , 1'', 18.04.

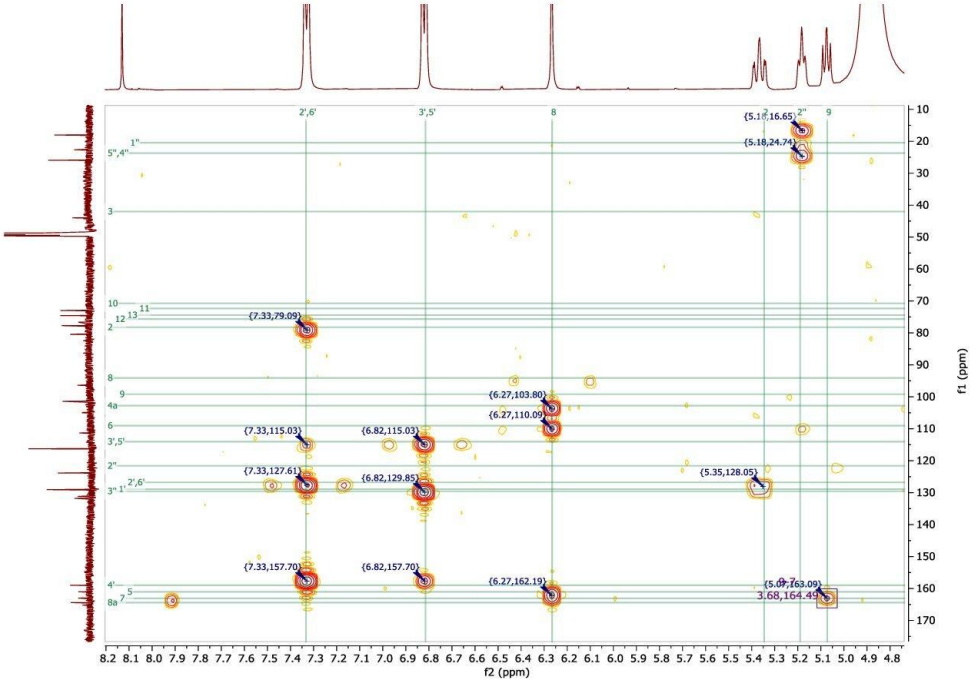

Figure S42: HMBC of 6-PN-7-O-glc

Indications that the glucuronide is attached to the 7 position is that there is a correlation between the anomeric proton of the glucuronide and the C7 as indicated in figure 42

Biosynthesised compounds

XN-4'OH-Glc and XN-7-OH-Glc

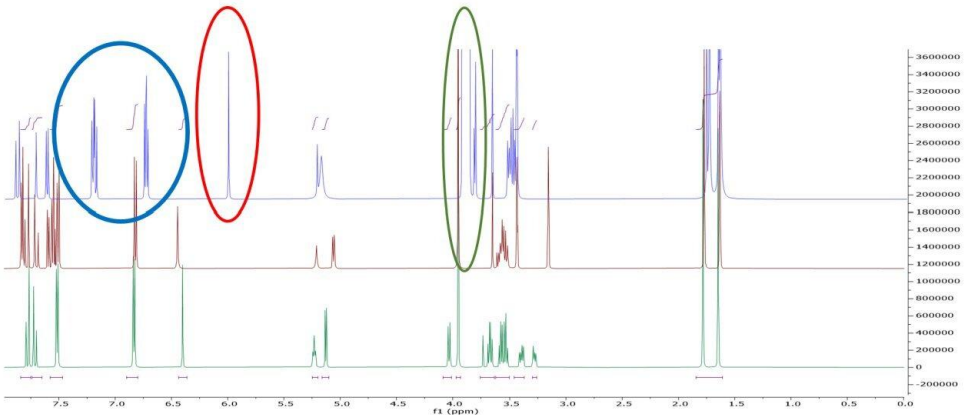

Figure S43:Green is synthesised XN-7-O-glc, Maroon is Biosynthesised XN-7-O-glc and, blue is bio 4'OH-glc

The NMR spectra of the biosynthesised compounds were contaminated and had extremely low abundance therefore, peaks were annotated and all artifacts and contaminated/solvent peaks were removed. An overlay of the H spectra are shown in figure 43 which shows that green and brown are similar, but key changes are in the blue spectra, i.e. the aromatic signals are shifted to lower frequencies and the singlet at position 6 is shifted to lower frequencies when the Glc is conjugated to the phenol.

IXN-C-Glc

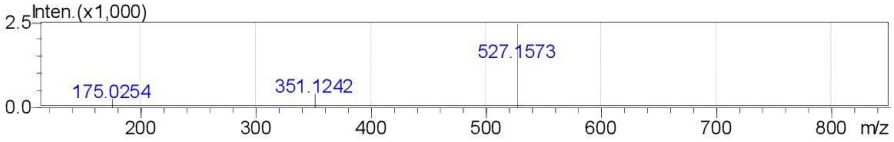

Figure S44: The fragmentation of IXN-C-Glc in DDA mode *XN-C-Glc*

Figure S45: The fragmentation of IXN-C-Glc in DDA mode

2. Enzymatic digestions

XN-7-O-Glc

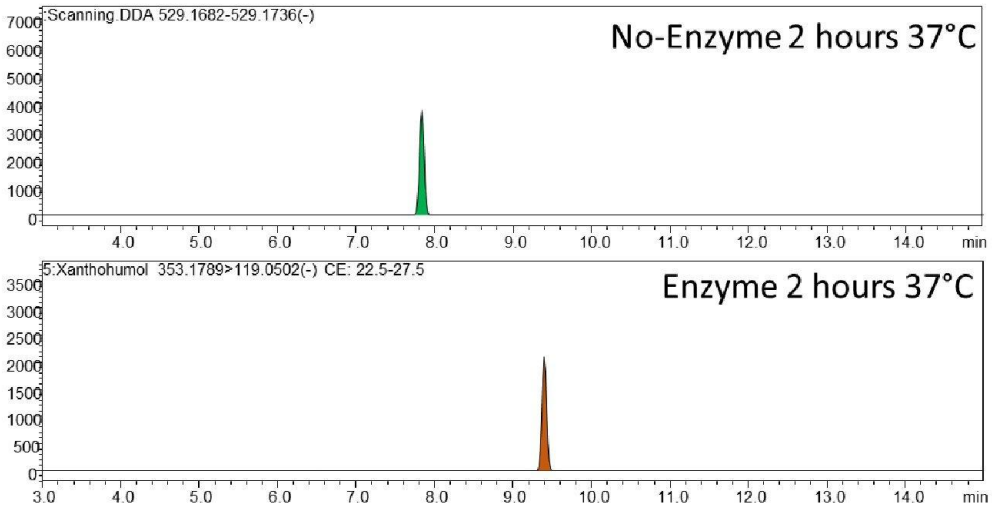

Figure S46: An LC-MS/MS chromatogram of XN-7-O-Glc after enzymatic digestion.

8-PN-7-O-Glc

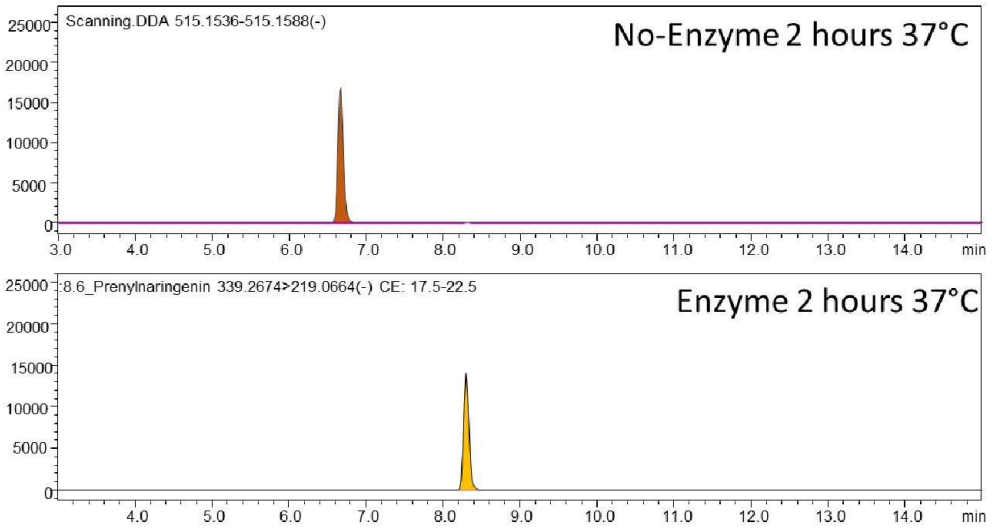

Figure S47: An LC-MS/MS chromatogram of 8PN-7-O-Glc after enzymatic digestion.

6-PN-7-O-Glc

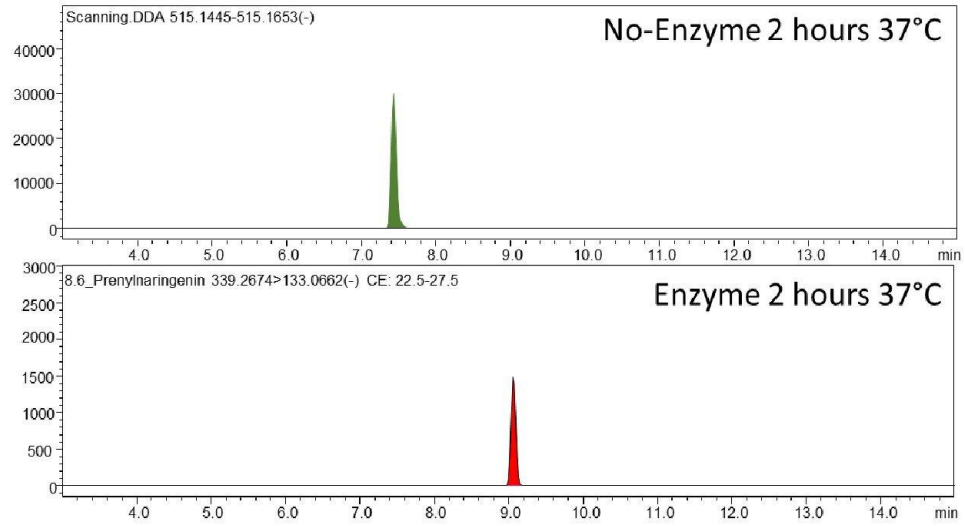

Figure S48: An LC-MS/MS chromatogram of 6PN-7-O-Glc after enzymatic

digestion. IXN-7-O-GLc

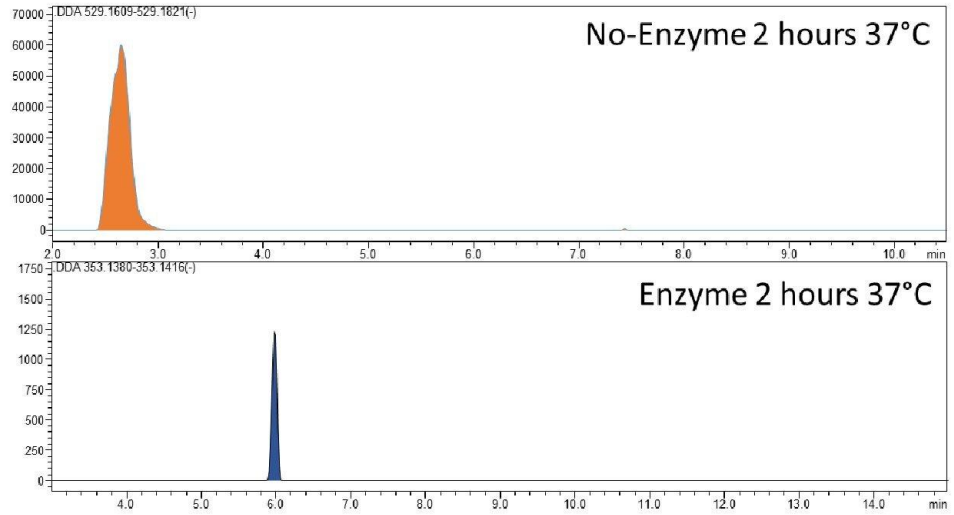

Figure S49: An LC-MS/MS chromatogram of IXN-7-O-Glc after enzymatic digestion. An earlier chromatogram was used where a steeper gradient was used, this was changed in the final runs of the blood hence the earlier elution.

XN-C-4'-O-GLc

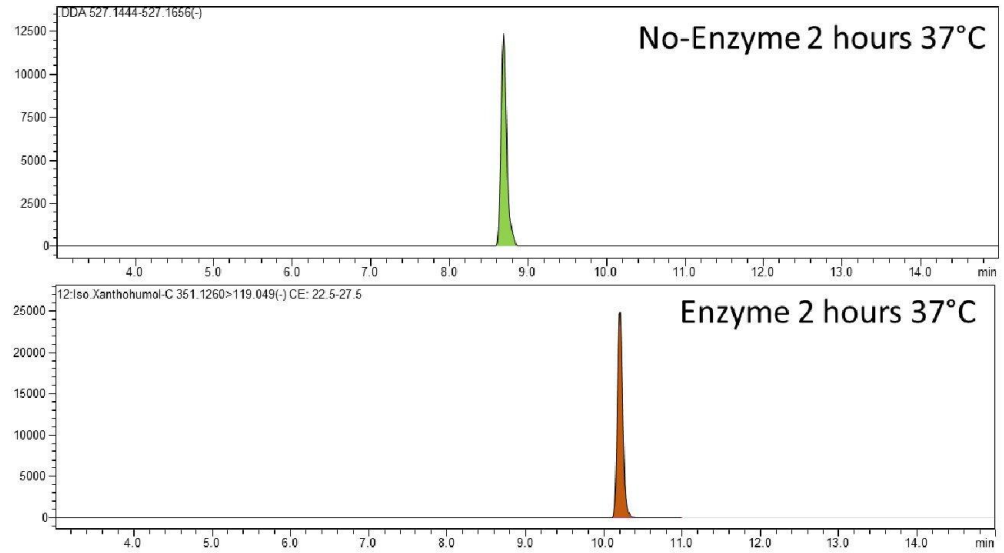

Figure S50: An LC-MS/MS chromatogram of XN-C-4'-O-Glc after enzymatic digestion. IXN-C-4'O-Glc

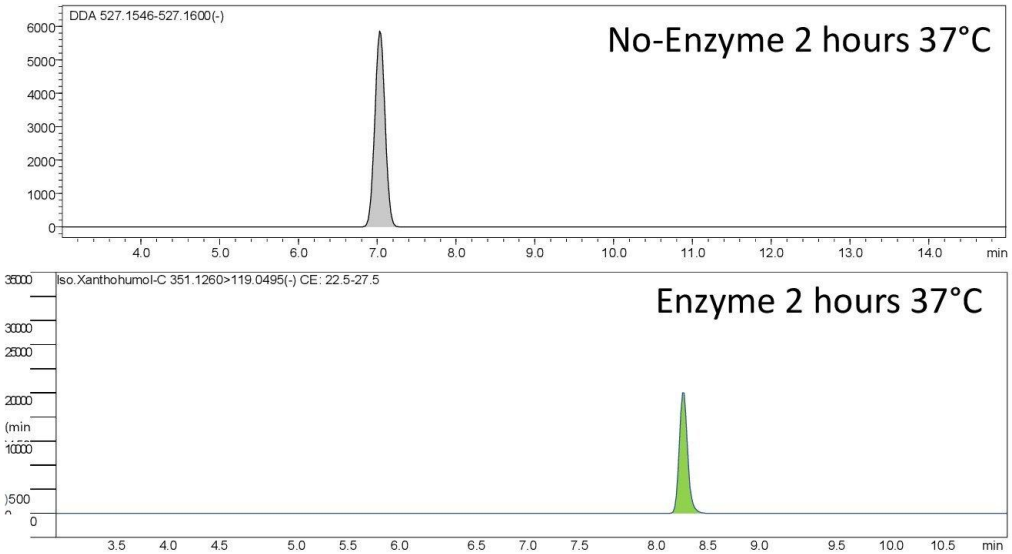

Figure S51: An LC-MS/MS chromatogram of IXN-C-4'-O-Glc after enzymatic digestion.

3. LC-MS/MS of hydroxylated compounds

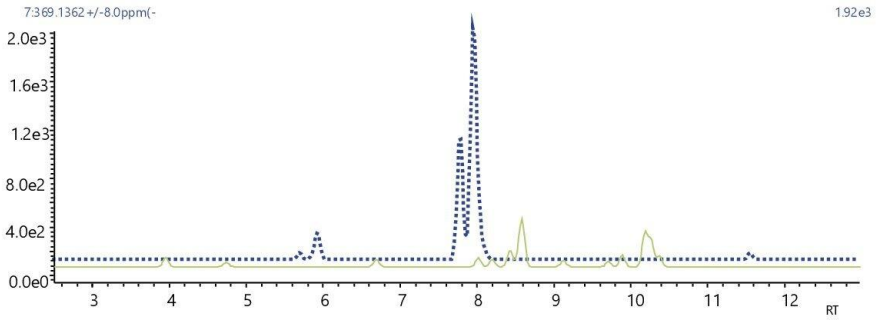

Figure S52: Compounds 5,6 and 7 (blue) overlaid with the analysis of the blood sample (green). No significant peaks were found.

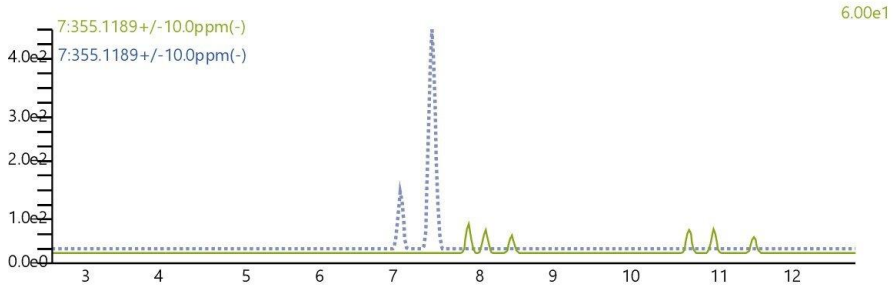

Figure S53: Compounds 8 and 9 (blue) overlaid with the analysis of the blood sample (green). No significant peaks were found.

4. LogP values of the synthesised compounds

Table S1: LogP values of the non-metabolites and the newly synthesised compounds

Non-metabolites	***Xanthohumol***	***Isoxanthohumol***	***8-Prenylnaringenin***	***6-Prenylnaringenin***
LogP	3.91	3.49	3.22	3.22
Hydroxyls	**XN-OH (*Z*) and (*E*)**	**IXN-OH (*E*)**	**8-PN-OH (*E*)**	**6-PN-OH (*E*)**
LogP	2.82	2.43	2.16	2.16
Sulfates	**XN-4'-O-sulfate**	**IXN-4'-O-sulfate**	**8-PN-4'O-sulfate**	**6-PN-7-O-sulfate**
LogP	1.92	1.26	0.74	0.74
Glucuronides	**XN-7-O-glc**	**IXN-7-O-glc**	**8-PN-O-7-glc**	**6-PN-O-7-glc**
LogP	2	1.61	1.34	1.34

References

1. Jongkees, S. A. K.; Withers, S. G., Glycoside Cleavage by a New Mechanism in Unsaturated Glucuronyl Hydrolases. *Journal of the American Chemical Society* **2011,** *133* (48), 19334-19337.
2. Buckett, L.; Schinko, S.; Urmann, C.; Riepl, H.; Rychlik, M., Stable Isotope Dilution Analysis of the Major Prenylated Flavonoids Found in Beer, Hop Tea, and Hops. *Front. Nutr.* **2020,** *7*, 11.

5.5 The pharmacokinetics of individual conjugated xanthohumol metabolites show higher bioavailability of micellar than native xanthohumol in a randomized, double-blind, crossover trial in healthy humans [203].

RESEARCH ARTICLE

Molecular Nutrition & Food Research
www.mnf-journal.com

The Pharmacokinetics of Individual Conjugated Xanthohumol Metabolites Show Efficient Glucuronidation and Higher Bioavailability of Micellar than Native Xanthohumol in a Randomized, Double-Blind, Crossover Trial in Healthy Humans

Lance Buckett, Nadine Sus, Veronika Spindler, Michael Rychlik, Christian Schoergenhofer, and Jan Frank**

Scope: Prenylated chalcones and flavonoids are found in many plants and are believed to have beneficial effects on health when consumed. Xanthohumol is present in beer and likely the most consumed prenylated chalcone, but poorly absorbed and rapidly metabolized and excreted, thus limiting its bioavailability. Micellar formulations of phytochemicals have been shown to improve bioavailability.

Methods and results: In a randomized, double-blind, crossover trial with five healthy (three males and two females) volunteers, a single dose of 43 mg was orally administered as a native or micellar formulation. The major human xanthohumol metabolites are quantified in plasma. Unmetabolized free xanthohumol makes 1% or less of total plasma xanthohumol. The area under the plasma concentration–time curve of xanthohumol-7-O-glucuronide following the ingestion of the micellular formulation is 5-fold higher and its maximum plasma concentration is more than 20-fold higher compared to native xanthohumol.

Conclusion: Metabolism of orally ingested xanthohumol is complex and efficiently converts the parent compound to predominantly glucuronic acid and to a lesser extent sulfate conjugates. The oral bioavailability of micellar xanthohumol is superior to native xanthohumol, making it a useful delivery form for future human trials.

1. Introduction

Many prenylated flavonoids native to hops have been studied for their health-beneficial and disease-preventive or even therapeutic activities.[1] The structurally related prenylated chalcone xanthohumol (XN) has promising activities against metabolic syndrome and cancer,[2] antibacterial and anti-viral activities, and may even have potential as a treatment against coronavirus infections, such as SARS-CoV-2.[2–4] XN is well tolerated in humans and does not alter clinical biomarkers, body weight, vital signs, or health-related quality of life.[5]

Prenylated flavonoids and chalcones are more lipophilic than their non-prenylated congeners and may thus more easily traverse cell membranes, which may facilitate their absorption.[6] Following oral ingestion, XN reaches the stomach, where the low pH facilitates its partial isomerization to isoxanthohumol (IXN).[7] XN is then absorbed in the small intestine and transported

L. Buckett, V. Spindler, M. Rychlik
Analytical Food Chemistry
Technical University of Munich
Maximus-von-Imhof Forum 2, 85354 Freising, Germany

N. Sus, J. Frank
Department of Food Biofunctionality (140b)
Institute of Nutritional Sciences
University of Hohenheim
Garbenstraße 28, 70599 Stuttgart, Germany
E-mail: jan.frank@nutres.de

C. Schoergenhofer
Department of Clinical Pharmacology
Medical University of Vienna
Währinger Gürtel 18–20, Vienna 1090, Austria
E-mail: christian.schoergenhofer@meduniwien.ac.at

The ORCID identification number(s) for the author(s) of this article can be found under https://doi.org/10.1002/mnfr.202200684

DOI: 10.1002/mnfr.202200684

to the liver where it may undergo metabolism by phase II enzymes, which catalyze conjugation reactions with water-soluble groups, such as glucuronic acid (GlcA) or sulfate. In healthy humans, the extent of phase II metabolism to generate O-glucuronides and O-sulfates of XN, administered as single doses of 60 or 180 mg, was nearly 100%.[8] The conjugated metabolites are secreted with the bile into the gut and the majority excreted in the feces, the remaining metabolites as well as the unmetabolized parent compound are excreted in the urine.[9] In addition, unabsorbed XN and biliary metabolites may undergo further biotransformation by the colonic microbiota, which can demethylate XN, resulting in 6-prenylnaringenin (6-PN) and 8-prenylnaringenin (8-PN) formation.[9]

The limited absorption of XN and its rapid metabolism are hurdles in the translation of the in vitro activities of XN to in vivo applications.[8] One other major issue, as described above, is that XN spontaneously cyclizes in the acidic environment of the stomach.[10] Consequently, the incorporation of XN into formulations that protect it from the acidic gastric conditions may aid in its absorption. Therefore, strategies to enhance XN solubility and to protect it from degradation, such as PEGylated graphene oxide nanosheet formulations of XN,[11] cyclodextrin formulations of the analogue xanthohumol-C,[12] and a micellar XN formulation,[13] have been developed in order to enhance its absorption and its biological activities. A protein-rich spent hops matrix enhanced XN absorption compared to a control spent hops preparation in humans.[14] A micellar formulation of XN inhibited Western-type diet-induced hepatic steatosis, inflammation, glucose intolerance, and body weight gain in mice and resulted in XN plasma concentration in the range of 100–330 nmol L^{-1}, whereas no XN was detectable after administration of native XN, which therefore was largely without effect in this mouse trial.[13] To the best of our knowledge, no study has investigated the absorption of XN from a micellular formulation compared to native XN in humans.

Most analytical methods used to quantify XN in human and animal trials employ enzymatic hydrolysis of the phase II conjugates and thus only quantify the sum parameter *total XN* (free + conjugated), which does not give a detailed overview of the diversity of compounds circulating in blood.[2] We recently published the synthesis of reference compounds for some XN metabolites, which now enables their identification and absolute quantification.[15]

Therefore, the aim of the present study was to identify the main metabolites formed after oral consumption of native and micellar XN and investigate their pharmacokinetics individually.

2. Results and Discussion

The present work aimed at identifying the main plasma metabolites of orally ingested XN in healthy humans and describing their individual pharmacokinetics rather than using the often-employed approach of quantifying total XN, which is the sum of parent compound plus conjugated phase II metabolites, after enzymatic hydrolysis. A further aim was to investigate if the metabolite profiles differed between native and micellar XN, because we hypothesized that the latter would be better bioavailable.

In a randomized, double-blind, crossover human trial, plasma samples were taken before and up to 24 h after ingestion of a single dose of 43 mg native or micellar XN and the plasma concentrations of the main metabolites were quantified to follow their pharmacokinetics. To the best of our knowledge, this is the first study reporting quantitative data on individual conjugated XN metabolites in humans and their pharmacokinetics following the intake of a micellular versus a native XN formulation. The employed data dependant acquisition (DDA) LC-MS/MS methodology combined with MS-Dial evaluation allowed targeted and untargeted approaches to simultaneously quantify and qualify pharmacokinetic data. The method here additionally allowed tentative confirmation of many metabolites and increased our understanding of XN metabolism.

2.1. Detected Metabolites of Xanthohumol

Metabolites were found initially by using the correlation function in MS-Dial when selecting reference compounds that were synthesized in previous work[15] by manually searching for glucuronic acid conjugates with an m/z of M+ GlcA (where M is the theoretical mass of XN/IXN or 8-PN/6-PN) and having the characteristic pharmacokinetic profile compared with XN-7-O-GlcA. Therefore, once all of the samples were uploaded, the MS1 spectra were compared for similarities in the abundance profile, but then, to confirm, the structures were tentatively annotated based on their MS2 spectra. An example of a confirmed annotation is given in **Figure 1** and shows the MS1 spectra over time to a very accurate MS1 of 0.008 Da. The MS2 spectra were taken from these time points and, using a mirror plot, were compared to a similar retention time (less than 5 s) of the reference compounds. Using the nominal mass of XN-7-O-GlcA 529.1715 (±0.008 Da) and 8-PN-7-O-GlcA 515.1524 (±0.010 Da), we identified four compounds at identification confidence level 1 (reference compound identified) and a further four at an identification confidence level 2 (MS2 and retention time), according to Schymanski et al.[16] **Table 1** shows all tentatively and identified compounds.

2.2. Recoveries and Precision

The recoveries of the metabolites were measured by spiking blank plasma with reference standards either before or after work-up. The areas of the reference standard peaks from MS-Dial were then compared between those before and after sample work-up. In general, recoveries from the metabolites were within 70–105%, but two analytes (colored red in **Table 2**), namely 6-PN-7-O-GlcA and 8-PN-7-O-sulfate, did not perform well. The low recoveries might be due to interfering peaks from the blood sample or due to the compound behaving differently than the other compounds during the extraction procedure. The method used was derived from van Breemen et al. where they did not calculate the recovery.[17] Because they were never calculated, the authors' recoveries during untargeted analysis might be similar to ours.

A pooled sample (quality control) was injected 12 times during each batch (4 times during each day over 3 days) and due to dilution (as blank samples were mixed in) not all analytes were resolvable. It was difficult to get MS2 spectra of many of the low-abundance compounds as they were below the DDA threshold.

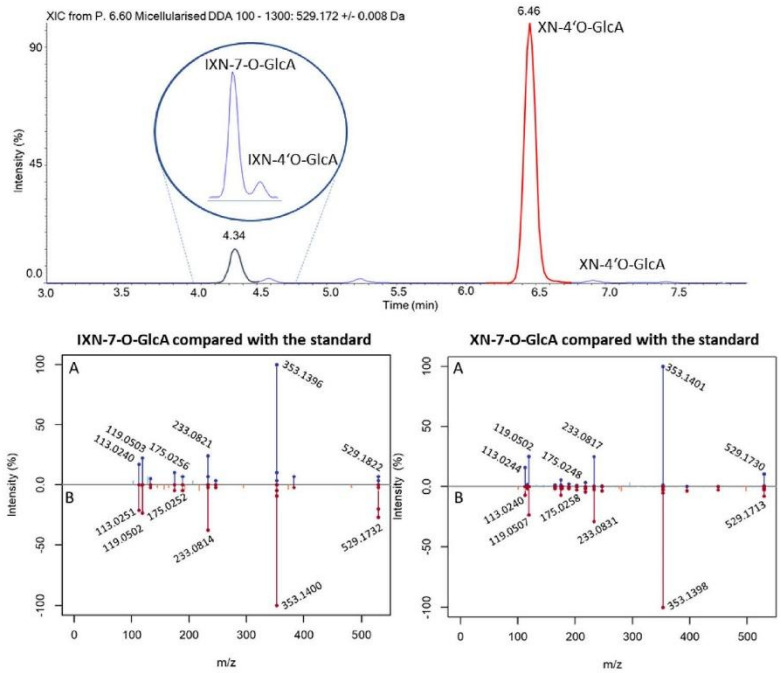

Figure 1. Top: An LC-MS/MS chromatogram of the xanthohumol (XN) and isoxanthohumol (IXN) glucuronides. Below: A is the compound found in human plasma and B is the reference standard represented as MS2 mirror plots.

Hence only the higher-abundance compounds were calculated and are presented in **Table 3**. Within the results of the precision over 3 days, the method was below the 20% range across multiple metabolites. Data independent analysis (DIA) would complement future analysis of prenylated flavonoids as spectral libraries are produced in public databases. However, this information is limited, but from the results of this study they can be added for future analysis. Therefore, as more metabolites are known and found in databases, future analyses should apply DIA as recent results indicated the improved accuracy of quantification.[18]

2.3. Calibration Graphs

The concentrations of the metabolites with available reference standards were calculated by comparing the ratio of analyte reference standard with the closest eluting internal standard in regards to retention time. As all samples were co-injected with blank plasma, the calibration graphs were matrix-matched to minimize any matrix effects from the blood plasma ionization efficiencies. Calibration graphs were created for the following analytes: XN-7-O-GlcA, IXN-7-O-GlcA, 8-PN-7-O-GlcA, 6-PN-7-

Table 1. Identified metabolites and corresponding IDs.

Glucuronides	Sulfates	Mixed	Unknown	Free
XN-7-O-GlcA *	XN-7-O-sulfate	XN-sulfate-GlcA	(m/z) 425.1961	XN*
IXN-7-O-GlcA *	6-PN-7-O-sulfate*	8/6-PN-sulfate-GlcA	(m/z) 423.1827	IXN*
6-PN-7-O-GlcA*	8-PN-7-O-sulfate	XN-di-GlcA	(m/z) 531.1883	6-PN*
8-PN-7-O-GlcA*	XN-4′O-sulfate*	6/8-PN-di-GlcA	(m/z) 533.1957	8-PN*
XN-4′O-GlcA	IXN-4′O-sulfate	-	(m/z) 517.1365	-
IXN-4′O-GlcA	6-PN-4′-O-sulfate	-	-	-
8-PN-4′O-GlcA	8-PN-4′-O-sulfate	-	-	-
6-PN-4′O-GlcA	-	-	-	-

The (*) denotes that identification was based on reference standards. All other metabolites were identified by retention time, MS2 spectra, and pharmacokinetic profile matching similar to XN-7-O-GlcA (where applicable). See supplementary information for detailed annotation.

Table 2. The recoveries as % average and (RSD) of each metabolite where reference compounds where used.

	Glucuronide metabolites			
	XN-7-O-GlcA	6-PN-7-O-GlcA	8-PN-7-O-GlcA	IXN-7-O-GlcA
High	73 (7.4)	74 (4.6)	79 (11.5)	95 (2.6)
Medium	71 (8.8)	67 (2.5)	79 (11.5)	105 (2.3)
Low	76 (8.0)	63 (21)	92 (3.9)	93 (3.6)
	Sulfate metabolites			
	XN-4′-O-sulfate	**6-PN-7-O-sulfate**	**8-PN-4′-O-sulfate**	**IXN-4′-O-sulfate**
High	95 (5.6)	75 (2.8)	78 (12.4)	88 (6.5)
Medium	84 (11)	70 (0.8)	69 (18.1)	105 (2.3)
Low	86 (1.4)	87 (7.6)	89 (5.8)	82 (10.0)

O-GlcA, XN-4′-O-sulfate, IXN,4′-O-sulfate, 8-PN-4′-O-sulfate, 6-PN-7-O-sulfate, XN, and IXN. See Table S1, Supporting Information showing the corresponding internal standards and m/z of each compound.

2.4. Pharmacokinetics of Xanthohumol

The primary goal of the study identified and quantified the major metabolites of XN using reference standards.[15] As the blood plasma samples were not digested using glucuronidases and sulfatases, it was additionally possible to calculate the free XN (<1.2% of total XN) compared with the total XN amongst all participants ingesting the micellar formulation (**Figure 2**). Comparing the pharmacokinetic plot of XN-7-O-GlcA, scarcely any free XN was present in blood plasma (**Figure 3**). A study by Legette et al. revealed comparable values (<1%) with 60 or 180 mg XN orally ingested as a self-emulsifying mixture by humans, demonstrating that XN circulates to nearly 100% as conjugated metabolites.[8] Plasma AUC-$_{0-24\,h}$ were 19.7 nmol L^{-1} h^{-1} and C_{max} 10.6 nmol L^{-1} for unmetabolized micellar XN and 0.5 and 5 nmol L^{-1}, respectively, for native XN (Figure 2), indicating that the micellarised formulation is much better bioavailable and delivers higher amounts of free XN than native XN. T_{max} was not significantly different between formulations, although micellar XN reached peak concentrations in 0.8 h and native XN in 2.1 h, which is in agreement with the above study of Legette et al. using enzymatic deconjugation.[8]

The pharmacokinetic plots revealed two maxima at 30 and 480 min for conjugated XN, which suggests that it may be undergoing enterohepatic recirculation (Figure 3). The double maxima might be explained by biliary secretion of the conjugates into the intestine and hydrolysis of the conjugates by intestinal bacteria, thus releasing free XN back into the gut where re-absorption might occur. Free XN had a single maximum and the C_{max} of conjugated XN was ca. 100-fold higher than for free XN, suggesting that conjugation of absorbed XN occurs rapidly and is nearly complete.

2.5. Pharmacokinetics of Xanthohumol Glucuronides

To the best of our knowledge, the present work is the first report of any XN glucuronides being quantified in humans. Glucuronides were the predominant XN conjugates, which is in agreement with previous findings,[5,8,14,19,20] although most of these studies did not quantify them as previously no reference standards were available.

The mean area under the plasma concentration–time curve (AUC) of **(1)** XN-7-O-GlcA was significantly higher following the consumption of micellar (250 nmol L^{-1} h^{-1}) than native XN (30 nmol L^{-1} h^{-1}), demonstrating the superior bioavailability of the micellar formulation (Figure 3). Also C_{max} was significantly higher (ca. 100-fold) after intake of micellar than native XN (Figure 3). These data are in agreement with previous findings in mice fed native or micellar XN for 3 weeks, in which total XN was not detectable following feeding of native XN, but plasma concentrations ranging from 100 to 330 nmol L^{-1} total XN were measured in mice fed the micellar formulation.[21] No differences were observed between micellar and native XN regarding T_{max} (Figure 3).

2.6. Pharmacokinetics of Xanthohumol Sulfates

The other major metabolite pathway for XN is sulfation resulting in metabolites XN-4′O-sulfate, 6-PN-7-O-sulfate, 8-PN-7-O-sulfate, and 6-PN-4′-O-sulfate (see supplementary information for semi-quantification results of 6-PN-4′-O-sulfate and MS2 spectra of the found sulfates). Reference standards were only available for XN-4′O-sulfate, which therefore was the only

Table 3. The precision of the method analyzing xanthohumol metabolites (n = 12) given as RSD percent of the mean over four times during the day and over 3 days.

XN-7-O-GlcA	IXN-7-O-GlcA	8-PN-7-O -GlcA	6-PN-7-O-GlcA	XN-4′O-sulfate	XN-sulfate-GlcA	(m/z) 531.1883	(m/z) 533.1957
6.4	3.3	10.4	14.8	13.7	16.6	5.4	10.5

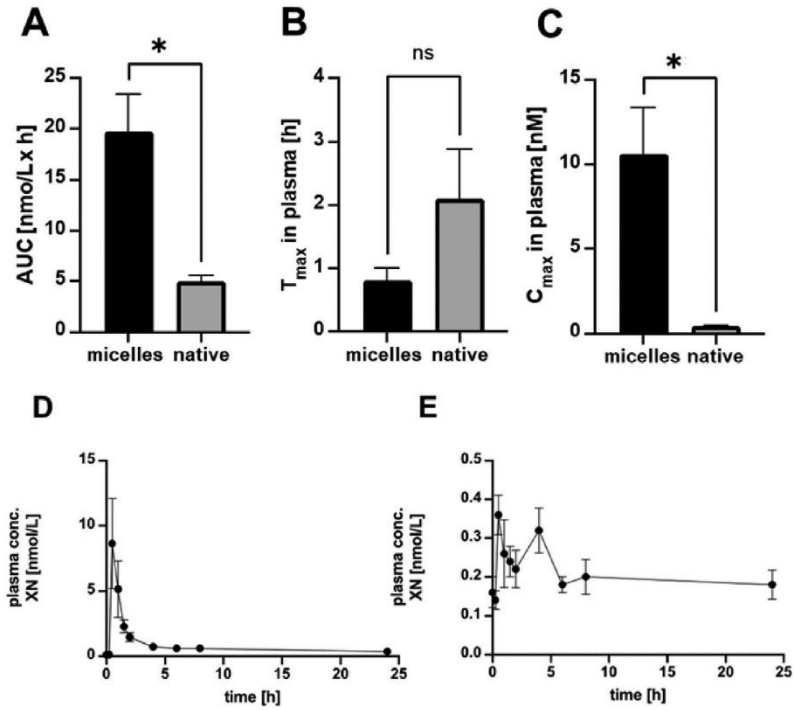

Figure 2. Mean ($n = 5$) xanthohumol (XN) area under the plasma concentration–time curve ($AUC_{0-24\,h}$) (A), T_{max} (B), C_{max} (C), and plasma concentrations over time of XN following the ingestion of a single dose of 43 mg of micellar (D) or native XN (E); * significantly different at $p < 0.05$.

sulfate quantifiable in the micellular treatment, due to an interfering signal and no MS2 data in the native formulation. Furthermore, no peak was detected at the retention time for IXN-4′-O-sulfate at 5.1 min. There is, however, an equal peak at 5.5 min, which is actually in-source fragmentation (ISF) of XN-sulfate-GlcA, tentatively a xanthohumol-sulfate-glucuronic acid conjugate. Many sulfate and glucuronic acid metabolites of XN detected in our volunteers were also identified in postmenopausal women given a hop supplement.[17] However, we believe that in the latter study the annotation of xanthohumol-sulfate may have been incorrect and may also be in-source fragmentation of XN-sulfate-GlcA at the retention time of 5.7 min (**Figure 4**, see supplementary information for all annotation data).

Interestingly, the mean AUC (micellular) of the XN-4′-O-sulfate (280 nmol L^{-1} h^{-1}) was similar to that of XN-7-O-GlcA (251 nmol L^{-1} h^{-1}, **Figure 5**) despite the interfering signal at the same mass being present in all samples. The interference exaggerated the $AUC_{0-24\,h}$ due to the zero point starting at 6 nmol L^{-1}. Therefore, the data are speculative but allow an estimation of the area under the curve revealing that the sulfates appear to peak at a similar time as the free XN glucuronic acid conjugates. In addition, as no MS2 information was found regarding the native XN supplementation, the micellular superiority in absorption is demonstrated. Regarding the 8- and 6-prenylnaringenin sulfate conjugates, an ISF at 5.3 min was observed (see supplementary information), this could easily be mistaken as a 8-/6-PN-sulfate metabolite. 6-PN′-4′-O-sulfate and small amounts of the 6-PN-7-O-sulfate were also detected.

2.7. Identification and Pharmacokinetics of Mixed Xanthohumol Metabolites

As no reference compounds for mixed metabolites, containing both sulfates and glucuronides, were available, only tentative evidence for the annotation of these compounds was achieved. Two major mixed metabolites were XN-sulfate-GlcA and 6-/8-PN-sulfate-GlcA, which have the same order of magnitude (above 30,000 cps) as XN-7-O-GlcA. Because no reference compounds for these metabolites were available, we assumed that the concentrations are in a similar range and kept possible differences in ionization efficiencies in mind. Other found metabolites include double glucuronides (substances XN-di-GlcA and 6-/8-PN-di-GlcA). See the online supplementary material for all data regarding the annotations of mixed metabolites.

Two compounds that have similar pharmacokinetic profiles have revealed interesting features as their molecular masses (m/z

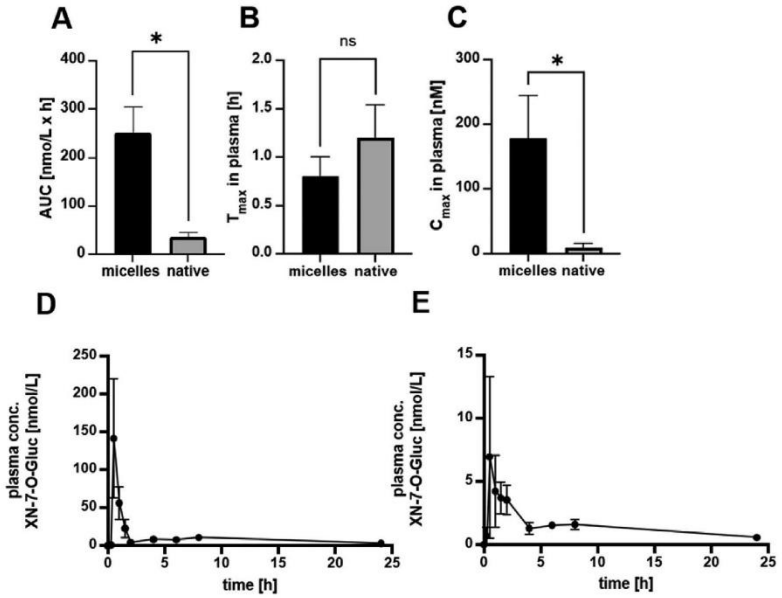

Figure 3. Mean ($n = 5$) XN-7-*O*-GlcA area under the plasma concentrations–time curve ($AUC_{0-24\,h}$) (A), T_{max} (B), C_{max} (C), and plasma concentrations over time of XN-7-O-GlcA following the ingestion of a single dose of 43 mg of micellar (D) or native XN; * significantly different at $p < 0.05$.

of 533.1672 and 531.1883) implying a hydrogenation reaction. To rule out that the compounds were present in the capsules, a sample was diluted 10,000-fold and analyzed using the same method (Figure S28, Supporting Information) and no parent masses of m/z of 355.1545 and 357.1352, which are theoretical deconjugated masses [M-GlcA]- containing the same MS2 spectra, were found.

Bacterial transformation of XN has been observed following in vitro digestion of IXN with *Eubacterium limosum*, which produces 8-PN.[22] Also *Eubacterium ramulus* is known to hydrogenate specifically the Michael system in many chalcones.[23] While this may appear to suggest that bacteria were involved in the transformation of XN to 533.1672 and 531.1883, as it has the corresponding mass of M-2H in our volunteers, certain observations contradict this. Namely, the AUC for these metabolites were higher following the intake of micellar than native XN (**Figure 6C**), suggesting that they are derived from XN absorbed in the small intestine, as more unabsorbed native XN is expected the reach the colon. In addition the MS2 spectra are very different than reported by Miranda et al., therefore these compounds were not tentatively annotated.[24] This is further supported by the early appearance of these metabolites within 2 h after intake

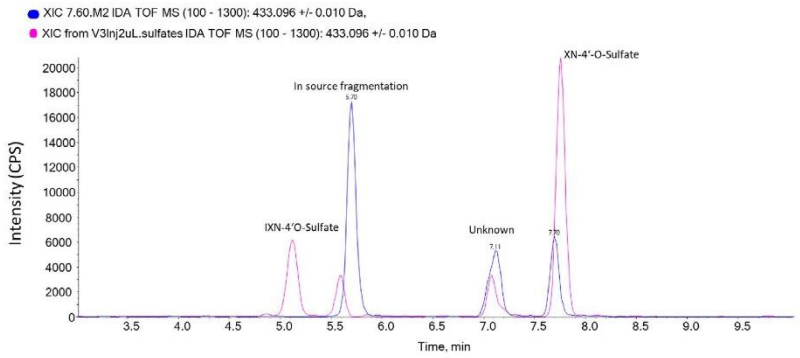

Figure 4. An extracted ion chromatogram of 433.0960 m/z analyzing the reference standards (pink) and the human plasma (blue). The in-source fragmentation is from the glucuronide sulfate conjugate of XN-sulfate-GlcA, which is based on having the same retention time.

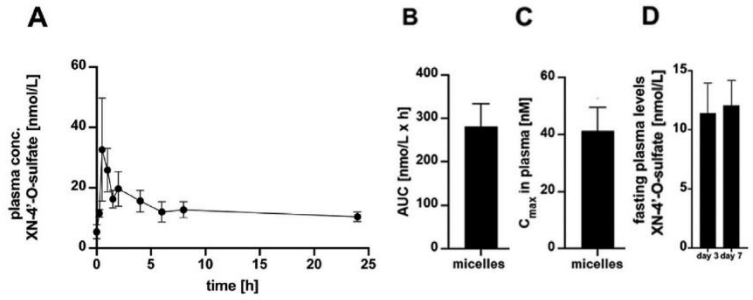

Figure 5. Plasma concentrations over time of XN-4′-O-sulfate following the ingestion of a single dose of 43 mg of micellar (A). Mean ($n = 5$) XN-4′-O-sulfate area under the plasma concentrations–time curve ($AUC_{0-24\,h}$) (B), and C_{max} (C) following the ingestion of a single dose of 43 mg of micellar. Fasting XN-4′-O-sulfate plasma concentrations after 3 and 7 days of daily ingestion of 129 mg micellar (D).

of XN, which is too short for compounds generated and absorbed in the colon. Hence, to answer the question where these metabolites originate from requires further experiments and cannot be answered with the presently available data. An additional compound that matched a demethylated version of m/z 531.1883 was also annotated as m/z 517.1365. Two additional compounds that followed similar pharmacokinetic data were not able to be annotated (m/z 425.1961) and (m/z 423.1827).

2.8. Pharmacokinetics of the Sum of Xanthohumol and its Metabolites

Combining all of the pharmacokinetic data from the quantified XN metabolites allowed us to show that significant absorption from the native and micellar formulations into the blood circulatory system occurred (**Figure 7**). The AUC of the sum of all XN and its metabolites quantified (apart from XN-4′O-sulfate due to an interfering signal) was significantly higher after intake of 43 mg of micellar than native XN (Figure 7C). T_{max} was significantly shorter for micellar (1 h) than native (1.5 h) XN (Figure 7D). The terminal elimination half-life could not be calculated due to increasing concentrations between 5 and 24 h, although a long half-life of native XN has been observed previously.[20]

Even though significant differences in the bioavailability of single doses of micellar and native XN were observed in the present human trial, fasting blood concentrations of the sum of all XN metabolites did not significantly differ after 3 or 7 days of daily intake of 129 mg XN (one 43 mg capsule with each principle meal) (Figure 7F). However, a small increase in fasting total XN from day 3 to day 7 was observed when micellar XN was taken. In a similar trial comparing native versus micellar curcumin, significantly higher fasting curcumin concentrations were observed after intake of the micellar compared to the native formulation at days 3 and 7.[25] The differences may be explained by differences

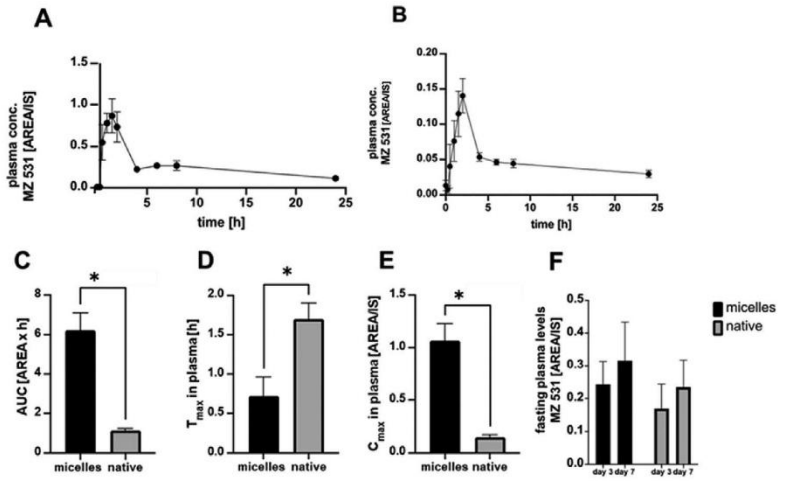

Figure 6. Plasma concentrations over time of m/z 531.1883 following the ingestion of a single dose of 43 mg of micellar (A) or native XN (B); mean ($n = 5$) 531.1883 area under the plasma concentrations–time curve ($AUC_{0-24\,h}$) (C), T_{max} (D), C_{max} (E), fasting levels comparing the micellular and native dosage (F). * significantly different at $p < 0.05$.

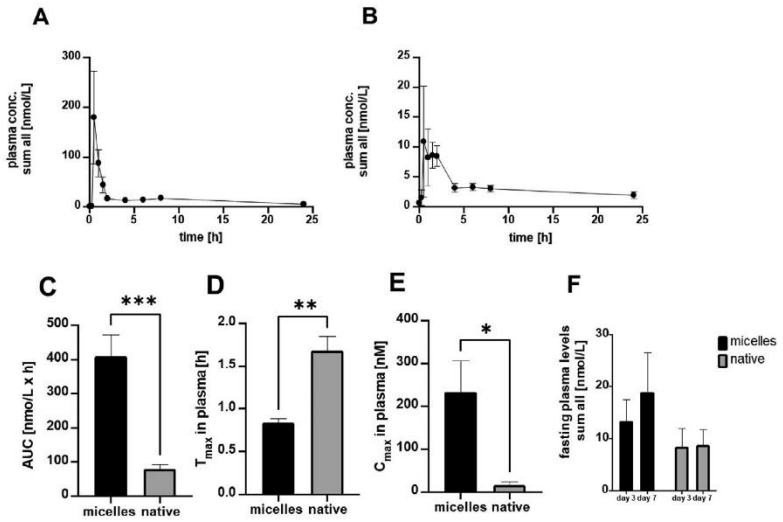

Figure 7. Plasma concentrations over time of all quantified metabolites following the ingestion of a single dose of 43 mg of micellar (A) or native xanthohumol (B); mean ($n = 5$) area under the plasma concentrations–time curve ($AUC_{0\text{-}24\,h}$) (C), T_{max} (D), and C_{max} (E) of all metabolites. Fasting concentrations of the sum of all quantified metabolites after 3 and 7 days of daily ingestion of 129 mg micellar or native XN (F). * significantly different at $p < 0.05$.

in the solubilities of the compounds. The lipid-soluble curcumin is insoluble in water and dependent on conjugation with glucuronic acid and sulfates for its excretion, whereas XN is slightly soluble in water and can thus be more easily excreted.[26] The main metabolites found were glucuronides, sulfates, and mixed metabolites for both formulations. Compared to native XN, C_{max} for the main metabolites were more than 20-fold higher for micellar formulation. From the results we have compiled an updated metabolic pathway of XN (**Figure 8**).[9,17,23] XN is consumed and isomerized into IXN in the stomach followed by combinations of modifications (e.g., demethylation) creating a number of pre-metabolites for the liver to actively produce extensive glucuronidation and sulfation products. The bioactivities of the metabolites are yet to be investigated and are paramount in understanding the effects of XN consumption on health.

3. Conclusion

The present study, for the first time, quantified individual metabolites of xanthohumol (XN) following the ingestion of native or micellar formulations. XN-7-O-GlcA and XN-4′-O-sulfate were the quantitatively most important metabolites. Smaller quantities of mixed metabolites containing sulfates and glucuronides as well as double glucuronide conjugates of XN and derived prenylated chalcones and flavonoids were also found. Free XN made up only about 1% or less of total XN in our volunteers, suggesting efficient conjugation of XN by phase II enzymes. The plasma concentrations of free XN, XN-7-O-GlcA, and of the sum of all XN metabolites were significantly higher following the intake of micellar compared to native XN, demonstrating the superior bioavailability of the micellar formulation and suggesting it may be a useful delivery form for future human trials investigating biological activities of XN.

4. Experimental Section

Human Trial: This double-blind, randomized crossover trial was conducted at the Department of Clinical Pharmacology of the Medical University of Vienna between October 2018 and August 2019 with the approval of an independent ethics committee (ethics number 1580/2018). All participants gave their oral and written informed consent and were free to withdraw from the trial at any time. Five healthy volunteers (three males and two females) received in random order a single capsule containing 43 mg of native or micellar XN after an overnight fast. Blood samples were drawn before and 0.25, 0.5, 1, 1.5, 2, 4, 6, 8, and 24 h after ingestion of the capsule. After this initial pharmacokinetic phase, the volunteers received one capsule of XN (43 mg) with each principal meal (3 times per day) for 7 days. A final blood sample was drawn after 7 days of drug intake to investigate possible accumulation. A washout period of at least 7 days was maintained before crossover to the respective other treatment. Blood samples were centrifuged at 2000 × *g* for 15 min at 4 °C. Plasma was aliquoted and stored at −80 °C until analysis.

Blood Pre-Treatment: Plasma samples were analyzed in duplicate and 150 µL plasma was spiked with 0.25 mg L^{-1} internal standards (IXN-D3, 8-PN-D3, 6-PN-D3, and XN-D3; synthesized previously).[27] Extraction and clean-up were performed according to van Breemen et al.[17]

Calibration: Reference standards were dissolved in acetonitrile:methanol (90:10, by volume) at the following initial concentrations: XN-4′O-sulfate (0.114 mg L^{-1}), IXN-4′-O-sulfate (0.110 mg L^{-1}), 8-PN-4′O-sulfate (0.109 mg L^{-1}), 6-PN-7-O-sulfate (0.106 mg L^{-1}), XN-7-O-glucuronide (0.263 mg L^{-1}), IXN-7-O- glucuronide (0.109 mg L^{-1}), 8-PN-7-O-glucuronide (0.195 mg L^{-1}), and 6-PN-7-O-glucuronide (0.144 mg L^{-1}). The free compounds XN, IXN, 8-PN, and 6-PN were dissolved

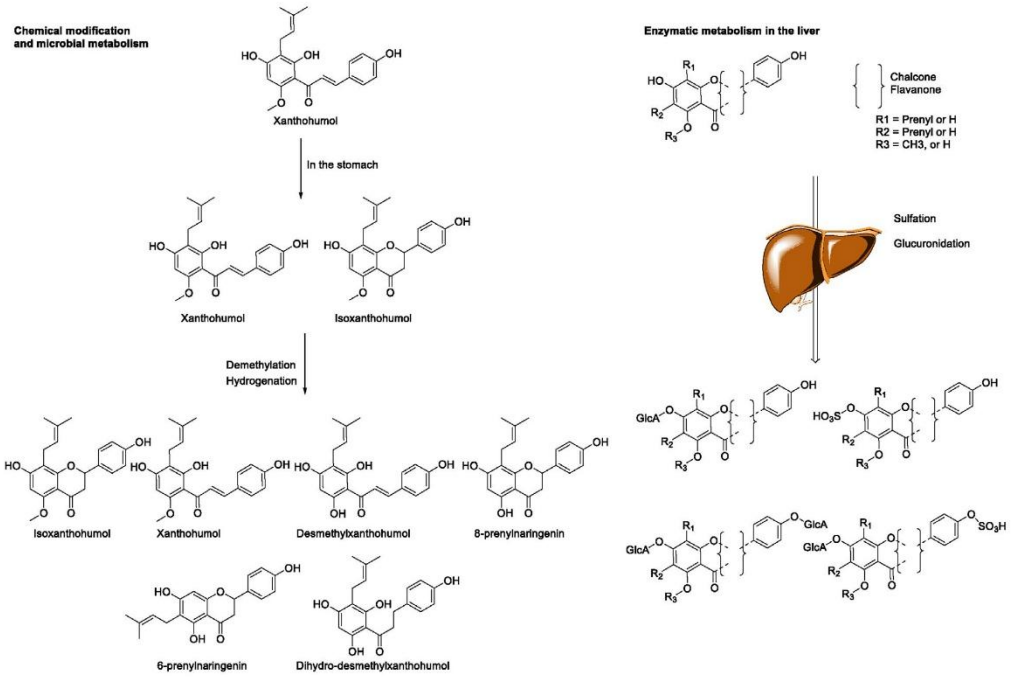

Figure 8. Human metabolism of XN and related prenylated flavonoids in vivo. No hydroxylated compounds, mercapturic acid, and no direct glutathione adducts were detected in this study.

at a concentration of 0.01 mg L^{-1}. The highly concentrated substances were then diluted 10- and 100-fold, generating high, medium, and low concentration stock solutions for each substance. The stock solutions were co-injected using the autosampler at injection volumes ranging from 0.5 to 5.0 µL with a blank plasma sample containing the internal standards (0.25 mg L^{-1}) in a separate vial and injected into the LC-MS/MS using the same method. See Table S1, Supporting Information.

Recoveries: Blank blood plasma (free from prenylated flavonoids) was spiked with concentrations at three different concentrations (high: XN-7-O-GlcA [0.026 mg L^{-1}], IXN-7-O-GlcA [0.011 mg L^{-1}], 8-PN-7-O-GlcA [0.020 mg L^{-1}], 6-PN-7-O-GlcA [0.014 mg L^{-1}], XN-4′-O-sulfate [0.011 mg L^{-1}], 6-PN-7-O-sulfate [0.011 mg L^{-1}] and 8-PN-4′-O-sulfate [0.011 mg L^{-1}]). The medium recoveries were tested at half the concentration as the high values and low recovery were tested at a 10-fold dilution of the high values. The recoveries were then calculated of the theoretical (spiked concentration) versus the calculated result using the determined calibration graphs. The lower limit of detection (LOD) was set at a peak found over 500 cps in height and the lower limit of quantification (LOQ) was estimated between the lowest and second lowest calibration points.

LC-MS/MS: LC-MS/MS was carried out on a Sciex Exion LC AD system coupled to a Sciex X500R QToF-MS (MDS Sciex, Concord, Canada). The system was calibrated every five samples and operated in information dependant acquisition (IDA) mode (also known as DDA). The ms range was set between 100 and 800 *m/z* and a selection of 10 precursors was set with a collision energy at 35 eV with a spread of 15 eV and fragmentation events above counts of 1000. The analytes were separated using the LC method developed by Buckett et al. (Supplementary information).[15] Each participant's samples were randomized and data were collected on a batch to batch within a time of 3 weeks.

MS-Dial and MS Convert: The Wiff. files were converted to mzML files using the Windows version of MS_convert and then grouped into the micellular and native groups manually.[28] Each participant's sample files were then incorporated into MS-dial (version 4.8 http://prime.psc.riken.jp/compms/msdial/main.html) using the following parameters, Ms1 and Ms2 tolerance of 0.05 Da, Ms range 338–1000 Da and MS/MS 100–1300 Da. Peak detection of 1000 amplitude and a mass slice of 0.5 Da with a smoothing level of 3 and a minimum peak of 10 scans. The MS/MS cut-off was set at 5. Due to computational limitations, each participant was uploaded individually and the alignment file used was 60 min. All known compounds were annotated manually and the metabolites' integrations at each time point were copied into Microsoft Excel (Excel 2019, Microsoft, WA, USA). The metabolites were found by comparing known reference standards features (MS, MS2, retention time pharmacokinetic profile) and the correlation feature in MS-dial (similar to Pearson correlation). The same process was applied to the calibration samples and graphs were produced using Microsoft Excel.

XCMS and See MS: To visualize some non-target MS2 spectra, the programme SeeMS (64-bit, version 3.0.21173.0) was used to extract MS2 spectra on a Windows 11 machine (SQ1 processor with 16 Gb RAM). These MS2 spectra were again processed using the XCMS programme in R-studio (version R 4.1.3).[29]

Statistical Analysis: Using the integrals of each peak obtained from MS-Dial calibration graphs were constructed. The linear trend line function was used and the concentrations of each analyte were calculated using linear regression extrapolation in Microsoft Excel. Using the concentrations that were calculated from Excel, pharmacokinetic plots were produced by plotting the concentration or compound ratio (qualitative analysis) over the retention time. All statistical analyses, including the calculation of AUC, were conducted with GraphPad Prism 9 (version 9.0.0, GraphPad Software, San Diego, CA, USA). Results were presented as arithmetic

mean with standard deviation (SD) or with standard error of the mean (SEM). Differences between the formulations regarding AUC, C_{max}, and t_{max} were computed by repeated-measures ANOVA followed by a Tukey post hoc test. Differences were considered significant at $p < 0.05$.

Supporting Information

Supporting Information is available from the Wiley Online Library or from the author.

Acknowledgements

We thank Prof. Phillipe Schmitt-Kopplin for allowing the use of the LC-MS/MS system, as without it the study would have not been possible.

Conflict of Interest

J.F. is a scientific consultant to AQUANOVA AG, the company producing micellular formulations of xanthohumol.

Author Contributions

L.B., C.S., J.F., and M.R. conceptualized the project. C.S. carried out the human trial. L.B. and V.S. carried out the sample work-up of the samples. L.B. carried out the analysis of the samples. L.B. and N.S. carried out the data analysis. L.B. and M.R. wrote the initial draft, which was revised by L.B., M.R., C.S., and J.F. All authors agreed to the manuscript before submission.

Data Availability Statement

The data that support the findings of this study are available from the corresponding author upon reasonable request.

Keywords

bioavailability, clinical trial, drug absorption, micelles, pharmacokinetics, phase II metabolism, xanthohumol glucuronide

Received: May 15, 2023
Published online:

[1] S. Venturelli, M. Burkard, M. Biendl, U. Lauer, J. Frank, C. Busch, *Nutrition* **2016**, *32*, 1171.
[2] H. F. Neumann, J. Frank, S. Venturelli, S. Egert, *Mol. Nutr. Food Res.* **2022**, *66*, 2100831.
[3] Y. Lin, R. Zang, Y. Ma, Z. Wang, L. Li, S. Ding, R. Zhang, Z. Wei, J. Yang, X. Wang, *Int. J. Mol. Sci.* **2021**, *22*, 12134.
[4] S. Yuan, B. Yan, J. Cao, Z.-W. Ye, R. Liang, K. Tang, C. Luo, J. Cai, H. Chu, T. W.-H. Chung, K. K.-W. To, I. F.-N. Hung, D.-Y. Jin, J. F.-W. Chan, K.-Y. Yuen, *Cell Discov.* **2021**, *7*, 100.
[5] B. O. Langley, J. J. Ryan, D. Hanes, J. Phipps, E. Stack, T. O. Metz, J. F. Stevens, R. Bradley, *Mol. Nutr. Food Res.* **2021**, *65*, 2001170.
[6] X. Chen, E. Mukwaya, M.-S. Wong, Y. Zhang, *Pharm. Biol.* **2014**, *52*, 655.
[7] D. Nikolic, Y. Li, L. R. Chadwick, G. F. Pauli, R. B. van Breemen, *J. Mass Spectrom.* **2005**, *40*, 289.
[8] L. Legette, C. Karnpracha, R. L. Reed, J. Choi, G. Bobe, J. M. Christensen, R. Rodriguez-Proteau, J. Q. Purnell, J. F. Stevens, *Mol. Nutr. Food Res.* **2014**, *58*, 248.
[9] L. Hanske, G. Loh, S. Sczesny, M. Blaut, A. Braune, *Mol. Nutr. Food Res.* **2010**, *54*, 1405.
[10] S. Possemiers, A. Heyerick, V. Robbens, D. De Keukeleire, W. Verstraete, *J. Agric. Food Chem.* **2005**, *53*, 6281.
[11] J. Zhang, L. Yan, P. Wei, R. Zhou, C. Hua, M. Xiao, Y. Tu, Z. Gu, T. Wei, *Eur. J. Pharmacol.* **2021**, *895*, 173866.
[12] M. Kirchinger, L. Bieler, J. Tevini, M. Vogl, E. Haschke-Becher, T. K. Felder, S. Couillard-Després, H. Riepl, C. Urmann, *Planta Med.* **2019**, *85*, 1233.
[13] A. Mahli, T. Seitz, K. Freese, J. Frank, R. Weiskirchen, M. Abdel-Tawab, D. Behnam, C. Hellerbrand, *Cells* **2019**, *8*, 359.
[14] A. O'Connor, V. R. Konda, R. L. Reed, J. M. Christensen, J. F. Stevens, N. Contractor, *Mol. Nutr. Food Res.* **2018**, *62*.
[15] L. Buckett, S. Schönberger, V. Spindler, N. Sus, C. Schoergenhofer, J. Frank, O. Frank, M. Rychlik, *Metabolites* **2022**, *12*, 345.
[16] E. L. Schymanski, J. Jeon, R. Gulde, K. Fenner, M. Ruff, H. P. Singer, J. Hollender, *Environ. Sci. Technol.* **2014**, *48*, 2097.
[17] R. B. van Breemen, L. Chen, A. Tonsing-Carter, S. Banuvar, E. Barengolts, M. Viana, S.-N. Chen, G. F. Pauli, J. L. Bolton, *J. Agric. Food Chem.* **2020**, *68*, 5212.
[18] C. Fernández-Costa, S. Martínez-Bartolomé, D. B. McClatchy, A. J. Saviola, N.-K. Yu, J. R. Yates, *J. Proteome Res.* **2020**, *19*, 3153.
[19] S. Bolca, J. Li, D. Nikolic, N. Roche, P. Blondeel, S. Possemiers, D. De Keukeleire, M. Bracke, A. Heyerick, R. B. van Breemen, H. Depypere, *Mol. Nutr. Food Res.* **2010**, *54*, S284.
[20] R. B. van Breemen, Y. Yuan, S. Banuvar, L. P. Shulman, X. Qiu, R. F. R. Alvarenga, S.-N. Chen, B. M. Dietz, J. L. Bolton, G. F. Pauli, E. Krause, M. Viana, D. Nikolic, *Mol. Nutr. Food Res.* **2014**, *58*, 1962.
[21] A. Mahli, T. Seitz, K. Freese, J. Frank, R. Weiskirchen, M. Abdel-Tawab, D. Behnam, C. Hellerbrand, *Cells* **2019**, *8*, 359.
[22] E. Moens, S. Bolca, T. Van de Wiele, A. Van Landschoot, J. L. Goeman, S. Possemiers, W. Verstraete, *AMB Express* **2020**, *10*, 79.
[23] I. L. Paraiso, L. S. Plagmann, L. Yang, R. Zielke, A. F. Gombart, C. S. Maier, A. E. Sikora, P. R. Blakemore, J. F. Stevens, *Mol. Nutr. Food Res.* **2019**, *63*, 1800923.
[24] C. L. Miranda, L. A. Johnson, O. de Montgolfier, V. D. Elias, L. S. Ullrich, J. J. Hay, I. L. Paraiso, J. Choi, R. L. Reed, J. S. Revel, C. Kioussi, G. Bobe, U. T. Iwaniec, R. T. Turner, B. S. Katzenellenbogen, J. A. Katzenellenbogen, P. R. Blakemore, A. F. Gombart, C. S. Maier, J. Raber, J. F. Stevens, *Sci. Rep.* **2018**, *8*, 613.
[25] J. Grafeneder, U. Derhaschnig, F. Eskandary, N. Buchtele, N. Sus, J. Frank, B. Jilma, C. Schoergenhofer, *Mol. Nutr. Food Res.* **2022**, *66*, e2200139.
[26] D. Kostrzewa, A. Dobrzyńska-Inger, E. Rój, *Fluid Phase Equilib.* **2013**, *360*, 445.
[27] L. Buckett, S. Schinko, C. Urmann, H. Riepl, M. Rychlik, *Front. Nutr.* **2020**, *7*, 619921.
[28] M. C. Chambers, B. Maclean, R. Burke, D. Amodei, D. L. Ruderman, S. Neumann, L. Gatto, B. Fischer, B. Pratt, J. Egertson, K. Hoff, D. Kessner, N. Tasman, N. Shulman, B. Frewen, T. A. Baker, M.-Y. Brusniak, C. Paulse, D. Creasy, L. Flashner, K. Kani, C. Moulding, S. L. Seymour, L. M. Nuwaysir, B. Lefebvre, F. Kuhlmann, J. Roark, P. Rainer, S. Detlev, T. Hemenway, et al., *Nat. Biotechnol.* **2012**, *30*, 918.
[29] J. Rainer, A. Vicini, L. Salzer, J. Stanstrup, J. M. Badia, S. Neumann, M. A. Stravs, V. Verri Hernandes, L. Gatto, S. Gibb, M. Witting, *Metabolites* **2022**, *12*.

5.6 Supplementary information. Manuscript III: The pharmacokinetics of individual conjugated xanthohumol metabolites show higher bioavailability of micellar than native xanthohumol in a randomized, double-blind, crossover trial in healthy humans [203].

Supplementary information

Identification of metabolites

Glucuronides

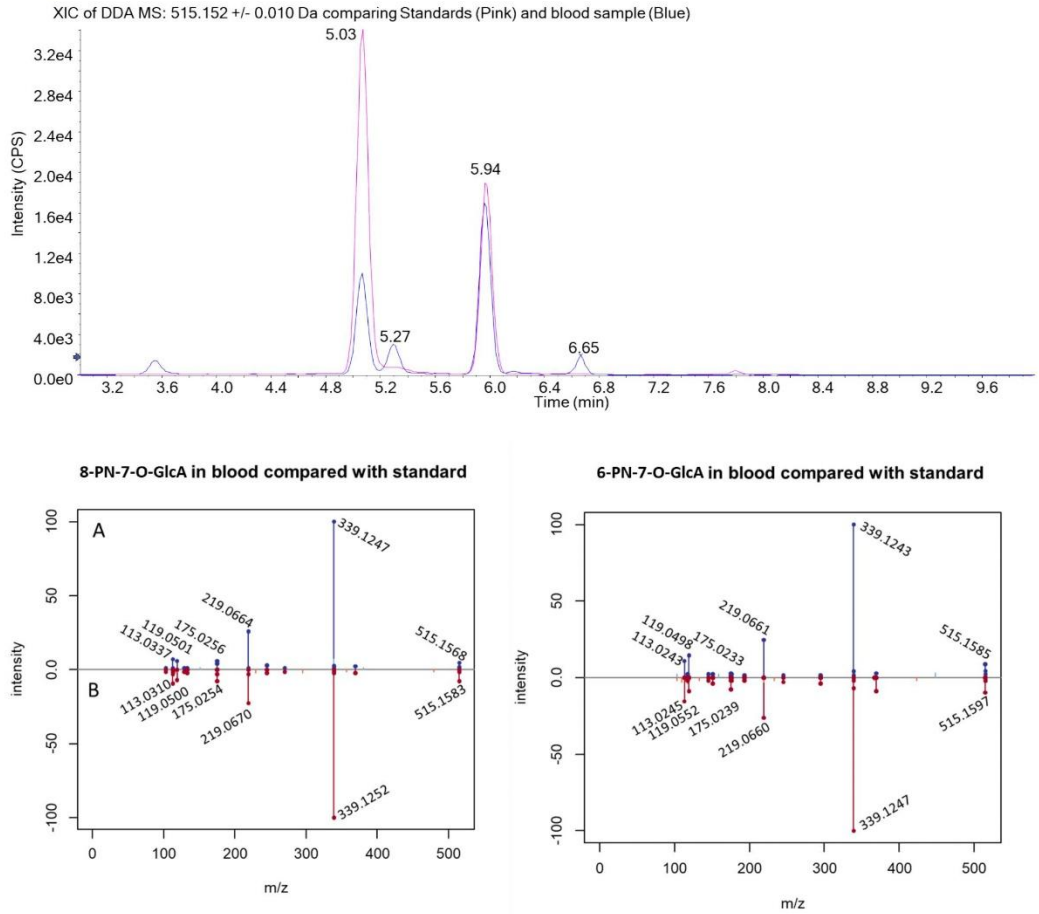

Figure 1. The identification of 8- and 6-PN-7-O-GlcA. The pink spectra are the reference compounds and the blue are a trace from the blood sample micellarised at T_{max} (60 min). Below is a mirror plot comparing the MS2 spectra of the blood with the standards (The retention time was matched).

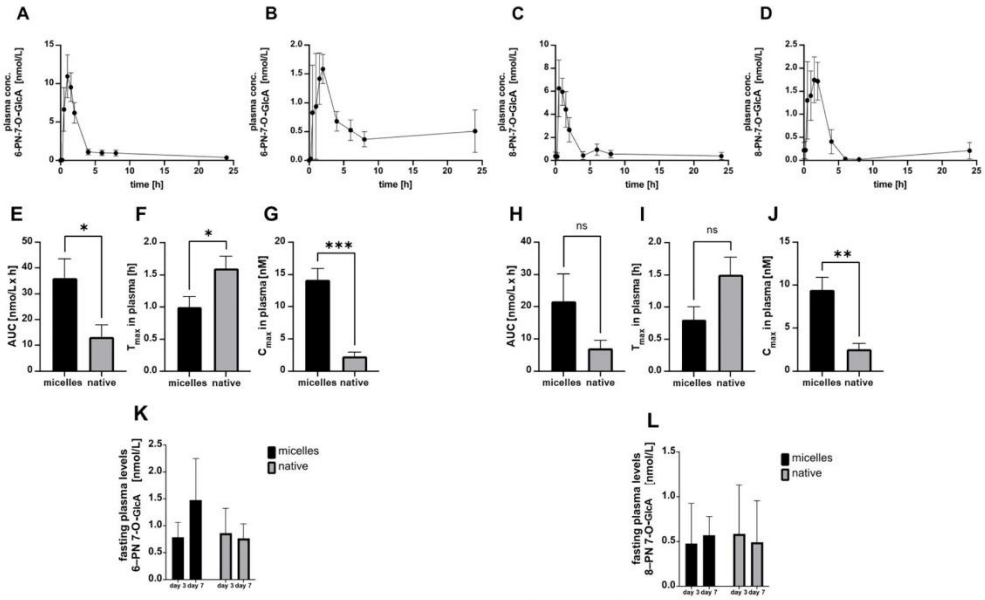

Figure 2. Plasma concentrations over time of 6-PN-7-O-GlcA following the ingestion of a single dose of 43 mg of micellar **(A)** or native XN **(B)**; Plasma concentrations over time of 8-PN-7-O-GlcA following the ingestion of a single dose of 43 mg of micellar **(C)** or native XN **(D)**; Mean (n=5) 6-PN-7-O-GlcA area under the plasma concentrations-time curve ($AUC_{0\text{-}24\ h}$) **(E),** 6-PN-7-O-GlcA T_{max} (**F**), 6-PN-7-O-GlcA C_{max} (**G**), Mean (n=5) 8-PN-7-O-GlcA area under the plasma concentrations-time curve ($AUC_{0\text{-}24\ h}$) **(H)** 8-PN-7-O-GlcA T_{max} (**I**), 8-PN-7-O-GlcA C_{max} (**J**), 6-PN-7-O-GlcA fasting levels comparing days of supplementation **(K),** 8-PN-7-O-GlcA fasting levels comparing days of supplementation **(L).** *significantly different at $P < 0.05$.

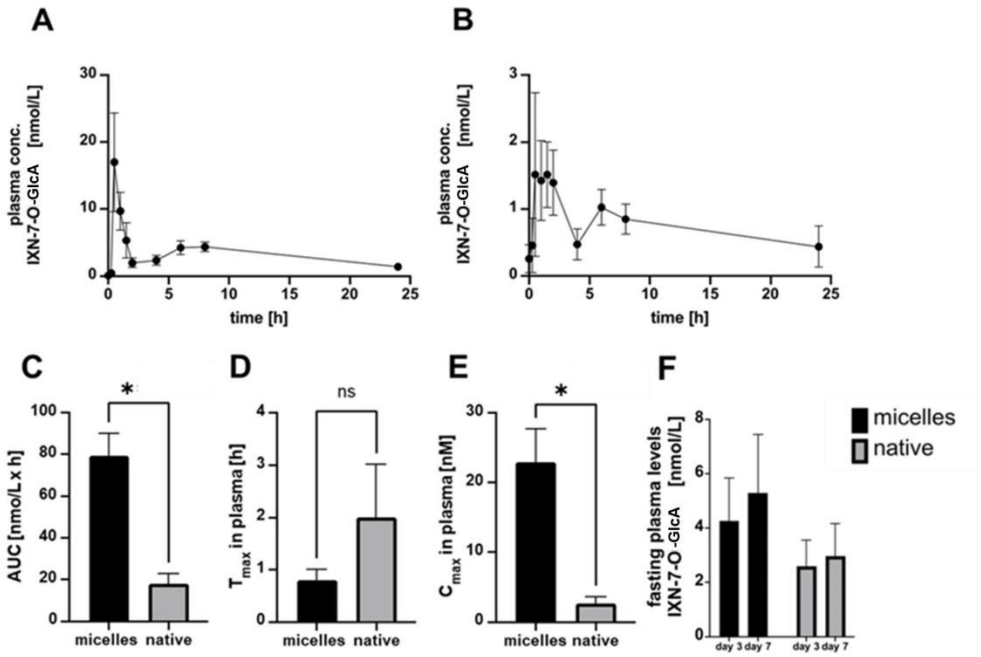

Figure 3: Plasma concentrations over time of IXN-7-O-GlcA following the ingestion of a single dose of 43 mg of micellar **(A)** or native xanthohumol **(B)**; Mean (n=5) IXN-7-O-GlcA area under the plasma concentrations-time curve ($AUC_{0\text{-}24\,h}$) **(C)**, T_{max} **(D)**, C_{max} **(E)**, Fasting levels comparing the micelles and native **(F)**. *significantly different at $P < 0.05$.

4'-O conjugated glucuronides

As no reference standards were available only MS2 spectra and retention time were used in the tentative identification.

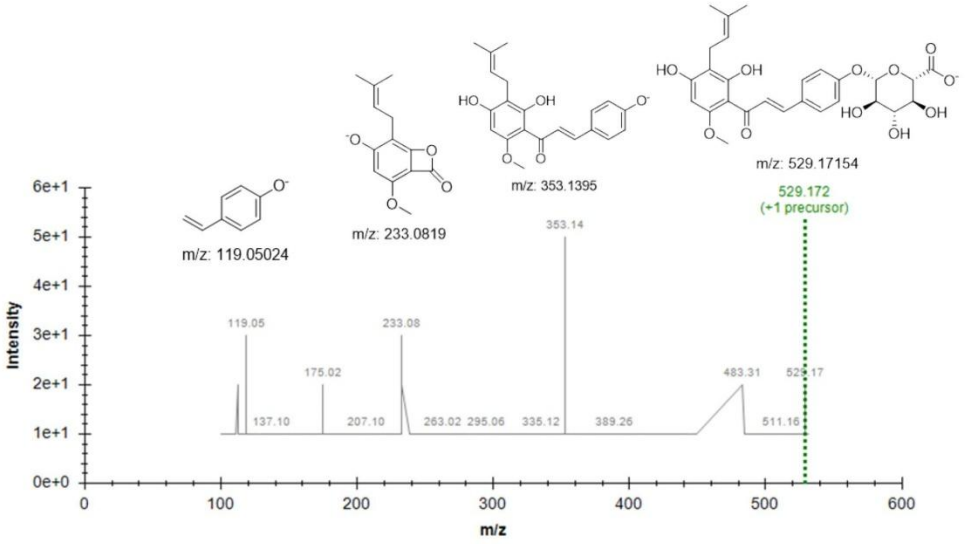

Figure 4: The MS2 of the tentatively annotated XN-4'O-GlcA found in blood plasma at retention time 6.9 min

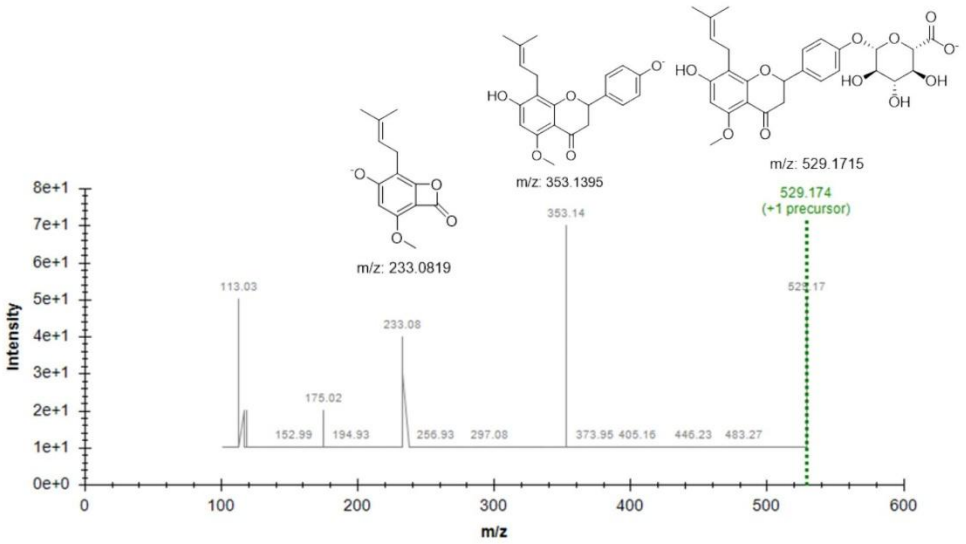

Figure 5: The MS2 of the tentatively annotated IXN-4'O-GlcA found in blood plasma at the retention time of 4.5 min

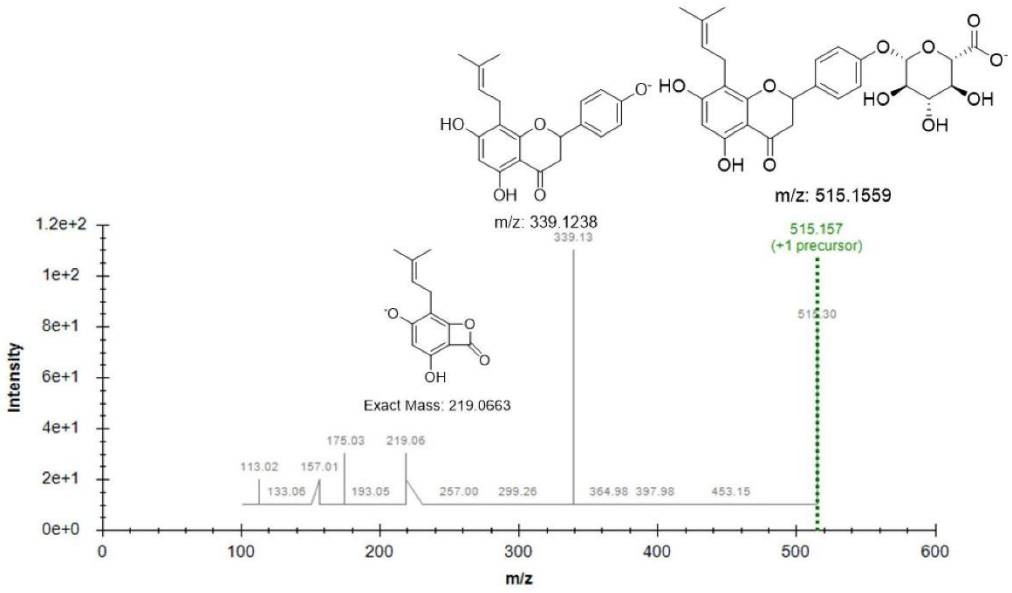

Figure 6. The MS2 of the tentatively annotated **(7.)** 8-PN-4'O-GlcA found in blood plasma at retention time of 5.3 min

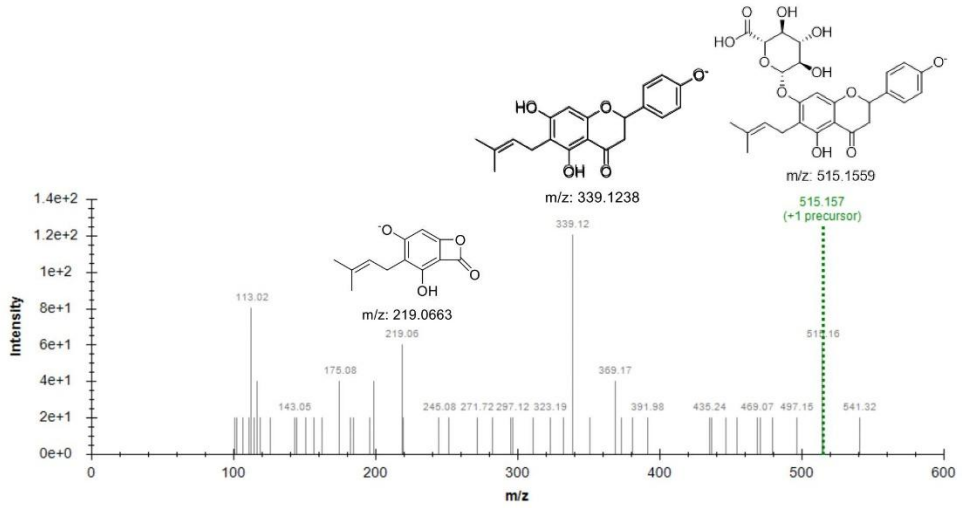

Figure 7: The MS2 of the tentatively annotated 6-PN-4'O-GlcA found in blood plasma at the retention time of 6.7 min

Sulfates

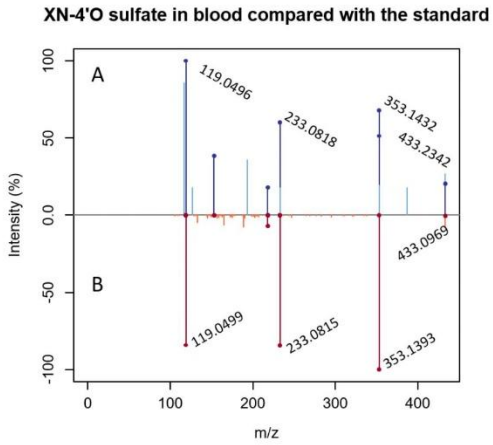

Figure 8: Mirror plot of XN-4'O-sulfate found in human plasma (blue) compared with the reference standard (red) at the retention time of 7.7 minutes

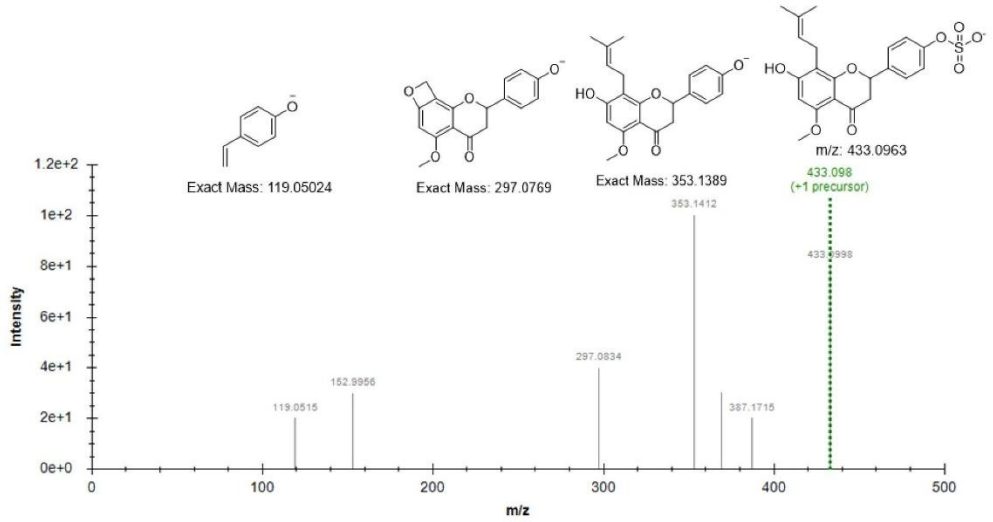

Figure 9: The MS2 spectra and proposed fragmentation of IXN-4'-O-sulfate at a retention time of 5.1 minutes.

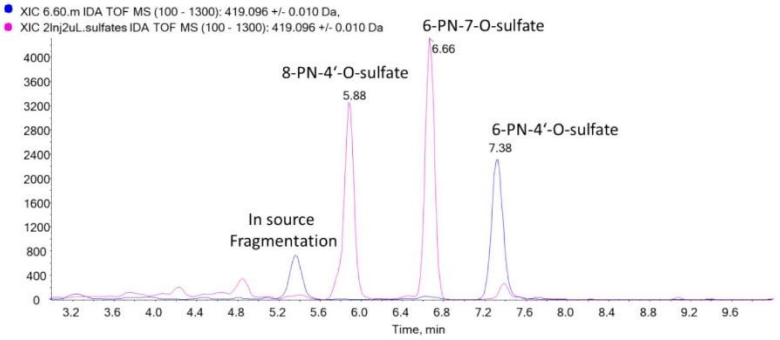

Figure 10: An extracted ion chromatogram of 419.0960 Da. Showing the reference standards (pink) and the human blood (blue)

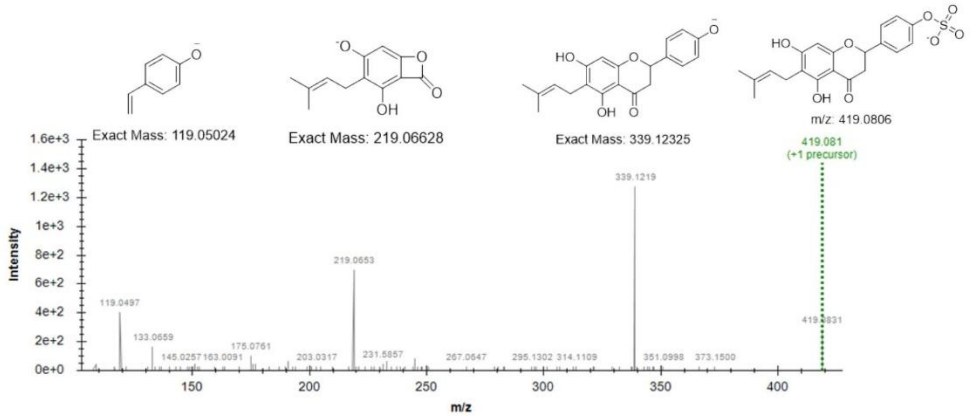

Figure 11: The MS2 spectra and proposed fragmentation of 6-PN-4'-O-sulfate at retention time of 7.38 minutes.

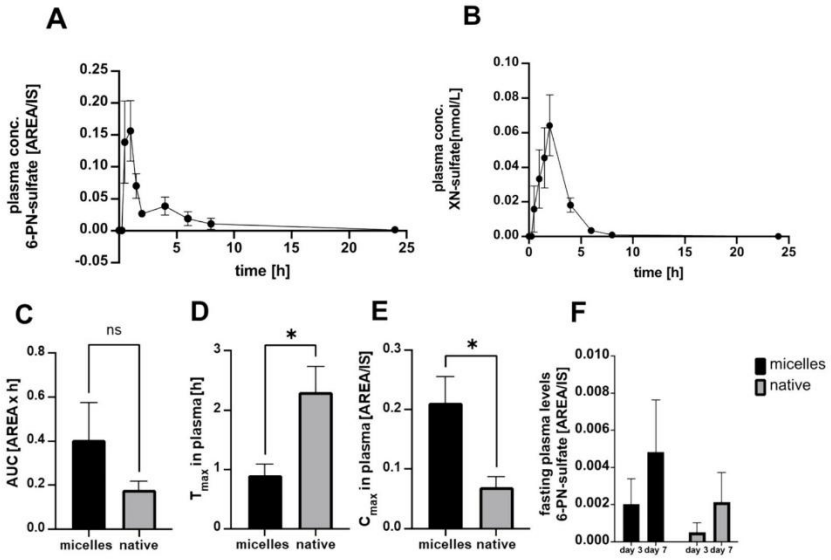

Figure 12: Plasma concentrations over time of 6-PN-4'-O-sulfate following the ingestion of a single dose of 43 mg of micellar **(A)** or native xanthohumol **(B)**; Mean (n=5) 6-PN-4'-O-sulfate area under the plasma concentrations-time curve ($AUC_{0\text{-}24\ h}$) **(C)**, T_{max} **(D)**, C_{max} **(E)**, Fasting levels comparing the micelles and native **(F)**. *significantly different at $P < 0.05$.

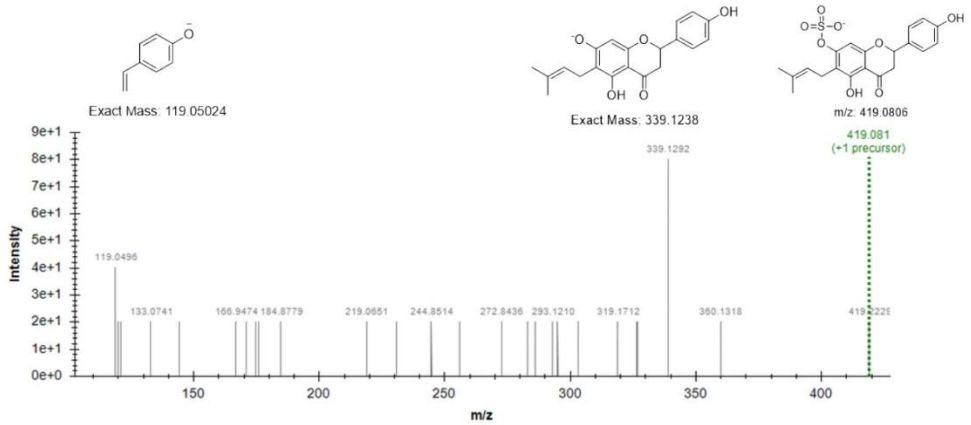

Figure 13: The MS2 spectra and proposed fragmentation of 6-PN-7-O-sulfate at retention time of 6.66 minutes.

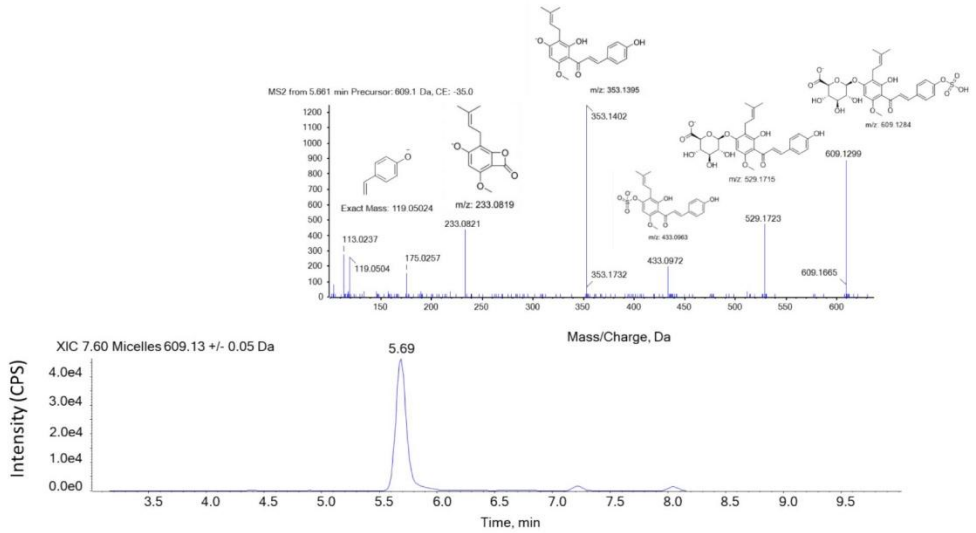

Figure 14:. The extracted ion chromatogram along with the MS2 of compound XN-sulfate-GlcA and the proposed fragmentation.

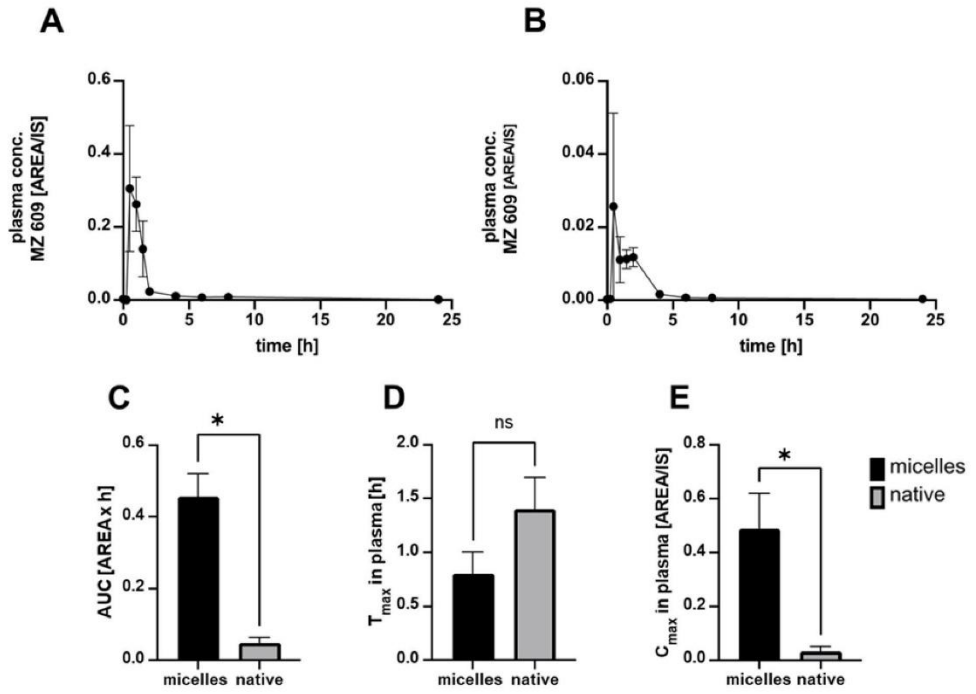

Figure 15: Plasma concentrations over time of XN-sulfate-GlcA following the ingestion of a single dose of 43 mg of micellar **(A)** or native XN **(B)**; Mean (n=5) XN-sulfate-GlcA area under the plasma concentrations-time curve ($AUC_{0\text{-}24\ h}$) **(C)**, T_{max} **(D)**, C_{max} **(E)**, Fasting levels comparing the micelles and native **(F)**. *significantly different at $P<0.05$.

The pharmacokinetics of **(20.)**. **A:** The pharmacokinetic profile for micelles. **B:** The pharmacokinetic profile for native. **C:** The $AUC_{0\text{-}24\ h}$ for the micelle and native. **D:** The T_{max} comparing the micelle and native. **E:** The C_{max} comparing the micelle and native. **F:** Fasting levels comparing days of supplementation. **E:** the C_{max} of the samples in plasma (qualitative).

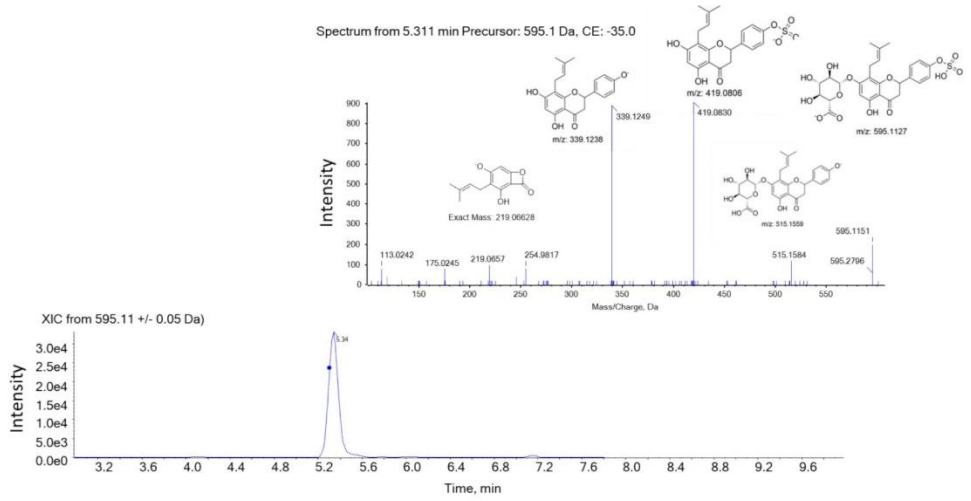

Figure 16: The extracted ion chromatogram along with the MS2 of compound 8/6-PN-sulfate-GlcA and the proposed fragmentation found at retention time of 5.3 min.

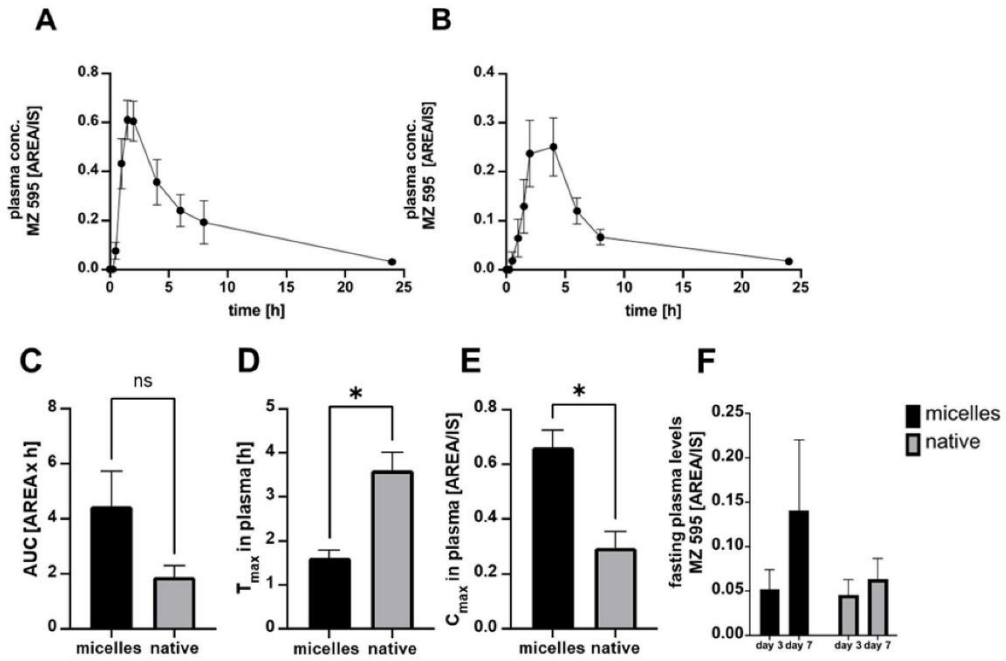

Figure 17: Plasma concentrations over time of 8/6-PN-sulfate-GlcA following the ingestion of a single dose of 43 mg of micellar **(A)** or native XN **(B)**; Mean (n=5) 8/6-PN-sulfate-GlcA area under the plasma concentrations-time curve ($AUC_{0\text{-}24\ h}$) **(C)**, T_{max} **(D)**, C_{max} **(E)**, Fasting levels comparing the micelles and native **(F)**. *significantly different at $P < 0.05$.

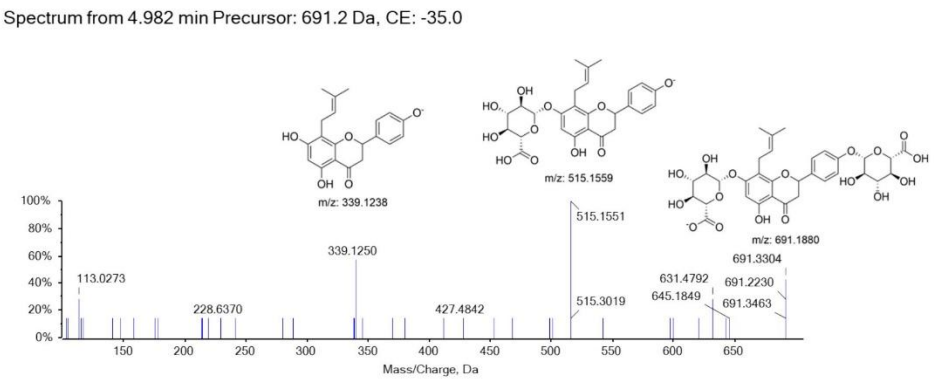

Figure 18: The MS2 of tentatively annotated 6/8-PN-di-GlcA and proposed fragmentation pattern found at RT 4.99 min.

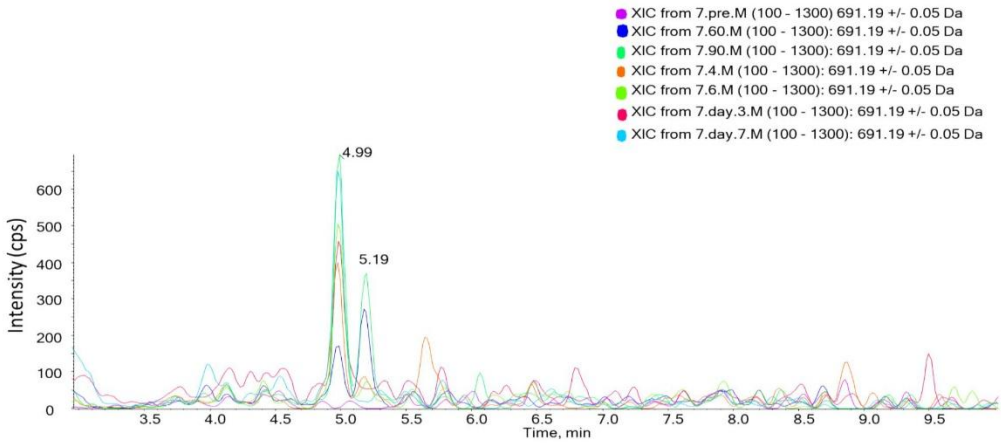

Figure 19: Extracted ion chromatogram of 691.19 Daltons from some samples at varying times from a participant. Suggesting that the T_{max} is 90 minutes after consumption. As this sample is near the cut-off for detection no pharmacokinetic data was calculated.

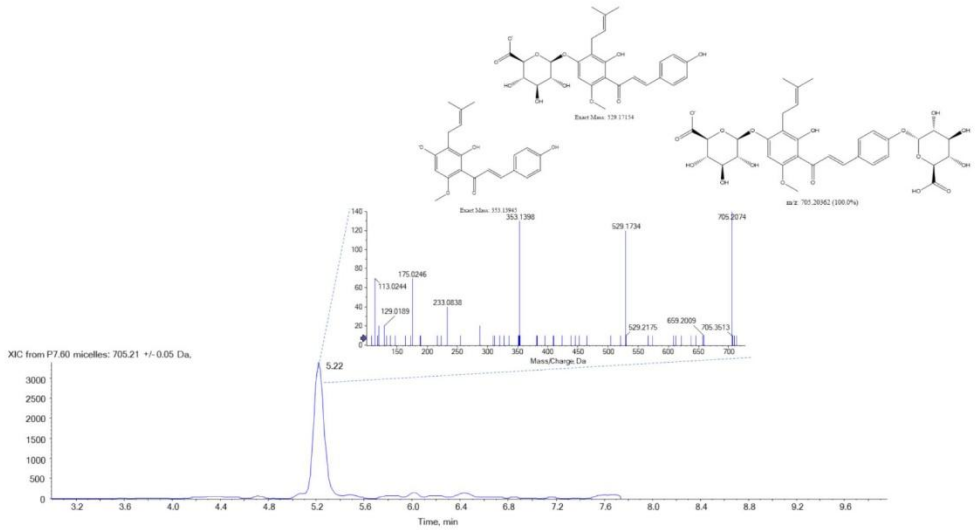

Figure 20: The LC chromatogram and MS2 spectra of an unknown metabolite that was tentatively denoted as XN-7,4'-O-di-GlcA. As the retention time is longer than IXN-7-O-GlcA it is thought that the metabolite found is in the chalcone configuration.

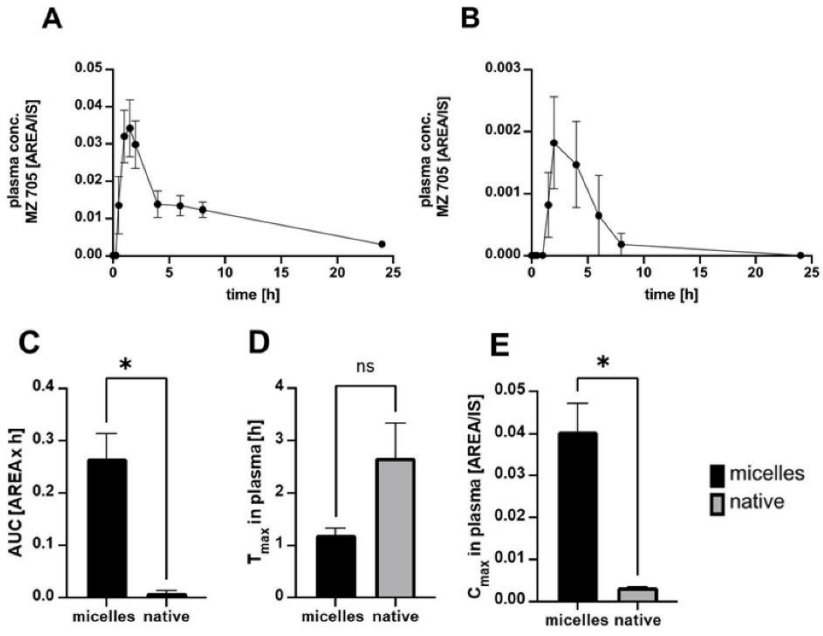

Figure 21: Plasma concentrations over time of Di-XN-GlcA following the ingestion of a single dose of 43 mg of micellar **(A)** or native XN **(B)**; Mean (n=5) Di-XN-GlcA area under the plasma concentrations-time curve ($AUC_{0\text{-}24\ h}$) **(C)**, T_{max} **(D)**, C_{max} **(E)**, Fasting levels comparing the micelles and native **(F)**. *significantly different at $P < 0.05$.

Unknown metabolites

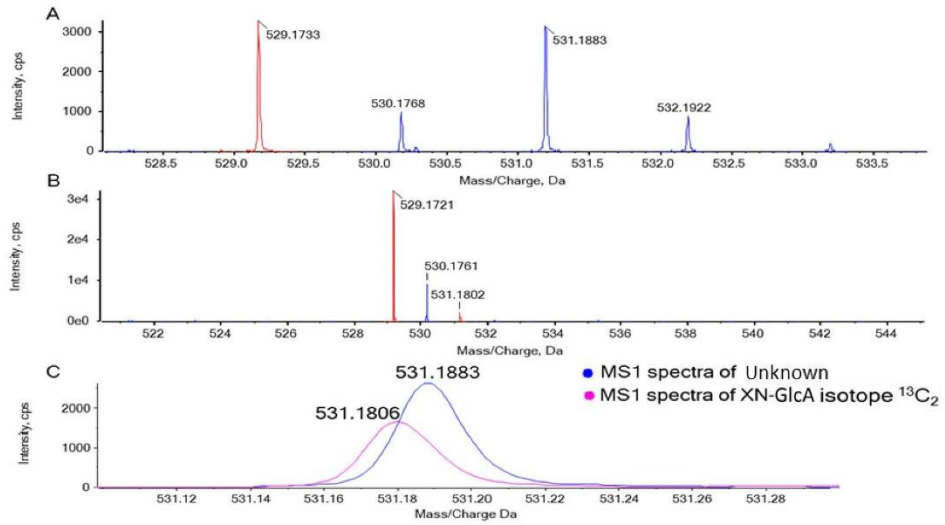

Figure 22: A: The MS1 between 4.291 to 4.396 min between 528 and 534 Daltons revealed an increased peak at 531.1883 Daltons with an intensity near 3000 CPS. B: MS1 from 6.400 to 6.505 min showing the natural isotope ratios for XN-7-O-GlcA. C: The MS1 of XN-7-O-GlcA 13C isotope and that of the unknown compound.

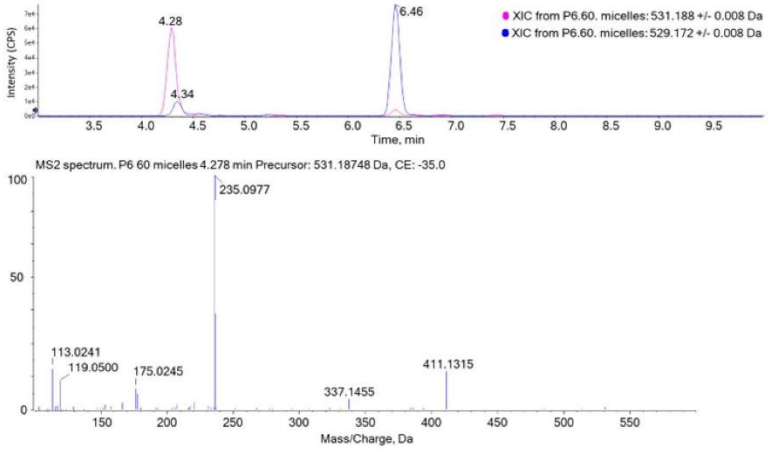

Figure 23: An extracted ion chromatogram (top) of 531.188 and 529.172 daltons revealing at around 4.3 min there are two compounds. The MS2 (bottom) of the unknown compound.

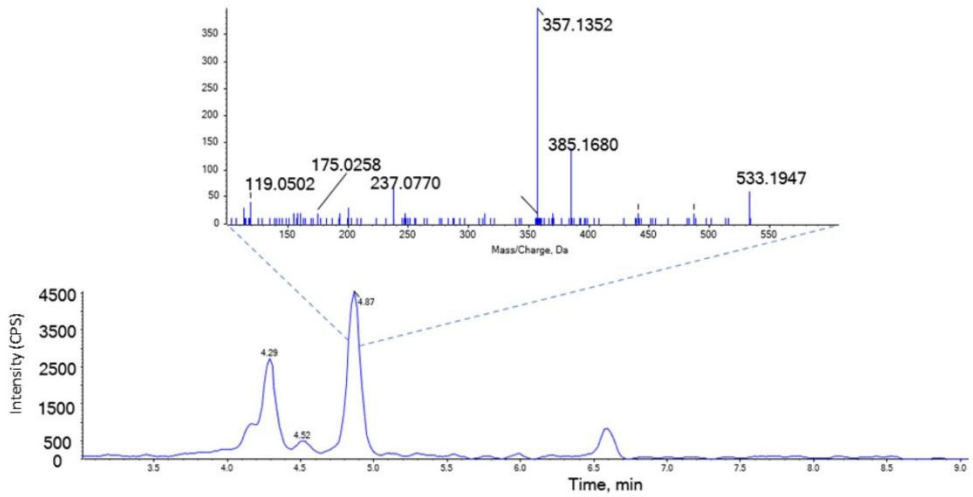

Figure 24: An extracted ion chromatogram from 533.1947 ± 0.001 Daltons showing the MS2 found at 4.87 min.

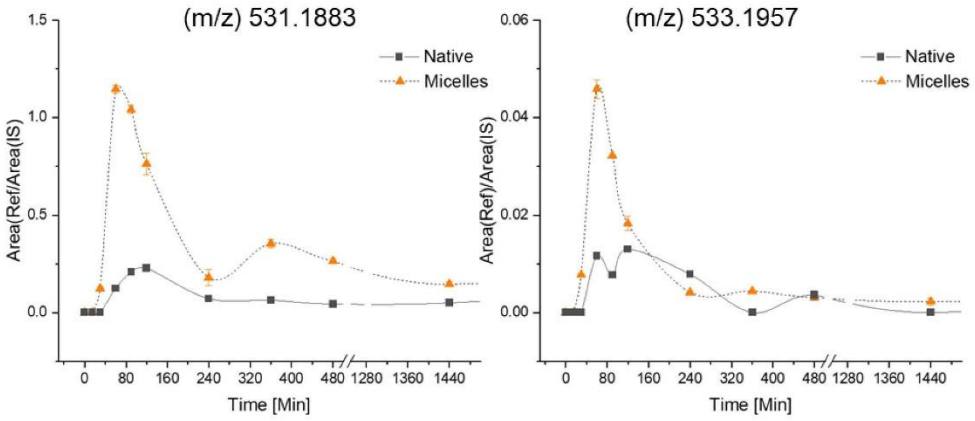

Figure 25: The Area ratio of unknown (m/z) 531.1883 and (m/z) 533.1957 with IXND in a participant.

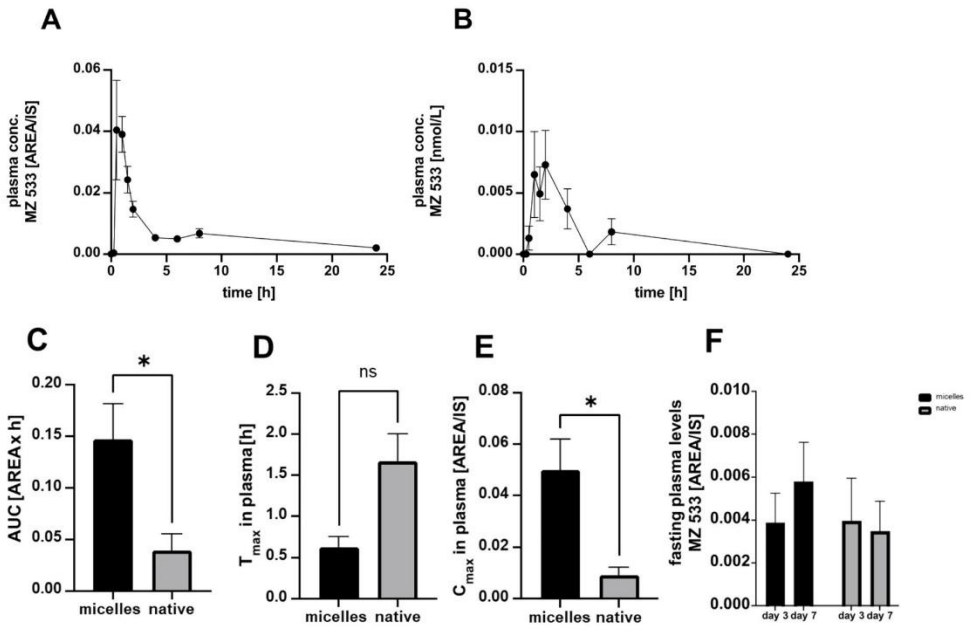

Figure 26: Plasma concentrations over time of (m/z) 533.1957 following the ingestion of a single dose of 43 mg of micellar **(A)** or native XN **(B)**; Mean (n=5) (m/z) 533.1957 area under the plasma concentrations-time curve ($AUC_{0\text{-}24\ h}$) **(C)**, T_{max} **(D)**, C_{max} **(E)**, Fasting levels comparing the micelles and native **(F)**. *significantly different at $P < 0.05$.

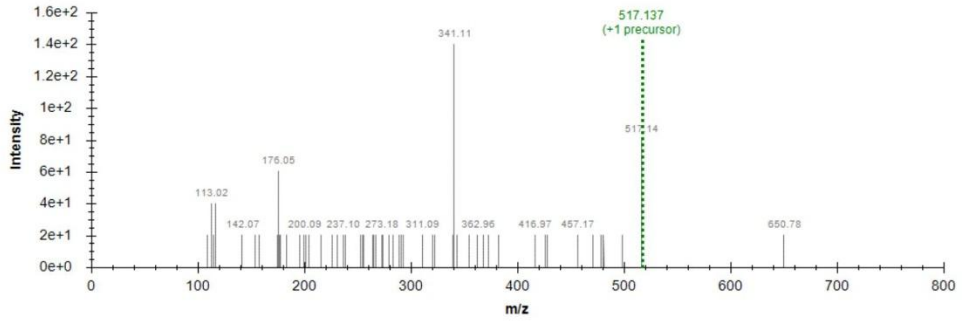

Figure 27: The MS2 of compound (m/z) 517.1365 was tentatively identified as a demethylated DXN-GlcA found at RT of 4.5 min.

Capsule

The liquid inside a capsule was diluted 100,000 times (serial dilution) and injected using the same method. Untargeted analysis revealed that none of the metabolites were found, although trace amounts of 8 and 6-prenylnaringenin were detected. Although, due to the amount of compared with XN it is assumed that they contributed little to the overall pool of 8-6-PN metabolites found and hence the metabolites were attributed from the transformation of XN. Based on the information the capsule

was 99% xanthohumol regarding its prenylated flavonoid content (AUC from each peak). An additional peak of desmethylxantohumol was tentatively detected.

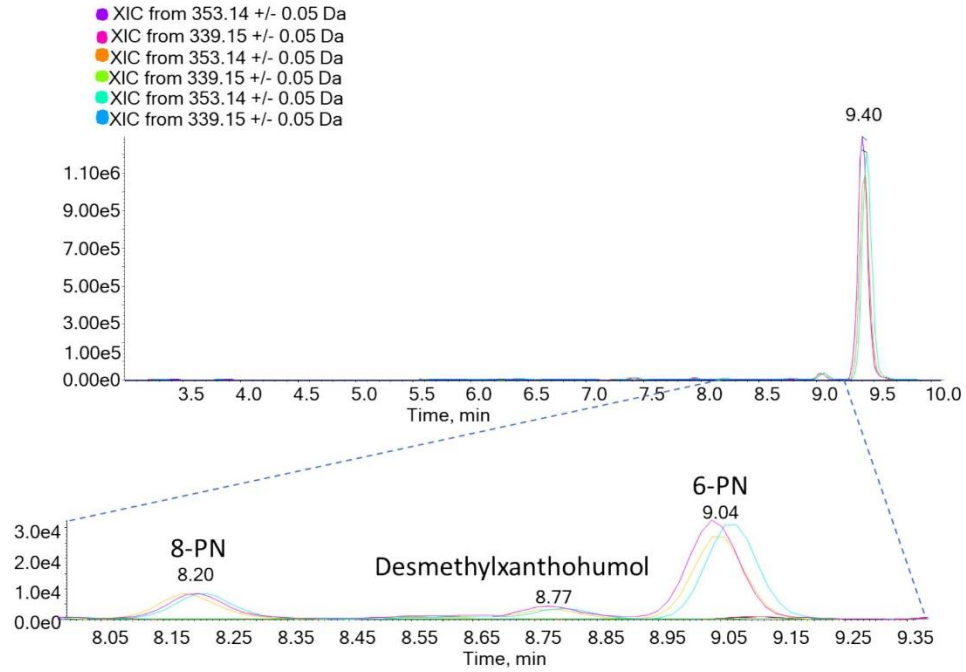

Figure 28: Extraction ion chromatograms of 353.14 and 339.15. (n = 3) Showing that the capsule is mainly composed of XN when searching for the mass of XN and 8-PN.

Calibration graphs

Calibration graphs from the resulting ratios of reference standard against the internal standard that eluted closest in retention time were constructed and linear regression was used in quantification of the found analytes.

Table 1. The internal standards and their corresponding reference compound that was used in quantification and semi-quantification (the reference m/z used +- 0.05).

IXND (357.1972)	**6-PND (343.1474)**	**XN-D (356.1577)**
IXN-7-O-GlcA (529.1702)	XN-7-O-GlcA (529.1737)	XN (353.1386)
6-PN-7-O-GlcA (515.1574)	XN-4'O-sulfate (433.0972)	-
8-PN-7-O-GlcA (515.1597)	-	-
IXN (353.1393)	-	-
6-PN-4'-O-sulfate (419.0801)	-	-
8/6-PN-sulfate-GlcA (595.1097)	-	-
XN-di-GlcA (705.2059)	-	-
(533.1660)	-	-
(531.2125)	-	

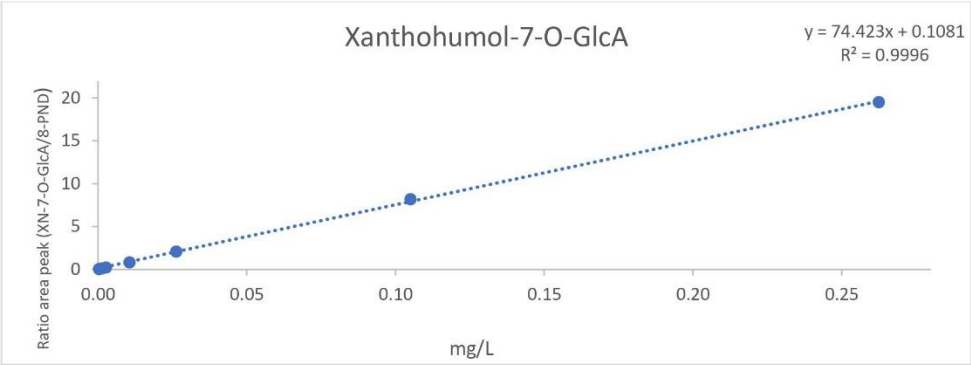

Figure 29: Calibration of XN-7-O-GlcA.

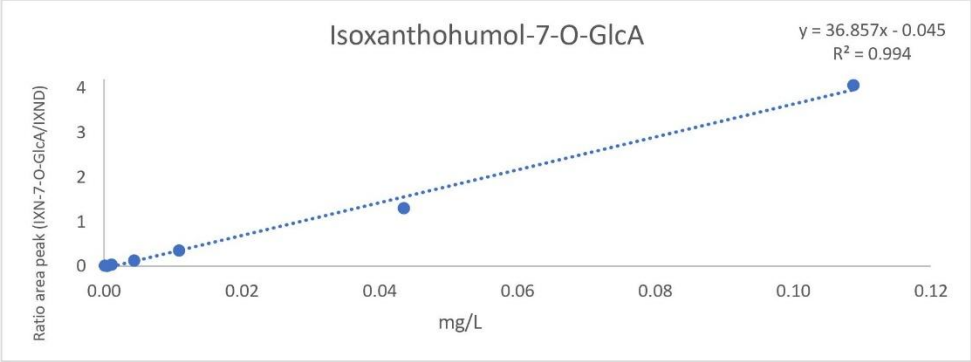

Figure 30: Calibration graph of IXN-7-O-GlcA.

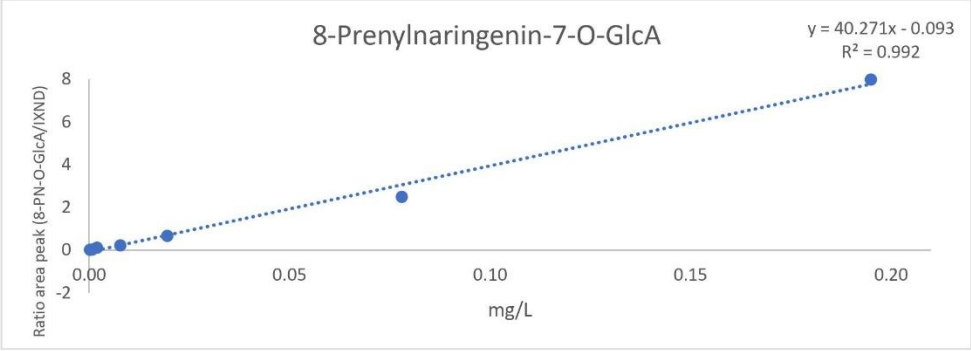

Figure 31: Calibration graph of 8-PN-7-O-GlcA.

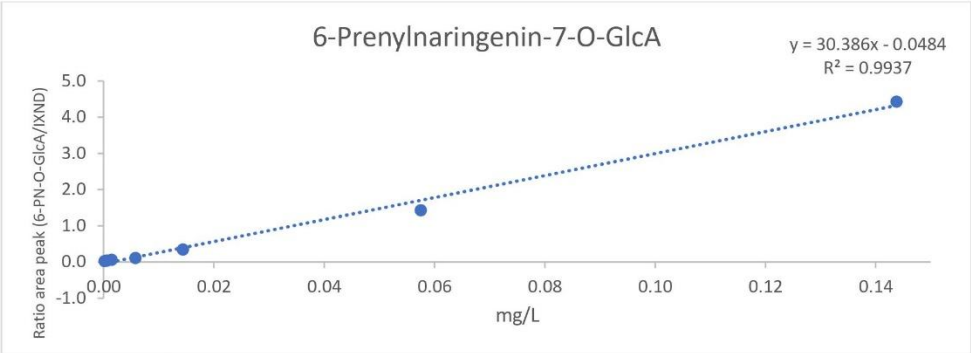

Figure 32: Calibration graph of 6-PN-7-O-GlcA

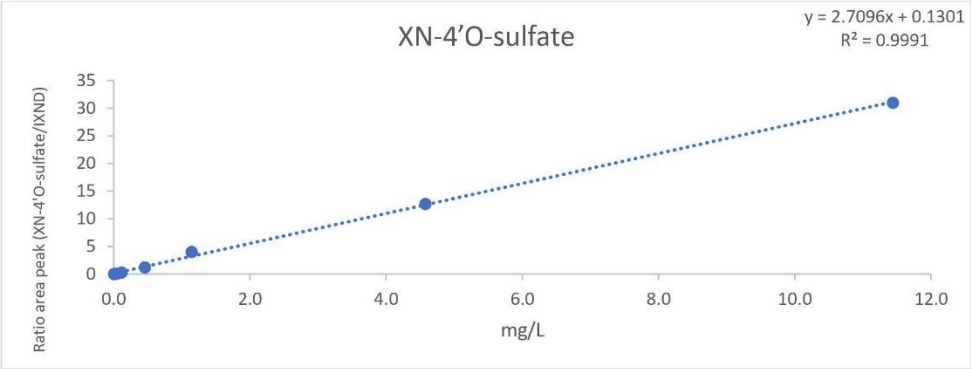

Figure 33: Calibration graph of XN-4'O-sulfate

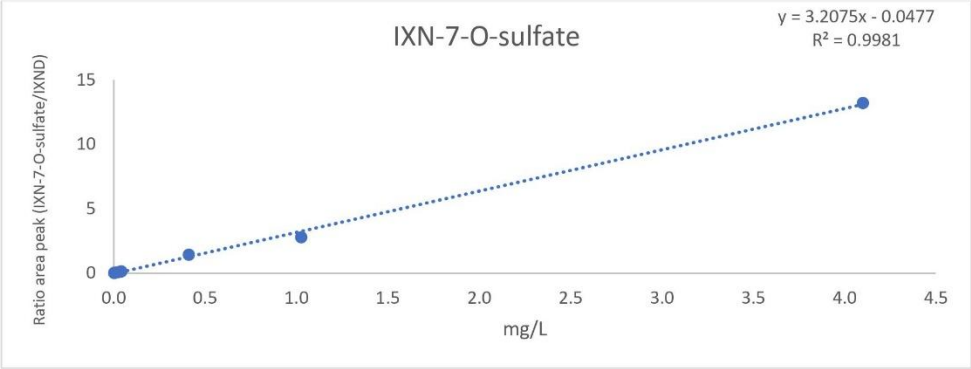

Figure 34: Calibration graph of IXN-7-O-sulfate. none was found in the plasma samples

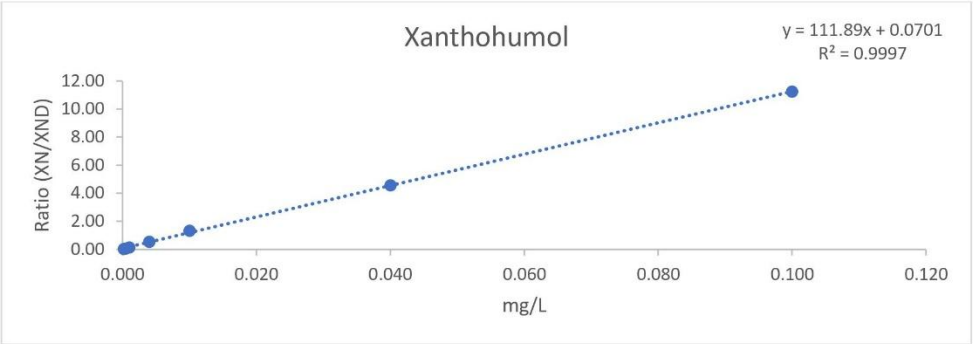

Figure 35: Calibration graph of XN

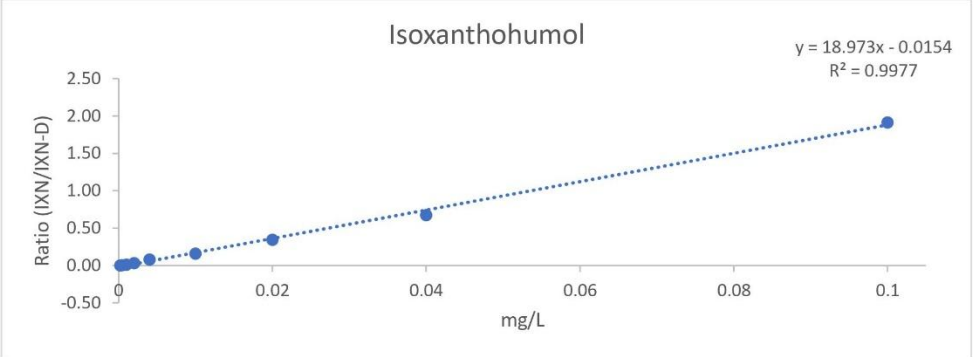

Figure 36: Calibration graph of IXN

6. References

1. Norn, S.; Permin, H.; Kruse, E.; Kruse, P. R., [Mercury--a major agent in the history of medicine and alchemy]. *Dan Medicinhist Arbog* **2008,** *36*, 21-40.
2. Garrett, R. H.; Grisham, C. M., *Biochemistry*. Cengage Learning: 2016.
3. Whitaker, T.; Dickens, J.; Monroe, R., Variability of aflatoxin test results. *Journal of the American Oil Chemists' Society* **1974,** *51* (5), 214-218.
4. Rychlik, M.; Asam, S., Stable isotope dilution assays in mycotoxin analysis. *Analytical and Bioanalytical Chemistry* **2008,** *390* (2), 617-628.
5. Stumpf, W. E., The dose makes the medicine. *Drug Discov Today* **2006,** *11* (11-12), 550-5.
6. Stevens, J. F.; Page, J. E., Xanthohumol and related prenylflavonoids from hops and beer: to your good health! *Phytochemistry* **2004,** *65* (10), 1317-1330.
7. Magalhães, P. J.; Carvalho, D. O.; Cruz, J. M.; Guido, L. F.; Barros, A. A., Fundamentals and Health Benefits of Xanthohumol, a Natural Product Derived from Hops and Beer. *Natural Product Communications* **2009,** *4* (5), 1934578X0900400501.
8. Friedman, R.; Sobel, D.; Myers, P.; Caudill, M.; Benson, H., Behavioral medicine, clinical health psychology, and cost offset. *Health psychology* **1995,** *14* (6), 509.
9. Baker, T. B.; McFall, R. M.; Shoham, V., Current Status and Future Prospects of Clinical Psychology:Toward a Scientifically Principled Approach to Mental and Behavioral Health Care. *Psychological Science in the Public Interest* **2008,** *9* (2), 67-103.
10. Vicente, A. M.; Ballensiefen, W.; Jönsson, J.-I., How personalised medicine will transform healthcare by 2030: the ICPerMed vision. *Journal of Translational Medicine* **2020,** *18* (1), 180.
11. Striegel, L.; Chebib, S.; Netzel, M. E.; Rychlik, M., Improved Stable Isotope Dilution Assay for Dietary Folates Using LC-MS/MS and Its Application to Strawberries. *Front Chem* **2018,** *6*, 11.
12. Lo, D. C.; Hughes, R. E., *Neurobiology of Huntington's Disease: Applications to Drug Discovery*. CRC Press: 2010.
13. Han, S.; Luo, Y.; Liu, B.; Guo, T.; Qin, D.; Luo, F., Dietary flavonoids prevent diabetes through epigenetic regulation: advance and challenge. *Critical Reviews in Food Science and Nutrition* **2022**, 1-17.
14. Downer, S.; Berkowitz, S. A.; Harlan, T. S.; Olstad, D. L.; Mozaffarian, D., Food is medicine: actions to integrate food and nutrition into healthcare. *BMJ* **2020,** *369*, m2482.
15. Funami, T., The Formulation Design of Elderly Special Diets. *Journal of Texture Studies* **2016,** *47* (4), 313-322.
16. Bin Rahman, A. N. M. R.; Zhang, J., Trends in rice research: 2030 and beyond. *Food and Energy Security* **2022,** *n/a* (n/a), e390.
17. Beyer, P., Golden Rice and 'Golden' crops for human nutrition. *New Biotechnology* **2010,** *27* (5), 478-481.
18. Winkelmann, L.; Schütze, M., Highly innovative products rich in xanthohumol. *Brauwelt International* **2004,** *5*, 300-301.
19. Ferk, F.; Mišík, M.; Nersesyan, A.; Pichler, C.; Jäger, W.; Szekeres, T.; Marculescu, R.; Poulsen, H. E.; Henriksen, T.; Bono, R.; Romanazzi, V.; Al-Serori, H.; Biendl, M.; Wagner, K.-H.; Kundi, M.; Knasmüller, S., Impact of xanthohumol (a prenylated flavonoid from hops) on DNA stability and other health-related biochemical parameters: Results of human intervention trials. *Molecular Nutrition & Food Research* **2016,** *60* (4), 773-786.
20. Poulsen, H. E.; Prieme, H.; Loft, S., Role of oxidative DNA damage in cancer initiation and promotion. *European Journal of Cancer Prevention* **1998,** *7* (1), 9-16.
21. EFSA Panel on Dietetic Products, N.; Allergies, Scientific Opinion on the substantiation of health claims related to various food(s)/food constituent(s) and protection of cells from premature ageing (ID 1668, 1917, 2515, 2527, 2530, 2575, 2580, 2591, 2620, 3178, 3179, 3180, 3181, 4329, 4415), antioxidant activity, antioxidant content and antioxidant properties (ID 857, 1306, 2515, 2527,

2530, 2575, 2580, 2591, 2629, 2728, 4327, 4365, 4380, 4390, 4394, 4455, 4464, 4507, 4694, 4705), protection of DNA, proteins and lipids from oxidative damage (ID 1196, 1211, 1216, 1306, 1312, 1440, 1441, 1666, 1668, 1692, 1900, 1914, 1948, 2023, 2158, 2517, 2522, 2527, 2575, 2591, 2620, 2637, 2639, 2663, 2860, 3079, 3276, 3564, 3818, 4324, 4329, 4351, 4397, 4416, 4424, 4507, 4527, 4528, 4542, 4611, 4629, 4659) and bioavailability of anthocyanins in black currants (ID 4220) pursuant to Article 13(1) of Regulation (EC) No 1924/2006. *EFSA Journal* **2010,** *8* (10), 1752.
22. Štern, A.; Furlan, V.; Novak, M.; Štampar, M.; Kolenc, Z.; Kores, K.; Filipič, M.; Bren, U.; Žegura, B., Chemoprotective Effects of Xanthohumol against the Carcinogenic Mycotoxin Aflatoxin B1. *Foods* **2021,** *10* (6), 1331.
23. Marcos, A.; Serra-Majem, L.; Pérez-Jiménez, F.; Pascual, V.; Tinahones, F. J.; Estruch, R., Moderate Consumption of Beer and Its Effects on Cardiovascular and Metabolic Health: An Updated Review of Recent Scientific Evidence. *Nutrients* **2021,** *13* (3), 879.
24. Morgan, S.; Grootendorst, P.; Lexchin, J.; Cunningham, C.; Greyson, D., The cost of drug development: A systematic review. *Health Policy* **2011,** *100* (1), 4-17.
25. Greenfield, D. P., Botanicals, Herbals, Nutraceuticals, and (Dietary) Supplements ("Natural Products"). In *Psychopharmacology for Nonpsychiatrists: A Primer*, Springer International Publishing: Cham, 2022; pp 101-107.
26. Mousavi Khaneghah, A.; Fakhri, Y.; Nematollahi, A.; Seilani, F.; Vasseghian, Y., The Concentration of Acrylamide in Different Food Products: A Global Systematic Review, Meta-Analysis, and Meta-Regression. *Food Reviews International* **2022,** *38* (6), 1286-1304.
27. Mesias, M.; Delgado-Andrade, C.; Holgado, F.; Morales, F. J., Acrylamide content in French fries prepared in food service establishments. *LWT* **2019,** *100*, 83-91.
28. Castaldo, L.; Narváez, A.; Izzo, L.; Graziani, G.; Gaspari, A.; Di Minno, G.; Ritieni, A., Red Wine Consumption and Cardiovascular Health. *Molecules* **2019,** *24* (19), 3626.
29. Boronat, A.; Soldevila-Domenech, N.; Rodríguez-Morató, J.; Martínez-Huélamo, M.; Lamuela-Raventós, R. M.; de la Torre, R., Beer Phenolic Composition of Simple Phenols, Prenylated Flavonoids and Alkylresorcinols. *Molecules* **2020,** *25* (11), 2582.
30. Pinto, C.; Cestero, J. J.; Galdón, B.; Macias, P., Xanthohumol, a prenylated flavonoid from hops (Humulus lupulus L.), protects rat tissues against oxidative damage after acute ethanol administration. *Toxicology Reports* **2014,** *1*.
31. Stanley, L. A., Chapter 27 - Drug Metabolism. In *Pharmacognosy*, Badal, S.; Delgoda, R., Eds. Academic Press: Boston, 2017; pp 527-545.
32. Zamboni, N.; Saghatelian, A.; Patti, Gary J., Defining the Metabolome: Size, Flux, and Regulation. *Molecular Cell* **2015,** *58* (4), 699-706.
33. Guo, Y.; Niu, K.; Momma, H.; Kobayashi, Y.; Chujo, M.; Otomo, A.; Fukudo, S.; Nagatomi, R., Irritable Bowel Syndrome Is Positively Related to Metabolic Syndrome: A Population-Based Cross-Sectional Study. *PLOS ONE* **2014,** *9* (11), e112289.
34. Mielko, K. A.; Jabłoński, S. J.; Łukaszewicz, M.; Młynarz, P., Comparison of bacteria disintegration methods and their influence on data analysis in metabolomics. *Scientific Reports* **2021,** *11* (1), 20859.
35. Hammerer, L.; Winkler, C. K.; Kroutil, W., Regioselective Biocatalytic Hydroxylation of Fatty Acids by Cytochrome P450s. *Catalysis Letters* **2018,** *148* (3), 787-812.
36. Shankar, K.; Mehendale, H. M., Cytochrome P450. In *Encyclopedia of Toxicology (Third Edition)*, Wexler, P., Ed. Academic Press: Oxford, 2014; pp 1125-1127.
37. Xu, C.; Li, C. Y.; Kong, A. N., Induction of phase I, II and III drug metabolism/transport by xenobiotics. *Arch Pharm Res* **2005,** *28* (3), 249-68.
38. Quintanilha, J. C. F.; de Sousa, V. M.; Visacri, M. B.; Amaral, L. S.; Santos, R. M. M.; Zambrano, T.; Salazar, L. A.; Moriel, P., Involvement of cytochrome P450 in cisplatin treatment: implications for toxicity. *Cancer Chemotherapy and Pharmacology* **2017,** *80* (2), 223-233.
39. Belcher, J.; McLean, K. J.; Matthews, S.; Woodward, L. S.; Fisher, K.; Rigby, S. E. J.; Nelson, D. R.; Potts, D.; Baynham, M. T.; Parker, D. A.; Leys, D.; Munro, A. W., Structure and Biochemical Properties of the Alkene Producing Cytochrome P450 OleT_{JE}

(CYP152L1) from the Jeotgalicoccus sp. 8456 Bacterium *. *Journal of Biological Chemistry* **2014,** *289* (10), 6535-6550.
40. DeVore, N. M.; Meneely, K. M.; Bart, A. G.; Stephens, E. S.; Battaile, K. P.; Scott, E. E., Structural comparison of cytochromes P450 2A6, 2A13, and 2E1 with pilocarpine. *The FEBS Journal* **2012,** *279* (9), 1621-1631.
41. Oesch, F.; Herrero, M. E.; Hengstler, J. G.; Lohmann, M.; Arand, M., Metabolic Detoxification: Implications for Thresholds. *Toxicologic Pathology* **2000,** *28* (3), 382-387.
42. Orzechowski, A.; Schrenk, D.; Bock, W., Metabolism of 1- and 2-naphthylamine in isolated rat hepatocytes. *Carcinogenesis* **1992,** *13* (12), 2227-2232.
43. Preuss, R.; Angerer, J.; Drexler, H., Naphthalene—an environmental and occupational toxicant. *International Archives of Occupational and Environmental Health* **2003,** *76* (8), 556-576.
44. Mytilineou, C.; Kramer, B. C.; Yabut, J. A., Glutathione depletion and oxidative stress. *Parkinsonism & Related Disorders* **2002,** *8* (6), 385-387.
45. Nikolic, D.; Li, Y.; Chadwick, L. R.; Pauli, G. F.; van Breemen, R. B., Metabolism of xanthohumol and isoxanthohumol, prenylated flavonoids from hops (Humulus lupulus L.), by human liver microsomes. *Journal of Mass Spectrometry* **2005,** *40* (3), 289-299.
46. Hanske, L.; Loh, G.; Sczesny, S.; Blaut, M.; Braune, A., Recovery and metabolism of xanthohumol in germ-free and human microbiota-associated rats. *Molecular Nutrition & Food Research* **2010,** *54* (10), 1405-1413.
47. Guo, J.; Nikolic, D.; Chadwick, L. R.; Pauli, G. F.; van Breemen, R. B., Identification of Human Hepatic Cytochrome p450 Enzymes involved in the Metabolism of 8-Prenylnaringenin and Isoxanthohumol from hops (Humulus Lupulus L.). *Drug Metabolism and Disposition* **2006,** *34* (7), 1152-1159.
48. Nookandeh, A.; Frank, N.; Steiner, F.; Ellinger, R.; Schneider, B.; Gerhäuser, C.; Becker, H., Xanthohumol metabolites in faeces of rats. *Phytochemistry* **2004,** *65* (5), 561-570.
49. Henderson, M. C.; Miranda, C. L.; Stevens, J. F.; Deinzer, M. L.; Buhler, D. R., In vitro inhibition of human P450 enzymes by prenylated flavonoids from hops, Humulus lupulus. *Xenobiotica* **2000,** *30* (3), 235-251.
50. Herath, W.; Ferreira, D.; Khan, S. I.; Khan, I. A., Identification and biological activity of microbial metabolites of xanthohumol. *Chem Pharm Bull (Tokyo)* **2003,** *51* (11), 1237-40.
51. Deng Yong, T. Z., Sang Zhipeiqiang, Xiaoming Liu Qiang Flavone alkylamine compounds as well as preparation method and application thereof. 2013.
52. Langley, B. O.; Ryan, J. J.; Hanes, D.; Phipps, J.; Stack, E.; Metz, T. O.; Stevens, J. F.; Bradley, R., Xanthohumol Microbiome and Signature in Healthy Adults (the XMaS Trial): Safety and Tolerability Results of a Phase I Triple-Masked, Placebo-Controlled Clinical Trial. *Molecular Nutrition & Food Research* **2021,** *65* (8), 2001170.
53. Xu, Y.-J.; Pieters, L., Recent Developments in Antimalarial Natural Products Isolated from Medicinal Plants. *Mini reviews in medicinal chemistry* **2012,** *13*.
54. Chen, Y.; Zhao, Y. H.; Jia, X. B.; Hu, M., Intestinal Absorption Mechanisms of Prenylated Flavonoids Present in the Heat-Processed Epimedium koreanum Nakai (Yin Yanghuo). *Pharmaceutical Research* **2008,** *25* (9), 2190-2199.
55. Shrestha, B.; Reed, J. M.; Starks, P. T.; Kaufman, G. E.; Goldstone, J. V.; Roelke, M. E.; O'Brien, S. J.; Koepfli, K. P.; Frank, L. G.; Court, M. H., Evolution of a major drug metabolizing enzyme defect in the domestic cat and other felidae: phylogenetic timing and the role of hypercarnivory. *PLoS One* **2011,** *6* (3), e18046.
56. Roy-Chowdhury, J.; Roy-Chowdhury, N., 58 - Bilirubin Metabolism and Its Disorders. In *Zakim and Boyer's Hepatology (Seventh Edition)*, Sanyal, A. J.; Boyer, T. D.; Lindor, K. D.; Terrault, N. A., Eds. Elsevier: Philadelphia, 2018; pp 898-925.e8.
57. Ruefer, C. E.; Gerhäuser, C.; Frank, N.; Becker, H.; Kulling, S. E., In vitro phase II metabolism of xanthohumol by human UDP-glucuronosyltransferases and sulfotransferases. *Molecular Nutrition & Food Research* **2005,** *49* (9), 851-856.

58. Habig, W. H.; Pabst, M. J.; Jakoby, W. B., Glutathione S-Transferases: The First Enzymatic step in Mercapturic Acid Formation. *Journal of Biological Chemistry* **1974,** *249* (22), 7130-7139.
59. Han, F.; Xiao, Y.; Lee, I. S., Microbial Conjugation Studies of Licochalcones and Xanthohumol. *Int J Mol Sci* **2021,** *22* (13).
60. Macherey, A.-C.; Dansette, P. M., 32 - Chemical Mechanisms of Toxicity: Basic Knowledge for Designing Safer Drugs. In *The Practice of Medicinal Chemistry (Second Edition)*, Wermuth, C. G., Ed. Academic Press: London, 2003; pp 545-560.
61. Legette, L.; Karnpracha, C.; Reed, R. L.; Choi, J.; Bobe, G.; Christensen, J. M.; Rodriguez-Proteau, R.; Purnell, J. Q.; Stevens, J. F., Human pharmacokinetics of xanthohumol, an antihyperglycemic flavonoid from hops. *Molecular Nutrition & Food Research* **2014,** *58* (2), 248-255.
62. Yilmazer, M.; Stevens, J. F.; Buhler, D. R., In vitro glucuronidation of xanthohumol, a flavonoid in hop and beer, by rat and human liver microsomes. *FEBS Letters* **2001,** *491* (3), 252-256.
63. Tronina, T.; Bartmańska, A.; Milczarek, M.; Wietrzyk, J.; Popłoński, J.; Rój, E.; Huszcza, E., Antioxidant and antiproliferative activity of glycosides obtained by biotransformation of xanthohumol. *Bioorganic & Medicinal Chemistry Letters* **2013,** *23* (7), 1957-1960.
64. Yoshimura, M.; Sano, A.; Kamei, J.-i.; Obata, A., Identification and quantification of metabolites of orally administered naringenin chalcone in rats. *Journal of agricultural and food chemistry* **2009,** *57 14*, 6432-7.
65. Fang, J.-B.; Nikolić, D.; Lankin, D. C.; Simmler, C.; Chen, S.-N.; Ramos Alvarenga, R. F.; Liu, Y.; Pauli, G. F.; van Breemen, R. B., Formation of (2R)- and (2S)-8-Prenylnaringenin Glucuronides by Human UDP-Glucuronosyltransferases. *Journal of Agricultural and Food Chemistry* **2019,** *67* (42), 11650-11656.
66. Wang, L.; Hong, X.; Yao, Z.; Dai, Y.; Zhao, G.; Qin, Z.; Wu, B.; Gonzalez, F. J.; Yao, X., Glucuronidation of icaritin by human liver microsomes, human intestine microsomes and expressed UDP-glucuronosyltransferase enzymes: identification of UGT1A3, 1A9 and 2B7 as the main contributing enzymes. *Xenobiotica* **2018,** *48* (4), 357-367.
67. Li, J.-j.; Zhang, X.; Shen, X.-c.; Long, Q.-d.; Xu, C.-y.; Tan, C.-j.; Lin, Y., Phytochemistry and biological properties of isoprenoid flavonoids from Sophora flavescens Ait. *Fitoterapia* **2020,** *143*, 104556.
68. Ye, Z. J.; He, X. A.; Wu, J. P.; Li, J.; Chang, X. W.; Tan, J.; Lv, W. Y.; Zhu, H.; Sun, H. H.; Wang, W. X.; Chen, Z. H.; Zhu, G. Z.; Xu, K. P., New prenylflavonol glycosides with xanthine oxidase inhibitory activity from the leaves of Cyclocarya paliurus. *Bioorg Chem* **2020,** *101*, 104018.
69. Buckett, L.; Schönberger, S.; Spindler, V.; Sus, N.; Schoergenhofer, C.; Frank, J.; Frank, O.; Rychlik, M., Synthesis of Human Phase I and Phase II Metabolites of Hop (Humulus lupulus) Prenylated Flavonoids. *Metabolites* **2022,** *12* (4).
70. Ibrahim, A. K.; Radwan, M. M.; Ahmed, S. A.; Slade, D.; Ross, S. A.; ElSohly, M. A.; Khan, I. A., Microbial metabolism of cannflavin A and B isolated from Cannabis sativa. *Phytochemistry* **2010,** *71* (8-9), 1014-9.
71. Paraiso, I. L.; Tran, T. Q.; Magana, A. A.; Kundu, P.; Choi, J.; Maier, C. S.; Bobe, G.; Raber, J.; Kioussi, C.; Stevens, J. F., Xanthohumol ameliorates Diet-Induced Liver Dysfunction via Farnesoid X Receptor-Dependent and Independent Signaling. *Frontiers in Pharmacology* **2021,** *12*.
72. Döring, B.; Petzinger, E., Phase 0 and phase III transport in various organs: Combined concept of phases in xenobiotic transport and metabolism. *Drug Metabolism Reviews* **2014,** *46* (3), 261-282.
73. Redgrave, L. S.; Sutton, S. B.; Webber, M. A.; Piddock, L. J. V., Fluoroquinolone resistance: mechanisms, impact on bacteria, and role in evolutionary success. *Trends in Microbiology* **2014,** *22* (8), 438-445.
74. Terao, J.; Mukai, R., Prenylation modulates the bioavailability and bioaccumulation of dietary flavonoids. *Archives of Biochemistry and Biophysics* **2014,** *559*, 12-16.
75. Brand, W.; Schutte, M. E.; Williamson, G.; van Zanden, J. J.; Cnubben, N. H. P.; Groten, J. P.; van Bladeren, P. J.; Rietjens, I. M. C. M., Flavonoid-mediated inhibition of intestinal ABC

transporters may affect the oral bioavailability of drugs, food-borne toxic compounds and bioactive ingredients. *Biomedicine & Pharmacotherapy* **2006,** *60* (9), 508-519.
76. Kimura, Y.; Morita, S. Y.; Matsuo, M.; Ueda, K., Mechanism of multidrug recognition by MDR1/ABCB1. *Cancer Sci* **2007,** *98* (9), 1303-10.
77. Burley, S. K.; Bhikadiya, C.; Bi, C.; Bittrich, S.; Chen, L.; Crichlow, G. V.; Christie, C. H.; Dalenberg, K.; Di Costanzo, L.; Duarte, J. M.; Dutta, S.; Feng, Z.; Ganesan, S.; Goodsell, D. S.; Ghosh, S.; Green, R. K.; Guranović, V.; Guzenko, D.; Hudson, B. P.; Lawson, C. L.; Liang, Y.; Lowe, R.; Namkoong, H.; Peisach, E.; Persikova, I.; Randle, C.; Rose, A.; Rose, Y.; Sali, A.; Segura, J.; Sekharan, M.; Shao, C.; Tao, Y. P.; Voigt, M.; Westbrook, J. D.; Young, J. Y.; Zardecki, C.; Zhuravleva, M., RCSB Protein Data Bank: powerful new tools for exploring 3D structures of biological macromolecules for basic and applied research and education in fundamental biology, biomedicine, biotechnology, bioengineering and energy sciences. *Nucleic Acids Res* **2021,** *49* (D1), D437-d451.
78. Ghosh, A. K.; Thapa, R.; Hariani, H. N.; Volyanyuk, M.; Ogle, S. D.; Orloff, K. A.; Ankireddy, S.; Lai, K.; Žiniauskaitė, A.; Stubbs, E. B.; Kalesnykas, G.; Hakkarainen, J. J.; Langert, K. A.; Kaja, S., Poly(lactic-co-glycolic acid) Nanoparticles Encapsulating the Prenylated Flavonoid, Xanthohumol, Protect Corneal Epithelial Cells from Dry Eye Disease-Associated Oxidative Stress. *Pharmaceutics* **2021,** *13* (9), 1362.
79. Nabekura, T.; Hiroi, T.; Kawasaki, T.; Uwai, Y., Effects of natural nuclear factor-kappa B inhibitors on anticancer drug efflux transporter human P-glycoprotein. *Biomedicine & Pharmacotherapy* **2015,** *70*, 140-145.
80. Beckles, D. M.; Roessner, U., 5 - Plant metabolomics: Applications and opportunities for agricultural biotechnology. In *Plant Biotechnology and Agriculture*, Altman, A.; Hasegawa, P. M., Eds. Academic Press: San Diego, 2012; pp 67-81.
81. Tissier, A.; Ziegler, J.; Vogt, T., Specialized Plant Metabolites: Diversity and Biosynthesis. In *Ecological Biochemistry*, 2014; pp 14-37.
82. Harbourne, J.; Mabry, T.; Mabry, H., The flavonoids. London, New York: Chapmann & Hall: 1994.
83. Levisson, M.; Araya-Cloutier, C.; de Bruijn, W. J. C.; van der Heide, M.; Salvador López, J. M.; Daran, J.-M.; Vincken, J.-P.; Beekwilder, J., Toward Developing a Yeast Cell Factory for the Production of Prenylated Flavonoids. *Journal of Agricultural and Food Chemistry* **2019,** *67* (49), 13478-13486.
84. Nagel, J.; Culley, L. K.; Lu, Y.; Liu, E.; Matthews, P. D.; Stevens, J. F.; Page, J. E., EST Analysis of Hop Glandular Trichomes Identifies an O-Methyltransferase That Catalyzes the Biosynthesis of Xanthohumol. *The Plant Cell* **2008,** *20* (1), 186-200.
85. Tsurumaru, Y.; Sasaki, K.; Miyawaki, T.; Uto, Y.; Momma, T.; Umemoto, N.; Momose, M.; Yazaki, K., HlPT-1, a membrane-bound prenyltransferase responsible for the biosynthesis of bitter acids in hops. *Biochemical and Biophysical Research Communications* **2012,** *417* (1), 393-398.
86. Montaño López, J.; Avalos, J. L., Genetically engineered yeast makes medicinal plant products. Nature Publishing Group: 2020.
87. Chajra, H.; Salwinski, A.; Guillaumin, A.; Mignard, B.; Hannewald, P.; Duriot, L.; Warnault, P.; Guillet-Claude, C.; Fréchet, M.; Bourgaud, F., Plant Milking Technology—An Innovative and Sustainable Process to Produce Highly Active Extracts from Plant Roots. *Molecules* **2020,** *25* (18), 4162.
88. Mobh, S., Research For Vitamin P. *The Journal of Biochemistry* **1939,** *29* (3), 487-501.
89. Robertson, N. U.; Schoonees, A.; Brand, A.; Visser, J., Pine bark (Pinus spp.) extract for treating chronic disorders. *Cochrane Database of Systematic Reviews* **2020,** (9).
90. Galeotti, F.; Barile, E.; Curir, P.; Dolci, M.; Lanzotti, V., Flavonoids from carnation (Dianthus caryophyllus) and their antifungal activity. *Phytochemistry Letters* **2008,** *1* (1), 44-48.

91. Brodziak-Jarosz, L.; Fujikawa, Y.; Pastor Flores, D.; Kasikci, S.; Jirásek, P.; Pitzl, S.; Owen, R.; Gerhäuser, C.; Amslinger, S.; Dick, T., A click chemistry approach identifies target proteins of xanthohumol. *Molecular nutrition & food research* **2016,** *60*.
92. Chun, O. K.; Chung, S. J.; Song, W. O., Estimated Dietary Flavonoid Intake and Major Food Sources of U.S. Adults. *The Journal of Nutrition* **2007,** *137* (5), 1244-1252.
93. Vogiatzoglou, A.; Mulligan, A. A.; Lentjes, M. A. H.; Luben, R. N.; Spencer, J. P. E.; Schroeter, H.; Khaw, K.-T.; Kuhnle, G. G. C., Flavonoid Intake in European Adults (18 to 64 Years). *PLOS ONE* **2015,** *10* (5), e0128132.
94. Buckett, L.; Schinko, S.; Urmann, C.; Riepl, H.; Rychlik, M., Stable Isotope Dilution Analysis of the Major Prenylated Flavonoids Found in Beer, Hop Tea, and Hops. *Front Nutr* **2020,** *7*, 619921.
95. Šmejkal, K., Cytotoxic potential of C-prenylated flavonoids. *Phytochemistry Reviews* **2014,** *13* (1), 245-275.
96. Boozari, M.; Soltani, S.; Iranshahi, M., Biologically active prenylated flavonoids from the genus Sophora and their structure–activity relationship—A review. *Phytotherapy Research* **2019,** *33* (3), 546-560.
97. Stompor, M.; Żarowska, B., Antimicrobial Activity of Xanthohumol and Its Selected Structural Analogues. *Molecules* **2016,** *21* (5), 608.
98. Chadwick, L. R.; Pauli, G. F.; Farnsworth, N. R., The pharmacognosy of Humulus lupulus L. (hops) with an emphasis on estrogenic properties. *Phytomedicine* **2006,** *13* (1), 119-131.
99. Fenselau, C.; Talalay, P., Is oestrogenic activity present in hops? *Food and Cosmetics Toxicology* **1973,** *11* (4), 597-603.
100. Milligan, S. R.; Kalita, J. C.; Heyerick, A.; Rong, H.; De Cooman, L.; De Keukeleire, D., Identification of a Potent Phytoestrogen in Hops (Humulus lupulus L.) and Beer. *The Journal of Clinical Endocrinology & Metabolism* **1999,** *84* (6), 2249-2249.
101. Rong, H.; Zhao, Y.; Lazou, K.; De Keukeleire, D.; Milligan, S. R.; Sandra, P., Quantitation of 8-prenylnaringenin, a novel phytoestrogen in hops (Humulus lupulus L.), hop products, and beers, by benchtop HPLC-MS using electrospray ionization. *Chromatographia* **2000,** *51* (9), 545-552.
102. Zhang, Y.; Bobe, G.; Revel, J. S.; Rodrigues, R. R.; Sharpton, T. J.; Fantacone, M. L.; Raslan, K.; Miranda, C. L.; Lowry, M. B.; Blakemore, P. R.; Morgun, A.; Shulzhenko, N.; Maier, C. S.; Stevens, J. F.; Gombart, A. F., Improvements in Metabolic Syndrome by Xanthohumol Derivatives Are Linked to Altered Gut Microbiota and Bile Acid Metabolism. *Molecular Nutrition & Food Research* **2020,** *64* (1), 1900789.
103. Zhang, X.-L.; Zhang, Y.-D.; Wang, T.; Guo, H.-Y.; Liu, Q.-M.; Su, H.-X., Evaluation on antioxidant effect of xanthohumol by different antioxidant capacity analytical methods. *Journal of Chemistry* **2014,** *2014*.
104. Khatib, N.; Varidi, M. J.; Mohebbi, M.; Varidi, M.; Hosseini, S. M. H., Replacement of nitrite with lupulon-xanthohumol loaded nanoliposome in cooked beef-sausage: experimental and model based study. *J Food Sci Technol* **2020,** *57* (7), 2629-2639.
105. Żołnierczyk, A. K.; Baczyńska, D.; Potaniec, B.; Kozłowska, J.; Grabarczyk, M.; Woźniak, E.; Anioł, M., Antiproliferative and antioxidant activity of xanthohumol acyl derivatives. *Medicinal Chemistry Research* **2017,** *26* (8), 1764-1771.
106. Wang, P.; Lindsey, J. S., Riley Oxidation of Heterocyclic Intermediates on Paths to Hydroporphyrins—A Review. *Molecules* **2020,** *25* (8), 1858.
107. Wongchum, N.; Dechakhamphu, A., Xanthohumol prolongs lifespan and decreases stress-induced mortality in Drosophila melanogaster. *Comparative Biochemistry and Physiology Part C: Toxicology & Pharmacology* **2021,** *244*, 108994.
108. Pinto, C.; Duque, A. L.; Rodríguez-Galdón, B.; Cestero, J. J.; Macías, P., Xanthohumol prevents carbon tetrachloride-induced acute liver injury in rats. *Food and Chemical Toxicology* **2012,** *50* (10), 3405-3412.
109. Rahman, S. U.; Ali, T.; Hao, Q.; He, K.; Li, W.; Ullah, N.; Zhang, Z.; Jiang, Y.; Li, S., Xanthohumol Attenuates Lipopolysaccharide-Induced Depressive Like Behavior in Mice:

Involvement of NF-κB/Nrf2 Signaling Pathways. *Neurochemical Research* **2021,** *46* (12), 3135-3148.
110. Bogdanova, K.; Röderova, M.; Kolar, M.; Langova, K.; Dusek, M.; Jost, P.; Kubelkova, K.; Bostik, P.; Olsovska, J., Antibiofilm activity of bioactive hop compounds humulone, lupulone and xanthohumol toward susceptible and resistant staphylococci. *Research in Microbiology* **2018,** *169* (3), 127-134.
111. Cermak, P.; Olsovska, J.; Mikyska, A.; Dusek, M.; Kadleckova, Z.; Vanicek, J.; Nyc, O.; Sigler, K.; Bostikova, V.; Bostik, P., Strong antimicrobial activity of xanthohumol and other derivatives from hops (Humulus lupulus L.) on gut anaerobic bacteria. *APMIS* **2017,** *125* (11), 1033-1038.
112. Bocquet, L.; Sahpaz, S.; Bonneau, N.; Beaufay, C.; Mahieux, S.; Samaillie, J.; Roumy, V.; Jacquin, J.; Bordage, S.; Hennebelle, T.; Chai, F.; Quetin-Leclercq, J.; Neut, C.; Rivière, C., Phenolic Compounds from Humulus lupulus as Natural Antimicrobial Products: New Weapons in the Fight against Methicillin Resistant Staphylococcus aureus, Leishmania mexicana and Trypanosoma brucei Strains. *Molecules* **2019,** *24* (6), 1024.
113. Kramer, B.; Thielmann, J.; Hickisch, A.; Muranyi, P.; Wunderlich, J.; Hauser, C., Antimicrobial activity of hop extracts against foodborne pathogens for meat applications. *Journal of Applied Microbiology* **2015,** *118* (3), 648-657.
114. Jung, F.; Staltner, R.; Tahir, A.; Baumann, A.; Burger, K.; Halilbasic, E.; Hellerbrand, C.; Bergheim, I., Oral intake of xanthohumol attenuates lipoteichoic acid-induced inflammatory response in human PBMCs. *European Journal of Nutrition* **2022**.
115. Stevens, J. F.; Revel, J. S., Xanthohumol, What a Delightful Problem Child! In *Advances in Plant Phenolics: From Chemistry to Human Health*, American Chemical Society: 2018; Vol. 1286, pp 283-304.
116. Wang, Q.; Ding, Z.-H.; Liu, J.-K.; Zheng, Y.-T., Xanthohumol, a novel anti-HIV-1 agent purified from Hops Humulus lupulus. *Antiviral Research* **2004,** *64* (3), 189-194.
117. Zhang, N.; Liu, Z.; Han, Q.; Chen, J.; Lv, Y., Xanthohumol enhances antiviral effect of interferon α-2b against bovine viral diarrhea virus, a surrogate of hepatitis C virus. *Phytomedicine* **2010,** *17* (5), 310-316.
118. Bartmańska, A.; Wałecka-Zacharska, E.; Tronina, T.; Popłoński, J.; Sordon, S.; Brzezowska, E.; Bania, J.; Huszcza, E., Antimicrobial Properties of Spent Hops Extracts, Flavonoids Isolated Therefrom, and Their Derivatives. *Molecules* **2018,** *23* (8), 2059.
119. Aydin, T.; Bayrak, N.; Baran, E.; Cakir, A., Insecticidal effects of extracts of Humulus lupulus (hops) L. cones and its principal component, xanthohumol. *Bulletin of Entomological Research* **2017,** *107* (4), 543-549.
120. Stompor, M.; Dancewicz, K.; Gabryś, B.; Anioł, M., Insect Antifeedant Potential of Xanthohumol, Isoxanthohumol, and Their Derivatives. *Journal of Agricultural and Food Chemistry* **2015,** *63* (30), 6749-6756.
121. Miranda, C. L.; Elias, V. D.; Hay, J. J.; Choi, J.; Reed, R. L.; Stevens, J. F., Xanthohumol improves dysfunctional glucose and lipid metabolism in diet-induced obese C57BL/6J mice. *Archives of Biochemistry and Biophysics* **2016,** *599*, 22-30.
122. Mahli, A.; Seitz, T.; Freese, K.; Frank, J.; Weiskirchen, R.; Abdel-Tawab, M.; Behnam, D.; Hellerbrand, C., Therapeutic Application of Micellar Solubilized Xanthohumol in a Western-Type Diet-Induced Mouse Model of Obesity, Diabetes and Non-Alcoholic Fatty Liver Disease. *Cells* **2019,** *8* (4), 359.
123. Smith, S. J.; Cases, S.; Jensen, D. R.; Chen, H. C.; Sande, E.; Tow, B.; Sanan, D. A.; Raber, J.; Eckel, R. H.; Farese, R. V., Obesity resistance and multiple mechanisms of triglyceride synthesis in mice lacking Dgat. *Nature Genetics* **2000,** *25* (1), 87-90.
124. Hirata, H.; Takazumi, K.; Segawa, S.; Okada, Y.; Kobayashi, N.; Shigyo, T.; Chiba, H., Xanthohumol, a prenylated chalcone from Humulus lupulus L., inhibits cholesteryl ester transfer protein. *Food Chemistry* **2012,** *134* (3), 1432-1437.

125. Paraiso, I. L.; Plagmann, L. S.; Yang, L.; Zielke, R.; Gombart, A. F.; Maier, C. S.; Sikora, A. E.; Blakemore, P. R.; Stevens, J. F., Reductive Metabolism of Xanthohumol and 8-Prenylnaringenin by the Intestinal Bacterium Eubacterium ramulus. *Mol Nutr Food Res* **2019,** *63* (2), e1800923.
126. Medicine, U. S. N. L. o. A Phase 2 Clinical Trial: Xanthohumol Metabolism and Signature (XMaS) in Crohn's Disease (XMaS). https://clinicaltrials.gov/ct2/show/NCT04590508 (accessed 23.08).
127. Girisa, S.; Saikia, Q.; Bordoloi, D.; Banik, K.; Monisha, J.; Daimary, U. D.; Verma, E.; Ahn, K. S.; Kunnumakkara, A. B., Xanthohumol from Hop: Hope for cancer prevention and treatment. *IUBMB Life* **2021,** *73* (8), 1016-1044.
128. Takezawa, K.; Okamoto, I.; Okamoto, W.; Takeda, M.; Sakai, K.; Tsukioka, S.; Kuwata, K.; Yamaguchi, H.; Nishio, K.; Nakagawa, K., Thymidylate synthase as a determinant of pemetrexed sensitivity in non-small cell lung cancer. *British Journal of Cancer* **2011,** *104* (10), 1594-1601.
129. Pritchard, K. I., Combining endocrine agents with chemotherapy: Which patients and what sequence? *Cancer* **2008,** *112* (S3), 718-722.
130. Dokduang, H.; Yongvanit, P.; Namwat, N.; Pairojkul, C.; Sangkhamanon, S.; Yageta, M.; Murakami, Y.; Loilome, W., Xanthohumol inhibits STAT3 activation pathway leading to growth suppression and apoptosis induction in human cholangiocarcinoma cells. *Oncology Reports* **2016,** *35*.
131. Lee, S. H.; Kim, H. J.; Lee, J. S.; Lee, I. S.; Kang, B. Y., Inhibition of topoisomerase I activity and efflux drug transporters' expression by xanthohumol. from hops. *Arch Pharm Res* **2007,** *30* (11), 1435-9.
132. Yong, W. K.; Ho, Y. F.; Malek, S. N., Xanthohumol induces apoptosis and S phase cell cycle arrest in A549 non-small cell lung cancer cells. *Pharmacogn Mag* **2015,** *11* (Suppl 2), S275-83.
133. Yang, X.; Jiang, Y.; Yang, J.; He, J.; Sun, J.; Chen, F.; Zhang, M.; Yang, B., Prenylated flavonoids, promising nutraceuticals with impressive biological activities. *Trends in Food Science & Technology* **2015,** *44* (1), 93-104.
134. Adamiak, K.; Sionkowska, A., The influence of UV irradiation on fish skin collagen films in the presence of xanthohumol and propanediol. *Spectrochimica Acta Part A: Molecular and Biomolecular Spectroscopy* **2022,** *282*, 121652.
135. Fournial, A. Cosmetic and topical use of xanthohumol including brightening skin complexion and reducing cutaneous redness. 2009.
136. Koo, J.-H.; Kim, H. T.; Yoon, H.-Y.; Kwon, K.-B.; Choi, I.-W.; Jung, S. H.; Kim, H.-U.; Park, B.-H.; Park, J.-W., Effect of xanthohumol on melanogenesis in B16 melanoma cells. *Experimental & Molecular Medicine* **2008,** *40* (3), 313-319.
137. Goenka, S.; Simon, S. R., Depigmenting effect of Xanthohumol from hop extract in MNT-1 human melanoma cells and normal human melanocytes. *Biochemistry and Biophysics Reports* **2021,** *26*, 100955.
138. Kanlayavattanakul, M.; Lourith, N., Therapeutic agents and herbs in topical application for acne treatment. *International Journal of Cosmetic Science* **2011,** *33* (4), 289-297.
139. Yamaguchi, N.; Satoh-Yamaguchi, K.; Ono, M., In vitro evaluation of antibacterial, anticollagenase, and antioxidant activities of hop components (Humulus lupulus) addressing acne vulgaris. *Phytomedicine* **2009,** *16* (4), 369-376.
140. Zheng, C.; Shao, W.; Chen, X.; Zhang, B.; Wang, G.; Zhang, W., Real-world effectiveness of COVID-19 vaccines: a literature review and meta-analysis. *International Journal of Infectious Diseases* **2022,** *114*, 252-260.
141. Chakraborty, C.; Bhattacharya, M.; Sharma, A. R., Emerging mutations in the SARS-CoV-2 variants and their role in antibody escape to small molecule-based therapeutic resistance. *Current Opinion in Pharmacology* **2022,** *62*, 64-73.
142. Syed, Y. Y., Molnupiravir: First Approval. *Drugs* **2022,** *82* (4), 455-460.

143. Jayk Bernal, A.; Gomes da Silva, M. M.; Musungaie, D. B.; Kovalchuk, E.; Gonzalez, A.; Delos Reyes, V.; Martín-Quirós, A.; Caraco, Y.; Williams-Diaz, A.; Brown, M. L.; Du, J.; Pedley, A.; Assaid, C.; Strizki, J.; Grobler, J. A.; Shamsuddin, H. H.; Tipping, R.; Wan, H.; Paschke, A.; Butterton, J. R.; Johnson, M. G.; De Anda, C., Molnupiravir for Oral Treatment of Covid-19 in Nonhospitalized Patients. *New England Journal of Medicine* **2021,** *386* (6), 509-520.
144. Gandhi, S.; Klein, J.; Robertson, A. J.; Peña-Hernández, M. A.; Lin, M. J.; Roychoudhury, P.; Lu, P.; Fournier, J.; Ferguson, D.; Mohamed Bakhash, S. A. K.; Catherine Muenker, M.; Srivathsan, A.; Wunder, E. A.; Kerantzas, N.; Wang, W.; Lindenbach, B.; Pyle, A.; Wilen, C. B.; Ogbuagu, O.; Greninger, A. L.; Iwasaki, A.; Schulz, W. L.; Ko, A. I., De novo emergence of a remdesivir resistance mutation during treatment of persistent SARS-CoV-2 infection in an immunocompromised patient: a case report. *Nature Communications* **2022,** *13* (1), 1547.
145. Lin, Y.; Zang, R.; Ma, Y.; Wang, Z.; Li, L.; Ding, S.; Zhang, R.; Wei, Z.; Yang, J.; Wang, X., Xanthohumol Is a Potent Pan-Inhibitor of Coronaviruses Targeting Main Protease. *International Journal of Molecular Sciences* **2021,** *22* (22), 12134.
146. Yuan, S.; Yan, B.; Cao, J.; Ye, Z.-W.; Liang, R.; Tang, K.; Luo, C.; Cai, J.; Chu, H.; Chung, T. W.-H.; To, K. K.-W.; Hung, I. F.-N.; Jin, D.-Y.; Chan, J. F.-W.; Yuen, K.-Y., SARS-CoV-2 exploits host DGAT and ADRP for efficient replication. *Cell Discovery* **2021,** *7* (1), 100.
147. Zeng, S.; Li, Y.; Zhu, W.; Luo, Z.; Wu, K.; Li, X.; Fang, Y.; Qin, Y.; Chen, W.; Li, Z.; Zou, L.; Liu, X.; Yi, L.; Fan, S., The Advances of Broad-Spectrum and Hot Anti-Coronavirus Drugs. *Microorganisms* **2022,** *10* (7), 1294.
148. Wang, J.; Zhang, X.; Omarini, A. B.; Li, B., Virtual screening for functional foods against the main protease of SARS-CoV-2. *Journal of Food Biochemistry* **2020,** *44* (11), e13481.
149. Stepulak, A. Xanthohumol as an Adjuvant Therapy in Critically Ill COVID-19 Patients. https://clinicaltrials.gov/ct2/show/NCT05463393?term=xanthohumol&draw=2&rank=1.
150. Boyd, R. K.; Basic, C.; Bethem, R. A., *Trace quantitative analysis by mass spectrometry*. John Wiley & Sons: 2011.
151. Nikolić, D.; van Breemen, R. B., Analytical methods for quantitation of prenylated flavonoids from hops. *Curr Anal Chem* **2013,** *9* (1), 71-85.
152. Kirkwood, J. S.; Legette, L. L.; Miranda, C. L.; Jiang, Y.; Stevens, J. F., A Metabolomics-driven Elucidation of the Anti-obesity Mechanisms of Xanthohumol *. *Journal of Biological Chemistry* **2013,** *288* (26), 19000-19013.
153. Vanhoecke, B.; Dolle, L.; Vercoutter-Edouart, A.; Antol, J.; Depypere, H.; Bracke, M., A proteomic approach to understand the anti-invasive and pro-apoptotic effect of xanthohumol in human breast cancer cells. *Molecular & Cellular Proteomics* **2005,** *4* (8), S57-S57.
154. Harikumar, K. B.; Kunnumakkara, A. B.; Ahn, K. S.; Anand, P.; Krishnan, S.; Guha, S.; Aggarwal, B. B., Modification of the cysteine residues in IκBα kinase and NF-κB (p65) by xanthohumol leads to suppression of NF-κB–regulated gene products and potentiation of apoptosis in leukemia cells. *Blood* **2009,** *113* (9), 2003-2013.
155. Roehrer, S.; Stork, V.; Ludwig, C.; Minceva, M.; Behr, J., Analyzing bioactive effects of the minor hop compound xanthohumol C on human breast cancer cells using quantitative proteomics. *Plos One* **2019,** *14* (3).
156. Huang, X.; Wang, J.; Chen, X.; Liu, P.; Wang, S.; Song, F.; Zhang, Z.; Zhu, F.; Huang, X.; Liu, J.; Song, G.; Spencer, P. S.; Yang, X., The Prenylflavonoid Xanthohumol Reduces Alzheimer-Like Changes and Modulates Multiple Pathogenic Molecular Pathways in the Neuro2a/APPswe Cell Model of AD. *Frontiers in Pharmacology* **2018,** *9*.
157. Rychlik, M.; Kanawati, B.; Roullier-Gall, C.; Hemmler, D.; Liu, Y. Z.; Alexandre, H.; Gougeon, R. D.; Gmelch, L.; Gotthardt, M.; Schmitt-Kopplin, P., *Foodomics assessed by Fourier transform mass spectrometry*. 2019; p 651-677.
158. Dresel, M.; Dunkel, A.; Hofmann, T., Sensomics Analysis of Key Bitter Compounds in the Hard Resin of Hops (Humulus lupulus L.) and Their Contribution to the Bitter Profile of Pilsner-Type Beer. *Journal of Agricultural and Food Chemistry* **2015,** *63* (13), 3402-3418.

159. Chadwick, L. R.; Nikolic, D.; Burdette, J. E.; Overk, C. R.; Bolton, J. L.; van Breemen, R. B.; Frohlich, R.; Fong, H. H. S.; Farnsworth, N. R.; Pauli, G. F., Estrogens and congeners from spent hops (Humulus lupulus). *Journal of Natural Products* **2004,** *67* (12), 2024-2032.
160. Wyns, C.; Derycke, L.; Soenen, B.; Bolca, S.; Deforce, D.; Bracke, M.; Heyerick, A., Production of monoclonal antibodies against hop-derived (Humulus lupulus L.) prenylflavonoids and the development of immunoassays. *Talanta* **2011,** *85* (1), 197-205.
161. Schaefer, O.; Bohlmann, R.; Schleuning, W. D.; Schulze-Forster, K.; Hümpel, M., Development of a radioimmunoassay for the quantitative determination of 8-prenylnaringenin in biological matrices. *J Agric Food Chem* **2005,** *53* (8), 2881-9.
162. Rad, M.; Hümpel, M.; Schaefer, O.; Schoemaker, R. C.; Schleuning, W. D.; Cohen, A. F.; Burggraaf, J., Pharmacokinetics and systemic endocrine effects of the phyto-oestrogen 8-prenylnaringenin after single oral doses to postmenopausal women. *Br J Clin Pharmacol* **2006,** *62* (3), 288-96.
163. Coldham, N. G.; Sauer, M. J., Identification, quantitation and biological activity of phytoestrogens in a dietary supplement for breast enhancement. *Food and Chemical Toxicology* **2001,** *39* (12), 1211-1224.
164. Češlová, L.; Holčapek, M.; Fidler, M.; Drštičková, J.; Lísa, M., Characterization of prenylflavonoids and hop bitter acids in various classes of Czech beers and hop extracts using high-performance liquid chromatography–mass spectrometry. *Journal of Chromatography A* **2009,** *1216* (43), 7249-7257.
165. Stevens, J. F.; Taylor, A. W.; Deinzer, M. L., Quantitative analysis of xanthohumol and related prenylflavonoids in hops and beer by liquid chromatography–tandem mass spectrometry. *Journal of Chromatography A* **1999,** *832* (1), 97-107.
166. Bolca, S.; Li, J.; Nikolic, D.; Roche, N.; Blondeel, P.; Possemiers, S.; De Keukeleire, D.; Bracke, M.; Heyerick, A.; van Breemen, R. B.; Depypere, H., Disposition of hop prenylflavonoids in human breast tissue. *Molecular Nutrition & Food Research* **2010,** *54* (S2), S284-S294.
167. Intelmann, D.; Haseleu, G.; Hofmann, T., LC-MS/MS Quantitation of Hop-Derived Bitter Compounds in Beer Using the ECHO Technique. *Journal of Agricultural and Food Chemistry* **2009,** *57* (4), 1172-1182.
168. De Bièvre, P. J.; Debus, G. H., Precision mass spectrometric isotope dilution analysis. *Nuclear Instruments and Methods* **1965,** *32* (2), 224-228.
169. Yang, Y.; Yu, L. X., Chapter 12 - Oral Drug Absorption, Evaluation, and Prediction. In *Developing Solid Oral Dosage Forms*, Qiu, Y.; Chen, Y.; Zhang, G. G. Z.; Liu, L.; Porter, W. R., Eds. Academic Press: San Diego, 2009; pp 289-308.
170. Avula, B.; Ganzera, M.; Warnick, J. E.; Feltenstein, M. W.; Sufka, K. J.; Khan, I. A., High-Performance Liquid Chromatographic Determination of Xanthohumol in Rat Plasma, Urine, and Fecal Samples. *Journal of Chromatographic Science* **2004,** *42* (7), 378-382.
171. Legette, L.; Ma, L.; Reed, R. L.; Miranda, C. L.; Christensen, J. M.; Rodriguez-Proteau, R.; Stevens, J. F., Pharmacokinetics of xanthohumol and metabolites in rats after oral and intravenous administration. *Molecular Nutrition & Food Research* **2012,** *56* (3), 466-474.
172. Zhang, J.; Yan, L.; Wei, P.; Zhou, R.; Hua, C.; Xiao, M.; Tu, Y.; Gu, Z.; Wei, T., PEG-GO@XN nanocomposite suppresses breast cancer metastasis via inhibition of mitochondrial oxidative phosphorylation and blockade of epithelial-to-mesenchymal transition. *European Journal of Pharmacology* **2021,** *895*, 173866.
173. Kirchinger, M.; Bieler, L.; Tevini, J.; Vogl, M.; Haschke-Becher, E.; Felder, T. K.; Couillard-Després, S.; Riepl, H.; Urmann, C., Development and Characterization of the Neuroregenerative Xanthohumol C/Hydroxypropyl-β-cyclodextrin Complex Suitable for Parenteral Administration. *Planta Med* **2019,** *85* (16), 1233-1241.
174. O'Connor, a.; Konda, V. R.; Reed, R. L.; Christensen, J. M.; Stevens, J. F.; Contractor, N., Rice Protein Matrix Enhances Circulating Levels of Xanthohumol Following Acute Oral Intake of Spent Hops in Humans. *Molecular Nutrition & Food Research* **2018,** *62*, &NA;.

175. Kamiński, D. M.; Gawęda, K.; Arczewska, M.; Senczyna, B.; Gagoś, M., A kinetic study of xanthohumol cyclization to isoxanthohumol – A role of water. *Journal of Molecular Structure* **2017,** *1139*, 10-16.
176. López-Yerena, A.; Perez, M.; Vallverdú-Queralt, A.; Escribano-Ferrer, E., Insights into the Binding of Dietary Phenolic Compounds to Human Serum Albumin and Food-Drug Interactions. *Pharmaceutics* **2020,** *12* (11), 1123.
177. Tronina, T.; Strugała, P.; Popłoński, J.; Włoch, A.; Sordon, S.; Bartmańska, A.; Huszcza, E., The Influence of Glycosylation of Natural and Synthetic Prenylated Flavonoids on Binding to Human Serum Albumin and Inhibition of Cyclooxygenases COX-1 and COX-2. *Molecules* **2017,** *22* (7), 1230.
178. Yilmazer, M.; Stevens, J. F.; Deinzer, M. L.; Buhler, D. R., In vitro biotransformation of xanthohumol, a flavonoid from hops (Humulus lupulus), by rat liver microsomes. *Drug Metabolism and Disposition* **2001,** *29* (3), 223-231.
179. Vanhoecke, B. W.; Delporte, F.; van Braeckel, E.; Heyerick, A.; Depypere, H. T.; Nuytinck, M.; de Keukeleire, D.; Bracke, M. E., A safety study of oral tangeretin and xanthohumol administration to laboratory mice. *In Vivo* **2005,** *19* (1), 103-107.
180. van Breemen, R. B.; Yuan, Y.; Banuvar, S.; Shulman, L. P.; Qiu, X.; Alvarenga, R. F. R.; Chen, S.-N.; Dietz, B. M.; Bolton, J. L.; Pauli, G. F.; Krause, E.; Viana, M.; Nikolic, D., Pharmacokinetics of prenylated hop phenols in women following oral administration of a standardized extract of hops. *Molecular Nutrition & Food Research* **2014,** *58* (10), 1962-1969.
181. Schmidt, C., First deuterated drug approved. *Nature Biotechnology* **2017,** *35* (6), 493-494.
182. Gester, S.; Metz, P.; Zierau, O.; Vollmer, G., An efficient synthesis of the potent phytoestrogens 8-prenylnaringenin and 6-(1,1-dimethylallyl)naringenin by europium(III)-catalyzed Claisen rearrangement. *Tetrahedron* **2001,** *57* (6), 1015-1018.
183. Diller, R. A.; Riepl, H. M.; Rose, O.; Frias, C.; Henze, G.; Prokop, A., Synthesis of Demethylxanthohumol, a New Potent Apoptosis-Inducing Agent from Hops. *Chemistry & Biodiversity* **2005,** *2* (10), 1331-1337.
184. Khupse, R. S.; Erhardt, P. W., Total Synthesis of Xanthohumol. *Journal of Natural Products* **2007,** *70* (9), 1507-1509.
185. Power, F. B.; Tutin, F.; Rogerson, H., CXXXV.—The constituents of hops. *Journal of the Chemical Society, Transactions* **1913,** *103* (0), 1267-1292.
186. Verzele, M.; Stockx, J.; Fontijn, F.; Anteunis, M., Xanthohumol, a New Natural Chalkone. *Bulletin des Sociétés Chimiques Belges* **1957,** *66* (1), 452-475.
187. Aniol, M.; Szymanska, K.; Zolnierczyk, A., An efficient synthesis of the phytoestrogen 8-prenylnaringenin from isoxanthohumol with magnesium iodide etherate. *Tetrahedron* **2008,** *64* (40), 9544-9547.
188. Santos, M. C.; Salvador, Â. C.; Domingues, F. M.; Cruz, J. M.; Saraiva, J. A., Use of High Hydrostatic Pressure to Increase the Content of Xanthohumol in Beer Wort. *Food and Bioprocess Technology* **2013,** *6* (9), 2478-2485.
189. Grudniewska, A.; Popłoński, J., Simple and green method for the extraction of xanthohumol from spent hops using deep eutectic solvents. *Separation and Purification Technology* **2020,** *250*, 117196.
190. Gagos, M. Process for the preparation of xanthohumol. 2014.
191. Chadwick, L. R.; Fong, H. H. S.; Farnsworth, N. R.; Pauli, G. F., CCC sample cutting for isolation of prenylated phenolics from hops. *Journal of Liquid Chromatography & Related Technologies* **2005,** *28* (12-13), 1959-1969.
192. Roehrer, S.; Behr, J.; Stork, V.; Ramires, M.; Médard, G.; Frank, O.; Kleigrewe, K.; Hofmann, T.; Minceva, M., Xanthohumol C, a minor bioactive hop compound: Production, purification strategies and antimicrobial test. *J Chromatogr B Analyt Technol Biomed Life Sci* **2018,** *1095*, 39-49.

193. Fang, Z.; Zhou, G.-C.; Zheng, S.-L.; He, G.-L.; Li, J.-L.; He, L.; Bei, D., Lithium chloride-catalyzed selective demethylation of aryl methyl ethers under microwave irradiation. *Journal of Molecular Catalysis A: Chemical* **2007,** *274* (1), 16-23.
194. Nakamura, A.; Nakada, M., Allylic Oxidations in Natural Product Synthesis. *Synthesis* **2013,** *45* (11), 1421-1451.
195. Nigudkar, S. S.; Demchenko, A. V., Stereocontrolled 1,2-cis glycosylation as the driving force of progress in synthetic carbohydrate chemistry. *Chem Sci* **2015,** *6* (5), 2687-2704.
196. Wang, Z., Schmidt Glycosylation. In *Comprehensive Organic Name Reactions and Reagents*, 2010; pp 2498-2502.
197. Schmidt, R. R., New Methods for the Synthesis of Glycosides and Oligosaccharides—Are There Alternatives to the Koenigs-Knorr Method? [New Synthetic Methods (56)]. *Angewandte Chemie International Edition in English* **1986,** *25* (3), 212-235.
198. Jongkees, S. A.; Withers, S. G., Glycoside cleavage by a new mechanism in unsaturated glucuronyl hydrolases. *J Am Chem Soc* **2011,** *133* (48), 19334-7.
199. Berwanger, S.; Frank, N.; Knauft, J.; Becker, H., Biosynthetic 14C-labelling of xanthohumol in hop cones. *Molecular Nutrition & Food Research* **2005,** *49* (9), 857-860.
200. Ellinwood, D. C.; El-Mansy, M. F.; Plagmann, L. S.; Stevens, J. F.; Maier, C. S.; Gombart, A. F.; Blakemore, P. R., Total synthesis of [13C]2-, [13C]3-, and [13C]5-isotopomers of xanthohumol, the principal prenylflavonoid from hops. *Journal of Labelled Compounds and Radiopharmaceuticals* **2017,** *60* (14), 639-648.
201. Turowski, M.; Yamakawa, N.; Meller, J.; Kimata, K.; Ikegami, T.; Hosoya, K.; Tanaka, N.; Thornton, E. R., Deuterium isotope effects on hydrophobic interactions: the importance of dispersion interactions in the hydrophobic phase. *J Am Chem Soc* **2003,** *125* (45), 13836-49.
202. Andrusiak, J.; Mylkie, K.; Wysocka, M.; Ścianowski, J.; Wolan, A.; Budny, M., Synthesis of xanthohumol and xanthohumol-d3 from naringenin. *RSC Advances* **2021,** *11* (46), 28934-28939.
203. Buckett, L.; Sus, N.; Spindler, V.; Rychlik, M.; Schoergenhofer, C.; Frank, J., The Pharmacokinetics of Individual Conjugated Xanthohumol Metabolites Show Efficient Glucuronidation and Higher Bioavailability of Micellar than Native Xanthohumol in a Randomized, Double-Blind, Crossover Trial in Healthy Humans. *Molecular Nutrition & Food Research*, 2200684.
204. Carvalho, D. O.; Guido, L. F., A review on the fate of phenolic compounds during malting and brewing: Technological strategies and beer styles. *Food Chemistry* **2022,** *372*, 131093.
205. Becker, H.; Berwanger, S.; Frank, N., Biolabeling of Xanthohumol in Hop Cones (Humulus Lupulus L., Cannabaceae) with Stable and Radioactive Precursors for Biosynthetic and Metabolic Studies. In *Beer in Health and Disease Prevention*, Preedy, V. R., Ed. Academic Press: San Diego, 2009; pp 795-799.
206. Schneider, F.; Bradbury, M.; Baillie, T. A.; Stamler, D.; Hellriegel, E.; Cox, D. S.; Loupe, P. S.; Savola, J.-M.; Rabinovich-Guilatt, L., Pharmacokinetic and Metabolic Profile of Deutetrabenazine (TEV-50717) Compared With Tetrabenazine in Healthy Volunteers. *Clinical and Translational Science* **2020,** *13* (4), 707-717.
207. Neumann, H. F.; Frank, J.; Venturelli, S.; Egert, S., Bioavailability and Cardiometabolic Effects of Xanthohumol: Evidence from Animal and Human Studies. *Molecular Nutrition & Food Research* **2022,** *66* (6), 2100831.
208. Xiao, J.; Muzashvili, T. S.; Georgiev, M. I., Advances in the biotechnological glycosylation of valuable flavonoids. *Biotechnology Advances* **2014,** *32* (6), 1145-1156.
209. Chen, S.-N.; Lankin, D. C.; Chadwick, L. R.; Jaki, B. U.; Pauli, G. F., Dynamic Residual Complexity of Natural Products by qHNMR: Solution Stability of Desmethylxanthohumol. *Planta Med* **2009,** *75* (07), 757-762.
210. Wang, M.-J.; Chao, P.-D.; Hou, Y.-C.; Hsiu, S.-L.; Wen, K.-C.; Tsai, S.-Y., Pharmacokinetics and conjugation metabolism of naringin and naringenin in rats after single dose and multiple dose administrations. *Journal of Food and Drug Analysis* **2006,** *14* (3), 4.

211. Felgines, C.; Texier, O.; Morand, C.; Manach, C.; Scalbert, A.; Régerat, F.; Rémésy, C., Bioavailability of the flavanone naringenin and its glycosides in rats. *American Journal of Physiology-Gastrointestinal and Liver Physiology* **2000,** *279* (6), G1148-G1154.
212. Cummins, G., Smart pills for gastrointestinal diagnostics and therapy. *Advanced Drug Delivery Reviews* **2021,** *177*, 113931.
213. Paolino, D.; Cosco, D.; Cilurzo, F.; Fresta, M., Innovative Drug Delivery Systems for the Administration of Natural Compounds. *Current Bioactive Compounds* **2007,** *3* (4), 262-277.